SIMULATION OF SOIL MOISTURE MIGRATION FROM A POINT SOURCE

by

© Krishanlal C. Khatri

A Thesis Submitted to
The Faculty of Graduate Studies and Research
in partial fulfilment of the requirements for the degree of
Doctor of Philosophy

Department of Agricultural Engineering
McGill University
Montreal, Quebec, Canada

September 1984

Short title:

SIMULATION OF SOIL MOISTURE MIGRATION.

K.C.Khatri

ABSTRACT

Ph.D. | Krishanlal C. Khatri | Agricultural Engineering

SIMULATION OF SOIL MOISTURE MIGRATION FROM A POINT SOURCE

A computer model simulating moisture migration in soil from a drip source considering root water extraction (RWE) was developed. The model was formulated using Continuous System Modeling Program (CSMP).

A two-dimensional non-linear unsaturated transient flow equation was solved using the principle of mass conservation and Darcy's law on soils of dwarf-apple orchards located in southwestern Quebec. A finite axisymmetric cylinder with homogeneous, isotropic and non-swelling soil was considered for the simulations. No flow conditions across the boundaries of the cylinder were fixed. The initial soil moisture contents in the soil profile observed in the field were input for the simulations.

The macroscopic approach was used to compute RWE as a function of θ, Z and t. The RWE was assumed to be equal to evapotranspiration (ET) which was estimated using temperatures and the solar radiation index of the location.

The moisture contents in the soil profile observed at the termination of emitter discharge were in close agreement with the simulated values. The soil moisture distribution was found to depend on the amount of water remaining in the soil and soil moisture retention characteristics. It is independent of the rate of emitter discharge, the depth of root zone and method of application.

RESUME

Ph.D. Krishanlal C. Khatri Génie Rural

SIMULATION DE L'ECOULEMENT DE L'EAU DANS LES SOLS
A PARTIR DE SOURCE PONCTUELLE

Un logiciel simulant la migration de l'eau dans le sol à partir de source ponctuelle (irrigation localisée) et prenant en considération l'extraction radiculaire de l'eau a été développé par le truchement de la programmation en langage CSMP (Continuous Systems Modeling Program).

Une équation non-lineaire bi-dimentionnelle d'écoulement transitoire non saturé a été solutionée en utilisant le principe de conservation de masse et la loi de Darcy sur les sols à vergers de pommiers nains du Sud-Ouest québécois. Un cylindre axisymmétrique de dimensions finies d'un sol homogène et isotrope non gonflant fut utilisé pour fins de simulation. Aucune condition d'écoulement fut établie à travers les limites dimensionnelles du cylindre. Les conditions initiales d'humidité du sol telles qu'observées dans les parcelles furent utilisées pour initier les simulations.

L'approche macroscopique fut utilisée pour le calcul de l'extraction radiculaire de l'eau du sol en fonction de Q, Z et t. Cette extraction fut prise comme étant égale à l'évapotranspiration, laquelle fut estimée à partir des températures ambiantes et de l'aide du rayonnement solaire du site expérimental.

La teneur en humidité du sol observée au terme des périodes d'apport d'eau à l'émetteur fut en accord avec les valeurs simulées. La distribution de l'eau dans le sol dépend de la quantité d'eau présenté et de la capacité de retention du sol en question, et est indépendante du

débit du goutteur, de la profondeur du système radiculaire ou de la méthode d'application.

ACKNOWLEDGEMENTS

The author wishes to express his appreciation to his thesis directors Professor P.J. Jutras and Dr. Robert S. Broughton for their guidance and encouragement throughout the course of this study.

I extend my appreciation to Dr. Shiv Prashar for their keen interest and assistance in the completion of this project.

I would like to thank my thesis committee including Dr. E. McKyes, Dr. G. Mehuys and Dr. D. Buszard for their interest and assistance in the completion of this project. The cooperation of Dr. R. Kok in providing computer facilities for this project is appreciated. Occasional advice from Dr. V. Raghavan was rewarding.

Field work for this project was made possible partially through a grant from Les Enterprise Harnois, St Thomas, Quebec. A subsidy from the McGill University Computer Center made computer time available for the completion of this project.

Thanks are extended to Ms. Suzelle Barrington and Messers Nisar Memon, Mohammad Issa Kalwar, L. Gauthier, Chandra Madramootoo, G. Sarwar Jakhro, Claude Weil Richard Eckerlin, John O. Ohu, G.M. Soomro and all my friends and fellow graduate students for their encouragement and assistance during the course of this research.

Special thanks are extended to Ms. Ann Anger for her time and help in collection of field data and Mr. Greg Bostock for his help in reviewing and correcting the manuscript.

The author would like to thank the Department of Agricultural

Engineering for partial financial support including the granting of the Jardin Bursary which made the completion of this study possible.

TABLE OF CONTENTS

PAGE

ABSTRACT i

RESUME ii

ACKNOWLEDGEMENTS iv

LIST OF TABLES ix

LIST OF FIGURES x

LIST OF SYMBOLS AND ABBREVIATIONS xviii

CHAPTER I. INTRODUCTION 1

1.1 Statement and Nature of the Problem 1
1.2 Objectives 3
1.3 Scope of the Work 4

CHAPTER II. REVIEW OF LITERATURE 5

2.1 General 5
2.2 Distribution of Irrigation Water in Soil 7
2.3 Simulation of Water Flow in Soils 9
2.4 Simulation of Water Extraction by Plant Roots 14
2.5 Estimation of Potential Evapotranspiration 19
2.6 Method of Irrigation Application 22

CHAPTER III. DEVELOPMENT AND SOLUTION OF THE MODEL 24

3.1 Description of the Problem 24
3.2 Assumptions 25
3.3 Theoretical Development 26
3.4 Solution Technique 31
3.5 Initial and Boundary Conditions 40
3.6 Actual Migration Time 40
3.7 Method of Drip Irrigation Application 42

CHAPTER IV. EXPERIMENTAL PROCEDURE AND DATA COLLECTION 44
4.1 General Description 44
4.2 Experimental Procedure 44
4.3 Input Data 45
4.4 Determination of Soil Properties 46
4.5 Estimation of Daily Potential Evapotranspiration 48
4.6 Determination of Root Zone Depth 50
4.7 Model Testing 50

CHAPTER V. DESCRIPTION OF THE COMPUTER PROGRAM 57

5.1 Introduction 57
5.2 The INITIAL Segment 59
5.3 The DYNAMIC Segment 61
5.3.1 SORT Section 61
5.3.2 NOSORT Section 62
5.4 The TERMINAL Segment 67
5.5 Execution Control Statements 68
5.6 Method of Integration 68
5.7 Output Control Statements 68

CHAPTER VI RESULTS AND DISCUSSION 70

6.1 Introduction 70
6.2 Rougemont Orchard Site 1 71
6.2.1 Orchard Experiments and Simulation Results 72
6.2.2 Simulation results after Redistribution of Water 75
6.2.2.1 Irrigation Application of 12 L of Water 76
6.2.2.2 Irrigation Application of 16 L of Water 82
6.2.2.3 Irrigation Application of 24 L of Water 84
6.3 Rougemont Orchard Site 2 85
6.3.1 Orchard Experiments and Simulation Results 86
6.3.2 Simulation Results After Redistribution of Water 88
6.3.2.1 Irrigation Application of 12 L of Water 88
6.3.2.2 Irrigation Application of 16 L of Water 93
6.4 Rougemont Orchard Site 3 94
6.4.1 Orchard Experiments and Simulation Results 94
6.4.2 Simulation Results after Redistributio of Water 96
6.4.2.1 Irrigation Application of 12 L of Water 97
6.4.2.2 Irrigation Application of 16 L of Water 97
6.5 Rockburn Orchard Site 1 101
6.5.1 Orchard Experiments and Simulation Results 101
6.5.2 Simulation Results after Redistributio of Water 103
6.5.2.1 Irrigation Application of 12 L of Water 103
6.5.2.2 Irrigation Application of 16 L of Water 106
6.6 Rockburn Orchard Site 2 108
6.6.1 Orchard Experiments and Simulation Results 108
6.6.2 Simulation Results after Redistributio of Water 110
6.6.2.1 Irrigation Application of 12 L of Water 110
6.6.2.2 Irrigation Application of 16 L of Water 114
6.7 Further Theoretical Investigations 114
6.7.1 Point Source vs Circular Loop Source 115
6.7.2 Research Site vs Moisture Migration 117
6.7.3 Amount of Irrigation Water versus Replenished Area . . 123
6.8 Sensitivity Analysis 124
6.8.1 Mesh Size in R-Direction 124
6.8.2 Mesh Size in Z-Direction 127
6.8.3 Hydraulic Conductivity 127
6.8.4 Rate of Irrigation Application 128

6.8.5 Amount of Irrigation Water 128
6.8.6 Root Zone Depth 131
6.8.7 Initial Soil Moisture Content 131
6.8.8 Daily evapotranspiration 134
6.8.9 Volume of Soil Ring 134

CHAPTER VII SUMMARY 139

CHAPTER VIII CONCLUSIONS 141

CHAPTER IX CONTRIBUTIONS TO KNOWLEDGE 145

CHAPTER X SUGGESSIONS FOR FUTURE RESEARCH 148

REFERENCES 151

APPEDICES 159

A. Listing of the Computer Program 160
B. Figures of Various Experiments and Simulations 179

LIST OF TABLES

Table		Page
3.1	Simulation time required for 12-hours AMT for various irrigation periods.	43
4.1	Initial volumetric moisture contents in soil profiles and other input parameters at the research sites.	51
4.2	Physical properties of soils existing in orchards.	54
4.3	Saturated hydraulic conductivity of soils.	54
4.4	Volumetric moisture contents of soils.	54
4.5	Basic parameters and their values in sensitivity analysis.	55
6.1	Summary of results predicted for Rougemont orchard site 1.	80
6.2	Summary of results predicted for Rougemont orchard site 2.	92
6.3	Summary of results predicted for Rougemont orchard site 3.	100
6.4	Summary of predicted results for Rockburn orchard site 1.	107
6.5	Summary of results predicted for Rockburn orchard site 2.	113
6.6	Summary of simulation results obtained with 12 L of water application from a point and a circular source for the five research sites.	120
6.7	Replenished areas (m^2) predicted with different volumes of irrigation water and time equivalent to 12-hours AMT.	125
6.8	Summary of simulation results obtained for sensitivity of mesh size.	126
6.9	Summary of simulation results obtained for sensitivity of various parameters.	136

LIST OF FIGURES

Figure		Page
3.1	Root water extraction as a function of root depth.	30
3.2	Root water extraction as a function of soil moisture content.	32
3.3	Schematic view of the soil cylinder for simulation.	33
3.4	Schematic view of a ring (i,j) for simulation.	36
4.1	Soil moisture retention curves of the soils.	47
4.2	Hydraulic conductivity curves of the soils.	49
5.1	Flow chart of the computer simulator.	58
6.1	Soil moisture content profiles before and after 12 L of water applied at 2 L.h^{-1} at Rougemont orchard site 1.	73
6.2	Water input predicted along horizontal distance with an irrigation application of 12 L at different discharge rates for Rougemont orchard site 1.	77
6.3	Water input predicted in soil profile with an irrigation application of 12 L at different discharge rates for Rougemont orchard site 1.	78
6.4	Soil moisture content profiles before and after 12 L of water applied at 2 L.h^{-1} at Rougemont orchard site 2	87
6.5	Water input predicted along horizontal distance with an irrigation application of 12 L at different discharge rates for Rougemont orchard site 2.	89
6.6	Water input predicted in soil profile with an irrigation application of 12 L at different discharge rates for Rougemont orchard site 2.	90
6.7	Soil moisture content profiles before and after 12 L of water applied at 2 L.h^{-1} at Rougemont orchard site 3	95
6.8	Water input predicted along horizontal distance with an irrigation application of 12 L at different discharge rates for Rougemont orchard site 3.	98

6.9 Water input predicted in soil profile with an irrigation application of 12 L at different discharge rates for Rougemont orchard site 3. 99

6.10 Soil moisture content profiles before and after 16 L of water applied at 4 $L.h^{-1}$ at Rockburn orchard site 1 102

6.11 Water input predicted along horizontal distance with an irrigation application of 16 L at different discharge rates for Rockburn orchard site 1. 104

6.12 Water input predicted in soil profile with an irrigation application of 16 L at different discharge rates for Rockburn orchard site 1. 105

6.13 Soil moisture content profiles before and after 12 L of water applied at 2 $L.h^{-1}$ at Rockburn orchard site 2 109

6.14 Water input predicted along horizontal distance with an irrigation application of 12 L at different discharge rates for Rockburn orchard site 2. 111

6.15 Water input predicted in soil profile with an irrigation application of 12 L at different discharge rates for Rockburn orchard site 2. 112

6.16 Water input predicted along horizontal distance with an irrigation application of 12 L from a point and a circular loop source for Rougemont orchard site 1. 116

6.17 Water input predicted along horizontal distance with an irrigation application of 12 L from a point source for the five research sites. 118

6.18 Water input predicted along horizontal distance with an irrigation application of 12 L from a circular loop source for the five research sites. 119

6.19 Water input predicted along horizontal distance with irrigation applications of 12, 16 and 24 L. 129

6.20 Water input predicted in soil profile with irrigation applications of 12, 16 and 24 L. 130

6.21 Water input predicted along horizontal distance with an irrigation application of 12 L and different initial soil moisture contents. 132

6.22 Water input predicted in soil profile with an irrigation application of 12 L and different initial soil moisture contents. 133

6.23 Water input predicted along horizontal distance with an irrigation application of 12 L using constant and variable volume soil rings. 135

B.1 Soil moisture content profiles before and after 12 L of water applied at 4 $L.h^{-1}$ at Rougemont orchard site 1. 180

B.2 Soil moisture content profiles before and after 12 L of water applied at 6 $L.h^{-1}$ at Rougemont orchard site 1. 181

B.3 Soil moisture content profiles before and after 16 L of water applied at 2 $L.h^{-1}$ at Rougemont orchard site 1. 182

B.4 Soil moisture content profiles before and after 16 L of water applied at 4 $L.h^{-1}$ at Rougemont orchard site 1. 183

B.5 Soil moisture content profiles before and after 16 L of water applied at 8 $L.h^{-1}$ at Rougemont orchard site 1. 184

B.6 Soil moisture content profiles before and after 24 L of water applied at 4 $L.h^{-1}$ at Rougemont orchard site 1. 185

B.7 Soil moisture content profiles before and after 24 L of water applied at 8 $L.h^{-1}$ at Rougemont orchard site 1. 186

B.8 Soil moisture content profiles before and after 24 L of water applied at 12 $L.h^{-1}$ at Rougemont orchard site 1. ... 187

B.9 Equimoisture curves at the cessation of irrigation water application of 12 L with discharge rate of 2 $L.h^{-1}$ for Rougemont orchard site 1. 188

B.10 Equimoisture curves at the cessation of irrigation water application of 12 L with discharge rate of 4 $L.h^{-1}$ for Rougemont orchard site 1. 189

B.11 Equimoisture curves at the cessation of irrigation water application of 12 L with discharge rate of 6 $L.h^{-1}$ for Rougemont orchard site 1. 190

B.12 Equimoisture curves at the cessation of irrigation water application of 16 L with discharge rate of 2 $L.h^{-1}$ for Rougemont orchard site 1. 191

B.13 Equimoisture curves at the cessation of irrigation water application of 24 L with discharge rate of 4 $L.h^{-1}$ for Rougemont orchard site 1. 192

B.14 Distribution of 12 L of water along horizontal distance with discharge rate of 2 $L.h^{-1}$ (expressed in mm) for Rougemont orchard site 1. 193

B.15 Distribution of 12 L of water along horizontal distance with pulse discharge rate of 4 $L.h^{-1}$ (expressed in mm) for Rougemont orchard site 1. 194

B.16 Distribution of 12 L of water along horizontal distance with discharge rate of 4 $L.h^{-1}$ (expressed in mm) for Rougemont orchard site 1. 195

B.17 Distribution of 12 L of water along horizontal distance with pulse discharge rate of 6 $L.h^{-1}$ (expressed in mm) for Rougemont orchard site 1. 196

B.18 Distribution of 12 L of water along horizontal distance with discharge rate of 6 $L.h^{-1}$ (expressed in mm) for Rougemont orchard site 1. 197

B.19 Distribution of 12 L of water along horizontal distance with discharge rate of 2 $L.h^{-1}$ (expressed as percentage) for Rougemont orchard site 1. 198

B.20 Distribution of 12 L of water along horizontal distance with pulse discharge rate of 4 $L.h^{-1}$ (expressed as percentage) for Rougemont orchard site 1. 199

B.21 Distribution of 12 L of water along horizontal distance with discharge rate of 4 $L.h^{-1}$ (expressed as percentage) for Rougemont orchard site 1. 200

B.22 Distribution of 12 L of water along horizontal distance with pulse discharge rate of 6 $L.h^{-1}$ (expressed as percentage) for Rougemont orchard site 1. 201

B.23 Distribution of 12 L of water along horizontal distance with discharge rate of 6 $L.h^{-1}$ (expressed as percentage) for Rougemont orchard site 1. 202

B.24 Distribution of 12 L of water in soil profile with discharge rate of 2 $L.h^{-1}$ for Rougemont orchard site 1. .. 203

B.25 Distribution of 12 L of water in soil profile with pulse discharge rate of 4 $L.h^{-1}$ for Rougemont orchard site 1. .. 204

B.26 Distribution of 12 L of water in soil profile with discharge rate of 4 L.h^{-1} for Rougemont orchard site 1. .. 205

B.27 Distribution of 12 L of water in soil profile with pulse discharge rate of 6 L.h^{-1} for Rougemont orchard site 1. .. 206

B.28 Distribution of 12 L of water in soil profile with discharge rate of 6 L.h^{-1} for Rougemont orchard site 1. .. 207

B.29 Equimoisture curves after redistribution of irrigation water application of 12 L with discharge rate of 2 L.h^{-1} for Rougemont orchard site 1. 208

B.30 Equimoisture curves after redistribution of irrigation water pulse application of 12 L with discharge rate of 4 L.h^{-1} for Rougemont orchard site 1. 209

B.31 Equimoisture curves after redistribution of irrigation water application of 12 L with discharge rate of 4 L.h^{-1} for Rougemont orchard site 1. 210

B.32 Equimoisture curves after redistribution of irrigation water pulse application of 12 L with discharge rate of 6 L.h^{-1} for Rougemont orchard site 1. 211

B.33 Equimoisture curves after redistribution of irrigation water application of 12 L with discharge rate of 6 L.h^{-1} for Rougemont orchard site 1. 212

B.34 Water input predicted along horizontal distance with an irrigation application of 16 L at different discharge rates for Rougemont orchard site 1. 213

B.35 Water input predicted in soil profile with an irrigation application of 16 L at different discharge rates for Rougemont orchard site 1. 214

B.36 Water input predicted along horizontal distance with an irigation application of 24 L at different discharge rates for Rougemont orchard site 1. 215

B.37 Water input predicted in soil profile with an irrigation application of 24 L at different discharge rates for Rougemont orchard site 1. 216

B.38 Soil moisture content profiles before and after 12 L of water applied at 4 L.h^{-1} at Rougemont orchard site 2. 217

B.39 Soil moisture content profiles before and after 16 L of water applied at 4 $L.h^{-1}$ at Rougemont orchard site 2 218

B.40 Soil moisture content profiles before and after 16 L of water applied at 8 $L.h^{-1}$ at Rougemont orchard site 2 219

B.41 Water input predicted along horizontal distance with an irrigation application of 16 L at different discharge rates for Rougemont orchard site 2. 220

B.42 Water input predicted in soil profile with an irrigation application of 16 L at different discharge rates for Rougemont orchard site 2. 221

B.43 Soil moisture content profiles before and after 12 L of water applied at 4 $L.h^{-1}$ at Rougemont orchard site 3 222

B.44 Soil moisture content profiles before and after 16 L of water applied at 4 $L.h^{-1}$ at Rougemont orchard site 3 223

B.45 Soil moisture content profiles before and after 16 L of water applied at 8 $L.h^{-1}$ at Rougemont orchard site 3 224

B.46 Water input predicted along horizontal distance with an irrigation application of 16 L at different discharge rates for Rougemont orchard site 3. 225

B.47 Water input predicted in soil profile with an irrigation application of 16 L at different discharge rates for Rougemont orchard site 3. 226

B.48 Soil moisture content profiles before and after 16 L of water applied at 8 $L.h^{-1}$ at Rockburn orchard site 1 227

B.49 Soil moisture content profiles before and after 24 L of water applied at 4 $L.h^{-1}$ at Rockburn orchard site 1 228

B.50 Soil moisture content profiles before and after 24 L of water applied at 8 $L.h^{-1}$ at Rockburn orchard site 1 229

B.51 Water input predicted along horizontal distance with an irrigation application of 24 L at different discharge rates for Rockburn orchard site 1. 230

B.52 Water input predicted in soil profile with an irrigation application of 24 L at different discharge rates for Rockburn orchard site 1. 231

B.53. Soil moisture content profiles before and after 12 L of water applied at 4 $L.h^{-1}$ at Rockburn orchard site 2 232

B.54 Soil moisture content profiles before and after 16 L of water applied at 2 $L.h^{-1}$ at Rockburn orchard site 2 233

B.55 Soil moisture content profiles before and after 16 L of water applied at 4 $L.h^{-1}$ at Rockburn orchard site 2 234

B.56 Water input predicted along horizontal distance with an irrigation application of 16 L at different discharge rates for Rockburn orchard site 2. 235

B.57 Water input predicted in soil profile with an irrigation application of 16 L at different discharge rates for Rockburn orchard site 2. 236

B.58 Water input predicted along horizontal distance with an irrigation application of 12 L from a point and a circular loop source for Rougemont orchard site 2. 237

B.59 Water input predicted along horizontal distance with an irrigation application of 12 L from a point and a circular loop source for Rougemont orchard site 3. 238

B.60 Water input predicted along horizontal distance with an irrigation application of 12 L from a point and a circular loop source for Rockburn Orchard Site 1. 239

B.61 Water input predicted along horizontal distance with an irrigation application of 12 L from a point and a circular loop source for Rockburn orchard site 2. 240

B.62 Water input predicted along horizontal distance with an irrigation application of 12 L and different mesh sizes in radial direction. 241

B.63 Water input predicted in soil profile with an irrigation application of 12 L and different mesh sizes in radial direction. 242

B.64 Water input predicted along horizontal distance with an irrigation application of 12 L and different mesh sizes in vertical direction. 243

B.65 Water input predicted in soil profile with an irrigation application of 12 L and different mesh sizes in vertical direction. 244

B.66 Water input predicted along horizontal distance with an irrigation application of 12 L and different hydraulic conductivity values. 245

B.67 Water input predicted in soil profile with an irrigation application of 12 L and different hydraulic conductivity values. 246

B.68 Water input predicted along horizontal distance with an irrigation application of 12 L for $K = 3.56$ m.day^{-1} at t=15 h and $K = 5.14$ m.day^{-1} at t=13 h. 247

B.69 Water input predicted in soil profile with an irrigation application of 12 L for $K = 3.56$ m.day^{-1} at t=15 h and $K = 5.14$ m.day^{-1} at t=13 h. 248

B.70 Water input predicted along horizontal distance with an irrigation application of 12 L and different root zone depths. 249

B.71 Water input predicted in soil profile with an irrigation application of 12 L and different root zone depths. 250

B.72 Water input predicted along horizontal distance with an irrigation application of 12 L and different PET values. .. 251

B.73 Water input predicted in soil profile with an irrigation application of 12 L and different PET values. 252

LIST OF SYMBOLS AND ABBREVIATIONS

a = A coefficient dependent on geographic and climatic region

A = Area, m^2

AET = Actual evapotranspiration, mm

AMT = Actual migration time, s, h

Av = Average

AW = Percentage of available water before evapotranspiration

AWRMM = Amount of water along horizontal distance expressed, mm

BRA = Below replenished area

BRZ = Below root zone

c = A constant used in Equation 4.2

C = Time period of pulse cycle, s, h

CUMPCR = Cumulative percentage of total irrigation water along horizontal distance from emitter

CUMPCZ = Cumulative percentage of total irrigation water along vertical distace from soil surface

D = Soil water diffusivity, $m^2.d^{-1}$

DELSTO = Rate of change of θ per unit volume of soil, $m^3.m^{-3}$

DL_m = Mean daylength for a month divided by the mean annual daylength, fraction

ET = Evapotranspiration, mm

H = Hydraulic potential, m

i = Counter in vertical direction

imax = Maximum number of soil rings in vertical direction

IMC = Initial moisture content (same as Θ_{in}), $m^3.m^{-3}$

IRR = Irrigation water input, mm

IRRWI = Irrigation water input, L

j = Counter in R-direction

jmax = Maximum number of soil rings in radial direction

K = Unsaturated hydraulic conductivity (function of Θ), $m.d^{-1}$, $m.s^{-1}$

K_s = Saturated hydraulic conductivity, $m.d^{-1}$, $m.s^{-1}$

L_s = Length of a soil sample for K_s test, m

L_r = Length of root system, m

LD = Daylength, s, h

MC = Volumetric moisture content (same as Θ), $m^3.m^{-3}$

m = Number of soil moisture content increaments for $K(\Theta)$

PET = Potential evapotranspiration, mm

PETR = PET rate with respect to the time of day, $m.s^{-1}$

$PETR_{max}$ = Maximum midday PET rate, $m.s^{-1}$

Q = Emitter discharge rate or flow rate across the boundaries of the soil rings, $m^3.s^{-1}$, $L.h^{-1}$

ΔQ = Net flow rate or rate of change in storage, $m^3.s^{-1}$

Q_e = Emitter discharge rate, $m^3.s^{-1}$, $L.h^{-1}$

Q_v = Volume of water that passes through a soil sample for K test, m^3

q = Flux of water, $m.s^{-1}$

QCON = Emitter discharge rate with continuous irrigation, $L.h^{-1}$

QPUL = Emitter discharge rate with pulse irrigation, $L.h^{-1}$

R = Radius or horizontal distance from the center, m

R_{max} = Radius of the finite soil cylinder, m

R_e = Length of roots, $m.m^{-3}$

ΔR = Width of the soil ring, m

RB1 = Rockburn orchard site 1

RB2 = Rockburn orchard site 2

RM1 = Rougemont orchard site 1

RM2 = Rougemont orchard site 2

RM3 = Rougemont orchard site 3

RWE = root water extraction, mm

RWE_{max} = maximum root water extraction, mm

RWEF = root water extraction, fraction of total

RWER = Rate of RWE, $mm.s^{-1}$

RZD = Root zone depth, m

SMC = Soil moisture content, $m^3.m^{-3}$

SWA_{fi} = Final amount of soil water, L

SWA_{in} = Initial amount of soil water, L

T = Mean monthly temperature, ^oC

T_a = An arbitrary AMT, s, h

T_{av} = Average transpiration, mm

T_{irr} = Time period of irrigation application, s, h

T_{obs} = Time required for observation or simulation, s, h

t = Time, s, h

TQ = Total amount of irrigation water, L

v = Volume of a soil ring, m^3

VMC = Volumetric moisture content, $m^3.m^{-3}$

WRA = Within replenished area

WRZ = Within root zone

WSC = Within soil cylinder

Z = Depth from the soil surface or gravity potential, m

Z_{max} = Depth from the top to the bottom of the soil cylinder, m

ΔZ = Thickness of a soil ring, m

Θ = Volumetric soil moisture content, $m^3.m^{-3}$

Θ_{an} = Θ at anaerobiosis point, $m^3.m^{-3}$

Θ_d = Θ at some anaerobiosis point where root water extraction is maximum, $m^3.m^{-3}$

Θ_{in} = Initial Θ, $m^3.m^{-3}$

Θ_{ob} = Observed Θ, $m^3.m^{-3}$

Θ_{pr} = Predicted Θ, $m^3.m^{-3}$

Θ_r = Θ at 50 percent available soil moisture, $m^3.m^{-3}$

Θ_s = Θ at saturation, $m^3.m^{-3}$

Θ_t = Θ at time t, $m^3.m^{-3}$

Θ_w = Θ at wilting point, $m^3.m^{-3}$

ϕ = Hydraulic potential, m, kPa

ψ = Matric potential, m, kPa

ψ_r = Root potential, m

π = A constant equal to 3.14159

1/b = Empirical constant (root effectiveness function), m^{-2}.

CHAPTER I

INTRODUCTION

1.1 Statement and Nature of the Problem

A large proportion of apple orchards in Quebec are located on valley slopes of the southwestern part of the Province. The soil of this area varies from gravelly sand to sandy loam. Available soil moisture capacity is low and drainage is excessive (Mailloux and Godbout, 1954). Precipitation is the major source of soil moisture supply for the crops. The uneven distribution of rainfall during the growing period results in soil moisture stress problems especially in young orchards (Soomro et al., 1983). Therefore, supplemental irrigation is necessary to provide satisfactory soil moisture conditions for optimal tree growth.

Drip irrigation is beneficially practiced by Quebec farmers in young orchards (Jutras et al., 1983). Emitters are usually placed on the soil surface and sometimes get buried into the soil due to erosion. Water from the emitters enters the soil which is in immediate contact with the emitter. The soil at the discharge point becomes saturated and water flows away into the soil matrix. Thus, this is a case of three dimensional, transient water flow into the soil (Brandt, et al., 1971).

The tree roots in drip-irrigated orchards, under Quebec conditions, are not restricted to the emitter-wetted soil volume.

They grow beyond the wetted soil volume. Under rainfall conditions, weeds grow throughout the entire surface area of the young orchards. Under drip irrigation weed growth is restricted to the emitter-wetted soil volume. Weeds help to reduce soil and water erosion. Thus, the root water extraction in the young apple orchards is the result of the transpiration needs of the trees and the weeds.

The future of drip irrigation is promising in Quebec (Jutras et al., 1983). Soomro et al. (1983) reported encouraging results on the response of semi-dwarf apple trees to supplementary drip irrigation. Irrigation systems in Quebec apple orchards are still designed and installed based on either work done elsewhere or on recommendations of dealers and equipment manufacturers. A properly designed drip irrigation system would minimize water and energy requirements. Local designers need data on soil moisture distribution with various emitter discharge rates and various quantities of water for proper design of drip irrigation systems.

Drip irrigation systems usually function continuously. In order to achieve lower application rates from a drip irrigation system, sequential or pulse irrigation is suggested (Karmeli and Peri, 1973). It is based on a series of pulses, where each pulse is composed of an operating phase and a resting phase. Mostaghimi et al. (1981b) compared soil moisture distribution from continuous and pulse irrigation applications on heavy soils. They reported that the pulse irrigation resulted in a significant reduction in water loss below the soil profile in comparison to the continuous treatments.

Brandt et al. (1971) were the first to investigate the problem of infiltration from a drip source onto a bare soil. The analysis of moisture movement into the soil becomes complex when water extraction by tree roots is considered. Very limited attempts have been made to study moisture movement considering root water uptake (Neuman et al., 1975; Feddes et al., 1975; Pall et al., 1981). No research of this type has been carried out in the past in Quebec.

1.2 Objectives

This research was conducted to study the soil moisture distribution from single emitters in newly developed dwarf apple orchards in Quebec with the following objectives:-

1. To study the moisture migration at various application rates and volumes of irrigation water.
2. To develop a computer model to simulate the migration of the soil moisture.
3. To estimate the loss of irrigation water below the root zone with various application rates and volumes.
4. To compare the predicted soil moisture distribution obtained from the continuous and pulse methods of irrigation application.

1.3 Scope of the Work

The results of the investigation of this research are expected to be applicable to the design of drip irrigation systems in orchards of southern Quebec. By using the appropriate data required by the simulation model one can predict the lateral and vertical extent of the soil volume wetted by an emitter. A designer can determine the number of emitters and their configuration, the rate of discharge, the amount of irrigation water to be applied, the method of application and the time of irrigation application for a tree. This model is applicable to homogeneous soils only. The model will not give good results in a situation where the moisture migration from adjacent emitters overlaps.

CHAPTER II

REVIEW OF LITERATURE

2.1 General

Drip irrigation is defined as the frequent application of water to the soil surface as discrete or continuous drops, or tiny streams, through emitters. Often the term drip and trickle irrigation are considered synonymous; however, in ASAE Engineering Practice (EP) 405 (ASAE, 1983), trickle irrigation also includes those systems (bubbler and spray irrigation) which have higher discharge rates than most drip systems. For drip irrigation, discharge rates for point-source emitters are generally less than 12 $L.h^{-1}$ for single-outlet emitters, and line source emitters are generally less than 12 $L.h^{-1}.m^{-1}$ of lateral.

The usual objective of irrigation is to recharge the soil to field capacity throughout the zone from which roots withdraw water and soil surface evaporation takes place. Then, after the soil has been dried by evapotranspiration to some allowable limit, another application is needed (Marshall and Holmes, 1979).

The upper limit of water availability to plants (field capacity) is generally based on water content after a saturated soil has freely drained for 2 or 3 days or by subjecting wetted soil to pressures in the range from 5 to 30 kPa (0.05 to 0.3 bar) in pressure membrane or pressure plate equipment. The lower values are generally applicable to sandy soils and the higher values to clay soils. While the soil is draining to field capacity, growing plants may use some of the water above field capacity. The lower limit (permanent wilting point) is estimated by determining the water content at which indicator plants growing in the soil wilt and fail to recover turgor when subjected overnight to a humid atmosphere. It can also be estimated by determining the equilibrium content of the wetted soil subjected to pressures of 1500 kPa (15 bars) in appropriate equipment (Kramer, 1969; Peters, 1965).

The principles of soil water flow due to irrigation have been investigated by many researchers. According to Miller and Klute (1967), for standard irrigation practice, water flow within soil may be classified in three phases:

(i) infiltration: This process starts with the application of water and ends with cessation of irrigation and depletion of surface storage.

(ii) redistribution: Water movement in the downward and horizontal directions does not cease immediately after infiltration and may persist for a long time as soil water redistributes within the profile. The soil volume wetted to near saturation during infiltration does not retain its full water content since some of its water moves into the soil matrix under the influence of gravity and suction gradients.

(iii) withdrawal: This is mainly absorption of water by plant roots to supply transpiration requirements. However, evaporation at the soil surface or drainage to the lower levels may be significant in certain situations.

Most of the processes involving soil-water interaction in the field, and particularly the flow of water in the rooting zone of most crop plants, occur while the soil is in an unsaturated condition. Unsaturated flow processes are in general complicated and difficult to describe quantitatively, since they often entail changes in the state and content of soil water during flow. Changes involve complex relations such as soil wetness, suction and conductivity, whose interaction may be further complicated by hysteresis. The formulation and solution of unsaturated flow problems very often require the use of indirect methods of analysis, based on approximation of numerical techniques (Hillel, 1977).

2.2 Distribution of Irrigation Water in Soil

Bresler et al. (1971) conducted laboratory and field experiments using loamy and sandy soils to study the effect of drip discharge rates on the water content distribution and the location of the wetting front. They reported that an increase in the drip discharge rate results in an increase in the horizontal wetted area and a decrease in the wetted depth.

Padmakumari and Sivanappan (1979) studied the wetting pattern for emitter discharge rates of 5 to 30 litres per hour with the total application of 10 liters per day for 6 weeks on bare silty clay loam soil. They found that the depth of wetting was greater for the lower application rates and longer times than for the higher application rates and shorter application times. They concluded that the water distribution is directly dependent on the discharge rate of dripping and duration of irrigation.

Leven et al. (1979a) investigated soil moisture distrbution from a trickle source on a 0.6-m-deep heavy basalt soil underlain with gravel. They found that the soil moisture and root system distribution covered a wider area when irrigated twice a week with 8 $L.h^{-1}$ emitters than when irrigated every day or once a week with 4 $L.h^{-1}$ emitters. They also found that the higher rate of application gave wider distribution.

Goldberg and Shmueli (1970) examined the effect of trickle irrigation intervals on distribution and utilization of soil moisture in a vineyard on sandy clay soil. They reported that the shorter irrigation intervals, with proportionally smaller amounts of water applied in a single irrigation, decreased the variations of moisture content in the root zone and established a continuously higher moisture content regime.

Ben-Asher (1979) investigated the effect of trickle irrigation timing on plant and soil water status. Tomato plants on Sinai sand dunes were irrigated daily by drip irrigation. The irrigation was applied during day time hours on one field and a short time after sunset on the second field. The results showed that daytime irrigation of soil with low water holding capacity increased the yield significantly and improved plant water potential as well as water use efficiency. When irrigation was applied at night, about 35-50 percent of the water was lost by deep drainage below the root zone between water application at 1800 hours and the beginning of evapotranspiration at 600 hours. This was due to the day time evapotranspiration which reduced the amount of water available for deep percolation.

2.3 Simulation of Water Flow into Soils

In the past, attempts have been made to predict moisture distribution into bare soils by analytical and numerical methods. A few simulation models have been developed which predict moisture distribution from a point source into a bare soil. To estimate root water uptake by plants and trees, a few models have been reported in the literature. However, no information is available about the moisture distribution from a point source considering root water uptake under supplementary irrigation conditions in orchards.

One of the most widely used approaches to predict soil moisture distribution into soils is numerical approximation. This approach can be applied either by the method of finite differences or by the method of finite elements. The basic principles of flow and energy conservation have also been applied directly for solution of saturated and unsaturated flow problems (Armstrong and Wilson, 1983; Hillel, 1977; van der Pleog and Benecke, 1974; Bhuiyan et al., 1971). The solution of flow problems can also be obtained by electrical analogs.

With the advancement of high speed digital computers, the electrical analogs are not considered an effective method of soil water simulation (Pall, 1980).

Klute (1952) was perhaps the first investigator to use numerical techniques for simulation of the unsaturated flow processes. The application of finite difference method for the study of soil water flow was introduced by Day and Luthin (1956). They solved the problem of vertical drainage by a Gauss-Seidel type of iterative method with a no-flow condition at the top surface and constant pressure boundary condition at the bottom.

Hanks and Bowers (1962) used the Crank-Nicolson finite difference scheme to study horizontal and vertical infiltration into uniform and layered soils. The difference equation in the tridiagonal was solved by Gaussian elimination. Ashcroft et al. (1962) applied a backward difference implicit scheme for the simulation of horizontal flow. Here, Gaussian elimination was used as the solution technique. The numerical approach of Hanks and Bowers (1962) was later used by Jensen and Hanks (1967) to investigate column drainage.

Bresler et al. (1969) used the modified approach of Hanks and Bowers (1962) to study the three different stages of soil water flow in terms of infiltration, redistribution, and evaporation. The modified approach has been outlined by Hanks et al. (1969). The effect of hysteresis was included in this investigation. Various types of boundary conditions were applied at the bottom. The surface boundary conditions were treated in an iterative manner by keeping a constant pressure at the surface during iteration.

Pall et al. (1978, 1979) approached the problem of simulation of unsaturated flow in a different way by avoiding the use of differential equations. Direct statements of Darcy's law and of mass conservation were applied for the solution of horizontal and vertical flow problems. Their results showed an excellent agreement with the solution of Hanks and Bowers (1962), Scott et al. (1962) and Philip (1955).

Rubin (1968) extended the approach of numerical simulation to two-dimensional unsteady flow. He studied horizontal infiltration into a partially air dry slab of soil and drainage from partially saturated soils into a ditch. The infiltration problem was solved with the alternate direction implicit procedure (ADI). For drainage, iterative alternate direction implicit procedure (ITADI) was used. No-flow boundary conditions and uniform initial conditions were used in this study.

Freeze (1971) was the first researcher to advance the approach of finite difference to three-dimensional flow problems. A very complex problem of transient flow into partially saturated soils was solved with the line successive over-relaxation (LSOR) method.

Brandt et al. (1971) were the first investigators to attack the problem of infiltration from a drip source into bare soils. A mathematical model for infiltration was developed from non-hysteretic, unsaturated flow theory. The differential equation of unsaturated flow in the diffusivity form was solved with noniterative alternate direction implicit (ADI) difference procedure with Newton's iterative method.

Bresler et al. (1971) tested the model of Brandt et al. (1971) in the field. At low trickle discharge, the predicted and experimental results were in good agreement. The disagreement at higher discharge was due to an increase in horizontal wetted area and decrease in wetted depth.

Bresler (1975) developed another model for multidimensional simultaneous transfer of noninteracting solute and water into soils. This model was also applicable to infiltration from a trickle source. The equation describing the two-dimensional transient transfer of solutes by diffusion and convection into unsaturated, homogeneous, isotropic, and stable porous media was solved by the finite difference method of Brandt et al. (1971).

Other complex mathematical models have been developed by Ben-Asher et al. (1978), Philip and Forrester (1975), Warrick and Lemon (1974), and Raats (1971). Several of these have been validated for field and laboratory testing in uniform soils (Mostaghimi et al. 1981a,b; Levin et al. 1979b; Merrill et al. 1978; and Bresler et al. 1971). These models are not readily adaptable when root water uptake is considered. Also, they require extensive mathematical skills to use.

There are several simulation languages available which simplify the task of writing simulation programs for a variety of different types of models. A few of these languages are identified by the following acronyms: SIMSCRIPT, GASP, MIDAS, SIMPAC, MIMIC, DYNAMO, SIMULATE, CSMP (Hillel, 1977) and ACSL (Morris and Hillel, 1983). Among these simulation languages Continuous System Simulation Program (CSMP) developed by Brennan and Silberberg (1968) is considered the most versatile and is widely used for simulating phenomena specified by a differential equation or by a set of differential equations with known boundary and initial conditions in systems changing with time.

Curry (1969) used S/1130 CSMP, an earlier version of S/360 CSMP (IBM Corporation, 1972) for dynamic modeling of plant growth. S/360 CSMP has been used for the solution of complex problems in the field of agronomy, engineering and biology by Armstrong and Wilson (1983), Morris and Hillel (1983), Carter, et al. (1982), Belmans, et al. (1979), Edwards, et al. (1979), de Wit, et al. (1978), Beese, et al. (1977), Hillel (1977), Hillel, et al. (1975a,b,c), van der Ploeg (1974), van der Ploeg and Benecke (1974), Beek and Frissel (1973), de Wit and van Keulen (1972), Bhuiyan et al. (1971), and Wierenga and de Wit (1970).

Armstrong and Wilson (1983) used CSMP to predict soil moisture flow from a trickle source in stratified bare soils. Field tests were conducted in a Lakeland sand and in two typical Piedmont soil profiles in South Carolina. The application rates ranged from 3.6 to 17.1 litres per hour. The volume of water applied ranged from 31 to 237 litres. They concluded that in all three of the soils tested, the shape and size of the wetted zone is more a function of the amount of water applied than of the rate of application, at least within the range of rates and volume tested. This was true in both field tests and simulations of Lakeland sand and in field tests of Cecil sandy loam and Hiwasee sandy loam. However, the application rate had a large effect on simulations with Cecil sandy loam, that is, the higher application rate resulting in more lateral movement and less downward movement.

2.2.4 Simulation of Water Extraction by Plant Roots

The distribution of roots in the soil is uneven. The root system explores a large volume of soil in search of water and nutrients. The development of the root system is sensitive to the method of application of irrigation. Water is absorbed mainly by the growing root tip (Westwood, 1978). Roots will turn and follow water in the soil when they are in direct contact or in very close proximity to water (Hunter and Kelly, 1946).

Water influences root systems in three general ways: (1) direction of root growth; (2) lateral extent and depth of penetration; and (3) relative weight of tops and roots. When the upper portion of the root zone is kept moist, most water used consumptively by the plant will be removed from the soil near the surface (Hansen et al., 1980). This may be due to the fact that more roots normally grow near the surface.

The effect of five irrigation treatments, applied for the four-year period on root distribution and water uptake from different depths of the 0-1.8 m profile, has been investigted by Levin et al. (1972). They found that most of the water extraction for evapotranspiration took place in the 0-0.6 m soil layer in all five treatments. Wetter treatments developed a higher percentage of roots in the 0-0.3 m layer. Further, they obtained the correlation of 0.944 between the relative water extraction and relative root density in each soil layer in the soil profile.

Whilloughby and Cockroft (1974) studied the root pattern of peach trees under trickle irrigation. At the end of their four-year experiment, they found the highest concentration of live roots (less than 0.5 mm dia.) within 300 mm to 600 mm from the dripper. In this zone, water was readily available and aeration was adequate. Poor aeration beneath the dripper inhibited root growth there; in fact, some roots were killed.

The idea of using an extraction function to calculate water uptake by plant roots has existed since at least the early 1960's (Belmans et al., 1979; van Bavel et al., 1968a,b; Whisler et al, 1968; Rose and Stern, 1967; Gardner, 1960, 1964; Gardner and Ehlig, 1962). The model developed by Gardner (1960) considers a root to be an infinitely long cylinder of uniform radius and water absorbing properties. The steady state soil water flow equation was then solved analytically assuming radial flow, and various water potential distributions surrounding the idealized root were calculated.

Molz and Remson (1970) suggested that it is not practical to develop models for water flow in soil containing roots, if flow to each individual rootlet of a complete root system must be considered. The detailed geometry of the root system is practically impossible to measure and is time dependent. In addition, the water permeability of a root system varies with position along the root (Kramer, 1969). Consequently, most of the root extraction functions have been developed using a macroscopic as opposed to a microscopic approach (Molz, 1981).

Feddes (1981) after reviewing the literature, concluded that the root water uptake depends, among others, on a number of factors such as soil hydraulic conductivity, rooting depth, rooting density, root distribution, soil moisture pressure head, demand set by the atmosphere (potential transpiration) on the plant system and the presence of water table. The enumeration indicates that it is not simple to model water uptake by roots, or to generalize on the effect of a single modification of the root zone.

Molz and Remson (1970, 1971) derived mathematical models to describe water movement to the plant roots. They suggested that the Richards equation be combined with a sink term representing water extraction by plant roots. The sink term may depend on space, time, water potential, water content, or a combination of these variables.

Generally, in a uniform soil, greater root development takes place in the upper layers of the soil than elsewhere. This influences the pattern of moisture extraction from the soil profile by the plant. For irrigation regimes, when soil moisture is maintained at high level one can use an empirical rule that 40 percent, 30 percent, 20 percent and 10 percent of the total transpiration occurs from each successive quarter of the root zone (Pair et al., 1975; Withers and Vipond 1974). Molz and Remson (1970) used the empirical rule to develop a water uptake term as given below:

$$RWE(Z) = -\frac{1.6T_{av}}{L_r^2} Z + \frac{1.8T_{av}}{L_r} \quad 0 \leq Z \leq L_r \qquad ....(2.1)$$

where $RWE(Z)$ = root water extraction, mm

Z = vertical distance positive downward, m

L_r = vertical length of root system, m

T_{av} = average transpiration, mm.

They used the experimental data of Gardner and Ehlig (1962) to show reasonable agreement with the computed results. Molz and Remson (1971) accounted for the water diffusivity, transpiration and root distribution function of Gardner (1964) to develop the following extraction term:

$$S(Z,\theta) = \frac{R_e(Z)\ D(\theta)}{\int_0^{L_r} R_e(Z)\ D(\theta)\ dZ} T_{av} \qquad ....(2.2)$$

where $RWE(Z,\Theta)$ = root water extraction, mm

$R_e(Z)$ = length of roots, $m.m^{-3}$

$D(\Theta)$ = soil water diffusivity, $m^2.d^{-1}$.

Feddes et al. (1974) assumed the rate of water uptake is proportional to the hydraulic conductivity and the potential difference between the roots, ψ_r, and the surroundings, ψ. According to this approach the sink term was expressed as

$$RWE = - K(\psi_r - \psi)/b \qquad ....(2.3)$$

where RWE = root water extraction, mm

K = unsatuarated hydraulic conductivity of soil, $m.d^{-1}$

1/b = empirical constant, known as root effectiveness function, representing the geometry of flow, and is directly proportional to the specific area (total area per unit bulk volume) of the soil root interface and inversely proportional to the impedance (the ratio of thickness to the hydraulic conductivity) of the soil root interface, m^{-2}.

An alternate expression based on soil moisture content was developed by Feddes et al. (1976). They assumed that under drier than wilting point (1500 kPa) and wetter than some anaerobiosis point (about 5 kPa) conditions, there was no water uptake by the plant. Between this anaerobiosis point and some moisture content where the water becomes limiting to plant growth, the water uptake was constant at a maximum rate (PET). It was also observed that the anaerbiosis point is very difficult to define, but the soil aeration characterized by oxygen diffusion rate (ODR) can be used for the estimation of this point. On this basis, Feddes et al. (1976) reported the values of the anaerobiosis point for various soils. The sink term with this approach was given by:

$$RWE(\theta) = RWE_{max} \frac{\theta - \theta_w}{\theta_d - \theta_w} \qquad \theta < \theta < \theta$$

....(2.4)

$$= RWE_{max} \qquad \theta_d \leq \theta \leq \theta_{an}$$

where $RWE(\theta)$ = root water extraction, mm

θ_w = moisture content at the wilting point, $m^3.m^{-3}$

θ_{an} = moisture content at the anaerobiosis point, $m^3.m^{-3}$

θ_d = moisture content at some point near the anaerobiosis point where the RWE was maximum, $m^3.m^{-3}$

RWE_{max} = maximum root water extraction, mm.

2.5 Estimation of Potential Evapotranspiration

Lake and Broughton (1969) investigated the irrigation water requirements of crops in southwestern Quebec using an evapotranspiration model and budgeting method. According to the evapotranspiration model:

$$PET = DL_m\ a\ (T/180) * 25.4 \qquad ....(2.5)$$

where PET is the potential evapotranspiration per month, mm;

DL_m is the mean daylength for the month divided by the the mean annual daylength, and

a is the coefficient dependent on geographic and climatic region,

T is the mean monthly temperature in °C.

The budget model is expressed as

$$SMC_i = SMC_{i-1} - PET + Rain \qquad \ldots.(2.6)$$

where SMC_i is the soil moisture content for the ith day.

They concluded that the models gave good estimates of deficits. The calculations of the potential evapotranspiration using the mathematical model are based on the assumption that the rate of evapotranspiration is not significantly affected before one-half of the water held in the soil between field capacity and permanent wilting point is depleted. This assumption was based on the findings of Holmes and Robertson (1963) that actual evapotranspiration equals the potential rate when soil is at or near field capacity, and the effect of soil moisture depletion on the rate of evapotranspiration is dependent on soil type. However, some of the researchers have found that actual evapotranspiration rate varied linearly with the amount of available moisture (Ayers, 1965). According to Baier and Robertson

(1967) this linear relationship does not hold for the entire range of available moisture and climatic demands. For this reason the soil-water budgeting model, developed by Verma and Whiteley (1981) for the climatic conditions of Southern Ontario, uses the non-linear variation for simulating irrigation need.

Bhattacharya (1977) developed a model for estimation of AET using PET values estimated from Russelo et al. (1974) and percentage of available water (AW) before evapotranspiration. The equation is represented as

$$AET = -0.2285 + 0.4753 * PET + 0.019 * AW \qquad \ldots(2.7)$$

The equation has two limitations. First, the computed AET becomes negative when both PET and AW are either zero or have very low magnitude; secondly, it will estimate AET in excess of PET, when the latter is less than 3.5167 mm at AW of 100 percent. The top layer of soil usually contains less than 100 percent of AW. Therefore, the use of this equation to calculate AET during simulation will cause an error.

Most researchers suggest that the equation given by Penman (cf. Hansen et al. 1980) for calculating the evapotranspiration (ET) can be used if the necessary data for its use are available. Since the many detailed climatic measurements needed are seldom available, some less precise means of estimating ET, such as those listed by Baier and Robertson (1966), are frequently used.

Baier and Robertson (1965) presented a technique for estimating latent evaporation from simple meteorological observations and astronomical data readily available from tables which include maximum and minimum air temperatures, and solar energy at the top of the atmosphere. The values of latent evaporation so obtained can be converted to potential evapotranspiration (PET) using the conversion factor for an irrigated field as defined by Holmes and Robertson (1957). The values of PET calculated to cover all parts of Canada were published by agriculture Canada (Russelo et al., 1974).

2.6 Method of Irrigation Application

Mostaghimi et al. (1981b) investigated the effect of pulsed trickling on the moisture distribution patterns in heavy soils. They conducted experiments on undisturbed samples of a Drummer silty clay loam soil located in Illinois. The discharge rates ranging from 1 to 8 litres per hour with a total volume of 16 litres were used for both the continuous and pulsed irrigation treatments. The simulation model proposed by Bresler (1975) was used to evaluate the laboratory results where it was assumed that the soil was a stable, isotropic, and homogeneous porous medium and Darcy's law was applied to both saturated and unsaturated zones. They found that the agreement between laboratory results and those calculated by the simulation model was quite good. Also, the pulsed irrigation resulted in a significant reduction in water loss below the soil profile in comparison to continuous treatment.

Zur (1976) compared soil water distribution between continuous and pulse irrigation application in a homogeneous soil column under laboratory conditions. He found that the volumetric soil water content distribution and the rate of advance of the wetting front in the soil columns were behaving as if the time averaged water application rate was being applied continuously.

Levin et al., (1979b) worked on the discharge rate and compared the effects of continuous and intermittent water application from a point source on sandy soils. They concluded that a low application rate of 1 litre per hour can be replaced by a higher discharge rate of 2 litres per hour with intermittent water application.

CHAPTER III

DEVELOPMENT AND SOLUTION OF THE MODEL

3.1 Description of the Problem

To design a drip irrigation system, information on the soil moisture distribution appropriate to the situation is necessary. It is not practical to collect information for each design problem in the field. Simulation models can be employed to generate data for meeting the needs of a designer. Some of the problems faced in the field are listed below:

1. Soil is neither homogeneous nor isotropic.

2. Soil moisture planes develop and water table fluctuations occur due to rainfall, root water extraction (RWE), evaporation and drainage.

3. Roots and weeds change the pore space and interconnecting pores with time.

4. Due to cultural practices such as the application of herbicides and fertilizers, traffic, tillage and irrigation, the infiltration characteristics do not remain constant.

5. The soil-water content with respect to the depth and the distance from an emitter or a tree does not remain constant due to irrigation and rainfall.

6. Timing of irrigation application, temperature, wind velocity, depth of water table, initial soil moisture content after rainfall or irrigation, and presence of stones affect the soil moisture

distribution in the soil matrix.

Since the initial and boundary conditions are usually not constant and the soil properties change with space and time, the prediction of soil water movement is highly complicated under field conditions.

3.2 Assumptions

The problem of soil-moisture from a drip source considering water uptake by a crop was studied with the following assumptions:-

1. The soil is homogeneous.
2. Soil properties do not change with time.
3. Soil does not shrink or swell with a change in moisture content.
4. Isothermal conditions prevail during the water flow to plant roots.
5. No water is stored by the tree and surrounding vegetation.
6. Root water extraction is equal to actual evapotranspiration.
7. The roots are distributed throughout the potential root volume.
8. Hydraulic conductivity is a single valued function of the moisture content.
9. There is no overlap between the wetted area of adjacent emitters.
10. Initial soil moisture content is evenly distributed in soil planes.

3.3 Theoretical Development

The theory for transient, isothermal flow of water in a non-swelling soil can be described by a combinition of two equations:

(1) Darcy's law, which states that the flux of water (q) is proportional to, and in the direction of, the driving force which is the effective potential gradient:

$$q = - K \nabla \emptyset \qquad \text{....(3.1)}$$

where

$\emptyset$ is the hydraulic potential, which is the sum of the matric potential (ψ) and the gravitational potential (Z).

K is the hydraulic conductivity, which in the unsaturated soil can be expressed as a function of water content (θ), or matric potential (ψ).

∇ is the del operator

The hydraulic potential can be expressed as

$$\partial \theta = \psi - Z \qquad \text{....(3.2)}$$

where

Z is the gravitational head expressed as depth below the soil surface.

(2) The continuity equation, which states that the time (t) rate of change of water content in a volume element of soil must equal the

divergence of the flux:

$$\partial\theta/\partial t = -\nabla\cdot q \qquad \ldots.(3.3)$$

By combining Equations 3.1 and 3.3, the general soil water flow equation is obtained as:

$$\partial\theta/\partial t = \nabla.(K\nabla\theta) \qquad \ldots.(3.4)$$

which in one-dimensional form becomes

$$\frac{\partial\theta}{\partial t} = \frac{\partial}{\partial X}(K\frac{\partial\psi}{\partial X}) \qquad \ldots.(3.5)$$

If the flow system is considered vertical and the Z direction is taken as positive from the soil surface downward, Equation 3.4 becomes

$$\frac{\partial\theta}{\partial t} = \frac{\partial}{\partial z}(K\frac{\partial(\psi - z)}{\partial z}) \qquad \ldots.(3.6)$$

Considering irrigation from a point source (source) and root water extraction (RWE), Equation 3.4 can be presented as:

$$\frac{\partial\theta}{\partial t} = \frac{\partial}{\partial x}(K\frac{\partial\psi}{\partial x}) + \frac{\partial}{\partial z}(K\frac{(\psi - z)}{\partial z}) - \text{RWE} + \text{source} \qquad \ldots.(3.7)$$

To estimate the RWE, the macroscopic approach is frequently considered due to its simplicity (Feddes et al., 1976, 1974; Nimah and Hanks, 1973a,b; Molz and Remson, 1970; Whisler et al., 1968). According to this approach the RWE depends on the moisture content and the depth of root zone.

In simulating the soil moisture distribution from a trickle source it is necessary to estimate the daily PET. Then AET which is assumed to be equal to RWE, can be calculated based on the moisture content in the soil. The PET is the maximum amount of water that will leave the soil system by ET when there is sufficient supply of water. The daily PET can be estimated using Tables published by Agriculture Canada (Russelo et al., 1974). This requires data on minimum and maximum temperatures and the radiation index of the location. This information is is available for most of the areas of the province of Quebec.

The PET rate increases from sunrise, reaches a maximum rate at about midday and then decreases until sunset. The rate of PET can be represented by a sine function (Hillel, 1977). However, during cloudy periods, this function is not applicable. The irrigation system design is usually based on the premise that evapotranspiration will occur during the day time. Thus, the assumption was made that during the simulation run, there were no clouds during daylight hours. Under this assumption PET with respect to t can be presented as

$$PETR(t) = PETR_{max} \sin(\pi * t/LD) \quad \ldots.(3.8)$$

where $PETR(t)$ is the PET rate with respect to the time of day from sunrise ($mm.s^{-1}$), LD is the length of the day (s), and t is the time from sunrise (s), $PETR_{max}$ is the maximum midday PET rate ($mm.s^{-1}$).

Upon integration with respect to t, Equation 3.8 becomes

$$PET = PETR_{max} \sin(\pi * t / LD)dt \qquad ....(3.9)$$

When t=LD, Equation 3.9 becomes

$$PET = (2\ LD * PETR_{max}) / \pi \qquad ....(3.10)$$

and from Equation 3.10 maximum midday rate of PET can be calculated as

$$PETR_{max} = (PET * \pi) / (2\ LD) \qquad ....(3.11)$$

The amount of moisture depleted from the root zone is a function of its depth. Under supplementary irrigation conditions, the roots of the tree grow into the potential soil volume including the soil volume irrigated by the emitter. Due to the presence of weeds in the orchards, the soil surface is covered with vegetation. Therefore, in these orchards the RWE patterns would be similar to those obtained under a crop cover. Figure 3.1 approximates the RWE pattern developed by Shockley (cf. Pair et al. 1975) from an examination of

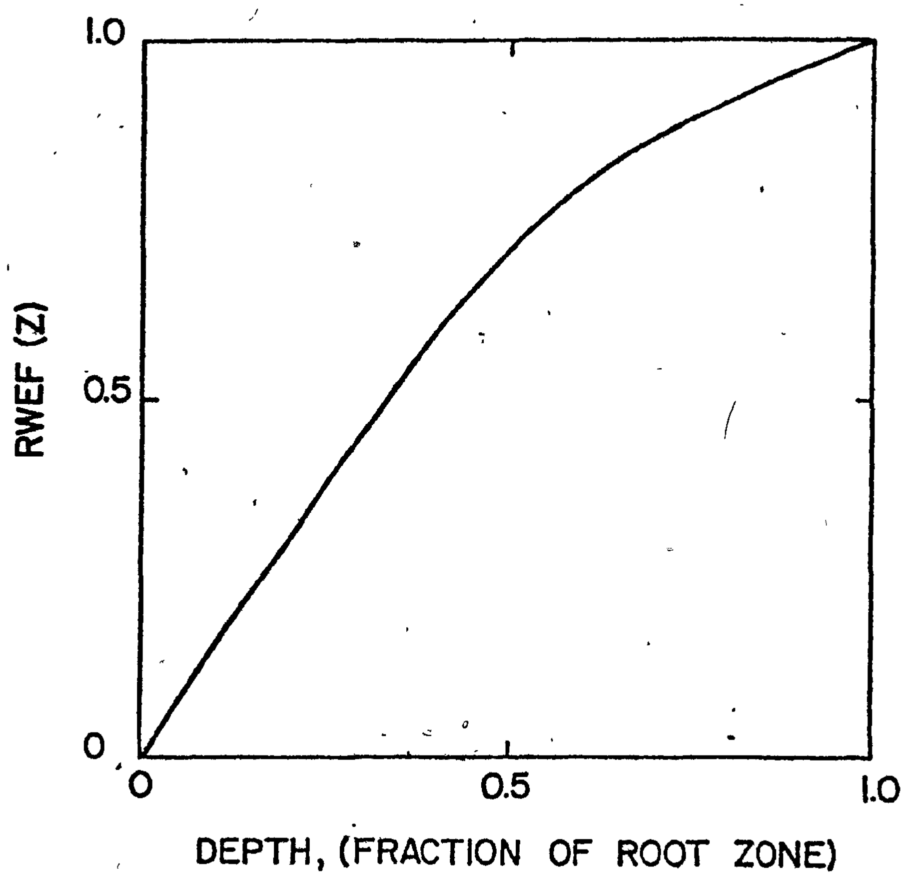

Figure 3.1. Root water extraction as a function of root depth.

soil-moisture extraction studies in the western United States.

The relationship of RWE with respect to the soil water content was developed by Feddes et al. (1976). They assumed that under conditions drier than wilting point (θ_w) (1500 kPa) and wetter than some anaerobiosis point (θ_{an}) (about 5 kPa) there was no water uptake by the roots. Between this anaerobiosis point and some moisture content (50 percent available soil moisture, θ_r) where water becomes limiting to plant growth, the water uptake was constant at maximum rate (PET). However, in this study it was assumed that anaerobiosis did not occur due to the occurrence of a temporary saturation under the emitter. Based on this assumption the RWE is considered to occur at the rate of the potential evapotranspiration between θ_s (soil moisture content at saturation) and θ_r. The relationship between RWE and soil moisture content is presented in Figure 3.2.

3.4 Solution Technique

To convert the mathematical model into a form soulble by a digital computer, the differential equations of water transport in the soil are cast into explicit algebraic equations, involving the values of the variables as they exist at discret points in space and time. Under this method, a mesh center grid system was selected. A finite cylindrical soil volume was divided into small concentric rings of width R and depth Z. This is shown in Figure 3.3. The center of all rings is a vertical line which passes through the center of the soil cylinder and the emitter on the soil surface.

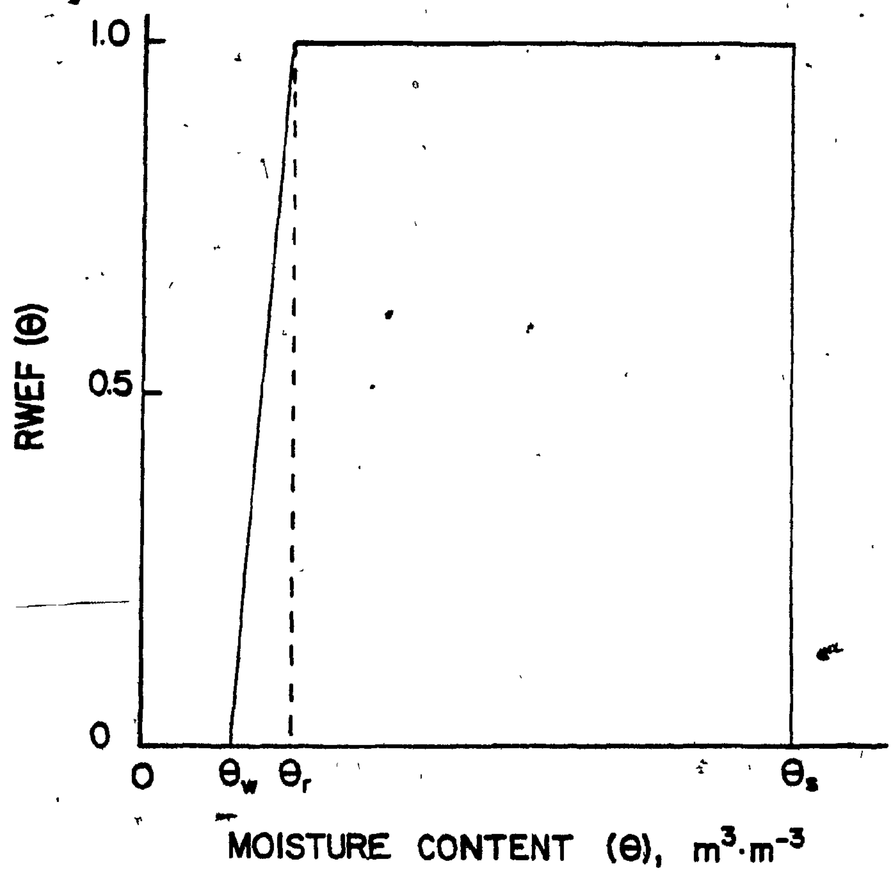

Figure 3.2. Root water extraction as a function of soil moisture content.

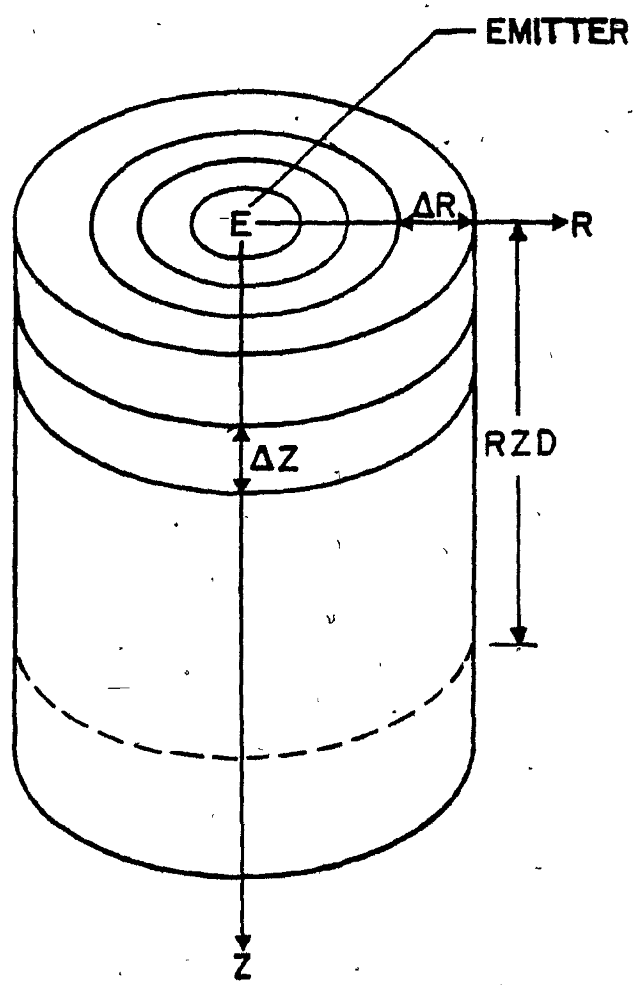

Figure 3.3. Schematic view of the soil cylinder for simulation.

The initial soil moisture content is specified at the nodal points. Irrigation is applied at the inner ring (1,1) of the finite soil cylinder. When the discharge rate exceeds the infiltration rate, the excess water runs laterally to the next ring (1,2). Similarly, excess water available on ring (i,j) after infiltration moves to the next adjacent ring (i,j+1). The index i (i=1,2.... imax) is measured along the Z-axis which is positive downward. The index j (j=1,2.... jmax) is measured along the R-axis. The imax and jmax represent the maximum number of soil rings along Z-axis and R-axis respectively.

The volume of the soil ring is calculated as

$$v_{i,j} = (R^2_{j+1} - R^2_j) * \Delta Z_i \qquad ....(3.12)$$

where $v_{i,j}$ = Volume of each soil ring, m^3

R_j and R_{j+1} = inner and outer radii of a soil ring, m

ΔZ_i = thickness of each soil ring, m.

The first step is to calculate $RWER_{i,j}$ rate for each of the soil ring as a function of θ , Z and t as

$$RWER_{i,j} = RWEF(\theta) \times RWEF(Z) \times PETR(t) \times A_{i,j} \qquad ....(3.13)$$

where $RWER_{i,j}$ is the volumetric rate of RWE from ring (i,j), $L.s^{-1}$; RWEF(θ) is RWE as a function of θ, calculated from θ versus AET/PET relationship given in Figure 3.2, fraction; RWEF(Z) is the RWE as a function of depth calculated using Figure 3.1 and the thickness of the ring, fraction; PETR(t) is the rate of ET at the time of simulation after sunrise, $mm.s^{-1}$; $A_{i,j}$ is the area of ring (i,j) as viewed from the soil surface, m^2.

The second step is to calculate the rate of flow (Q) across each boundary of ring (i,j). The schematic view of the ring (i,j) and its adjoining rings used for simulation presented in Figure 3.4. The flow rate ($m^3.s^{-1}$) across the boundaries between rings (i,j-1) and (i,j); (i,j) and (i,j+1); (i-1,j) and (i,j); and, (i,j) and (i+1,j) is respectively presented by the equations:

$$Q_{i,j-1} = - K_{i,j-1}\ (H_{i,j} - H_{i,j-1})/[(R_j + R_{j-1})/2](2\pi R_j)(\Delta Z_i) \quad \ldots(3.14)$$

$$Q_{i,j+1} = - K_{i,j+1}\ (H_{i,j+1} - H_{i,j})/[(R_j + R_{j+1})/2](2\pi R_j)(\Delta Z_i) \quad \ldots(3.15)$$

$$Q_{i-1,j} = - K_{i-1,j}\ (H_{i,j} - H_{i-1,j})/[(Z_i + Z_{i-1})/2](\pi(R^2_{j+1} - R^2_j)) \quad \ldots(3.16)$$

$$Q_{i+1,j} = - K_{i+1,j}\ (H_{i+1,j} - H_{i,j})/[(Z_i + Z_{i+1})/2](\pi(R^2_{j+1} - R^2_j)) \quad \ldots(3.17)$$

where subscripts i and j refer to the position of the ring,

H = the total potential as a function of θ and Z, m

K = the hydraulic conductivity as a function of θ, $m.s^{-1}$

R_j = inside radius of ring (j), m

Z_i = depth from soil surface to the top of soil ring (i), m

θ = volumetric moisture content, $m^3.m^{-3}$.

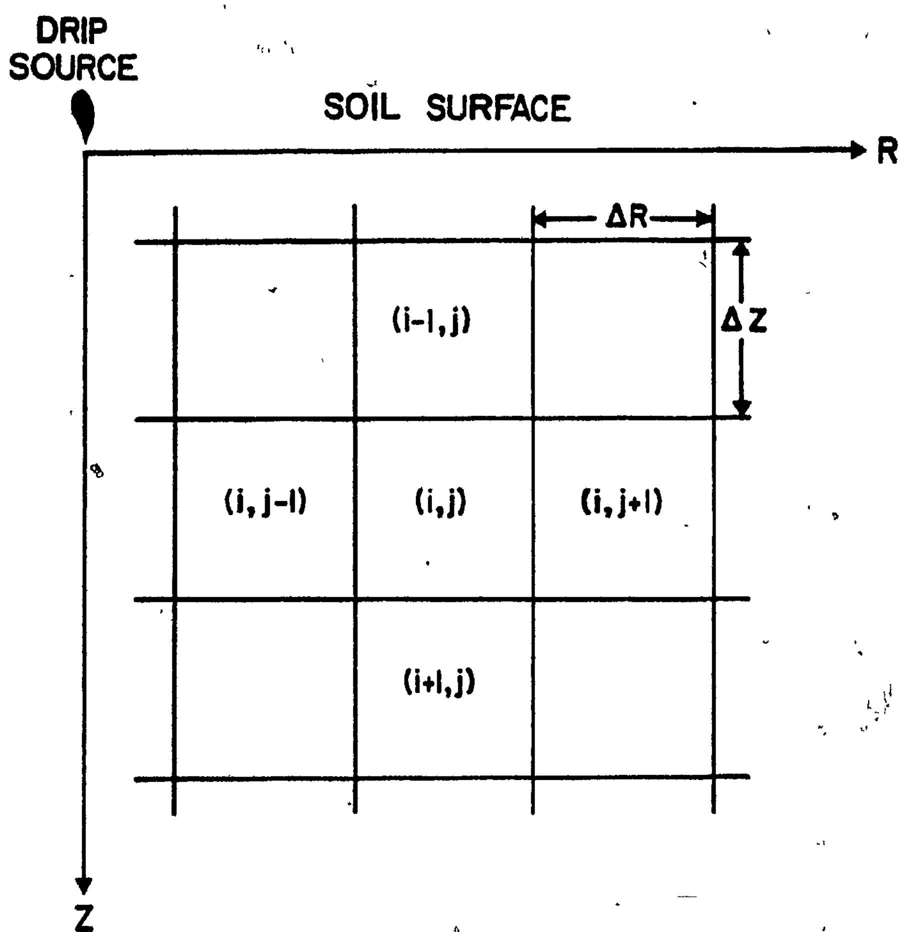

Figure 3.4. Schematic view of a ring (i,j) for simulation.

$$K_{i,j-1} = (K_{i,j-1}\, v_{i,j-1} + K_{i,j}\, v_{i,j})/(v_{i,j-1} + v_{i,j}) \quad \ldots.(3.18)$$

$$K_{i,j+1} = (K_{i,j}\, v_{i,j} + K_{i,j+1}\, v_{i,j+1})/(v_{i,j} + v_{i,j+1}) \quad \ldots.(3.19)$$

$$K_{i-1,j} = (K_{i-1,j}\, v_{i-1,j} + K_{i,j}\, v_{i,j})/(v_{i-1,j} + v_{i,j}) \quad \ldots.(3.20)$$

$$K_{i+1,j} = (K_{i,j}\, v_{i,j} + K_{i+1,j}\, v_{i+1,j})/(v_{i,j} + v_{i+1,j}) \quad \ldots.(3.21)$$

$Q_{i,j-1}$ = flow rate across interface of (i,j-1) and (i,j), m^3s^{-1}
$Q_{i,j+1}$ = flow rate across interface of (i,j) and (i,j+1), m^3s^{-1}
$Q_{i-1,j}$ = flow rate across interface of (i-1,j) and (i,j), m^3s^{-1}
$Q_{i+1,j}$ = flow rate across interface of (i,j) and (i+1,j), m^3s^{-1}
$K_{i,j-1}$ = average hydraulic conductivity of (i,j-1) and (i,j), $m.s^{-1}$
$K_{i,j+1}$ = average hydraulic conductivity of (i,j) and (i,j+1), $m.s^{-1}$
$K_{i-1,j}$ = average hydraulic conductivity of (i-1,j) and (i,j), $m.s^{-1}$
$K_{i+1,j}$ = average hydraulic conductivity of (i,j) and (i+1,j), $m.s^{-1}$.

The third step is to calculate net flow rate per unit volume of soil in each of the rings. The net flow rate into ring (i,j), according to its position is given below:

(1) $1 < i < imax$, $1 < j < jmax$

$$\Delta Q_{i,j} = Q_{i,j-1} - Q_{i,j+1} + Q_{i-1,j} - Q_{i+1,j} - RWER_{i,j} \quad \ldots.(3.22)$$

(2) $i = 1,\ j = 1$

$$\Delta Q_{i,j} = Q_e - Q_{i,j+1} - Q_{i+1,j} - RWER_{i,j} \qquad \text{....(3.23)}$$

(3) $1 < i < imax,\ j = 1$

$$\Delta Q_{i,j} = Q_{i-1,j} - Q_{i+1,j} - Q_{i,j+1} - RWER_{i,j} \qquad \text{....(3.24)}$$

(4) $i = imax,\ j = jmax$

$$\Delta Q_{i,j} = Q_{i-1,j} - Q_{i,j+1} - RWER_{i,j} \qquad \text{....(3.25)}$$

(5) $i = 1,\ 1 < j < jmax$

$$\Delta Q_{i,j} = Q_{i,j-1} - Q_{i,j+1} - Q_{i+1,j} - RWER_{i,j} \qquad \text{....(3.26)}$$

(6) $i = imax,\ 1 < j < jmax$

$$\Delta Q_{i,j} = Q_{i,j-1} + Q_{i-1,j} - Q_{i,j-1} - RWER_{i,j} \qquad \text{....(3.27)}$$

(7) $i = 1,\ j = jmax$

$$\Delta Q_{i,j} = Q_{i,j-1} - Q_{i-1,j} - RWER_{i,j} \qquad \text{....(3.28)}$$

(8) $1 < i < imax,\ j = jmax$

$$\Delta Q_{i,j} = Q_{i,j-1} + Q_{i-1,j} - Q_{i+1,j} - RWER_{i,j} \qquad \text{....(3.29)}$$

(9) $i = imax,\ j = jmax$

$$\Delta Q_{i,j} = Q_{i,j-1} + Q_{i-1,j} - RWER_{i,j} \qquad \text{....(3.30)}$$

where $\Delta Q_{i,j}$ = net flow rate into ring (i,j), m^3s^{-1}

Q_e = emitter discharge rate, $m^3 s^{-1}$

$RWER_{i,j}$ = root water extraction rate, $m^3 s^{-1}$.

The rate of change in volumetric moisture content per unit volume of soil in ring (i,j) is calculated by the following equation:

$$DELSTO_{i,j} = [\Delta Q_{i,j} / (\pi(\Delta Z_i)(R^2_{j+1} - R^2_j))] \qquad ....(3.31)$$

where $DELSTO_{i,j}$ is the rate of change in volumetric moisture content per unit volume of soil in ring (i,j), $m^3.m^{-3}.s^{-1}$.

Since the soil moisture migration from a point source is a non-steady process, $DELSTO^{i,j}$ is not constant. It is a function of time and may change from one second to the another. When θ_{in} is known the soil moisture content at any time later (θ_t) can be calculated as

$$\theta_t = \theta_{in} + \int_{t=0}^{t} DELSTO_{i,j}\, dt \qquad ....(3.32)$$

As with ring (i,j), any ring in the flow region may be treated. Using the initial moisture content (an input to the program) to calculate hydraulic conductivity and total potential, the Θ is calculated for each ring (i,j), beginning with (1,1) nearest to the emitter and ending with (imax,jmax). CSMP then finds the updated moisture content. The updated moisture content values become the new initial conditions and the process continues for a second time increment, Δt. This process is repeated to the time specified to stop simulation.

3.5 Initial and Boundary Conditions:

At $t = 0$

$$\theta = (\theta_{in})_i \qquad 0 \leq R \leq R_{max} \qquad Z_i \leq Z \leq Z_{i+1} \qquad \ldots.(3.33)$$

Where i = 1 to imax

At $t > 0$

$$\partial\theta/\partial R = 0 \text{ for } \qquad R = R_{max}; \qquad 0 \leq Z \leq Z_{max} \qquad \ldots.(3.34)$$

$$\partial\theta/\partial Z = 0 \text{ for } \qquad Z = Z_{max}; \qquad 0 \leq R \leq R_{max} \qquad \ldots.(3.35)$$

$$\theta_W \leq \theta \leq \theta_s \text{ for } \qquad 0 \leq R \leq R_{max}; \qquad 0 \leq Z \leq Z_{max} \qquad \ldots.(3.36)$$

3.6 Actual Migration Time

The termination of irrigation application occurs earlier when water is applied at higher rates when compared with the lower rates of application for the same amount of irrigation water. For example: 12.0 L of irrigation water are applied at the the rate of 2, 4, and 6 L/h with irrigation termination occuring at 6, 3 and 2 hours respectively. If the comparison for the soil moisture migration is made without considering the time period of irrigation application, the potential migration to total irrigation water would be inconsistent at different discharge rates. It is, therefore, necessary to consider the migration time of total irrigation water in the soil. A concept of actual migration time of total irrigation water (AMT) is proposed.

Actual Migration Time (AMT) is defined as the time taken by the total irrigation water to migrate in the soil at some specified time. The AMT for drip irrigation at the time of termination of emitter discharge is calculated as

(a) for continuous application

$$AMT = T_{irr}/2 \qquad ....(3.37)$$

(b) for pulse application

$$AMT = T_{irr}/2 + C/4 \qquad ....(3.38)$$

where T_{irr} = time required for irrigation application, h

C = time period of pulse cycle, h.

Considering a sufficient time of redistribution of soil water after the termination of irrigation, an arbitrary AMT (T_a) of 12-hour was selected for this study. The time required for simulation or observation (T_{obs}) can be calculated as

$$T_{obs} = T_a - AMT + T_{irr} \qquad ....(3.39)$$

The AMT and the simulation time required for various irrigation periods are given in Table 3.1. Even though this criterion does not consider the changing moisture conditions during irrigation application at various rates, this seems to be a better method to compare the moisture distributions.

3.7 Method of Drip Irrigation Application

The continuous and pulse methods of drip irrigation application were considered for simulation in this study. The pulse irrigation consisted of a series of pulse cycles of 1-hour duration. Each cycle consisted of 1/2-hour operating phase followed by 1/2-hour resting phase. Thus, the pulse irrigation reduced the average rate of water application to half the rate of continuous irrigation. The time of pulse irrigation termination increased to twice the continuous irrigation for the same amount of total irrigation water. This is due to the fact that the operating phase of each pulse cycle was provided with a square wave function of time. The migration of soil moisture with pulse irrigation application was simulated with the same initial and boundary conditions and parameters as the continuous irrigation. To compare the performance of both methods and application rates giving sufficient time of soil moisture migration after termination of discharge, an arbitrary 12-hour actual migration time for the total amount of irrigation water (AMT) was selected. Therefore, in both methods of application, the simulation runs were continued after irrigation termination, to the time equivalent to the 12-hour AMT (Table 3.1).

Table 3.1. Simulation time required for 12-hour AMT for various irrigation application periods.

Method of Irrigation Application					
Continuous			Pulse (1-hour cycle)		
Irrigation time h	AMT h	Simulation time h	Irrigation time h	AMT h	Simulation time h
8.0	4.0	16.0	-	-	-
6.0	3.0	15.0	-	-	-
4.0	2.0	14.0	8.0	4.25	15.75
3.0	1.5	13.5	6.0	3.25	14.75
2.0	1.0	13.0	4.0	2.25	13.75

CHAPTER IV

EXPERIMENTAL PROCEDURE AND DATA COLLECTION

4.1 General Description

The soil water migration studies were conducted in apple orchards located near Rougemont and Rockburn both in southern Quebec. The existing drip irrigation system was designed and installed by Les Enterprises Harnois, Inc., St. Thomas, Quebec. The system served as supplemental irrigation with one emitter for each tree. The emitters were placed at the distance of about 0.3-0.35 m from each tree.

The Rougemont orchard was two years old as of 1980. The irrigation water for the system in the orchard was pumped from a pond which was filled with seepage water and runoff from heavy rainfall. The water table remained within the range of 1.0 to 2.0 metres from the ground surface, and it fluctuated due to rainfall, drainage and evapotranspiration.

The apple orchard near Rockburn was four years old as of 1981. The irrigation water for the orchard was pumped from ground water storage. The water table at this experimental site exceeded 2.0 m below ground surface.

4.2 Experimental Procedure

The experiments were conducted only on sunny days in both apple orchards. The irrigation water was applied continuously at predetermined rates and amounts. A soil probe with a diameter of 0.02 m was used to obtain soil samples for the determination of moisture contents. After rainfall the soil moisture content was considered evenly distributed with respect to the depth from soil surface throughout the young orchard. To determine initial moisture content in the soil profile, soil samples were taken at the depths of 0.0, 0.05, 0.1, 0.2, 0.3, 0.5, 0.6 and 0.9 m before the start of emitter discharge. These samples were taken at the distance of 0.8 m from an emitter. Thus, the soil volume used for the moisture migration experiment was not disturbed. The soil samples were also taken immediately after the termination of the emitter discharge at the depths of 0.0, 0.05, 0.1, 0.2, 0.3, 0.5, 0.6, 0.9 m from the soil surface and at the horizontal distances of 0.0, 0.1, 0.25 and 0.5 m from the emitter. The moisture contents were determined in the laboratory by the oven dry method.

4.3 Input Data

The basic data required for the solution of the model developed in this study are as follows:

1. Matric potential versus soil moisture content,
2. Hydraulic conductivity versus soil moisture content,
3. Root water extraction patterns with respect to depth and root zone depth,
4. Daylength and time of the day,
5. Daily potential evapotranspiration,

6. Soil moisture contents at saturation, 50 percent available moisture and wilting point,
7. Initial soil moisture contents with respect to depth, and
8. Emitter discharge rate and time of application.

4.4 Determination of Soil Properties

The soil texture was determined using hydrometer and sieve analysis methods (Lambe, 1951). The soil samples were taken from 0-0.30, and 0.30-0.60 m depths. The samples from each depth were air dried in the laboratory and mixed well for analysis. The bulk density was determined using undisturbed soil samples from the orchards. The soil moisture retention curves given in Figure 4.1 were determined by pressure-plate method.

To determine hydraulic conductivity, undisturbed samples for all the soils were obtained in soil cores of 0.1 m diameter and 0.1 m high. The samples were taken at depths of 0-0.1, 0.2-0.3, and 0.5-0.6 m. The saturated hydraulic conductivity was measured by the constant head method and calculations were made using the equation (Klute, 1965):-

$$K_s = (Q_v / (A * t))(L_s / \Delta H) \qquad \text{.... (4.1)}$$

where K_s = saturated hydraulic conductivity, $m.s^{-1}$

Q_v = volume of water that passes through the sample, m^3

A = cross-sectional area of the sample, m^2

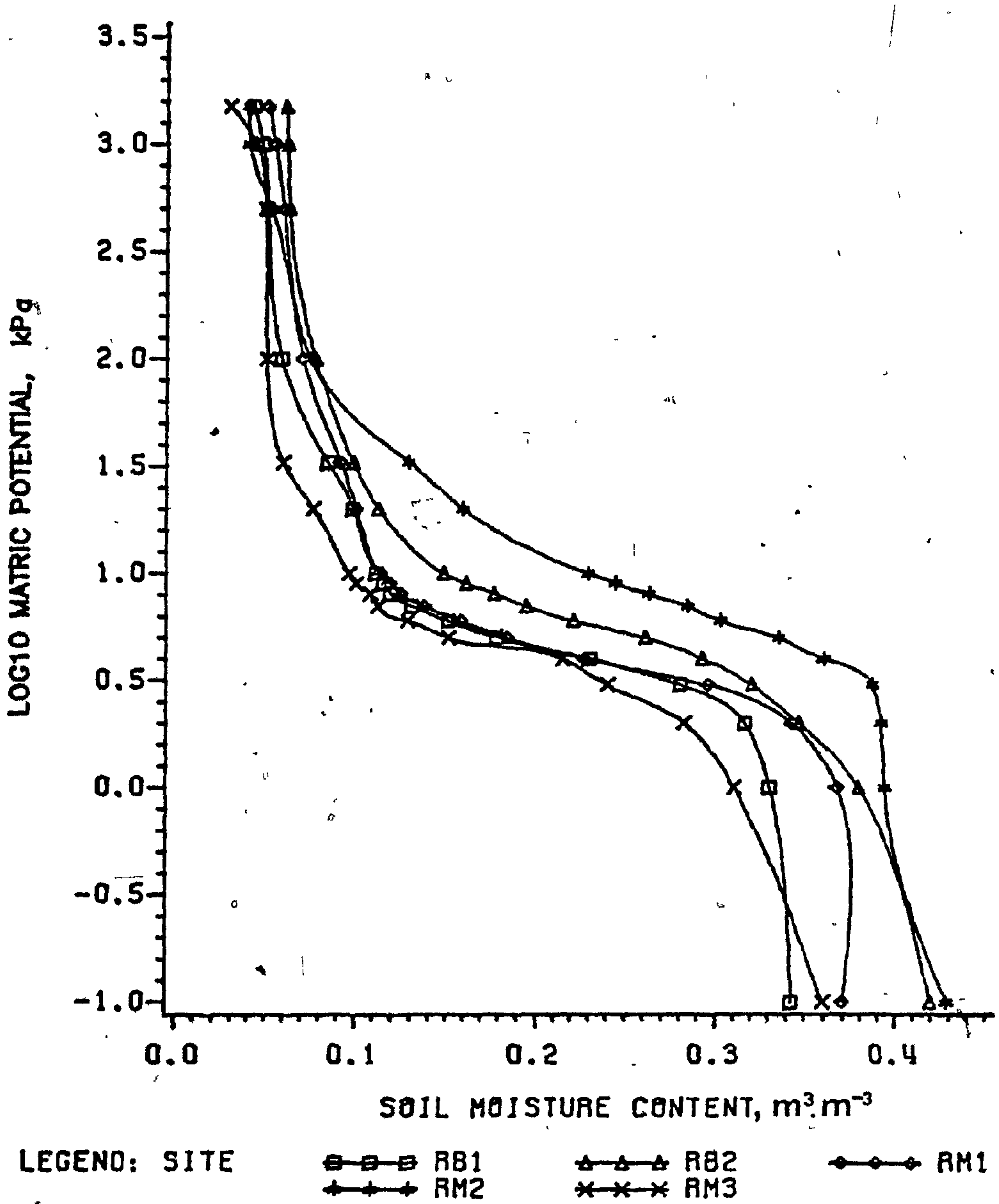

Figure 4.1. Soil moisture retention curves of the soils.

t = time, s

ΔH = hydraulic head difference across the sample, m

L_s = length of the sample, s.

The unsaturated hydraulic conductivity versus moisture content function for each soil was determined by using the method of Jackson (1972). The soil moisture characteristic function was divided into m equal moisture content (θ) increments and suction head (ψ) at each increment was determined from a moisture characteristic curve. Then at the midpoint of each increment suction head was calculated and value of hydraulic conductivity was computed according to the equation:

$$K_i = K_s\,(\theta_i/\theta_s)^c \sum_{i=1}^{m} ((2j + 1 - 2i)\,\psi_j^{-2}) / \sum_{i=1}^{m} ((2j-1)\,\psi_j^{-2}) \quad \ldots.(4.2)$$

where K_i is the hydraulic conductivity at θ_i; m is the number of increments of θ; ψ is the suction head at the midpoint of each θ increment; c is equal to 1; and, j and i are summation indices. The calculated hydraulic conductivities as a function of volumetric moisture content are given in Figure 4.2.

4.5 Estimation of Daily Potential Evapotranspiration (PET)

The daily PET was estimated from the "Agrometeorological Tables" published by Agriculture Canada (Russelo et al., 1974). The parameters required for estimation of daily PET for the model are:

1) maximum temperature,

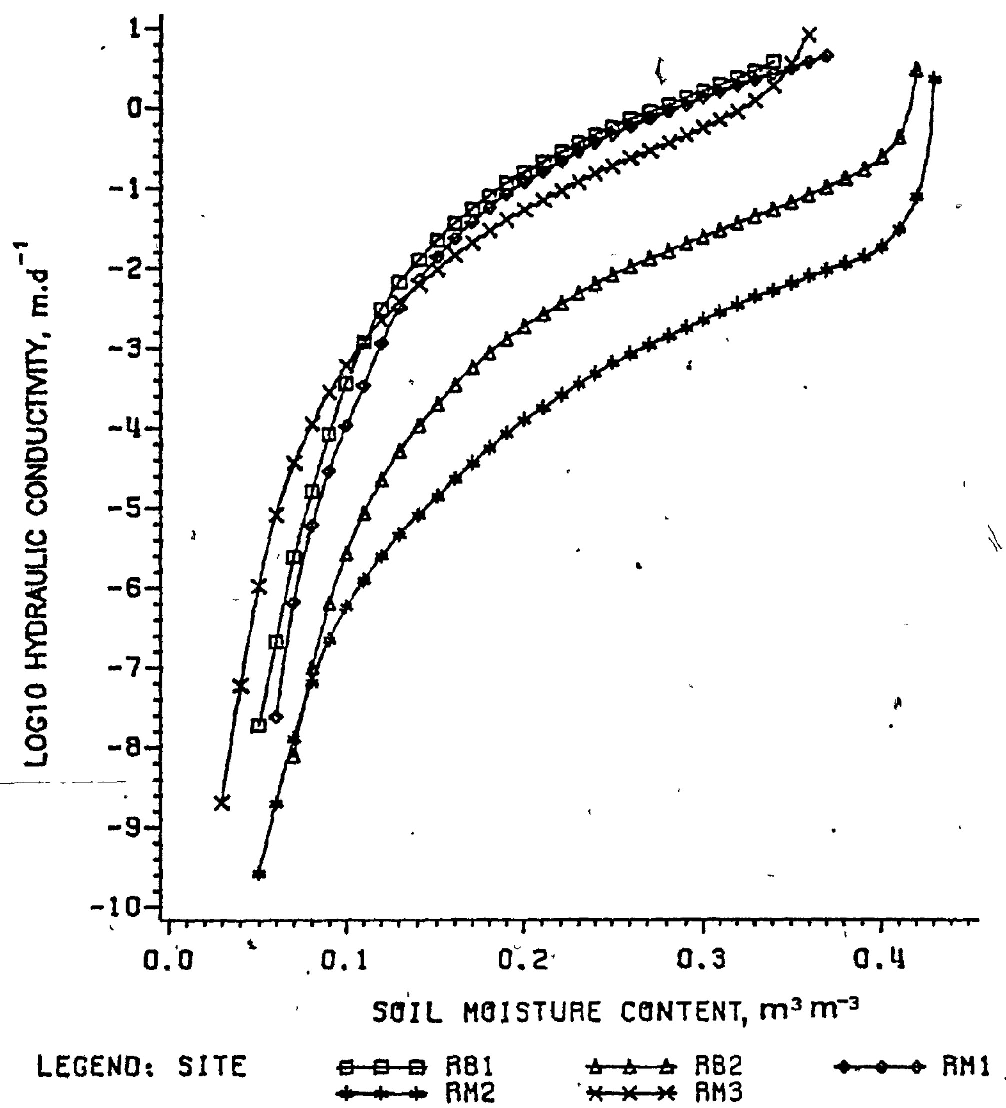

Figure 4.2. Hydraulic conductivity curves of the soils.

2) minimum temperature,

3) latitude of the experimental site.

These were obtained from Ministere de l'Environnment, Gouvernement du Quebec. The Rockburn orchard is located at 45,02' N latitude and 73,54' longitude and the Rougement orchard is located at 45,27' latitude and 73,04' longitude.

4.6 Determination of Root Zone Depth

The roots were unearthed after the completion of the experiment. The depth of the roots was determined by visual inspection.

4.7 Model Testing

The model was tested under various soils and flow conditions. The data on intial soil moisture content and some other parameters used for testing this model are presented in Table 4.1. The emitter discharge rates for each of the sites are given in Chapter 6. The physical properties of the soils are presented in Tables 4.2, 4.3, and 4.4. The basic values of of the parameters used in sensitivity analysis are given in Table 4.5.

The simulated moisture content data generated by the model were fed into a computer, and GCONTOUR procedure of the Statistical Analysis System was used to draw iso-soil moisture content curves. The figures showing soil moisure content profiles and water input along vertical and horizontal directions were drawn using GPLOT procedure of SAS.

Table 4.1. initial volumetric soil moisture contents in the soil profiles and other input parameters at the research sites

Location	Rougemont RM1	Rougemont RM2	Rougemont RM3	Rockburn RB1	Rockburn RB2
Root zone, (m)	0.36	0.36	0.48	0.60	0.60
			12 liters		
Depth (m)					
0.0	0.076	0.089	0.071	-	0.123
0.05	0.078	0.128	0.083	-	0.152
0.10	0.078	0.149	0.096	-	0.158
0.20	0.079	0.171	0.098	-	0.156
0.30	0.081	0.178	0.105	-	0.166
0.50	0.083	0.180	0.105	-	0.164
0.60	0.086	0.183	0.119	-	0.170
0.90	0.086	0.245	0.126	-	0.186
Av WRZ	0.079	0.159	0.099	-	0.159
Av BRZ	0.085	0.207	0.120	-	0.180
Av WSC	0.083	0.187	0.109	-	0.166
Date (D M Y)	24-8-80	9-7-80	13-6-81	-	2-8-1981
Time (h)	4.4	5.75	5.88	-	5.35
Daylength (h)	13.43	15.50	15.62	-	14.75
Daily PET (mm)	4.9	4.2	4.4	-	4.2

continued next page

Table 4.1 continued.....

Location	RM1	RM2	RM3	RB1	RB2
		16 liters			
Depth (m)					
0.0	0.055	0.098	0.059	0.067	0.130
0.05	0.076	0.123	0.080	0.089	0.151
0.10	0.078	0.144	0.088	0.094	0.159
0.20	0.082	0.198	0.097	0.114	0.158
0.30	0.086	0.201	0.101	0.114	0.166
0.50	0.088	0.200	0.101	0.119	0.172
0.60	0.091	0.224	0.107	0.123	0.170
0.90	0.102	0.226	0.128	0.146	0.181
Av WRZ	0.080	0.173	0.096	0.110	0.160
Av BRZ	0.092	0.223	0.115	0.137	0.177
Av WSC	0.087	0.203	0.105	0.119	0.166
Date	19-7-80	1-8-80	16-7-81	6-7-81	31-7-81
Time (h)	5.08	5.3	5.63	5.78	4.38
Daylength (h)	15.23	14.75	15.32	15.57	14.82
Daily PET (mm)	5.1	5.1	4.7	4.6	4.9

continued next page

Table 4.1 continued.....

Location	RM1	RM2	RM3	RB1	RB2
			24 liters		
Depth (m)					
0.0	0.067	-	-	0.071	-
0.05	0.078	-	-	0.096	-
0.10	0.080	-	-	0.099	-
0.20	0.080	-	-	0.106	-
0.30	0.082	-	-	0.106	-
0.50	0.086	-	-	0.106	-
0.60	0.086	-	-	0.110	-
0.90	0.098	-	-	0.116	-
Av WRZ	0.079	-	-	0.101	-
Av BRZ	0.088	-	-	0.114	-
Av WSC	0.085	-	-	0.105	-

Date	18-7-80	-	-	2-7-81	-
Time (h)	5.10	-	-	5.07	-
Daylength (h)	15.27	-	-	15.62	-
Daily PET (mm)	5.1	-	-	5.6	-

Table 4.2. Physical properties of soils existing in the orchards

Location	Texture	Sand %	Silt %	Clay %	Bulk Density $Mg.m^{-3}$
RB1	Sandy	90.8	5.9	3.3	1.65
RB2	Loamy sand	82.9	12.2	4.9	1.52
RM1	Sandy	94.7	4.9	0.4	1.61
RM2	Sandy	88.1	6.3	5.6	1.46
RM3	Sandy	98.4	1.6	0.0	1.65

Table 4.3. Saturated hydraulic conductivity of the soils

Site	No. of samples	K_s (mean) $m.d^{-1}$	Std. Dev. $m.d^{-1}$	Range $m.d^{-1}$
RB1	12	3.6576	0.5141	3.154 - 4.363
RB2	12	2.9520	0.2257	2.647 - 3.336
RM1	12	4.3488	0.6178	3.643 - 5.558
RM2	12	2.2032	0.3038	1.814 - 2.650
RM3	12	8.0208	0.7214	7.013 - 8.917

Table 4.4. Volumetric soil moisture content of the soils

Site	Saturation	FC	WP	Available Moisture	MC @ 50% Available Moisture
RB1	0.34	0.112	0.043	0.069	0.0775
RB2	0.42	0.149	0.061	0.088	0.0105
RM1	0.37	0.114	0.051	0.063	0.0825
RM2	0.43	0.230	0.041	0.189	0.1355
RM3	0.36	0.097	0.022	0.075	0.0595

Table 4.5. Basic parameters and their values used in sensitivity analysis.

Parameter	Base Value
1. Mesh size R direction	0.06 m
2. Mesh size Z direction	0.06 m
3. Hydraulic conductivity	4.35 $m.d^{-1}$
4. Discharge rate	2.0 $L.h^{-1}$
5. Total irrigation water	16.0 L
6. Root zone depth	0.36 m
7. Initial moisture content	0.085 $m^3.m^{-3}$
8. Daily PET	5.0 $mm.d^{-1}$
9. Volume of soil ring	variable
10. Time of start	2.0 h
11. Daylength	14.0 h
12. Radius of soil cylinder	0.60 m
13. Depth of soil cylinder	0.90 m

In order to calculate irrigation water input in mm, soil profile from surface to bottom of the finite soil cylinder was considered. The calculations were done as follows:

$$IRR_j = \sum_{i=1}^{imax} IRRWI_j / A_j \qquad ....(4.3)$$

where j = 1 to jmax

imax = maximum number of rings in Z-direction,

jmax = maximum number of rings in R-direction,

IRR_j = irrigation water input in soil rings (j), mm

$IRRWI_j$ = irrigation water input in soil rings (j), L

A_j = surface area of rings (j), m^2

i and j are subscripts in Z and R direction repectively.

For the details of calculations regarding water distribution, the reader is advised to refer to the computer program given in Appendix A.

CHAPTER V

DESCRIPTION OF THE COMPUTER PROGRAM

5.1 Introduction

The geometric structure of the model is shown in Figures 3.3 and 3.4 which depict a uniform soil profile of finite depth Z with root zone depth RZD and finite radius R. The soil profile is divided into IMAX rings each of thickness DELTAZ. The finite radius (R) is divided into JMAX rings each of width DELTAR.

The rate of water movement between soil rings obeys Darcy's law in finite difference form. The moisture content of a soil ring at any moment determines the hydraulic conductivity and matric potential of the soil ring. The matric potential and time after sunrise at any moment, and position of the soil ring relative to the soil surface determine the root moisture extraction from the soil ring.

The computer program was written using IBM System/360 Continuous System Modeling Program (CSMP). Apart from the formal STORAGE, DIMENSION, EQUIVALENCE, and FIXED statements, the program consists of three segments: (1) INITIAL, (2) DYNAMIC and (3) TERMINAL. These describe the computations to be performed before, during, and after each simulation run. The description of the variables and the details of the computer program, are given in appendix A. The flow chart of computer simulator is shown in Figure 5.1.

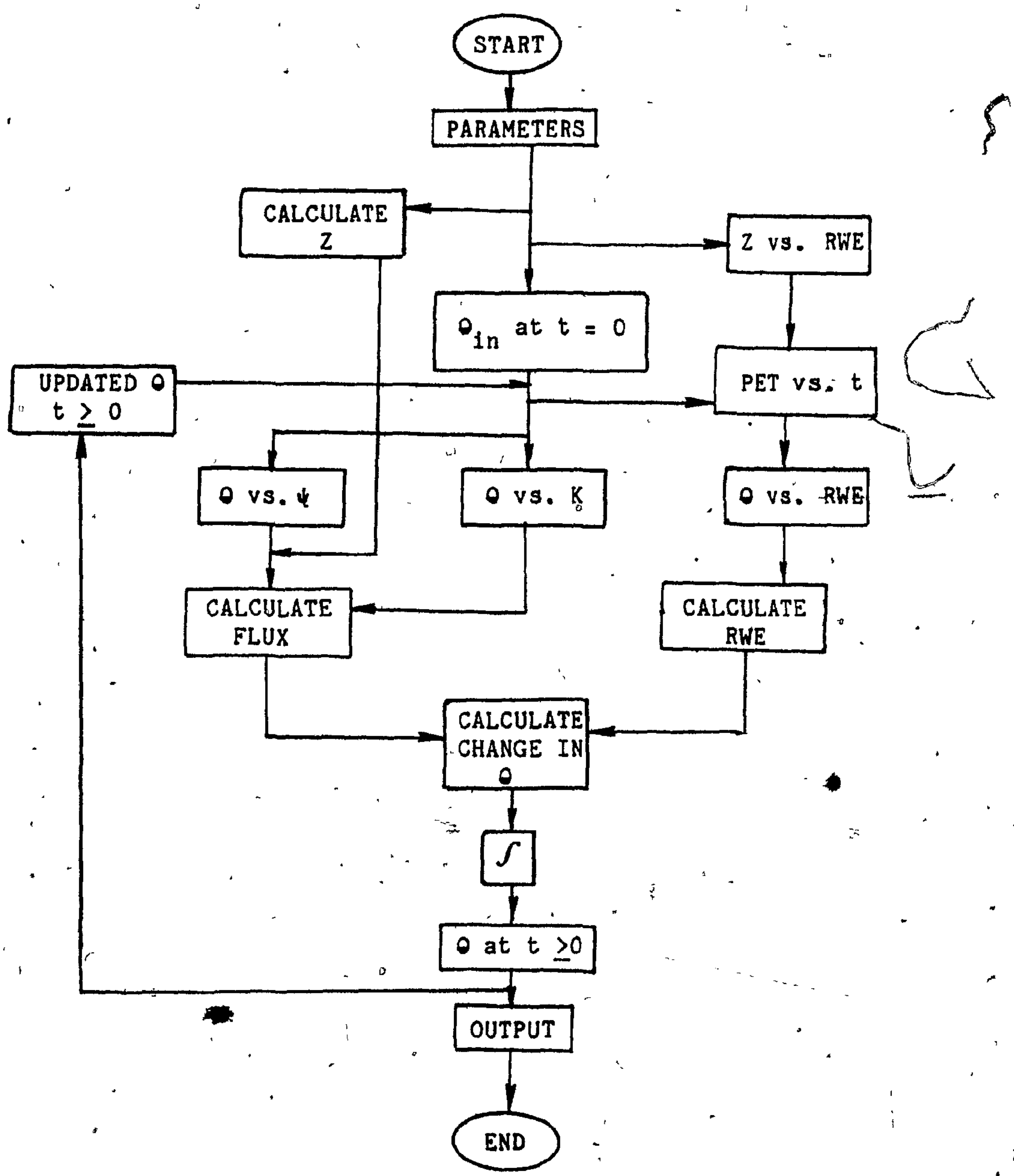

Figure 5.1. Flow chart of the computer simulator.

5.2. The INITIAL segment

This segment is intended exclusively for computing initial condition values and basic parameters. The segment begins with the TABLE statements where the initial soil moisture content of the soil rings, radial distances from the axis and depths from the soil surface to the interface between soil rings and the boundaries of the soil cylinder are provided. This follows the functions THMPOT, THK, RZDRWE and the parameters.

The number of soil rings for this study were set arbitrarily at 165. The thickness and width of the soil rings were determined from TABLE RADRNG and TABLE Z respectively. The TABLEs are written to facilitate the input of variable or constant mesh size of the soil rings for simulation. For this study the thickness and the width of each of the soil rings were 0.06 m. The total profile depth was 0.9 m and the distance R from the vertical axis passing through emitter was 0.66 m.

The values of matric potential dependent on soil moisture content are given as a tabulated FUNCTION THMPOT, in which the first of each pair of numbers is the independent variable (moisture content) and the second of each pair the dependent variable (matric potential). Similarly, the values of hydraulic conductivity dependent on moisture content are given as tabulated FUNCTION THK; values of the root water extraction term dependent on root depth are tabulated as a FUNCTION RZDRWE. Note that the root zone depth must fall on the horizontal interface between the soil rings or the bottom of the finite soil cylinder.

The following parameters are specified in this segment using PARAMETER statements:

```
PARAMETER IMAX, JMAX, RZD, THETAS, TRUN, HBOUND, KSAT, PI, P1,
PARAMETER TSTART, EQHR, LDMIN, MCWIL, MC50AV, WRTDEL, PET
```

The initial soil moisture content ITHETA given in scalar array is changed to IMC, the vector array using the following statements:

```
      DO 10 I=1,IMAX
      DO 10 J=1,JMAX
      M=(I-1)*JMAX+J
 10   IMC(I,J)=ITHETA(M)
```

The calculations for the following variables are done using NOSORT option and FORTRAN statements:

JMAX1, IMAX1, TWOPI, EQMIN, EQMIN1, RWEMDR, P2, IMC(I,J), DELTAR(J), RADDIS(J), ARNGJ(J), AVDELR(J), DELTAZ(I), GPOT(I), AVDELZ(I), ARNGIJ(I,J), VOLRNG(I,J), RWEZF(M), RZDF(I), N, RWEZ(I), MP50AV, MPDEN, VWROWI(I), VWCOLI(J), VWWRZI, VWBRZI, VWWSCI.

5.3. The DYNAMIC segment

This segment is the main segment in the model. It includes the complete description of the system dynamics, together with other computations needed during the run. The structure statements within this segment are a mixture of S/360 CSMP and FORTRAN statements. The segment consists of SORT and NOSORT sections. The CSMP assumes the statements to be sorted by the CSMP unless NOSORT is specified. In the NOSORT section the statement are executed as provided in the program.

5.3.1. SORT section

The integrations to update the volumetric moisture contents of each of the soil rings at each time step are carried out by the CSMP function :

```
MC1=INTGRL(IMC1,DELST1,165)
```

The third argument represents the number of soil rings in the integrator array to keep track of their moisture contents. The variables MC1, IMC1 and DELST1 are dummies. These appear in EQUIVALENCE statements corresponding to the first soil ring (1,1) of vector arrays of variables MC, IMC and DELST respectively. The volumetric moisture contents are stored in an array MC. This array is used in the beginning of the dynamic segment to calculate the moisture content of each soil ring at the current time. The first argument of the integral function states that the initial value of the volumetric moisture content is given by an array IMC. The second argument states that the net rates of change in volumetric moisture content into integral is given by the array DELST. At current time all net rates of change in moisture content in all the rings are calculated from the state of the system. Then all integrations are performed.

Similarly, the integrations to update the root water extraction from each soil rings (nn) within the root zone, the PET and the volume of water applied are carried out by the CSMP functions respectively:

```
RWE1=INTGRL(0.,RWEZP1,nn)
PETCUM=INTGRL(0.,RWET)
VWAPPL=INTGRL(0.,EQMIN)
```

At the time equal to zero, the root water extraction, cumulative PET and the volume of water applied are equal to zero. Therefore, the first argument in each of the above three functions is zero.

5.3.2. NOSORT section

This section starts with resetting each soil ring within the lower and upper limits of moisture contents provided in the functions THMPOT and THK. This is done to avoid any chance of instability during a simulation run. The upper and lower limits of MC in the functions are given at saturation THETAS and wilting point MCWIL respectively.

The values of the hydraulic conductivity, matric potential, hydraulic potential at the center of each ring are calculated using AFGEN function which interpolates linearly in the tabulated function defined by the first name in the argument, using the second name in the argument as the independent variable.

```
K(I,J)=AFGEN(THK,MC(I,J))
MPOT(I,J)=-AFGEN(THMPOT,MC(I,J))
HMPOT=MPOT(I,J)-GPOT(I)
```

The average conductivity for flow through boundary (J) between adjoining rings (I,J-1) and (I,J) and for boundary (I), between adjoining rings (I-1,j) and (I,J) is weighted according to their volume:

```
AVKR(I,J)=(K(I,J-1)*VOLRNG(I,J-1)+K(I,J)*VOLRNG(I,J))/...
          (VOLRNG(I,J-1)+VOLRNG(I,J))
AVKZ(I,J)=(K(I-1,J)*VOLRNG(I-1,J)+K(I,J)*VOLRNG(I,J))/...
          (VOLRNG(I-1,J)+VOLRNG(I,J))
```

The root water extraction RWET is assumed to take place during the day time only and is considered as a sine function from sunrise to sunset with its maximum rate at midday. This is calculated at current time using the statement:

```
RWET=RWEMDR*SIN(PI*T/LDMIN)
```

The root water extraction RWEMP of each soil ring is calculated at current matric potential for each soil ring. Then the volumetric root water extraction rate from each soil ring at current time, considering the position of the ring and matric potential in the ring, is calculated using the following statements:

```
RWER=RWET*RWEMP*RWEZ(I)
RWEZP(I,J)=RWER*ARNGJ(J)
```

Based on the soil moisture content, the position of the soil ring (I,J) with respect to the emitter and soil surface, the time of day and the volume of the ring, RWEZP(I,J) are calculated for each of the soil rings. Then control is transferred to the desired statement for calculating DELST(I,J) based on the position of the ring (I,J) in the soil volume considered.

The flow of soil moisture between rings is calculated using Darcy's law. The change in storage is calculated using the law of conservation of mass. The rate of change in storage per unit volume of soil in a soil ring DELST(I,J) depends on its position in the soil cylinder. DELST(I,J) with its position 1<I<IMAX and 1<J<JMAX is calculated as follows:

```
DELST(I,J)=(-RWEZP(I,J)...
 +AVKZ(I,J)*ARNGIJ(I,J)*(HPOT(I,J-1)-HPOT(I,J))/AVDELR(J)...
 -AVKR(I,J+1)*ARNGIJ(I,J+1)*(HPOT(I,J)-HPOT(I,J+1))/AVDELR(J+1)...
 +AVKZ(I,J)*ARNGJ(J)*(HPOT(I-1,J)-HPOT(I,J))/AVDELZ(I)...
 -AVKZ(I+1,J)*ARNGJ(J)*(HPOT(I,J)-HPOT(I+1,J))/AVDELZ(I+1))...
 /VOLRNG(I,J)
```

Similarly, the DELST(I,J) of other soil rings are calculated according to their position in the soil cylinder. It is also taken into account that water does not move across the circumferential and bottom boundaries of the soil cylinder.

Irrigation is applied at the ring (1,1). When the irrigation application at the soil ring (1,1) exceeds the intake, the excess water runs off to the next ring (1,2). If the amount of run off from any ring (1,J) exceeds the intake, the excess amount of water runs off to the next ring (1,J+1).

The pulse irrigation is generated by using the combination of PULSE and IMPULS functions as follows:

```
Y=PULSE(P1,IMPULS(0.,P2))
```

The IMPULS function is used to trigger the PULSE function. The IMPULS function generates a series of impulses having a value of 1.0 starting at time equal to zero and continuing at times equal to P2*(1,2,3,....). The input to the PULSE function is the impulse generator which triggers the pulse of minimum width P1 whenever its value is greater than zero, providing a pulse is not already being generated. When the value of P2 is twice the value of P1, a square-wave function is generated. Thus, the time of irrigation TRUN for pulse irrigation is twice that of continuous irrigation for the same amount of irrigation application.

The timings for the calculation of the variables in the remainder of the program and output of desired variable are controlled by the impulse generator. FORTRAN is used for these calculations and output of the variables.

The calculations are performed for the following variables at the interval equal to PRDEL:

VWCOLT(J), VWROWT(I), VWWRZT, VWBRZT, DSTROW(I), DSTCOL(J), RWECUM, VWWSCT, DSTWRZ, DSTBRZ, DSTWSC, VWSIMU, VWERR, VWACCT

The output of the following variables is obtained at PRDEL interval:

TIMHR, RADDIS(J), GPOT(I), MC(I,J), DELTAZ(I), DSTROW(I), DELTAR(J), DSTCOL(J), VWWRZI, VWWRZT, DSTWRZ, VWBRZI, VWBRZT, DSTBRZ, VWWSCI, VWWSCI, WWSCT, DSTWSC, RWECUM, VWAPPL, VWSIMU, VWERR, VWACCT.

Calculations for the following variables are performed at the interval equal to P2, at and before sunset:

PETCU, AET(I,J), AEPE(I,J), AEPEL(I,J), AETAR(J), AEPEAR(J)

The output of the following variables is obtained at an interval equal to P2, at and before sunset, and at the end of simulation run:

RADRNG(J), Z(I), AET(I,J), AEPE(I,J), AEPEL(I,J), AETAR, AEPEAR, PETCU, EQHR

Structure statements are translated and placed into a FORTRAN subroutine called UPDATE, which is executed at each iteration cycle.

5.4. The TERMINAL segment

This segment of the program enters into simulation at the end of a simulation run. The calculations of the variable which were needed at the termination of the run are performed here. All the format statements are given in this segment. The following variables are calculated:

AETALL, AETPET, ARRPC, DSRZPC, DSLSPC, DSSCPC, RWEPC

The output for the following variables is obtained at the termination of the simulation run:

AETALL, PETCU, AETPET, N, MP50AV, VWACCT, ERRPC, DSRZPC, DSLSPC, DSSCPC, RWEPC

5.5. Execution control statements

These statements are used to specify certain items relating to actual simulation run.

TIMER is the label which identifies the card as a timer card. The following system variables are used in the program.

PRDEL is the increment for printing output. Even though this system variable has not been used for output control, it must be specified.

FINTIM is the maximum simulation value for the independent variable, time. Its value must be a multiple of PRDEL.

DELT is the integral interval or the step size for the independent variable, time.

5.6. Method of Integration

Various methods of integration can be employed using centralized integration routine for a simulation. In this simulation program integration is performed by the Milne fifth order predictor-corrector method with a variable time step as stated by the statement:

METHOD MILNE

5.7 Output control statements

The output can be obtained in graphic or numeric form using PRTPLOT or PRINT statement respectively. The print statement is limited to only 50 variables which include TIME. To obtain output of more than 50 variables one can use impulse generator. The IMPULS functions are used in DYNAMIC segment to control the timings for the calculations and output of variables as specified therein, using FORTRAN statements:

```
      IF(TIME.EQ.FINTIM)GO TO 403
      A=IMPULS(0.,PRDEL)
      IF(A*KEEP.LT.1.) GO TO 999
      GO TO 405
403   IF(KEEP.LT.1.) GO TO 999
405   TIMHR=.....
      .....
999   CONTINUE
```

The series of impulses are generated at time equal to zero and are continued at a time interval equal to WRTDEL, until the end of simulation run, if the FINTIM is a multiple of WRTDEL. The FINTIM need not be a multiple of WRTDEL. In that case, the step of the impulse generator is skipped at FINTIM and the rest of the program is executed. The output with the system variable KEEP equal to 1.0 represents a valid integration step, otherwise it is a trial integration step.

CHAPTER VI

RESULTS AND DISCUSSION

6.1 Introduction

The simulation results obtained from the solution of this model are discussed and compared with the field data obtained immediately after termination of emitter discharge. The soil moisture distributions predicted at the AMT of 12-hours are compared with different discharge rates, amounts of irrigation water and methods of irrigation application.

Distance, depth, replenishing front, percentage and irrigation application are frequently used in the presentation of results and discussions. The definitions of the words as used in this text are given below:

Distance: horizontal distance from the vertical axis passing through the center of the finite soil cylinder.

Depth: depth from the soil surface.

Replenishing front: The replenishing front rather than wetting front is used in this study. At this point the depth of root water extraction (RWE) and net water input (inflow-outflow) are exactly equal. Thus, the change in soil moisture content at this point is equal to zero.

This condition in radial direction (R) is fulfilled when the amount of migrating moisture in a soil profile at some horizontal distance from the emitter is equal to the RWE or when the change in storage at that point tends to approach zero. This definition applies to the vertical direction (Z) when the depth is considered from the soil surface in the column (Z,1).

Throughout the discussion 'i' refers to Z, the depth or row number and 'j' refers to the radial distance, or column or ring number in radial (R) direction.

The percentage refers to the percentage of total irrigation water.

The irrigation application is to be considered as the continuous application method unless the pulse method is specified.

Water distribution in the soil profile refers to the water distribution for the total wetted radius.

Water input or distribution along the horizontal distance refers to the water input or the distribution for the total wetted depth.

Loss of water refers to the irrigation water which is deep drained below the root zone.

Soil moisture content profiles, in figures, are shown as (Z,R) where Z is the depth from soil surface to the bottom of the finite soil cylinder and R is the distance, m.

6.2. <u>Rougemont Orchard Site 1.</u>

The experiments were conducted using 12, 16 and 24 L of irrigation water applied from an emitter. The moisture contents in the soil profile were measured and predicted at the distances of 0.0, 0.1 and 0.25 m from the emitter. The results are presented and discussed in the following sections.

6.2.1 Orchard Experiments and Simulation Results

When the experiments were conducted with an irrigation application of 12 L, water was applied at the emitter discharge rates (Q) of 2, 4, and 6 $L.h^{-1}$ and the results are presented in Figures 6.1, B.1 and B.2 respectively. The predicted soil moisture content (Θ_{pr}) in the soil ring (1,1) ranged from 0.31 $m^3.m^{-3}$ at a Q of 2 $L.h^{-1}$ to 0.35 $m^3.m^{-3}$ at a Q of 6 $L.h^{-1}$.

The experiments were also conducted with 16 L of irrigation water applied at the discharge rate of 2, 4 and 8 $L.h^{-1}$. The moisture contents in the soil profile obtained from the field experiments and simulations are presented in Figures B.3, B.4 and B.5 respectively. The Θ_{pr} in the soil ring (1,1) ranged from 0.31 $m^3.m^{-3}$ at a Q of 2 $L.h^{-1}$ to 0.36 $m^3.m^{-3}$ at a Q of 8 $L.h^{-1}$.

The moisture contents obtained for the total irrigation application of 24 L applied at the discharge rates of 4, 8 and 12 $L.h^{-1}$ are presented in Figures B.6, B.7 and B.8 respectively. The Θ_{pr} in the soil ring (1,1) ranged from 0.34 $m^3.m^{-3}$ at a Q of 4 $L.h^{-1}$ to 0.36 $m^3.m^{-3}$ at the Q of 8 $L.h^{-1}$.

The results show that the field situation gave higher moisture contents and deeper migration of water under the emitter when compared to the computed results. One of the reasons is that the mesh size was kept constant at 0.06 m during all simulations. The soil moisture is

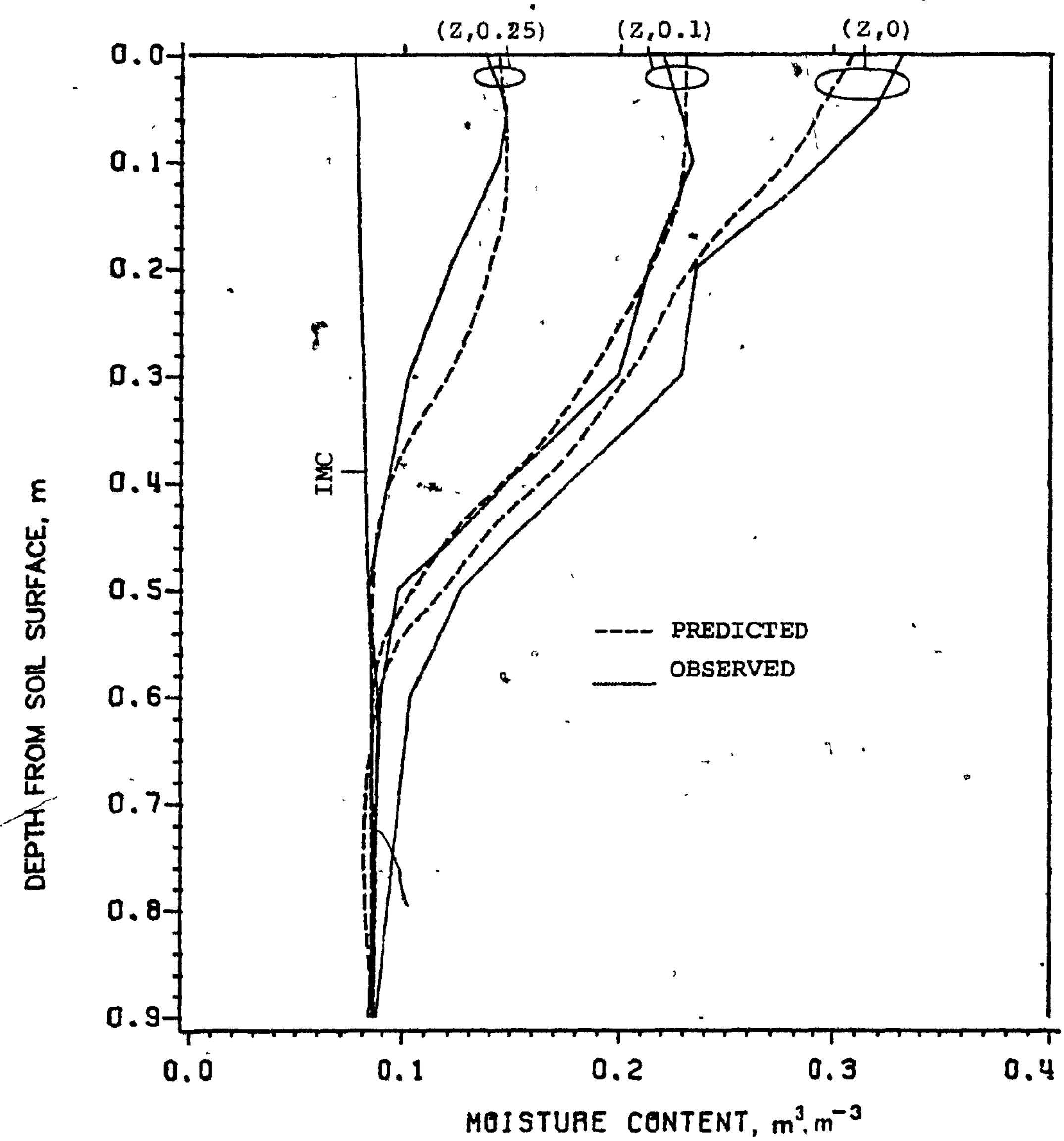

Figure 6.1. Soil moisture content profiles before and after 12 L of water applied at 2 $L.h^{-1}$ at Rougemont orchard site 1.

considered uniformly distributed within a soil ring. In reality, the soil moisture movement is a continuous function of the distance and the depth from the emitter. The model considers the moisture movement as a step function of the distance and the depth from the emitter, the step size is equal to the mesh size.

When water is discharged from an emitter, a zone of saturation develops up to a certain distance from the source (Leven et al., 1974). The saturation zone is larger with higher rates of emitter discharge. Figures B.9 to B.13 show the iso-soil moisture content curves for different amounts of irrigation water application at different rates. If the zone of saturation is less than the volume of the soil ring (1,1), uniform distribution of moisture within the ring by the model, results in a moisture content value less than saturation. This is evident from the fact that Θ_{pr} values in ring (1,1) were higher at the higher Q when compared with the low Q.

When the soil moisture content (Θ) is near saturation in sandy soils, gravity forces dominated in soil moisture movement. Thus the loss of water beyond the root zone tends to increase with increase in the Q. The higher Θ_{pr} in ring (1,1) resulted in deeper migration of water. Also, the higher moisture contents observed under an emitter in the field resulted in faster and deeper moisture migration under the emitter when compared to the predicted values. The soil moisture retention characteristics were used to simulate the soil moisture movement. However, during the wetting period, water moves faster with the same moisture contents when compared to the redistribution period.

The simulated values are calculated at the center of a mesh which, in this case, is 0.03 m away from the vertical axis and the horizontal axis passing through the emitter. The simulation technique distributes soil moisture in a mesh 0.06 m deep. The extrapolation technique is not applicable for the prediction of soil moisture content at the vertical axis or horizontal axis passing through the emitter. The observed soil moisture content (θ_{ob}) at the soil surface were lower as compared to the calculated values at a distance of 0.10 and 0.25 m from an emitter. The soil surface is usually open directly to the atmospheric demand. Thus, a low moisture content may be found at the soil surface away from an emitter. At the emitter where water is applied, the soil remains saturated during irrigation and immediately after termination of irrigation. At this point one should expect higher moisture content from the field in comparison to calculated values which depend on the extent of the zone of saturation. There were stones and heterogeniety in the field. Therefore, at some points, departure from the simulated smooth curve was observed. Comparing the soil moisture profiles at the horizontal distances of 0.10 and 0.25 m from an emitter, the agreement with computed results is reasonably good.

6.2.2 Simulation Results after Redistribution of Water

The soil moisture distributions predicted for 12, 16, 24 L of irrigation water applied at different discharge rates and methods are presented and discussed.

6.2.2.1 Irrigation Application of 12 L of Water

The distributions of water input, along the horizontal distance and in the soil profile obtained with different discharge rates and methods are presented in Figures 6.2 and 6.3 respectively. The results show that the lower discharge rates gave higher input close to the emitter when compared to the higher discharge rates. The water input at the emitter ranged between 32.0 mm obtained with 2 $L.h^{-1}$, and 30.4 mm obtained with 6 $L.h^{-1}$. The difference in water input close to the emitter is caused by the difference in the period of infiltration and redistribution. When water is applied at lower discharge rates the infiltration time is higher and the redistribution time is lower when compared to the higher rates of emitter discharge (Table 6.1). The pulse irrigation application at the rate of 4 $L.h^{-1}$ gave the same results as the continuous irrigation application at the discharge rate of 2 $L.h^{-1}$.

The simulation results are summarized in Table 6.1. The results obtained with different discharge rates and methods of irrigation application are in close agreement with each other. There are very small differences which occured due to the difference in time of infiltration and redistribution.

The loss of water tends to increase with an increase in the rate of discharge. When the soil is close to saturation the gravity potential dominates resulting in faster movement of water downwards. However, the differences resulting from the discharge rates are very small and can be ignored.

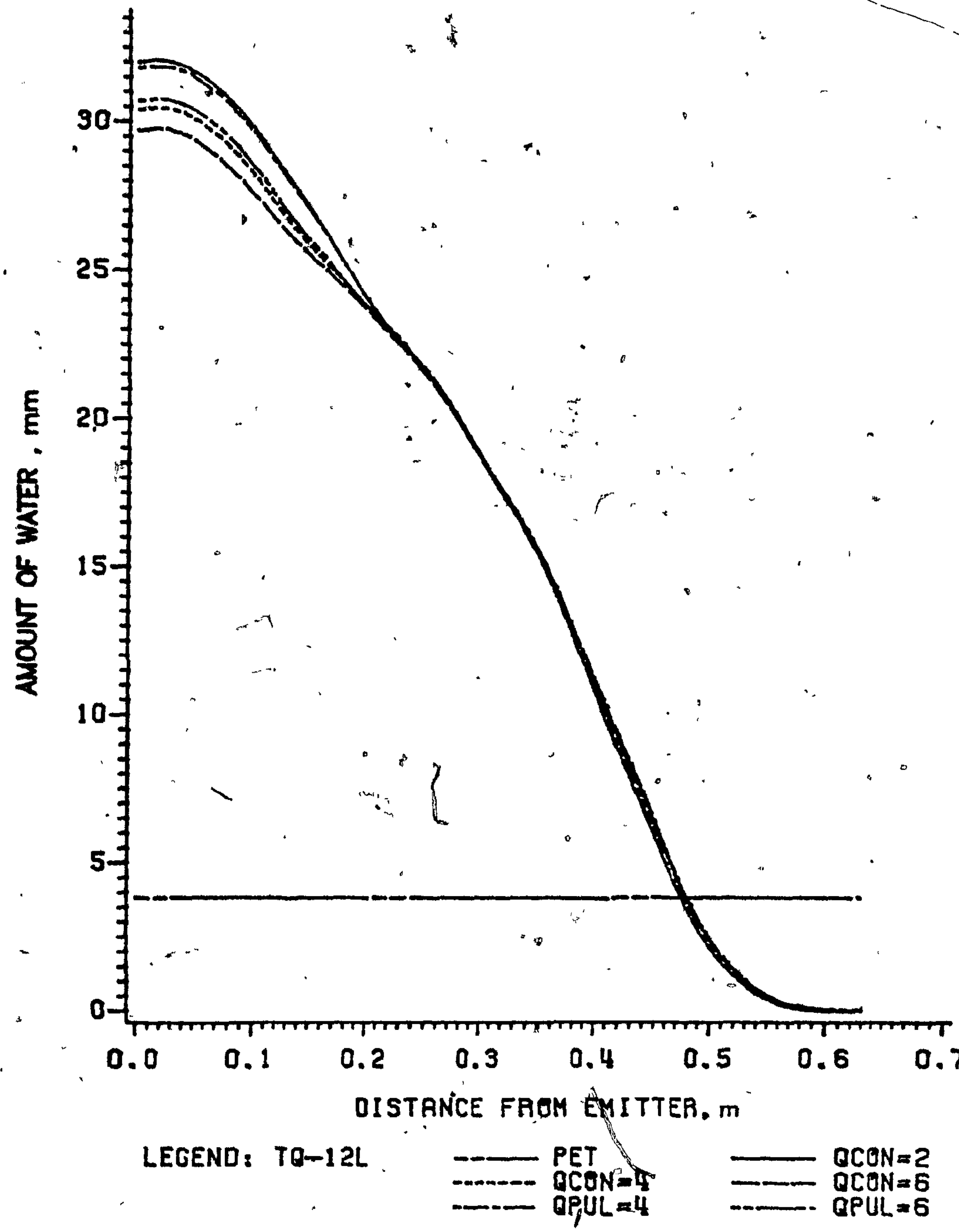

Figure 6.2. Water input predicted along horizontal distance with an irrigation application of 12 L at different discharge rates for Rougemont orchard site 1.

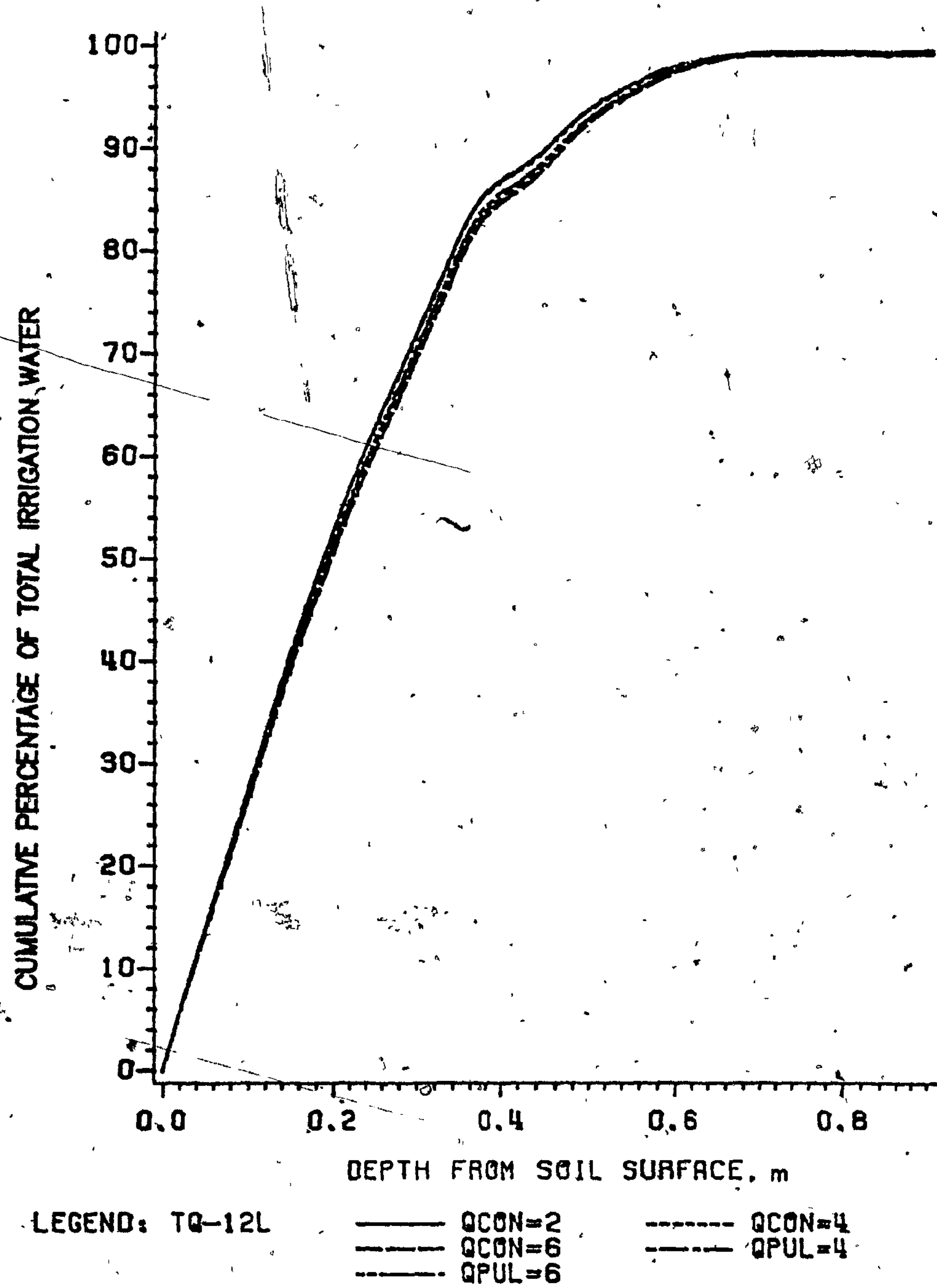

Figure 6.3. Water input predicted in soil profile with an irrigation application of 12 L at different discharge rates for Rougemont orchard site 1.

The model accounted for more than 99 percent of the total irrigation water in each simulation. This shows that the model is stable.

The average initial soil moisture contents (Θ) in all simulations were close to 50 percent available soil moisture content. The irrigation application of 12 L yielded a replenished area of 0.74 m^2. The amount of water that moved beyond the replenished area ranged between 2.4 and 2.9 percent; it remained within root zone but did not meet the RWE demand.

The average water input over the replenished area was 16.2 mm and the RWE was 3.6 mm. The application of more than 30 mm resulted in a loss of 9 mm under the emitter, an upward flux of 0.3 mm and moisture storage deficits at the outer boundary of the soil cylinder.

The range of irrigation water input over the replenished area was wide and the average water input was too high when compared to the RWE demand. The large amount of water input close to the emitter results in a loss of water beyond the root zone, and the low input of water far from the emitter results in a deficit in storage. Therefore, the irrigation application from a point source was not uniform and was inefficient.

The water input, RWE, change in soil water storage and loss of water beyond the root zone along the horizontal distance are presented in Figures B.14 to B.23. The water input, RWE and the change in soil water storage in the soil profile are given in Figures B.24 to B.28. The iso-soil moisture curves are presented in Figures B.29 to B.33.

Table 6.1. Summary of results predicted for Rougemont orchard site 1.

	Amount of Irrigation Water = 12 L				
Rate (L.h^{-1})	2.0	4.0	4.0	6.0	6.0
Application Method	Continuous	Continuous	Pulse	Continuous	Pulse
Wetting Time (h)	6.0	3.0	6.0	2.0	4.0
Redistribution Time (h)	9.0	10.5	8.75	11.0	9.75
Simulation Time (h)	15.0	13.5	14.75	13.0	13.75
Replenished R (m)	0.48	0.49	0.48	0.49	0.49
Replenished Z (m)	0.79	0.80	0.79	0.80	0.80
Area (m^2)	0.74	0.74	0.74	0.75	0.74
RWE (%)	22.2	22.7	22.3	22.9	22.6
Storage (%)	57.3	54.8	57.1	53.9	55.4
Loss (%)	17.4	19.1	17.3	19.7	18.4
Input WRA (%)	96.9	96.6	96.6	96.9	96.5
Input BRA (%)	2.6	2.9	2.4	2.5	2.7
Simulated (%)	99.5	99.5	99.0	99.5	99.2
Error (%)	0.5	0.5	1.0	0.5	0.8
Total (%)	100.0	100.0	100.0	100.0	100.0

	Amount of Irrigation Water = 16 L				
Rate (L.h^{-1})	2.0	4.0	4.0	8.0	8.0
Method	Continuous	Continuous	Pulse	Continuous	Pulse
Wetting Time (h)	8.0	4.0	8.0	2.0	4.0
Redistribution Time (h)	8.0	10.0	7.75	11.0	9.75
Simulation Time (h)	16.0	14.0	15.75	13.0	13.75
Replenished R (m)	0.52	0.53	0.52	0.53	0.53
Replenished Z (m)	0.86	0.89	0.87	0.90	0.89
Area (m^2)	0.86	0.88	0.86	0.89	0.89
RWE (%)	19.0	20.0	19.0	20.6	20.2
Storage (%)	55.2	52.1	55.0	50.6	52.1
Loss (%)	23.3	25.6	23.0	26.1	24.9
Input WRA (%)	97.5	97.6	97.1	97.3	97.3
Input BRA (%)	2.0	1.9	1.9	1.9	1.8
Simulated (%)	99.5	99.5	99.1	99.2	99.2
Error (%)	0.5	0.5	0.9	0.8	0.9
Total (%)	100.0	100.0	100.0	100.0	100.0

continued...

Table 6.1 continued....

	Amount of Irrigation Water = 24 L				
Rate ($L.h^{-1}$)	4.0	8.0	8.0	12.0	12.0
Application Method	Continuous	Continuous	Pulse	Continuous	Pulse
Wetting Time (h)	6.0	3.0	6.0	2.0	4.0
Redistribution Time (h)	9.0	10.5	8.75	11.0	9.75
Simulation Time (h)	15.0	13.5	14.75	13.0	13.75
Replenished R (m)	0.57	0.58	0.57	0.59	0.58
Replenished Z (m)	> 0.90	> 0.90	> 0.90	> 0.90	> 0.90
Area (m^2)	1.02	1.05	1.02	1.08	1.06
RWE (%)	16.5	17.3	16.6	17.7	17.4
Storage (%)	47.7	45.7	48.0	45.6	47.0
Loss (%)	33.3	34.4	32.6	34.1	33.0
Input WRA (%)	97.6	97.4	97.2	97.5	97.4
Input BRA (%)	2.0	1.8	1.9	1.8	1.8
Simulated (%)	99.6	99.2	99.1	99.3	99.1
Error (%)	0.4	0.8	0.9	0.7	0.9
Total (%)	100.0	100.0	100.0	100.0	100.0

Comparing the figures showing different discharge rates and methods, and ignoring minor differences in their values, it can be concluded that the soil moisture distribution is not dependent on the rate of discharge and the method of irrigation application. However, the pulse method of irrigation reduces the average irrigation application rate and permits low application rates from high discharging emitters.

6.2.2.2.3 Irrigation application of 16 L

The distribution of water input along the horizontal distance and in the soil profile obtained with different discharge rates are presented in Figures B.34 and B.35, respectively.

The soil moisture distribution obtained with pulse irrigation is the same as that obtained with continuous irrigation at an average rate of pulse irrigation application. Thus, the pulse irrigation method reduces the rate of irrigation application from high discharging emitters.

The simulation results are summarized in Table 6.1. The results obtained with different discharge rates and methods of irrigation application are in close agreement with each other. There are a few minor differences wich occurred due to the inconsistency in conditions developed with different discharge rates at each time step which serve as initial conditions for the subsequent time steps. Also, the time of infiltration is higher and redistribution time is lower when water is applied at low rates of application.

The input under the emitter ranged from 38.3 mm at the Q of 2 $L.h^{-1}$ to 35.1 mm at the Q of 8 $L.h^{-1}$. The loss of water ranged from 13.1 mm at the Q of 8 $L.h^{-1}$ to 13.6 mm at the Q of 2 $L.h^{-1}$. under the emitter. However, the amount of water that moved beyond the root zone ranged between 23.3 percent at the Q of 2 $L.h^{-1}$ to 26.1 percent at the Q of 8 $L.h^{-1}$. The replenished area with Q of 2 $L.h^{-1}$ was 0.86 m^2 and it increased to 0.89 m^2 when the Q was increased to 8 $L.h^{-1}$. This indicates that the replenished area tends to increase when the emitter discharge rate is increased. This is due to the fact that the intake and the zone of saturation increases with increasing rates. The increase of area by 0.03 m^2 over an area of 0.086 m^2 is very small and does not warrant running an irrigation system with high discharge rates.

The average input over the replenished area was 18.1 mm and RWE of 3.5 mm with daily PET of 5.4 mm. The wide range of water input over the replenished area and the loss of water indicate that the irrigation application from the point source is not uniform and it is inefficient in water use.

The total amount of water accounted for at 0.72 m depth was more than 100 percent. The difference in the simulated amount of water occurred due to upward flux from lower rings into the root zone. The boundary conditions did not permit the entry or exit of water. Thus, there occurred a deficit of storage water below 0.72 m in the simulated amount. The simulation accounted for more 99 percent of the total water applied.

6.2.2.3 Irrigation application of 24 L

The distribution of water input along the horizontal distance and in the soil profile obtained with different discharge rates are presented in Figures B.36 and B.37. The replenished area ranged from 1.02 m^2 with 4 l. h^{-1} to 1.08 m^2 with 12 $L.h^{-1}$ irrigation application. The input under the emitter ranged from 47.5 mm at 4 $L.h^{-1}$ to 44.7 mm at 12 $L.h^{-1}$. The average RWE of 3.9 mm over the replenished area with 4 $L.h^{-1}$ application with a high range indicates that the irrigation application was not uniform. The amount of water applied was too high compared to the daily requirement of 5.4 mm. According to the replenished area the maximum daily RWE would have been 5.5 L or 11.0 L for a two-day period. However, when the volume of irrigation is reduced, the replenished area reduces which in turn reduces the need of irrigation water to be applied from a point source. Thus, an irrigator may need to apply a small volume of water from an emitter and use many emitters around a tree to irrigate a required area.

The loss of water ranged from 21.9 mm with 4 $L.h^{-1}$ to 20.8 mm with 12 $L.h^{-1}$ under the emitter. The total loss of water was high with an emitter discharge rate of 8 $L.h^{-1}$. This is due to the fact that the higher rates of discharge develop larger areas of saturation. The lower discharge rates develop smaller areas of saturation and if the saturation zone is smaller than the mesh size, the averaging reduces the moisture content in the ring (1,1) which in turn will reduce the moisture movement.

Pulse irrigation behaviour seems to shift from the previous criterion and in this case it tends to behave as continuous irrigation when water is applied at the rate of 12 $L.h^{-1}$.

The differences in results with different discharge rates and methods are very small. The distributions of moisture were also compared with respect to RWE, change in soil water content, and input along horizontal distance, and in the soil profile. The results indicated that the soil moisture distributions were same with all discharge rates in this study. The figures show that small differences in water input occurred close to the emitter. The input was higher at the emitter with low discharge rates. However, the irrigation water loss beyond the root zone, considering the replenished area, was higher with higher discharge rates. The results obtained with different discharge rates and methods of application are summarized in Table 6.1. Ignoring minor differences in the results, it seems that the distribution of soil moisture is not dependent on the rate or method of irrigation application.

The simulation results accounted for more than 99 percent of the water applied which indicates that the model is stable under these conditions also.

6.3 Rougemont Orchard Site 2

The experiments were conducted with 12 and 16 L of water applied from an emitter. The moisture contents in the soil profile were measured and predicted at a distance of 0.0, 0.1 and 0.25 m from the emitter. The results are presented and discussed in the following sections.

6.3.1 Orchard Experiments and Simulation Results

The moisture contents in the soil profile measured in the field and predicted by the model with discharge rates of 2 $L.h^{-1}$ are presented in Figures 6.4 and B.38 respectively. The Θ_{pr} in soil ring (1,1) ranged from 0.426 $m^3.m^{-3}$ at a Q of 2 $L.h^{-1}$ to 0.427 at a Q of 4 $L.h^{-1}$.

The moisture contents in the soil profile obtained with the discharge rates of 4 and 8 $L.h^{-1}$ with 16 L of irrigation application are presented in Figures 6.12 and B.77 respectively. The Θ_{pr} in soil ring (1,1) ranged from 0.426 $m^3.m^{-3}$ at a Q of 4 $L.h^{-1}$ to 0.427 at a Q of 8 $L.h^{-1}$. Thus, the moisture content in ring (1,1) reached saturation. This was also clear from the fact that the moisture contents were near saturation in the soil rings close to the source of water application.

The soil moisture content profiles predicted by the model show high moisture contents close to the soil surface. The Θ_{ob} values were higher below 0.1 m depth indicating that the moisture movement was faster in the field. It was not possible to find the exact width of moisture migration in the field.

The results indicate that the field situation gave deeper moisture migration than the simulated results. In this case it seems that hysteresis played an important role. The departure of observed moisture content curves from that of predicted values is no doubt due

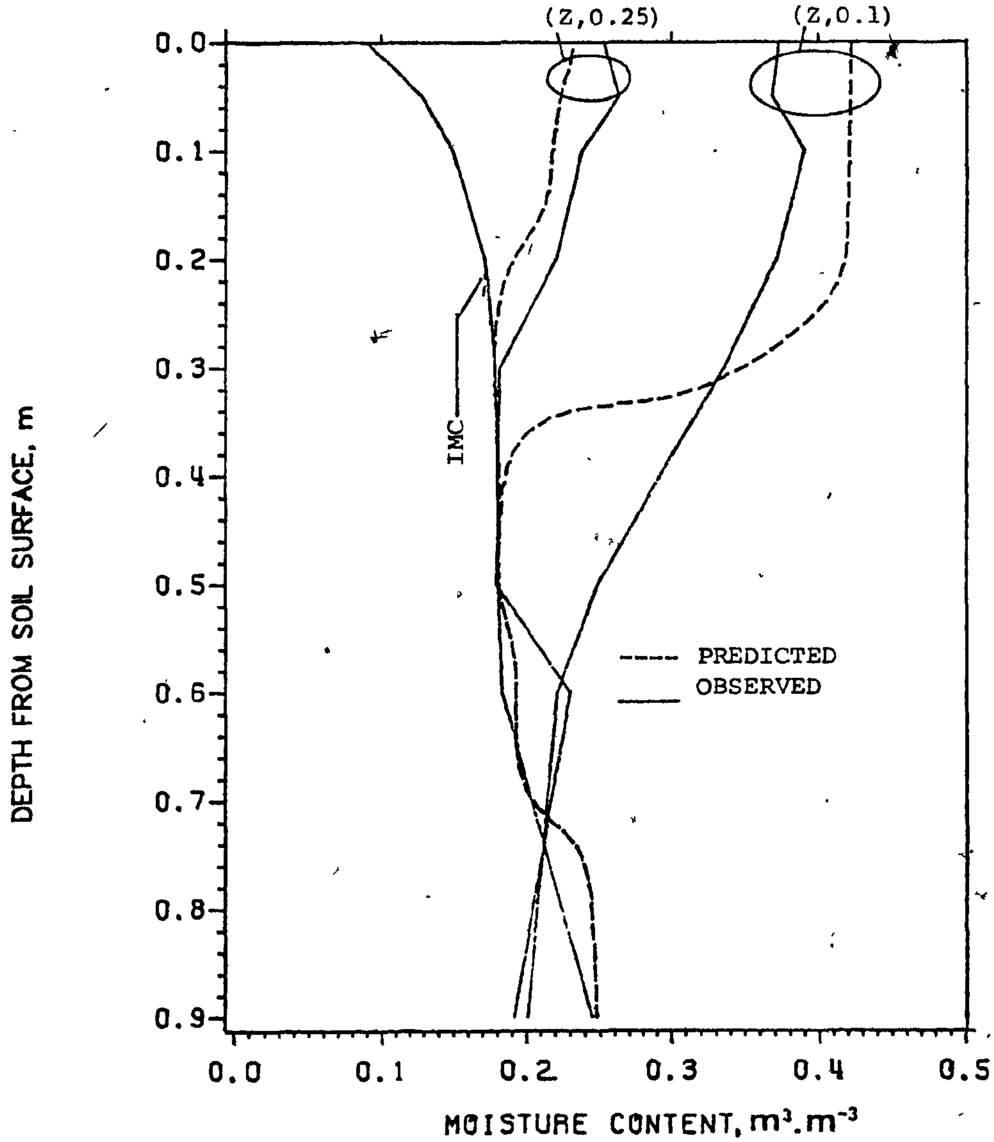

Figure 6.4. Soil moisture content profiles before and after 12 L of water applied at 2 $L.h^{-1}$ at Rougemont orchard site 2.

to the hysteresis. There were errors involved in measuring the hydraulic conductivity and the moisture characteristic curve because these were measured in the laboratory. The problem of spatial variabilty and heterogeniety in the field could cause the error in observed values when assumptions are made in simulations. Also, hydraulic conductivity (K) values reduce tremendously with a small decrease in moisture content as shown in Figure 4.2. This caused slow movement of water in the soil and the moisture content remained at its high value close to an emitter. The problem of saturation thus would occur under the emitter in the soils having similar properties.

6.3.2 Simulation Results after Redistribution of Water

The soil moisture distribution was predicted with 12 and 16 L of water at different discharge rates. The simulation results are presented and discussed as follows:

6.3.2.1 Irrigation Application of 12 L of water

The distributions of water input, along the horizontal distance and in the soil profile, obtained with different discharge rates and methods are presented in Figures 6.5 and 6.6 respectively. The results show that the lower discharge rates gave higher input close to the emitter when compared to the higher discharge rates. The water input at the emitter ranged between 76.7 mm obtained with 2 $L.h^{-1}$, and 71.9 mm obtained with 4 $L.h^{-1}$. The difference in water input close to the emitter is caused by the difference in the hours of

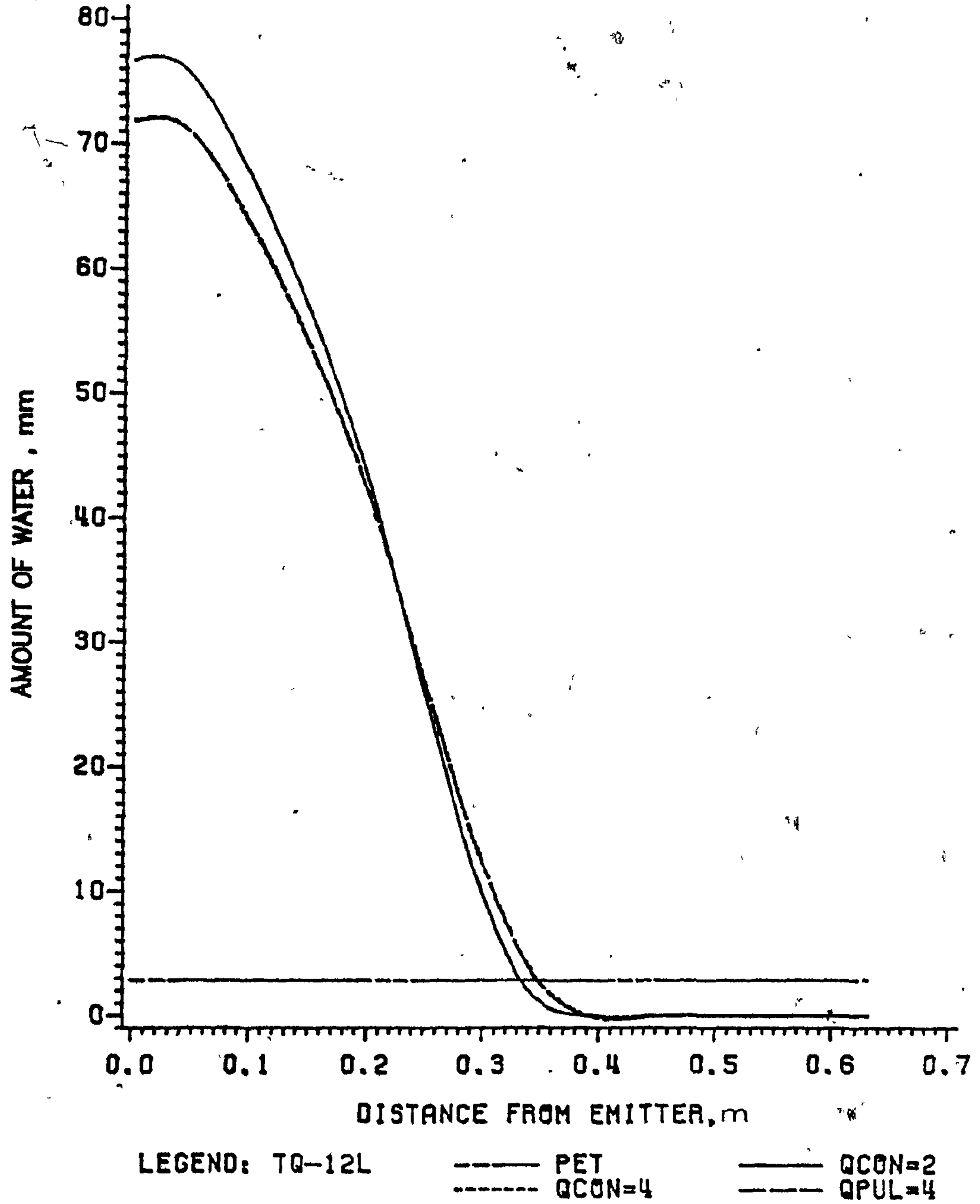

Figure 6.5. Water input predicted along horizontal distance with an irrigation application of 12 L at different discharge rates for Rougemont orchard site 2.

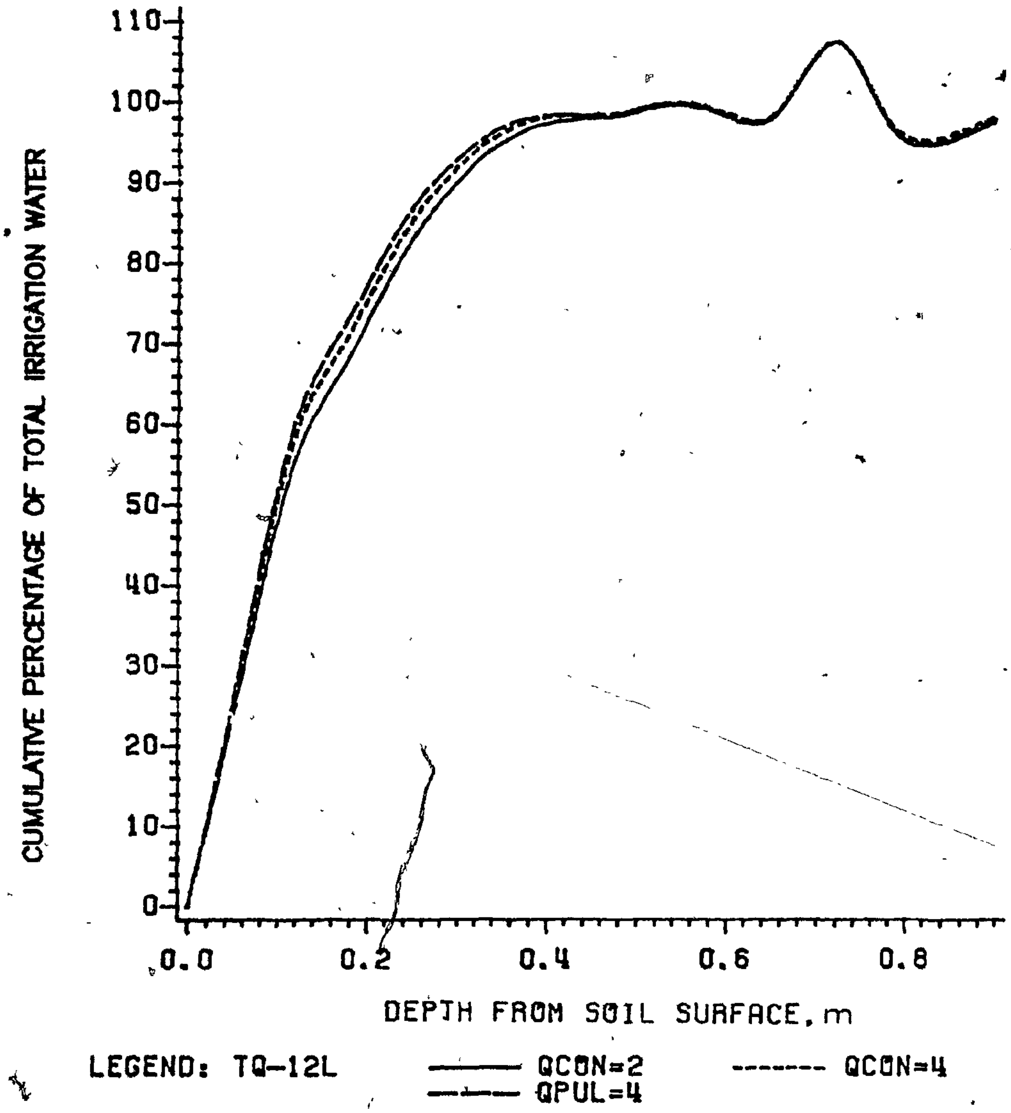

Figure 6.6. Water input predicted in soil profile with an irrigation application of 12 L at different discharge rates for Rougemont orchard site 2.

infiltration and redistribution. When water is applied at lower discharge rates the infiltration time is higher and the redistribution time is lower when compared to the higher rates of emitter discharge (Table 6.2).

The pulse irrigation at an application at the rate of 4 $L.h^{-1}$ gave the same results as the continuous irrigation at an application rate of 4 $L.h^{-1}$. In this case the pulse irrigation behaved as the continuous irrigation at the same discharge rate. This is due to very low K values at θ less than saturated soil moisture content (θ_s).

The summary of simulation results is given in Table 6.2. The results obtained with different discharge rates and methods of irrigation application are in close agreement with each other. There are very small differences which occured due to the difference in time of infiltration and redistribution. Also the saturation zone developed with higher discharge rates is larger.

The loss of water tends to increase with the decrease in the rates of discharge. This is due to the fact that the infiltration area increases with the increase in discharge rate. This behaviour is opposite to that found in RM1 soil. However, the differences resulting from the discharge rates are very small and can be ignored.

The model accounted for more than 97 percent of the total irrigation water in each simulation. The input beyond the replenished area is negative. The predicted values show more deficit than RWE beyond the replenished area. This, is evident since the model accounts for 97 to 98 percent of the water applied.

Table 6.2. Summary of results predicted for Rougemont orchard site 2.

	Amount of Irrigation Water = 12 L		
Rate ($L.h^{-1}$)	2.0	4.0	4.0
Application Method	Continuous	Continuous	Pulse
Wetting Time (h)	6.0	3.0	6.0
Redistribution Time (h)	9.0	10.5	8.75
Simulation Time (h)	15.0	13.5	14.75
Replenished R (m)	0.34	0.36	0.36
Replenished Z (m)	0.58	0.55	0.55
Area (m^2)	0.35	0.40	0.40
RWE (%)	8.7	9.8	9.8
Storage (%)	86.3	87.2	87.9
Loss (%)	2.9	2.1	1.3
Input WRA	97.9	99.1	99.0
Input BRA (%)	-0.5	-1.0	-1.2
Simulated (%)	97.4	98.1	97.8
Error (%)	2.6	1.9	2.2
Total (%)	100.0	100.0	100.0

	Amount of Irrigation Water = 16 L		
Rate ($L.h^{-1}$)	4.0	8.0	8.0
Application Method	Continuous	Continuous	Pulse
Wetting Time (h)	4.0	2.0	4.0
Redistribution Time (h)	10.0	11.0	9.75
Simulation Time (h)	14.0	13.0	13.75
Replenished R (m)	0.37	0.39	0.39
Replenished Z (m)	0.66	0.60	0.60
Area (m^2)	0.44	0.47	0.47
RWE (%)	10.2	10.6	10.6
Storage (%)	81.4	83.6	84.2
Loss (%)	7.3	3.8	3.2
Input WRA	98.9	98.0	98.0
Input BRA (%)	-0.6	0.6	0.5
Simulated (%)	98.3	98.6	98.5
Error (%)	1.7	1.4	1.5
Total (%)	100.0	100.0	100.0

The average water input over the replenished area was 33.5 mm and the RWE was 3.0 mm. with daily PET of 4.2 mm. The high application of more than 76 mm resulted in a loss of 9.8 mm under the emitter, upward flux of 0.5 mm and moisture storage deficits at the outer boundary of the soil cylinder.

The range of irrigation water input over the replenished area was wide and the average water input was too high when compared to the RWE demand. The large amount of water input close to the emitter results in a loss of water below the root zone and the low input of water far from the emitter results in a deficit in storage. Therefore, the irrigation application from a point source was not uniform and was inefficient.

Comparing the results obtained with different discharge rates and methods, and ignoring minor differences in their values, it is concluded that the soil moisture distribution is not dependent on the rate of discharge and the method of irrigation application. However, the pulse method of irrigation in this soil behaves as continuous irrigation at the same rate of application and demonstrates no advantage over continuous irrigation.

6.3.2.2 Irrigation Application of 16 L of Water

The distribution of irrigation water, along the horizontal distance and in the soil profile, is presented in Figures B.41 and B.42 respectively. The figures show that the input ranged from 82.2 mm with 4 $L.h^{-1}$ to 73.3 mm with 8 $L.h^{-1}$. This indicates that with high rate of application, water moved laterally resulting in a smaller increase in the replenished area. Thus, the area increases with the increase in the discharge rate.

Pulse irrigation behaved in a manner similar to continuous irrigation with the same rate of application. The loss of water tended to increase with a decrease in the discharge rate. The irrigation resulted in an average application of 36 mm over the replenished area of 0.44 m^2. The daily PET of 5.1 mm and RWE of 3.7 mm do not justify an average application of 36 mm of water (over the replenished area) which eventually gets distributed nonuniformly in the soil and possibly becomes available for deep drainage.

6.4 Rougemont Orchard Site 3

The experiments were conducted for 12 and 16 L of irrigation water applied at different discharge rates from an emitter. The moisture contents in the soil profile measured and predicted at distances of 0.1 and 0.25 m from an emitter are presented and discussed.

6.4.1 Orchard Experiments and Simulation Results

The moisture contents in the soil profile obtained at the rate of 2 and 4 $L.h^{-1}$ with a total irrigation application of 12 L are presented in Figures 6.7 and B.43 respectively. The Θ_{in} in the soil profile varied between 0.083 and 0.126 $m^3.m^{-3}$. The Θ_{pr} in the soil ring (1,1) ranged from 0.324 $m^3.m^{-3}$ at a Q of 2 $L.h^{-1}$ to 0.345 at a

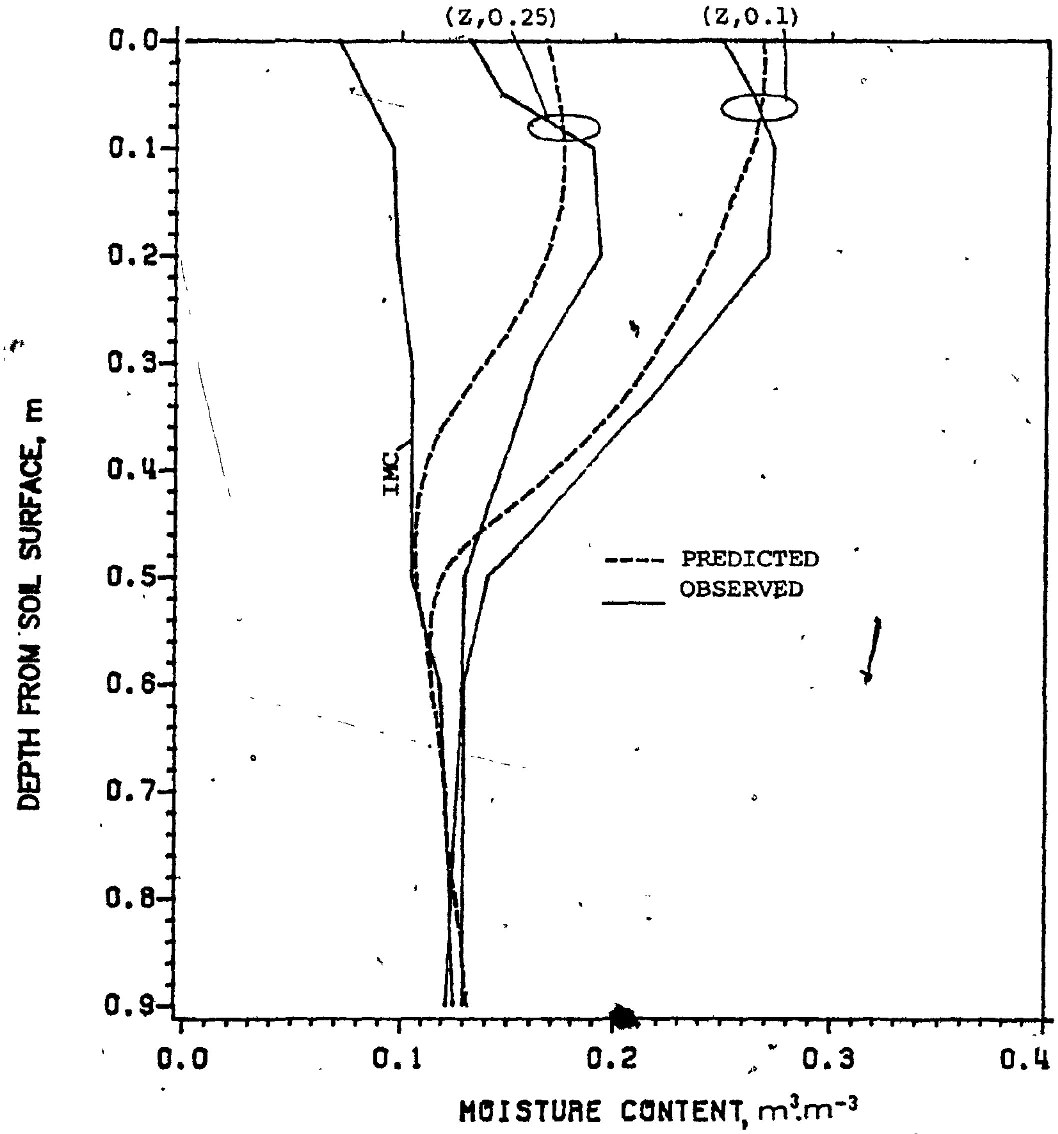

Figure 6.7. Soil moisture content profiles before and after 12 L of water applied at 2 $L.h^{-1}$ at Rougemont orchard site 3.

Q of 4 $L.h^{-1}$.

The results of 16 L of irrigation water application at the emitter discharge rates of 4 and 8 $L.h^{-1}$ are presented in Figures B.44 and B.45 respectively. The Θ_{pr} in the soil ring (1,1) ranged from 0.344 $m^3.m^{-3}$ at a Q of 4 $L.h^{-1}$ to 0.352 at a Q of 8 $L.h^{-1}$. The Θ_{pr} lower than Θ_s indicated that the ring did not reach saturation. As the emitter discharge rate was increased the moisture content in the ring (1,1) approached saturation.

The soil moisture content profiles predicted by the model are in close agreement with the field data. The close agreement is due to the fact that the soil was sandy and homogeneous in nature. This site was developed by filling the low lying area with sand.

The moisture contents observed under the emitter were higher than the predicted ones. Due to the coarse nature of the soil and high hydraulic conductivity, the saturation zone developed was not large enough and the water migration was faster in the downward vertical direction. The average over 0.06 m mesh size resulted in the reduced soil moisture content.

6.4.2 Simulation Results after Redistribution of Water

The soil moisture distribution was predicted with 12 and 16 L of irrigation water application at different discharge rates. the results are presented and discussed as follows:

6.4.2.1 Irrigation Application of 12 L of Water

The results are presented in Figures 6.8 and 6.9. The figures show that the lower rates of discharge gave higher input under the emitter. However, the loss of water was higher with 4 $L.h^{-1}$ when compared to 2 $L.h^{-1}$ irrigation application. The input of water under the emitter was 34.9 mm with 2 $L.h^{-1}$ and 32.2 mm with 4 $L.h^{-1}$ The RWE during simulation was 3.0 mm with a daily PET of 4.4 mm. An average input over an area of 0.71 m^2 was about 16 mm. The replenished area tends to increase when emitter discharge rate in increased. But the increase in the area is a very small. The loss of water tends to decrease with the increase in the emitter discharge rate. Pulse irrigation behaves similarly to continuous irrigation with its average rate of discharge.

The differences in the results are very small as shown in Table 6.3. It can therefore be concluded that the distribution of soil moisture is not dependent of the rate or method of irrigation application.

6.4.2.2 Irrigation Application of 16 L of Water

The results are presented in Figures B.46 and B.47. The water input ranged from 40.7 mm with 4 $L.h^{-1}$ to 38.9 mm with 8 $L.h^{-1}$ irrigation application. The average input over the replenished area of 0.8 m^2 was 19.3 mm. The RWE was 3.3 mm with daily PET of 4.7 mm. Pulse irrigation behaviour starts shifting at 8 $L.h^{-1}$ from an average rate continuous irrigation to its emitter discharge rate.

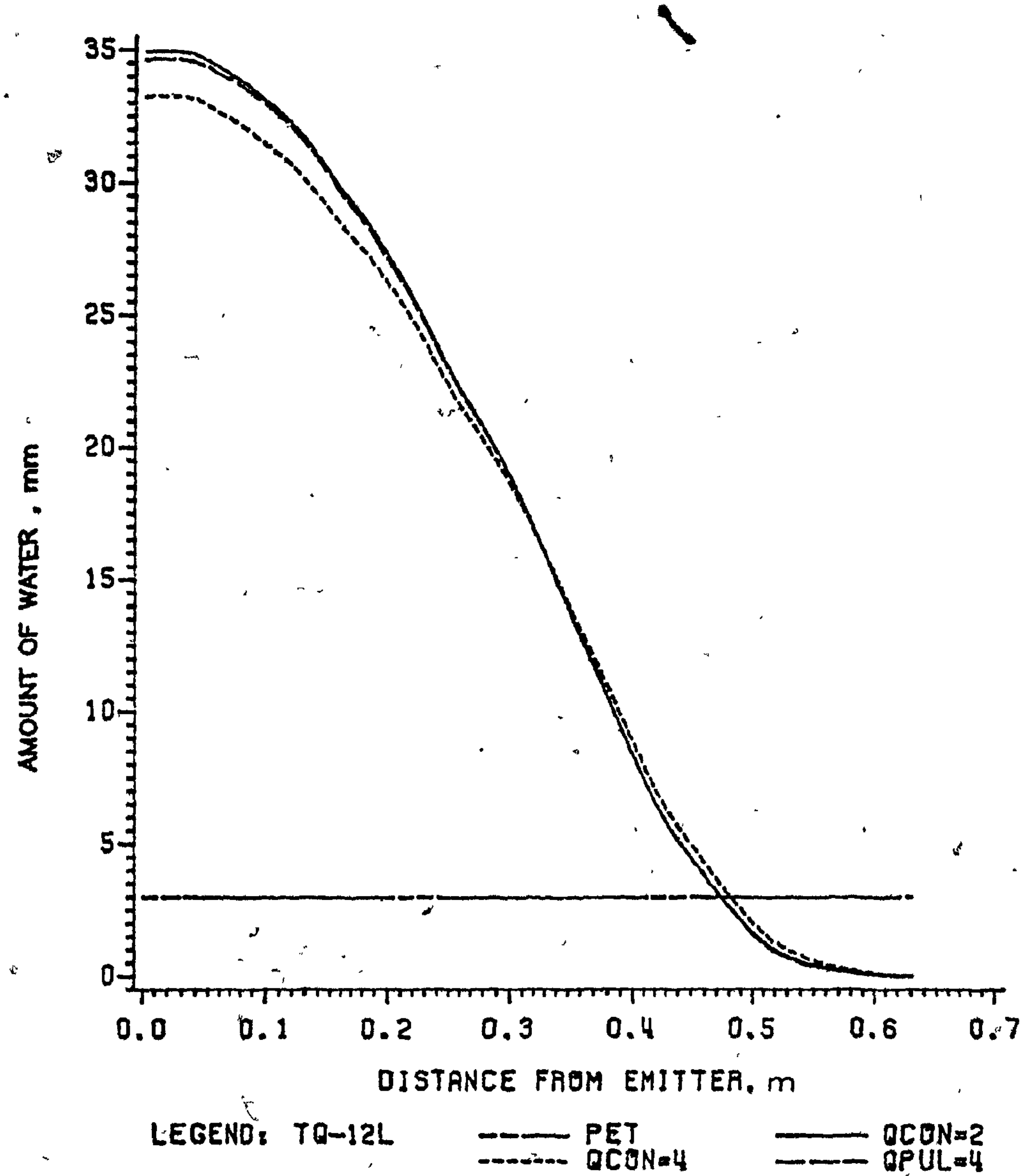

Figure 6.8. Water input predicted along horizontal distance with an irrigation application of 12 L at different discharge rates for Rougemont orchard site 3.

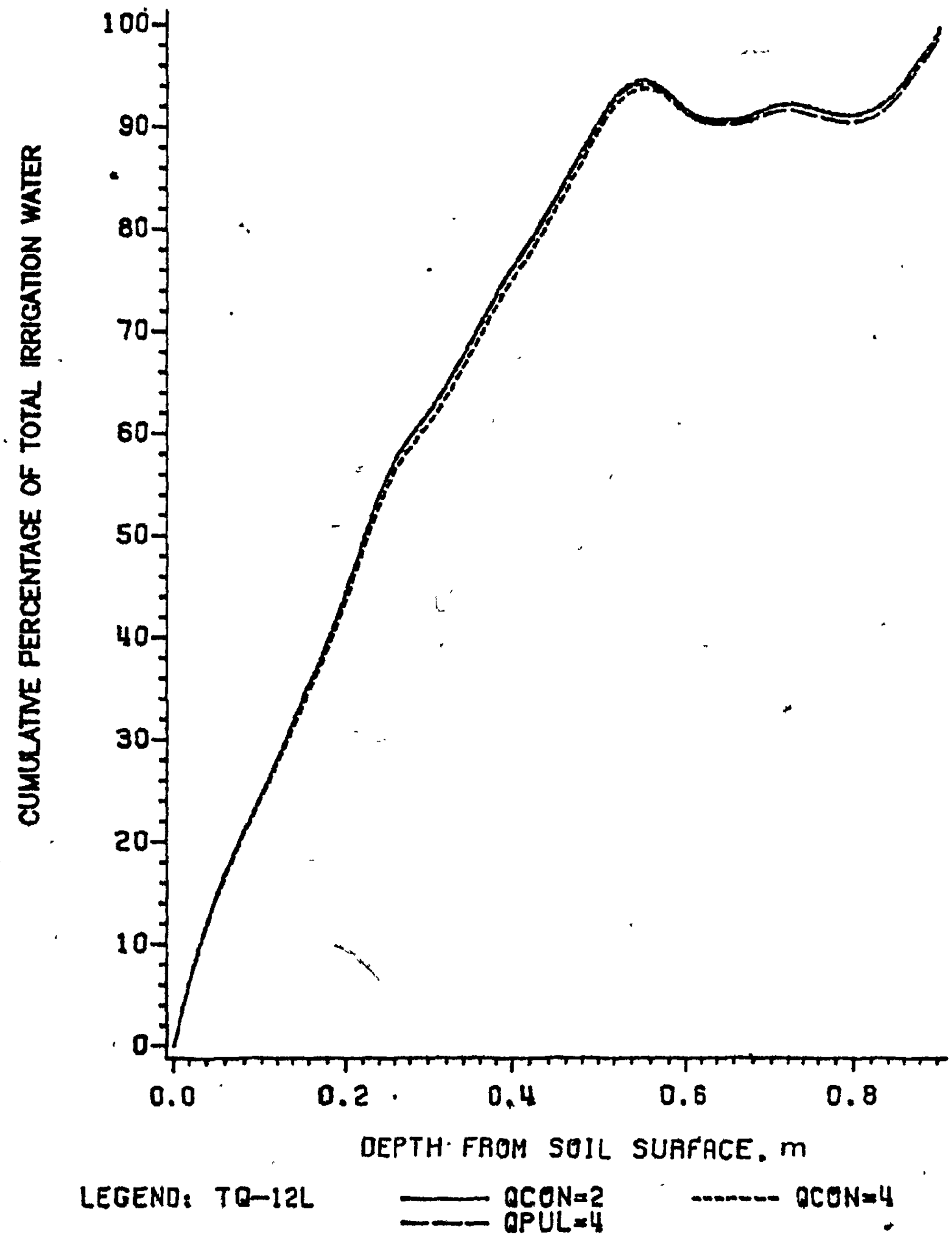

Figure 6.9. Water input predicted in soil profile with an irrigation application of 12 L at different discharge rates for Rougemont orchard site 3.

Table 6.3. Summary of results predicted for Rougemont orchard site 3.

	Amount of Irrigation Water = 12 L		
Rate ($L.h^{-1}$)	2.0	4.0	4.0
Application Method	Continuous	Continuous	Pulse
Wetting Time (h)	6.0	3.0	6.0
Redistribution Time (h)	9.0	10.5	8.75
Simulation Time (h)	15.0	13.5	14.75
Replenished R (m)	0.48	0.48	0.48
Replenished Z (m)	0.90	0.90	0.89
Area (m^2)	0.71	0.74	0.71
RWE (%)	18.0	18.7	18.0
Storage (%)	67.3	65.1	67.0
Loss (%)	11.3	12.3	11.1
Input WRA	96.6	96.0	96.1
Input BRA (%)	2.8	3.0	2.4
Simulated (%)	99.4	99.0	98.5
Error (%)	0.6	1.0	1.5
Total (%)	100.0	100.0	100.0

	Amount of Irrigation Water = 16 L		
Rate ($L.h^{-1}$)	4.0	8.0	8.0
Application Method	Continuous	Continuous	Pulse
Wetting Time (h)	4.0	2.0	4.0
Redistribution Time (h)	10.0	11.0	9.75
Simulation Time (h)	14.0	13.0	13.75
Replenished R (m)	0.50	0.52	0.51
Replenished Z (m)	> 0.90	0.90	0.90
Area (m^2)	0.80	0.84	0.81
RWE (%)	16.5	17.4	16.8
Storage (%)	64.8	64.3	65.4
Loss (%)	15.0	14.7	14.7
Input WRA	96.3	96.4	96.2
Input BRA (%)	2.7	3.0	2.9
Simulated (%)	99.0	99.4	99.1
Error (%)	1.0	0.6	0.9
Total (%)	100.0	100.0	100.0

Table 6.3 indicates that the soil moisture distribution with different discharge rates and methods of application is the same in this soil.

6.5 Rockburn Orchard Site 1

The experiments were conducted for 16 and 24 L of irrigation water applied at different discharge rates. The mesh size in the radial direction was changed from 0.06 to 0.08 m for the simulations for this site. The soil moisture profiles measured in the orchard and predicted by the model are presented and discussed.

6.5.1 Orchard Experiments and Simulation Results

The results of 16 liters of irrigation application at the rate of 4 and 8 $L.h^{-1}$ are given in Figures 6.10 and B.48 respectively. The Θ_{pr} in the soil ring (1,1) ranged from 0.305 $m^3.m^{-3}$ at a Q of 4 $L.h^{-1}$ to 0.328 at a Q of 8 $L.h^{-1}$.

The moisture contents in the soil profile obtained at irrigation application rates of 4 and 8 $L.h^{-1}$ for 24 L of water are presented in Figures B.49 and B.50. The Θ_{pr} in the soil ring (1,1) ranged from 0.305 $m^3.m^{-3}$ at a Q of 4 $L.h^{-1}$ to 0.328 at a Q of 8 $L.h^{-1}$.

The soil moisture content profiles predicted by the model show low moisture contents below o.1 m depth. This indicates that the moisture movement was faster in the field.

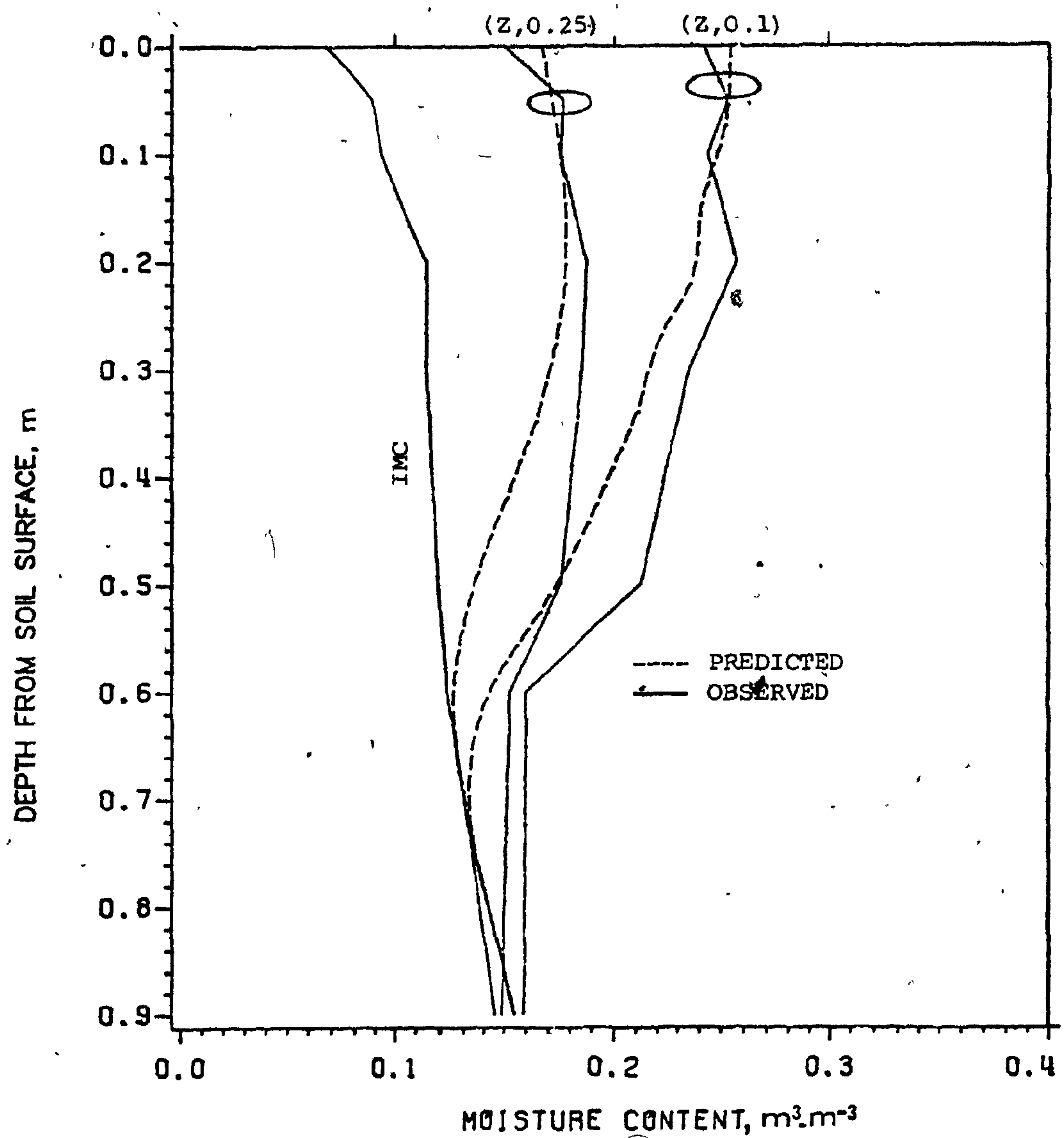

Figure 6.10. Soil moisture content profiles before and after 16 L of water applied at 4 $L.h^{-1}$ at Rockburn orchard site 1.

6.5.2 Simulation Results after Redistribution of Water

Soil moisture distribution was predicted using 16 and 24 L of irrigation water. Water was applied at different discharge rates and methods of application. The results are presented and discussed as follows:

6.5.2.1 Irrigation Application of 16 L of Water

The distributions of water input, along the horizontal distance and in the soil profile obtained with different discharge rates and methods are presented in Figures 6.11 and 6.12 respectively. The results show that the lower discharge rates gave higher input close to the emitter when compared to the higher discharge rates. The water input at the emitter ranged between 23.8 mm obtained with 4 $L.h^{-1}$, and 22.8 mm obtained with 8 $L.h^{-1}$. Pulse irrigation application at the rate of 8 $L.h^{-1}$ gave the same results as the continuous irrigation application at the discharge rate of 4 $L.h^{-1}$.

A summary of simulation results is given in Table 6.4. The results obtained with different discharge rates and methods of irrigation application are in close agreement with each other.

The average water input over the replenished area was 11.9 mm and the RWE was 3.2 mm with a daily PET of 4.6 mm. The loss of water tends to increase with the increase in the rates of discharge. When the soil is close to saturation the gravity potential dominates

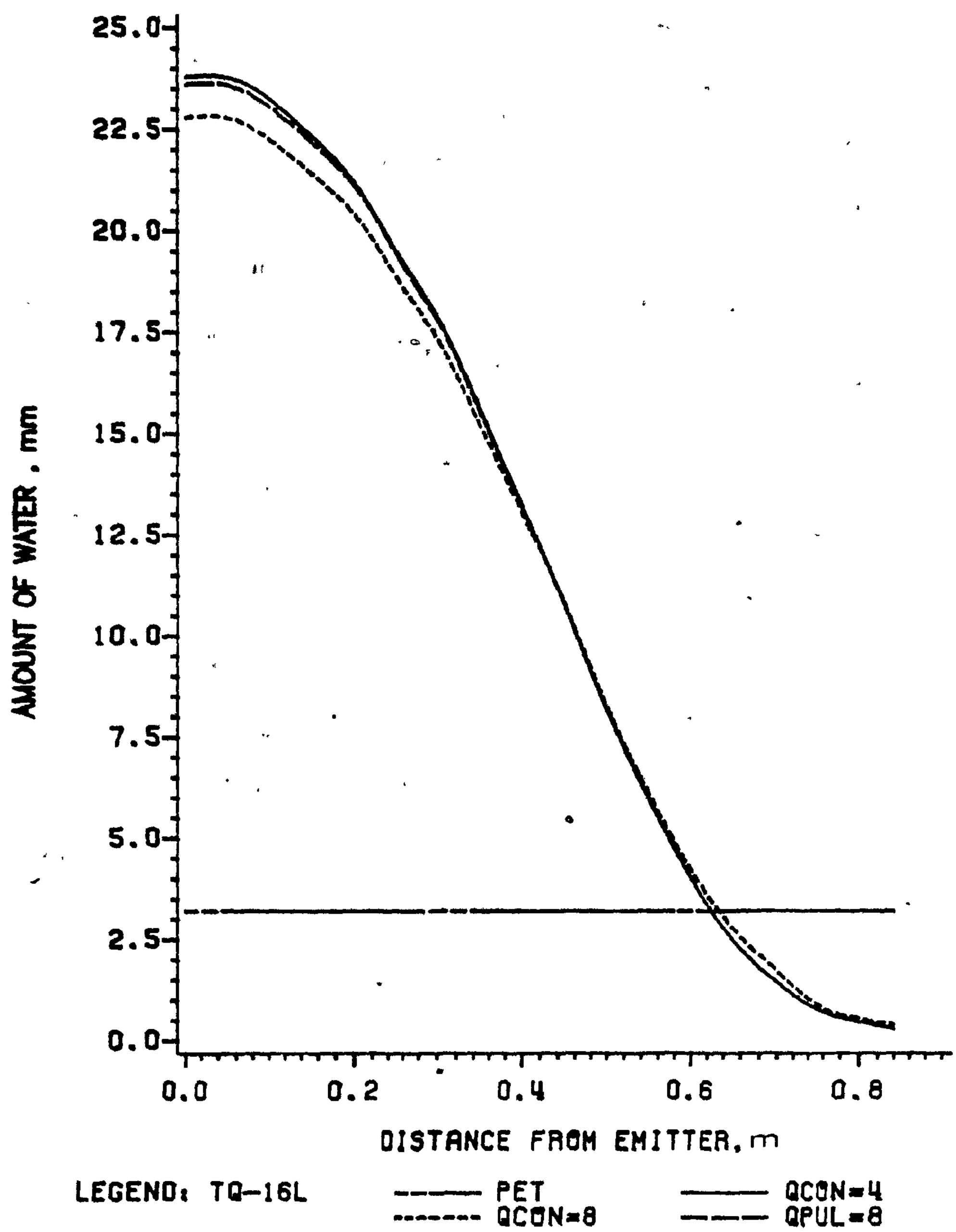

Figure 6.11. Water input predicted along horizontal distance with an irrigation application of 16 L at different discharge rates for Rockburn orchard site 1.

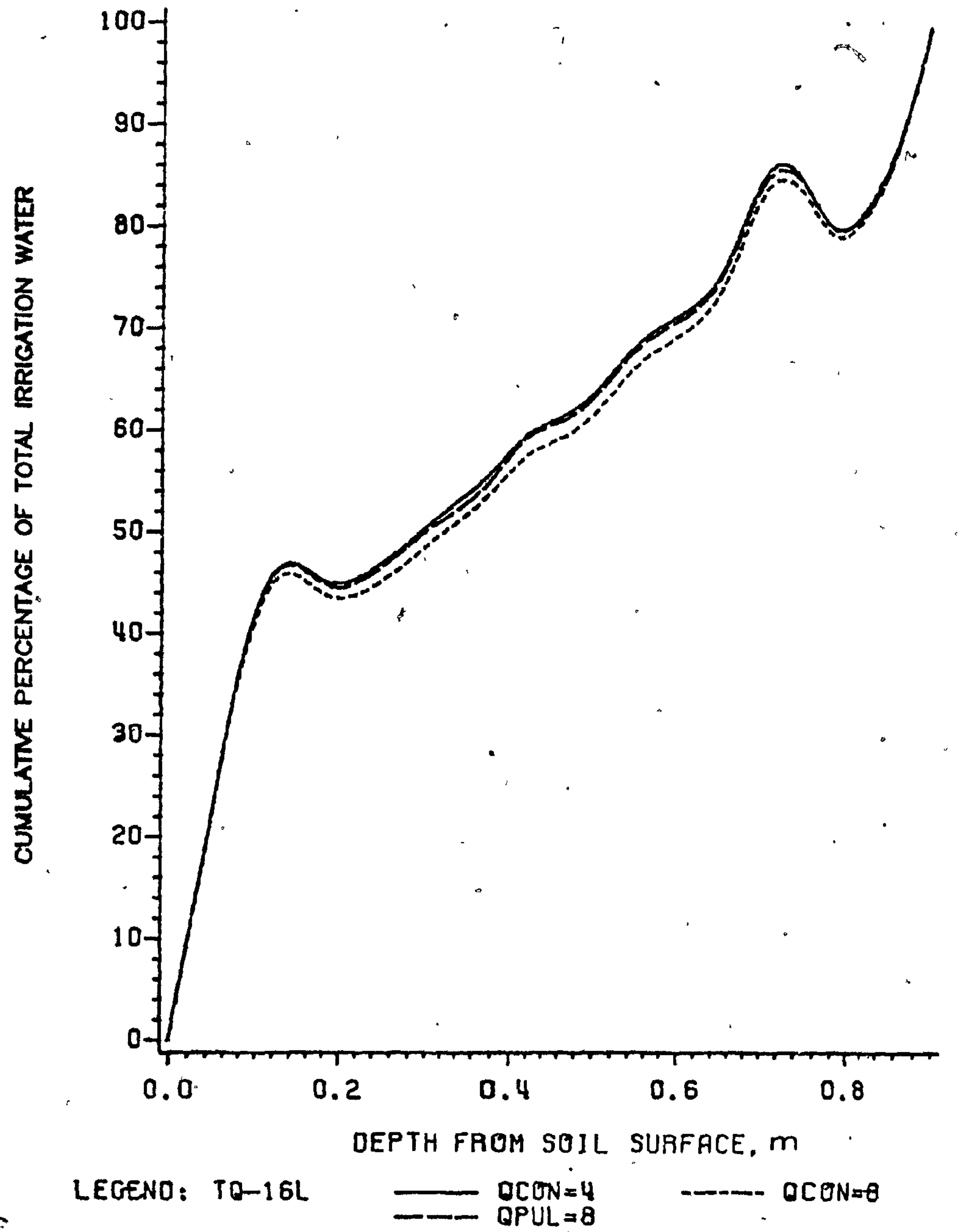

Figure 6.12. Water input predicted in soil profile with an irrigation application of 16 L at different discharge rates for Rockburn orchard site 1.

resulting in faster movement of water downwards. However the differences resulting from the dischage rates are very small and can be ignored.

The model accounted for more than 99 percent of the total irrigation water in each simulation. This shows that the model is stable in this soil.

6.5.2.2 Irrigation application of 24 L of water

The distribution of water, along the horizontal distance and in the soil profile, obtained with different discharge rates and methods are presented in Figures B.51 and B.52 respectively.

The water input under the emitter ranged from 35.7 mm with 4 $L.h^{-1}$ to 33.8 mm with 8 $L.h^{-1}$ irrigation applications. The average input over the area of 1.28 m^2 was 17.7 mm. The RWE was 4.3 mm with daily PET of 5.6 mm.

The distribution of soil moisture with respect to replenished area is summarized in Table 6.4. The Table shows that the moisture distribution in the soil is not dependent on the rate of emitter discharge. The simulations with the pulse method were less precise than the those using continuous irrigation. However, all the simulations accounted for more than 98 percent of the irrigation water applied.

Table 6.4 shows that the results obtained with different discharge rates and method of application are not different from each other. Thus, the distribution of soil moisture is not dependent on

Table 6.4. Summary of results predicted for Rockburn site 1.

	Amount of Irrigation Water = 16 L		
Rate ($L.h^{-1}$)	4.0	8.0	8.0
Application Method	Continuous	Continuous	Pulse
Wetting Time (h)	4.0	2.0	4.0
Redistribution Time (h)	10.0	11.0	9.75
Simulation Time (h)	14.0	13.0	13.75
Replenished R (m)	0.63	0.64	0.63
Replenished Z (m)	> 0.90	> 0.90	> 0.90
Area (m^2)	1.24	1.28	1.24
RWE (%)	24.9	25.6	24.9
Storage (%)	42.9	40.4	42.5
Loss (%)	24.0	25.4	24.0
Input WRA	91.9	91.4	91.4
Input BRA (%)	7.4	7.7	7.3
Simulated (%)	99.3	99.1	98.7
Error (%)	0.7	0.9	1.3
Total (%)	100.0	100.0	100.0

	Amount of Irrigation Water = 24 L		
Rate ($L.h^{-1}$)	4.0	8.0	8.0
Application Method	Continuous	Continuous	Pulse
Wetting Time (h)	6.0	3.0	6.0
Redistribution Time (h)	9.0	10.5	8.75
Simulation Time (h)	15.0	13.5	14.75
Replenished R (m)	0.64	0.65	0.64
Replenished Z (m)	> 0.90	> 0.90	> 0.90
Area (m^2)	1.28	1.32	1.28
RWE (%)	22.8	23.6	22.8
Storage (%)	50.8	47.1	50.4
Loss (%)	20.6	22.8	20.6
Input WRA	94.2	93.5	93.8
Input BRA (%)	5.2	5.7	5.0
Simulated (%)	99.4	99.2	98.8
Error (%)	0.6	0.8	1.2
Total (%)	100.0	100.0	100.0

the rate and method of irrigation application in this soil.

6.6 Rockburn Orchard Site 2

The experiments were conducted using 12 and 16 L of irrigation water. The moisture contents in the soil profile measured in the field and predicted by the model are presented and discussed.

6.6.1 Orchard Experiments and Simulation Results

The results of 12 L irrigation water application at the rates of 2 and 4 $L.h^{-1}$ are presented in Figures 6.13 and B.53 respectively. The Θ_{pr} in the soil ring (1,1) ranged from 0.4156 $m^3.m^{-3}$ at a Q of 2 $L.h^{-1}$ to 0.4162 $m^3.m^{-3}$ at a Q of 4 $L.h^{-1}$.

The distribution of Θ in the soil profile obtained with irrigation application of 16 L at the rates of 2 and 4 $L.h^{-1}$ The Θ_{pr} in the soil ring (1,1) ranged from 0.4155 $m^3.m^{-3}$ at a Q of 2 $L.h^{-1}$ to 0.4162 at a Q of 4 $L.h^{-1}$.

The figures show that the soil moisture migrated deeper in all the treatments. The values of Θ were lower in a soil profile (Z,0.10) close to the soil surface when compared to the generated values. The Θ_{ob} values in a soil profile (Z,0.25) were higher close to the soil surface which indicate that the moisture migration was wider in the field. The problem seems to have occured due to the soil moisture retention curves which were measured in a laboratory. The soil moisture distribution patterns are similar in both the simulated and field data. The departure of observed data from generated data is

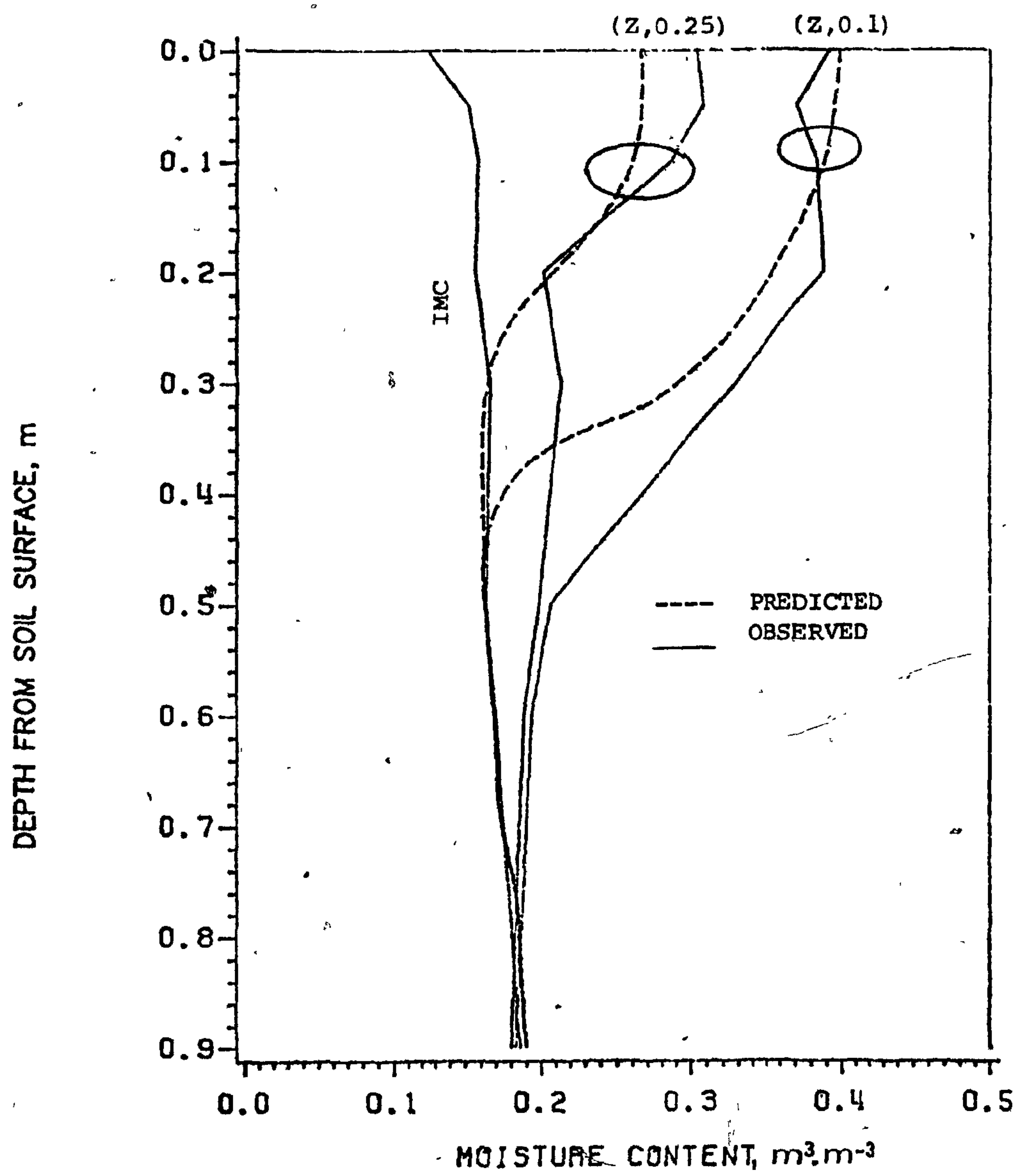

Figure 6.13. Soil moisture content profiles before and after 12 L of water applied at 2 L.h^{-1} at Rockburn orchard site 2.

due to causes already mentioned in previous sections.

6.6.2 Simulation Results after Redistribution of Water

The experiments were conducted for 12 and 16 L of irrigation water applied at different discharge rates from an emitter. The soil moisture distribution predicted at the distances of 0.1 and o.25 m from an emitter are presented and discussed.

6.6.2.1 Irrigation Application of 12 L of Water

The distributions of water input, along the horizontal distance and in the soil profile, obtained with different discharge rates and methods are presented in Figures 6.14 and 6.15 respectively. The results show that the lower discharge rates gave higher input close to the emitter when compared to the higher discharge rates. The water input at the emitter ranged between 51.4 mm obtained with 2 $L.h^{-1}$, and 50.0 mm obtained with 4 $L.h^{-1}$. The pulse irrigation application at the rate of 4 $L.h^{-1}$ gave the same results as the continuous irrigation application at the discharge rate of 2 $L.h^{-1}$.

The summary of simulation results is given in Table 6.5. The results obtained with different discharge rates and methods of irrigation application are in close agreement with each other. There was no loss of water beyond the root zone during the simulation time. However, the water movement was deeper with 4 $L.h^{-1}$ when compared to 2 $L.h^{-1}$ irrigation application. The average input over the replenished area of 0.49 m^2 was 23.8 mm. The RWE was 3.0 mm with the

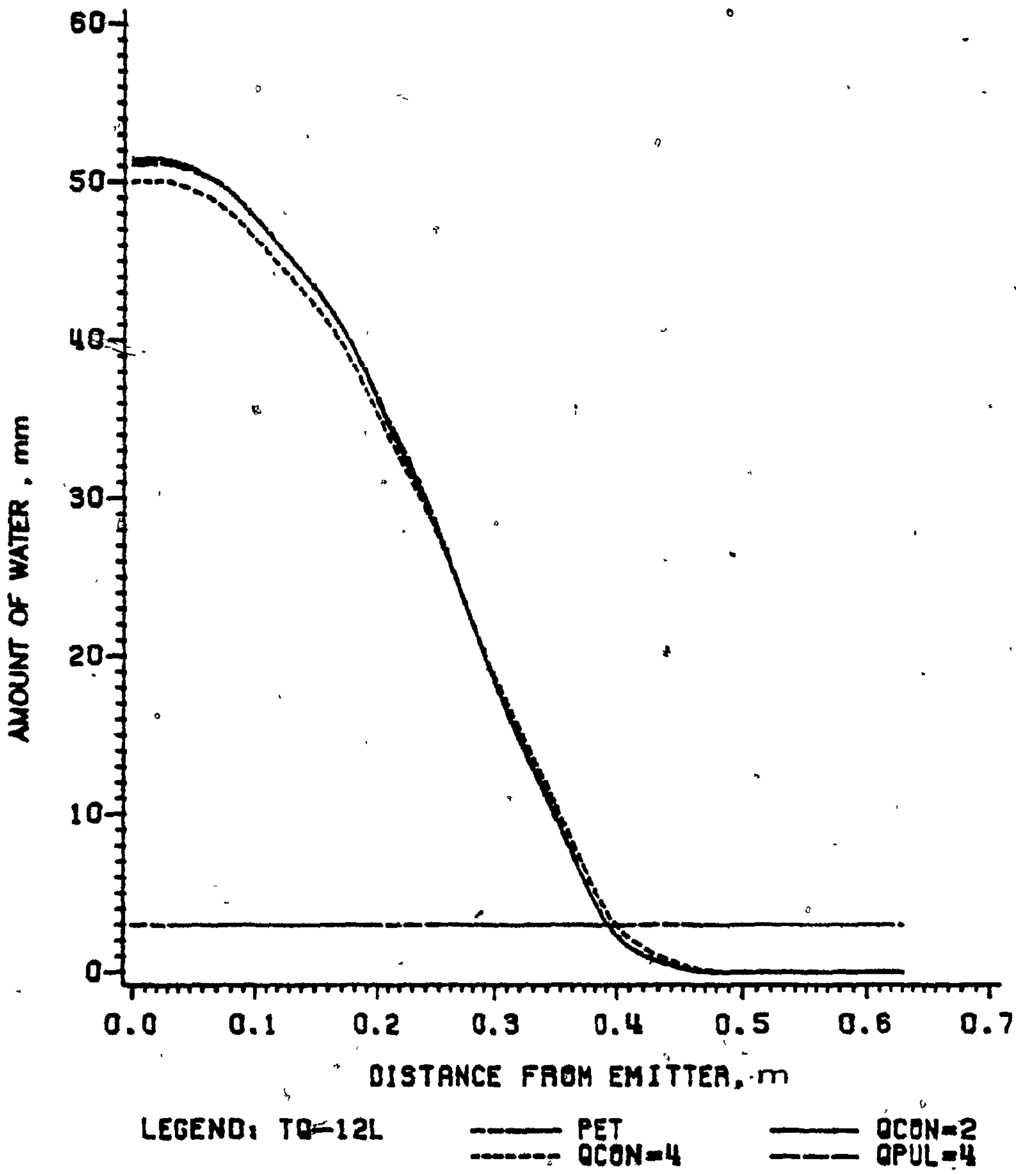

Figure 6.14. Water input predicted along horizontal distance with an irrigation application of 12 L at different discharge rates for Rockburn orchard site 2.

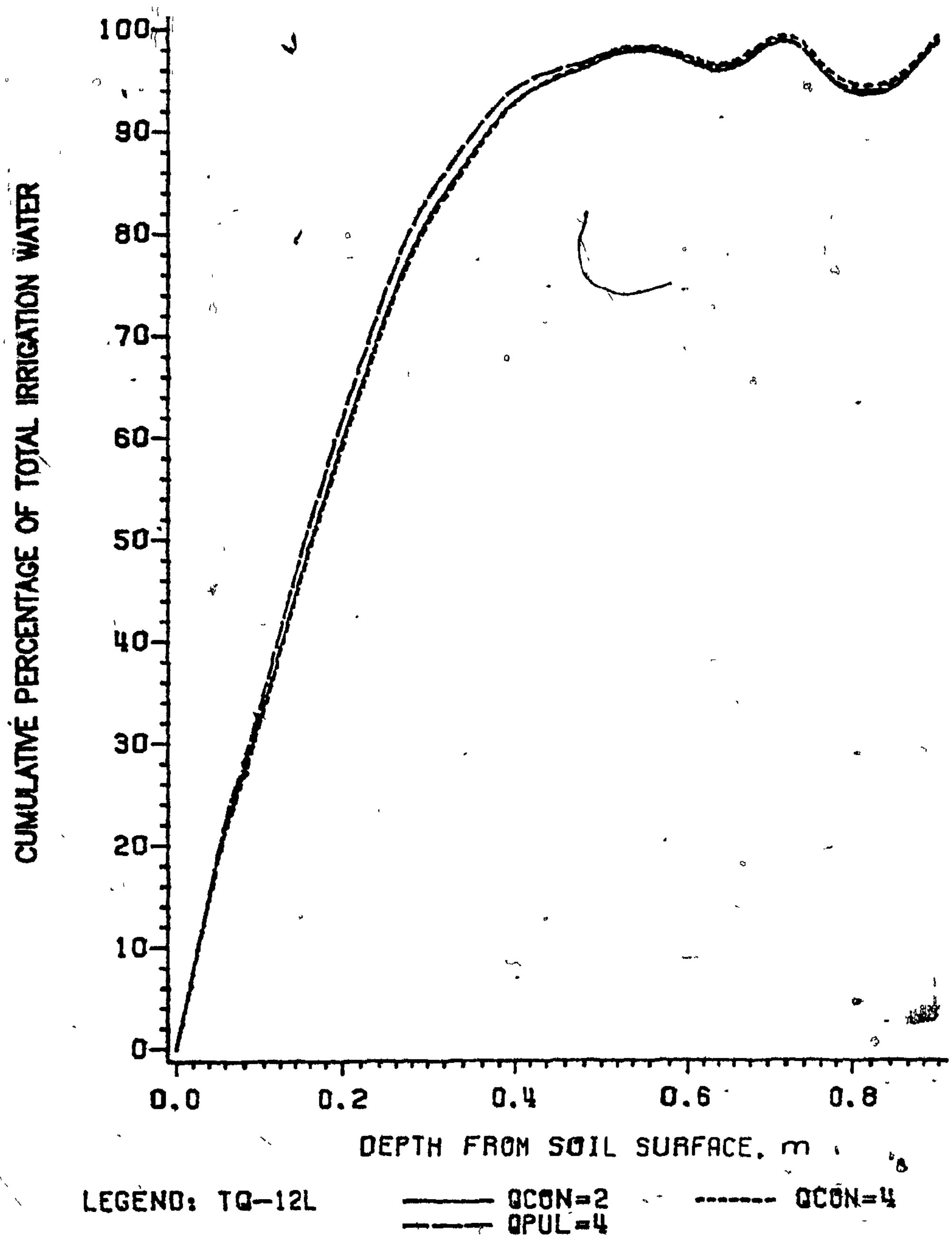

Figure 6.15. Water input predicted in soil profile with an irrigation application of 12 L at different discharge rates for Rockburn orchard site 2.

Table 6.5. Summary of results predicted for Rockburn orchard site 2.

	Amount of Irrigation Water = 12 L		
Rate ($L.h^{-1}$)	2.0	4.0	4.0
Application Method	Continuous	Continuous	Pulse
Wetting Time (h)			
Redistribution Time (h)			
Simulation Time (h)			
Replenished R (m)	0.40	0.41	0.41
Replenished Z (m)	0.61	0.66	0.61
Area (m^2)	0.49	0.52	0.49
RWE (%)	12.2	12.9	12.2
Storage (%)	84.4	84.2	84.5
Loss (%)	0.7	0.8	0.7
Input WRA	97.3	97.9	97.4
Input BRA (%)	1.2	1.2	1.3
Simulated (%)	98.5	99.1	98.7
Error (%)	1.5	0.9	1.3
Total (%)	100.0	100.0	100.0

	Amount of Irrigation Water = 16 L		
Rate ($L.h^{-1}$)	2.0	4.0	4.0
Application Method	Continuous	Continuous	Pulse
Wetting Time (h)			
Redistribution Time (h)			
Simulation Time (h)			
Replenished R (m)	0.42	0.43	0.42
Replenished Z (m)	0.66	0.69	0.66
Area (m^2)	0.56	0.57	0.56
RWE (%)	13.5	13.9	13.7
Storage (%)	84.1	83.6	83.9
Loss (%)	0.7	0.8	0.7
Input WRA	98.3	98.3	98.3
Input BRA (%)	0.3	0.9	0.4
Simulated (%)	98.6	99.2	98.7
Error (%)	1.4	0.8	1.3
Total (%)	100.0	100.0	100.0

daily PET of 4.2 mm.

The model accounted for more than 97 percent of the total irrigation water in each simulation. This shows that the model is stable.

6.6.2.2 Irrigation Application of 16 L of Water

The distributions of water input, along the horizontal distance and in the soil profile obtained with different discharge rates and methods are presented in Figures B.56 and B.57 respectively. The water input ranged from 59.4 mm with 2 $L.h^{-1}$ to 58.0 mm with 2 $L.h^{-1}$ irrigation application. The results with high irrigation application seems to behave as continuous irrigation indicating that the pulse irrigation behaviour is dependent on initial soil moisture content, type of soil and the amount of irrigation water.

6.7. Further Theoretical Investigations

In previous sections the comparison of results obtained from various research sites was not done due to the variation in the conditions under which experiments were conducted. From the results, it was noticed that the moisture content in the soil tends to approach field capacity during moisture redistribution. One of the objectives of drip irrigation is to maintain the soil moisture content between field capacity and 50 percent available soil moisture. Therefore, further investigations were carried out by keeping the Θ_{in} at field capacity. The physical properties of each of the sites were used keeping all other parameters constant in each of the simulations.

Two types of emitters were studied: (1) discharge from an emitter at the center, (2) discharge from a circular loop emitter.

A circular loop emitter was placed at the 0.3 m from an apple tree. To simulate moisture migration from the circular loop emitter using the model, the origin of input in the simulation process was shifted to the ring (4,1). The excess water after infiltration moves out to either side of the rings (3,1) and (5,1). The simulation were carried out for two days with a daily PET of 4.5 $mm.day^{-1}$. The irrigation application of 12.0 liters of water at the rate of 2.0 $L.h^{-1}$ was started at midday on the second day. The results of each of the research sites thus obtained are presented and compared.

6.7.1 Point Source versus Circular Loop Source

The distribution of water input at the termination of simulation is presented in Figures 6.16, and B.58 to B.61. The discharge from a point source gave high water input at the center which resulted in a loss of water below the root zone. The discharge from the loop emitter gave fairly even distribution with some gain of water due to upward flux into the root zone. Therefore, it is possible to apply larger amounts of water with the circular loop source emitters without loosing water below the root zone and wetting larger areas around growing trees.

In addition to the above investigations, a circular loop emitter was placed o.42 m, instead of 0.3 m, away from the tree in Rockburn

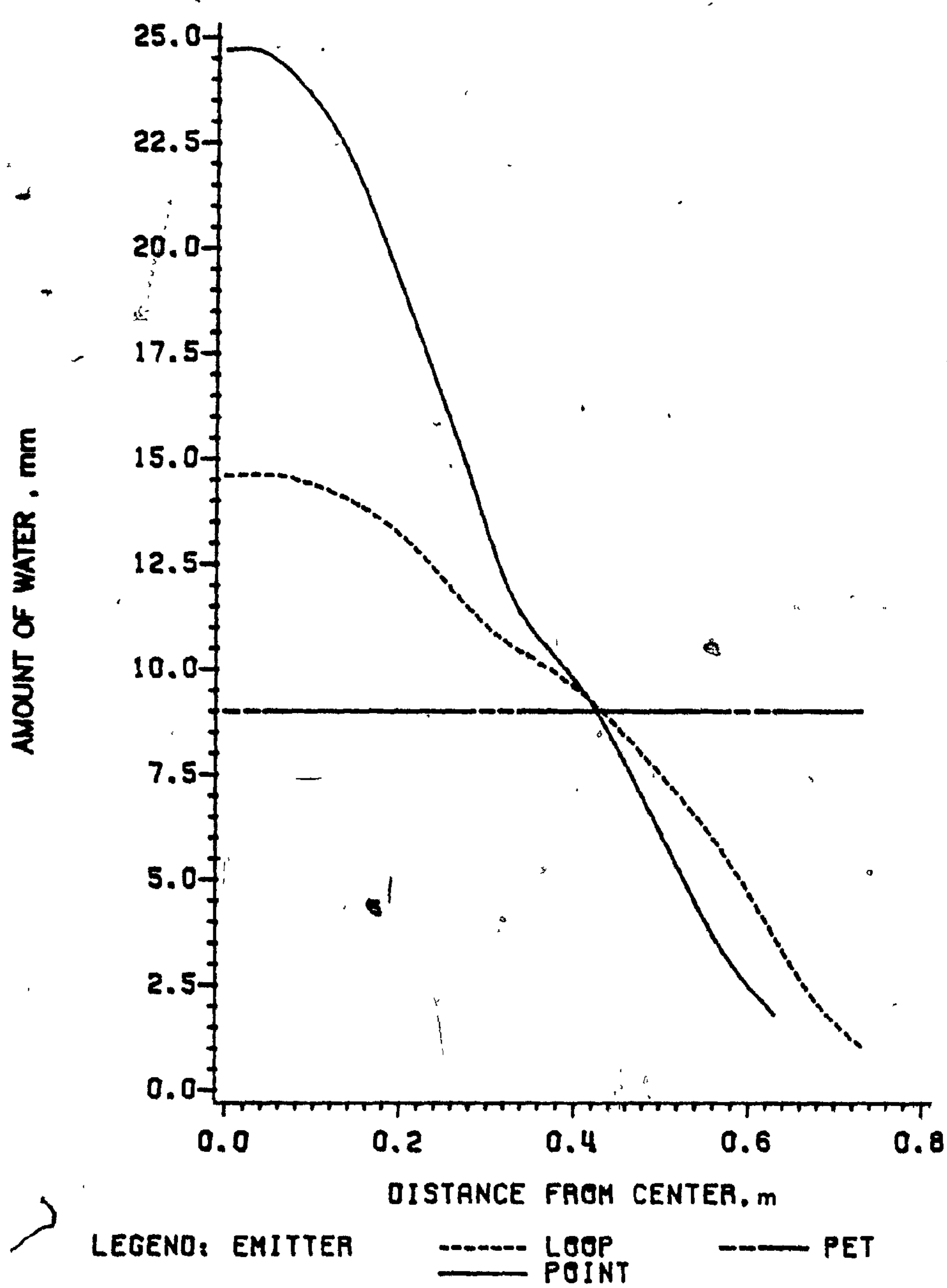

Figure 6.16. Water input predicted along horizontal distance with an irrigation application of 12 L from a point and a circular loop source for Rougemont orchard site 1.

field 1. Figure B.60 shows that an emitter at o.42 m away from the tree gave a wider wetted area. However, the water input predicted for the emitter with a larger radius of application was a little lower than the PET. Thus, further increase in the radius of application of a loop emitter may not provide enough moisture close to the tree in the field without increasing the amount of irrigation water.

6.7.2 Research Site versus Soil Moisture Migration

The results of theoretical investigations conducted for the five research sites are compared. Irrigation from a point and a circular source is considered. The results are summarized in Table 6.6. Water input along the horizontal distance obtained from a point source and a circular loop source is presented in Figures 6.17 and 6.18 respectively. The results show that the distribution of water is not only dependent on the K_s value but also on the soil moisture characteristics. The soil moisture characteristics (Figures 4.1 and 4.2) as well as the predicted soil moisture distribution for the Rockburn field 1 and Rougemont field 1 are similar. On the other hand, the soil moisture migration for the Rockburn field 1 and Rougemont field 1 is wider than that for Rougemont field 3. This is due to the coarser texture and higher hydraulic conductivity of the soil at Rougemont field 3.

The soil moisture content remained high close to both types of sources at Rockburn field 2 and Rougemont filed 2. The unsaturated hydraulic conductivity values reduce tremendously with a small

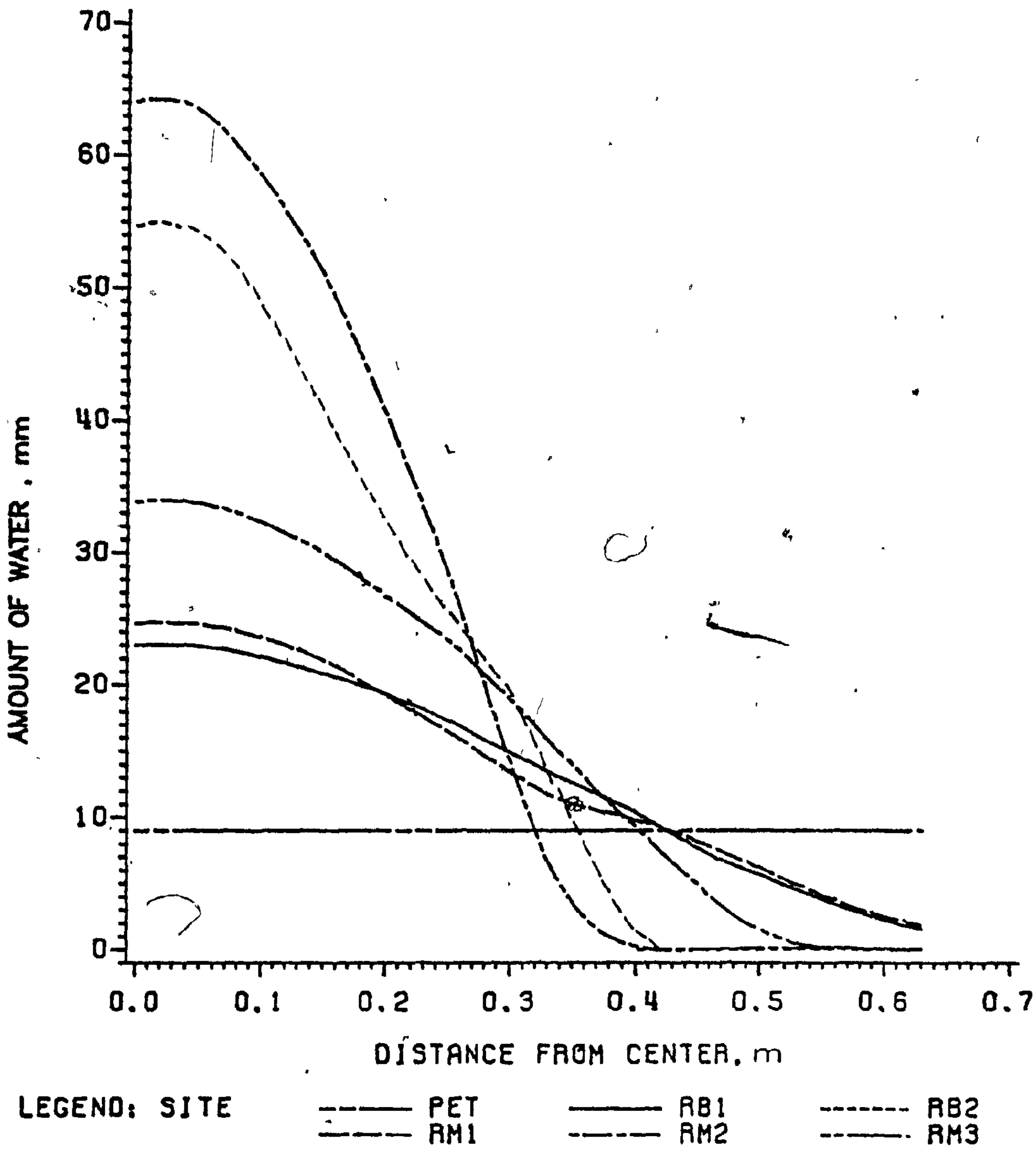

Figure 6.17. Water input predicted along horizontal distance with an irrigation application of 12 L from a point source for the five research sites.

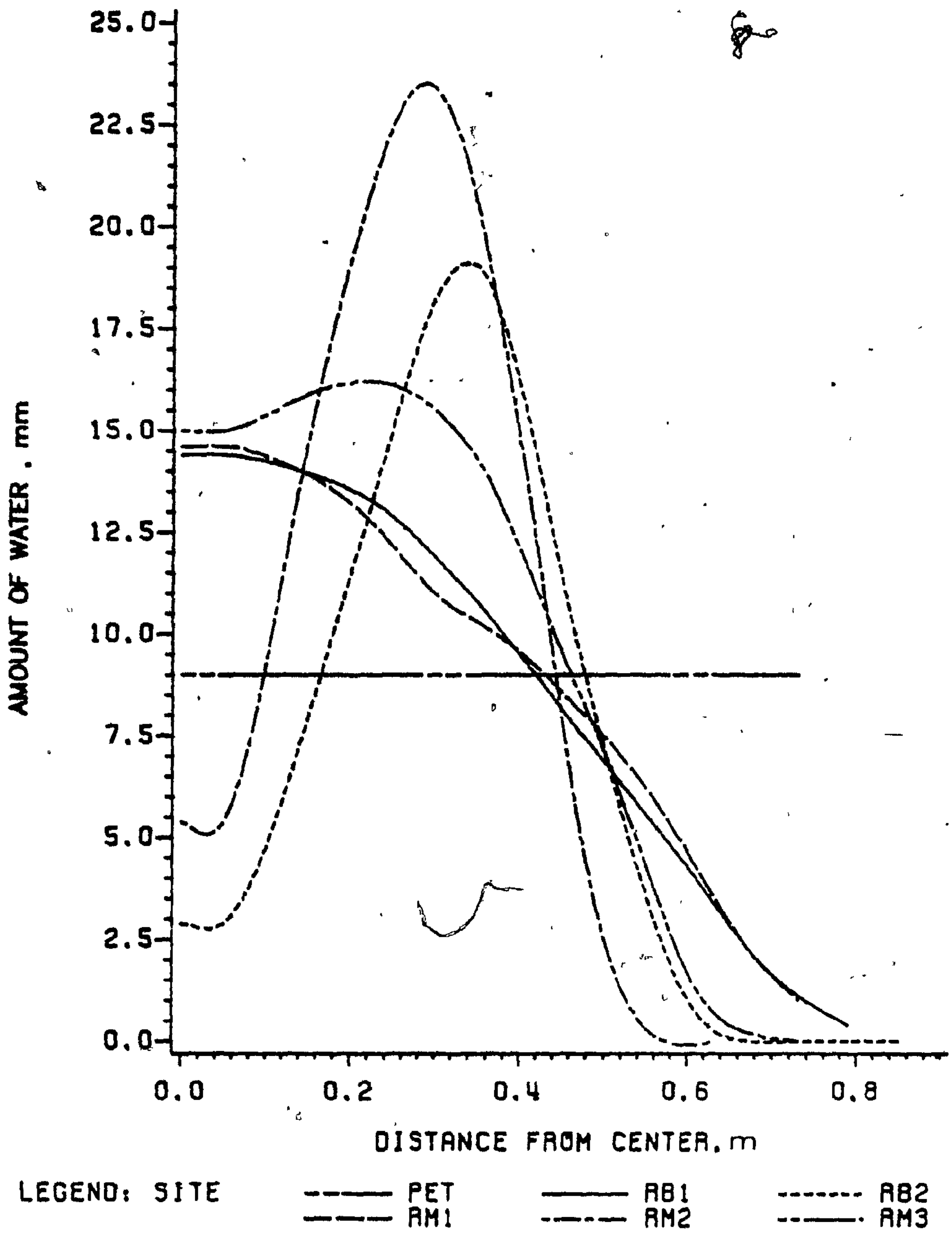

Figure 6.18. Water input predicted along horizontal distance with an irrigation application of 12 L from a circular loop source for the five research sites.

Table 6.6. Summary of simulation results obtained with 12 L of water application from a point and a circular source for the five research sites.

Rougemont Orchard Site 1

Source	Point	Circular loop
Replenished R (m)	0.42	0.43
Replenished Z (m)	0.90	0.36
Area (m^2)	0.56	0.58
RWE (%)	41.9	43.5
Storage (%)	9.8	17.7
Loss (%)	17.5	-6.1
Input WRA (%)	69.2	55.1
Input BRA (%)	29.9	44.3
Simulated (%)	99.1	99.4
Error (%)	0.9	0.6
Total (%)	100.0	100.0

Rougemont Orchard Site 2

Source	Point	Circular loop
Replenished R (m)	0.32	0.44
Replenished Z (m)	0.66	0.36
Area (m^2)	0.32	0.62
RWE (%)	24.5	46.6
Storage (%)	61.8	44.0
Loss (%)	7.5	-0.6
Input WRA	93.8	90.0
Input BRA (%)	3.5	9.5
Simulated (%)	97.3	99.5
Error (%)	0.7	0.5
Total (%)	100.0	100.0

continued...

Table 6.6 continued .....

Rougemont Orchard Site 3		
Source	Point	Circular loop
Replenished R (m)	0.40	0.46
Replenished Z (m)	0.86	0.60
Area (m^2)	0.51	0.67
RWE (%)	38.3	50.2
Storage (%)	41.6	29.7
Loss (%)	7.2	-2.0
Input WRA	87.1	77.9
Input BRA (%)	12.0	21.6
Simulated (%)	99.1	99.5
Error (%)	0.9	0.5
Total (%)	100.0	100.0

Rockburn Orchard Site 1		
Source	Point	Circular loop
Replenished R (m)	0.42	0.42
Replenished Z (m)	> 0.90	0.60
Area (m^2)	0.57	0.55
RWE (%)	42.5	41.5
Storage (%)	32.0	21.1
Loss (%)	-2.0	-7.6
Input WRA	72.5	55.0
Input BRA (%)	26.7	44.4
Simulated (%)	99.2	99.4
Error (%)	0.8	0.6
Total (%)	100.0	100.0

continued...

Table 6.6 continued .....

	Rockburn Orchard Site 2	
Source	Point	Circular loop
Replenished R (m)	0.35	0.48
Replenished Z (m)	0.60	0.36
Area (m^2)	0.38	0.73
RWE (%)	29.0	54.8
Storage (%)	62.9	30.2
Loss (%)	-0.9	-1.5
Input WRA	91.0	83.5
Input BRA (%)	6.7	15.9
Simulated (%)	97.7	99.4
Error (%)	2.3	0.6
Total (%)	100.0	100.0

decrease in moisture content as shown in Figure 4.2. This caused slow movement of water in the soil and the moisture content remained at its high value close to an emitter. The problem of saturation thus would occur under the emitter in the soils having similar properties. Therefore, placement of an emitter close to the tree should be avoided at these sites.

6.7.3 Amount of Irrigation Water versus Replenished Area

As pointed out in previous discussions, the soil moisture migration is not dependent on the rate of irrigation application or the method of application. The conditions and the parameters used for the simulations with 12, 16 and 24 L of water are similar and are given in Table 4.1. Thus, the results obtained with different amounts of water are compared and discussed. The results show that the replenished area and loss of water below root zone increases with the increase in the amount of irrigation application. The increase in the replenished area is not proportional to the increase in the amount of water. There seems to be some relationship between the amount of water and the area replenished. The relationship between replenished area and amount of water can be expressed as:

$$A_2 = A_1 \sqrt{TQ_2 / TQ_1} \qquad \text{.... (6.1)}$$

where TQ is the total amount of irrigation water, L

A is the replenished area, m

Subscripts 1 and 2 refer to the amount of water and the corresponding replenished area.

In comparing the resulting replenished areas with different amounts of water the relationship developed in Eq. 6.1 is necessary to have similar conditions for different amounts of irrigation water. Also, this relationship holds within the volumes of water tested as shown in Table 6.7.

6.8 Sensitivity Analysis

The effects of the various parameters on the soil water migration were studied to examine the sensitivity of the simulation model. The parameters and their values used in this analysis are listed in Table 6.8. The results obtained at the termination of the simulation runs are presented and discussed.

6.8.1. Mesh Size in R-Direction

The mesh size was changed to 0.05 and 0.08 m. The variable mesh size was also examined. The mesh sizes starting from an emitter to the outer boundary, in order, were: 0.02, 0.04 0.08, 0.10, 0.06, 0.04, 0.06, 0.06, and 0.06 m. The distribution of irrigation water input along R and Z directions is presented in Figures B.62 and B.63 respectively. The summary of water distribution results is presented in Table 6.8. The Figures and the Table show that the distribution of water in the soil is similar with various mesh sizes.

Table 6.7 Replenished areas (m^2) predicted with different volumes of irrigation water and time equivalent to 12-hours AMT

Site	Volume of Water (L)		
	12	16	24
Rougemont Orchard Site 1	0.70	0.81	1.0
Rougemont Orchard Site 2	0.40	0.46	-
Rougemont Orchard Site 3	0.74	0.84	-
Rockburn Orchard Site 1	-	1.28	1.58
Rockburn Orchard Site 2	0.52	0.60	-

Table 6.8. Summary of simulation results obtained for sensitivity of mesh size.

	Radial Direction			
Mesh Size (m)	0.05	0.06	0.08	Variable
Replenished R (m)	0.50	0.50	0.51	0.50
Replenished Z (m)	0.85	0.85	0.85	0.83
Area (m^2)	0.77	0.78	0.83	0.78
RWE (%)	22.7	23.1	24.5	23.2
Storage (%)	49.0	48.6	48.8	49.2
Loss (%)	25.3	24.5	22.6	22.3
Input WRA (%)	97.0	96.2	95.9	94.6
Input BRA (%)	2.5	3.4	3.9	3.3
Simulated (%)	99.5	99.6	99.7	97.9
Error (%)	0.5	0.4	0.3	2.1
Total (%)	100.0	100.0	100.0	100.0

	Vertical Direction		
Mesh Size (m)	0.05	0.06	0.08
Replenished R (m)	0.50	0.50	0.50
Replenished Z (m)	0.85	0.85	0.86
Area (m^2)	0.78	0.78	0.78
RWE (%)	23.1	23.1	23.0
Storage (%)	48.9	48.6	48.6
Loss (%)	24.1	24.5	24.6
Input WRA (%)	96.1	96.2	96.3
Input BRA (%)	3.5	3.4	3.4
Simulated (%)	99.5	99.6	99.7
Error (%)	0.5	0.4	0.3
Total (%)	100.0	100.0	100.0

6.8.2 Mesh size Z-direction

The mesh size was changed to 0.05 and 0.08 m. The input of irrigation water along the R and Z direction is presented in Figures B.64 and B.65. The summary of ressults is given in Table 6.8. The Figures and the Table indicate that the distribution of water in the soil is similar.

To accomodate the soil moisture migration various PET and initial moisture content values, within the same finite soil, the base values of the total irrigation water was changed to 12.0 litres in the sensitivity analysis of the remaining parameters.

6.8.3 Hydraulic conductivity

The K values were changed to 3.56 and 5.14 $m.day^{-1}$. Unsaturated K values were calculated using the soil moisture retention curve of Rougemont orchard site 1. The distribution of water input along the R and Z directions are presented in Figures B.66 and B.67. The Figures indicate that the moisture migration is faster in the R and Z direction with higher K values when compared to lower values. However, the moisture migration obtained at 12 hours after the start of irrigation with a K value of 5.1396 $m.day^{-1}$ when compared to the moisture migration obtained at 15 hours after start of irrigation with K value of 3.56 $m.day^{-1}$ show no difference in water input in the R (Figure B.66) or Z (Figure B.67) direction. This indicates that the K values with the same soil moisture characteristic curve do not influence the soil migration patterns. Water moves faster with higher K values when compared with lower K values. The results obtained from other soils having different soil moisture characteristics are discussed in previous sections. The results indicate that the moisture migration is dependent on the soil moisture characteristics rather than only on the saturated hydraulic conductivity.

3.8.4 Rate of irrigation application

The effects of various rates of irrigation applications of irrigation water were examined in previous sections. The results indicate that the moisture migration was independent of emitter discharge rates.

3.8.5 Amount of irrigation water

The total water input was changed to 16 and 24 liters. Since it is evident from the results obtained with various application rates that the moisture migration is independent of emitter discharge rate, the total water in all these cases was applied within the same period of 6.0 hours. The input of water along R and Z directions is presented in Figures 6.19 and 6.20 respectively. A summary of simulation results is presented in Table 6.9. The Figures and the Table indicate that the higher amount of irrigation water gave wider and deeper migration of soil moisture when compared to the lower amounts of irrigation water applications. The migration of soil moisture is dependent on total quantity of irrigation water rather

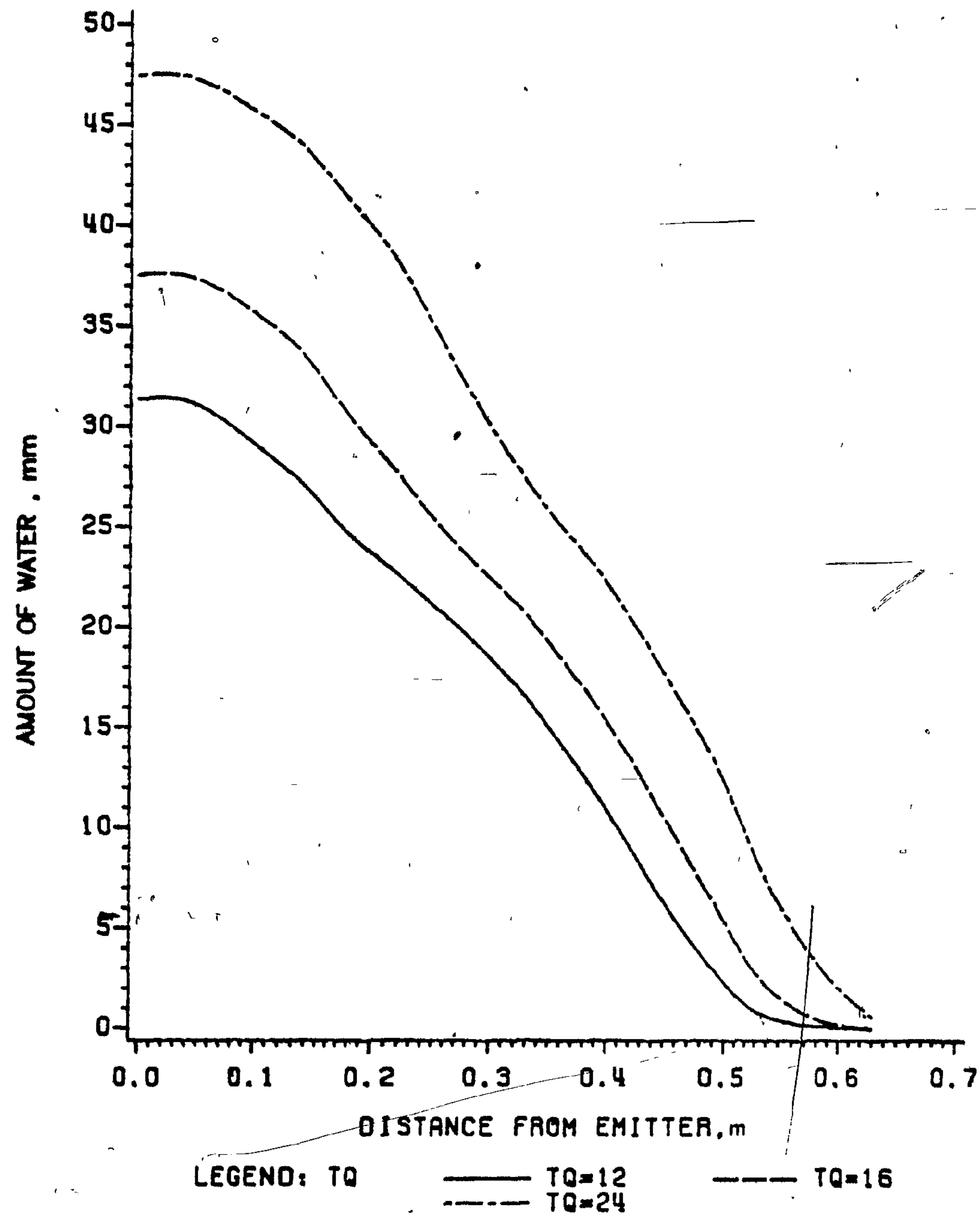

Figure 6.19. Water input predicted along horizontal distance with irrigation applications of 12, 16 and 24 L.

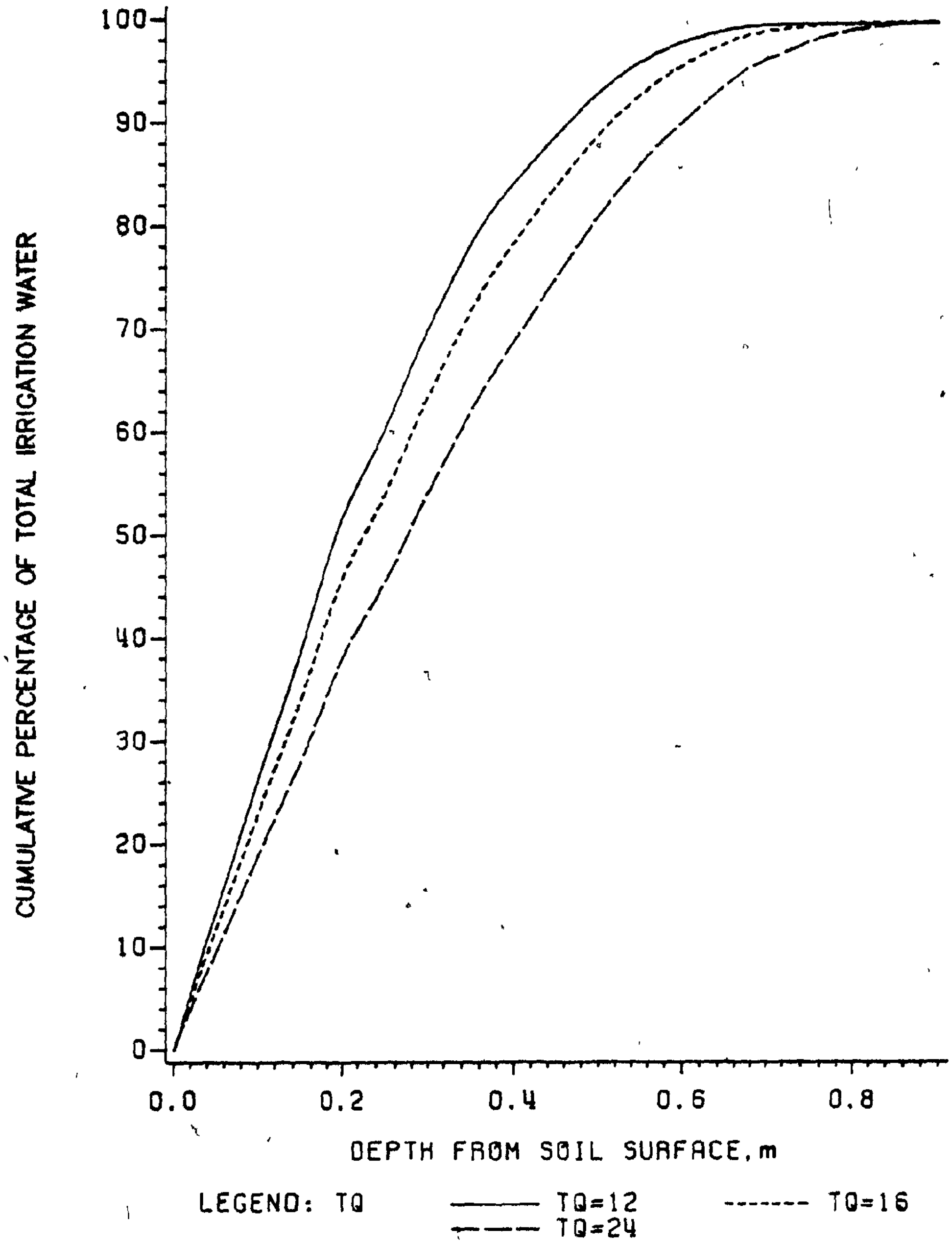

Figure 6.20. Water input predicted in soil profile with irrigation applications of 12, 16 and 24 L.

than on the rate of irrigation application.

The higher amount of water gave higher water input along the radial and vertical directions. Figure 6.20 shows that the higher percentage of total irrigation water was obtained with a lower amount of water at the same depth. Thus, the loss of water increases with an increase in the amount of water. The replenished area increases with an increased amount of water input.

6.8.6 Root zone depth

The root zone depth was changed to 0.48 and 0.60 m respectively. The irrigation water input along the R and Z directions is presented in Figures B.70 and B.71. The Figures show that the distribution of irrigation water in both directions is similar with different root zone depths. The loss of water decreases with the increase in root zone depth. This is due to the fact that the loss of water is considered beyond the specified root zone depth.

6.8.7 Initial soil moisture content

The initial moisture content was changed to 0.07 and 0.10 $m^3.m^{-3}$. The input of irrigation water along R and Z directions is presented in Figures 6.21 and 6.22 respectively. The Figures indicate that the amount of water retained near the emitter was higher with lower initial moisture content. The migration of moisture was wider and deeper with high initial soil moisture content.

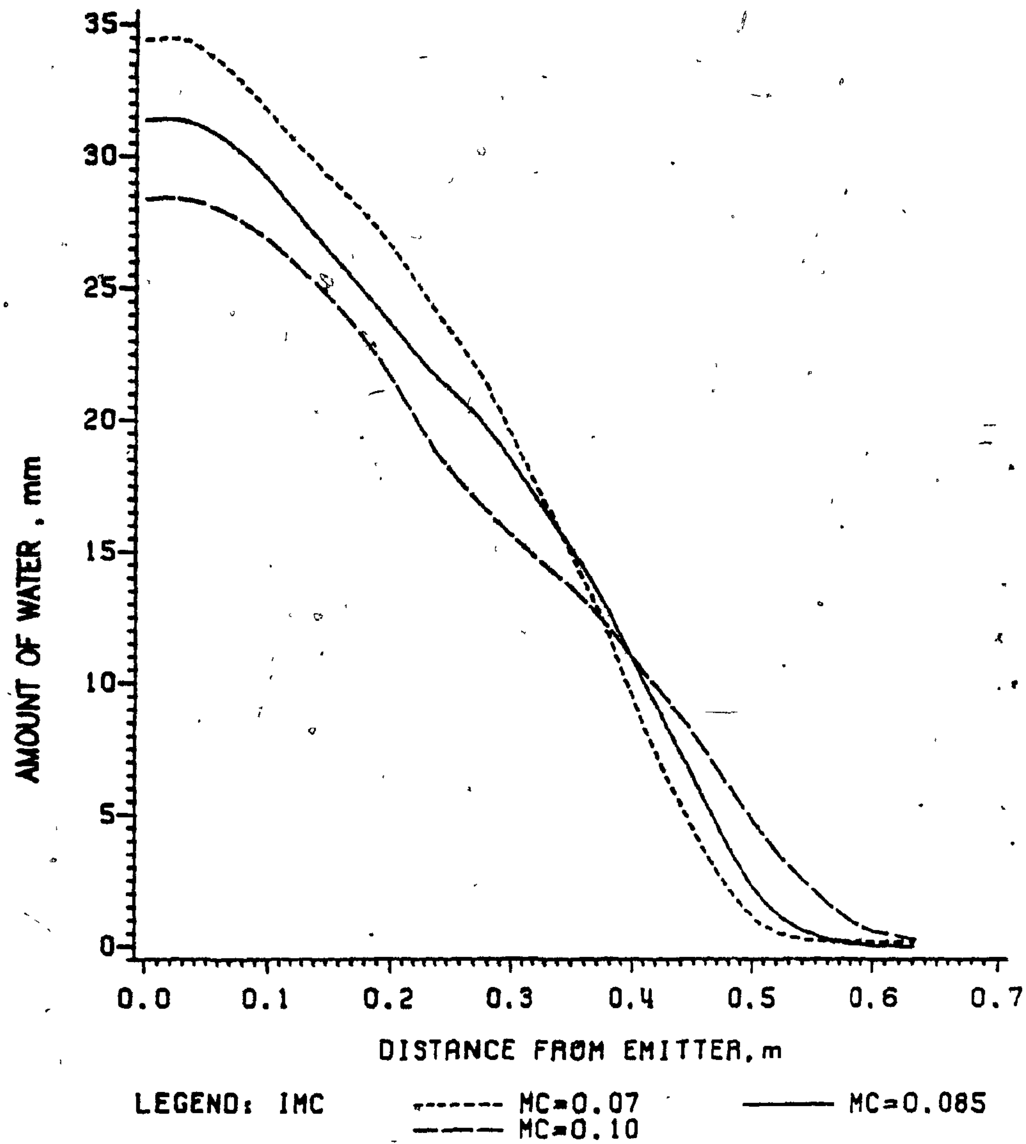

Figure 6.21. Water input predicted along horizontal distance with an irrigation application of 12 L and different initial soil moisture contents.

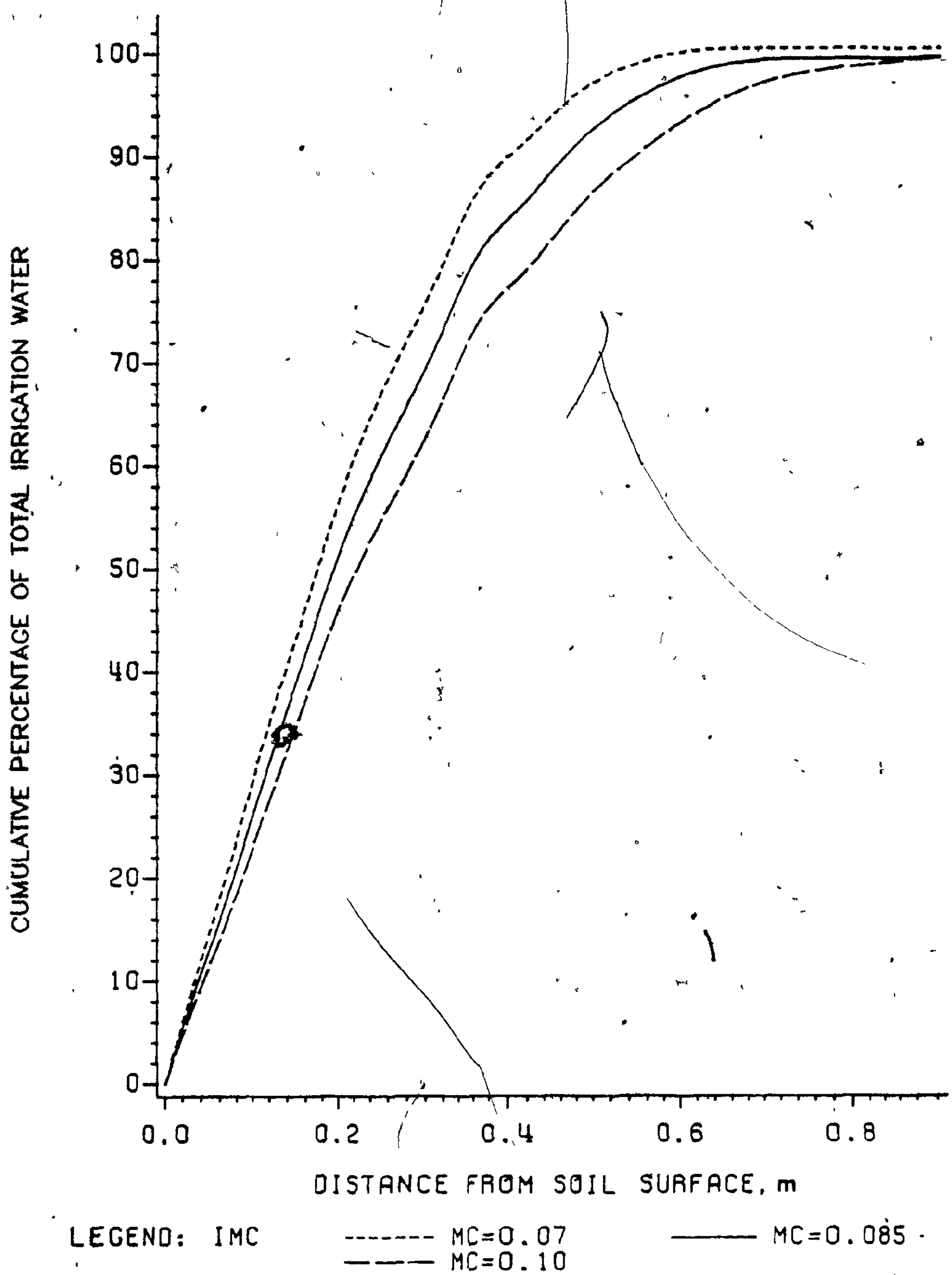

Figure 6.22. Water input predicted in soil profile with an irrigation application of 12 L and different initial soil moisture contents.

6.8.8 Daily evapotranspiration.

The daily PET values were changed to 0.0, 2.5 and 7.5 mm. The irrigation water input along the R and Z directions is presented in Figures B.72 and B.73 respectively. The summary of water distribution is presented in Table 6.9. The Figures and the Table indicate that the moisture migration was wider and deeper with low PET values when compared to the high PET values. This is due to the fact that the amount of water available to migrate into the soil was higher when PET values were lower.

6.8.9 Volume of soil ring

The volume of all the soil rings was maintained. The mesh size in Z direction and all other parameters were held unchanged. The mesh size in the R direction and the radius of the soil cylinder were changed to accomodate the same volume of each soil ring. The distribution of water along R is presented in Figure 6.23. The summary of water distribution is presented in Table 6.9. The Figure shows lower water input under the emitter with constant volume soil rings. By keeping the volume constant the width of inner most ring is greater when compared to the variable volume soil rings with constant mesh size. The saturation zone in this case probably was not large enough and the average of the input over larger area reduced the water input. However, the replenished area obtained with both treatments is the same as shown in Table 6.9.

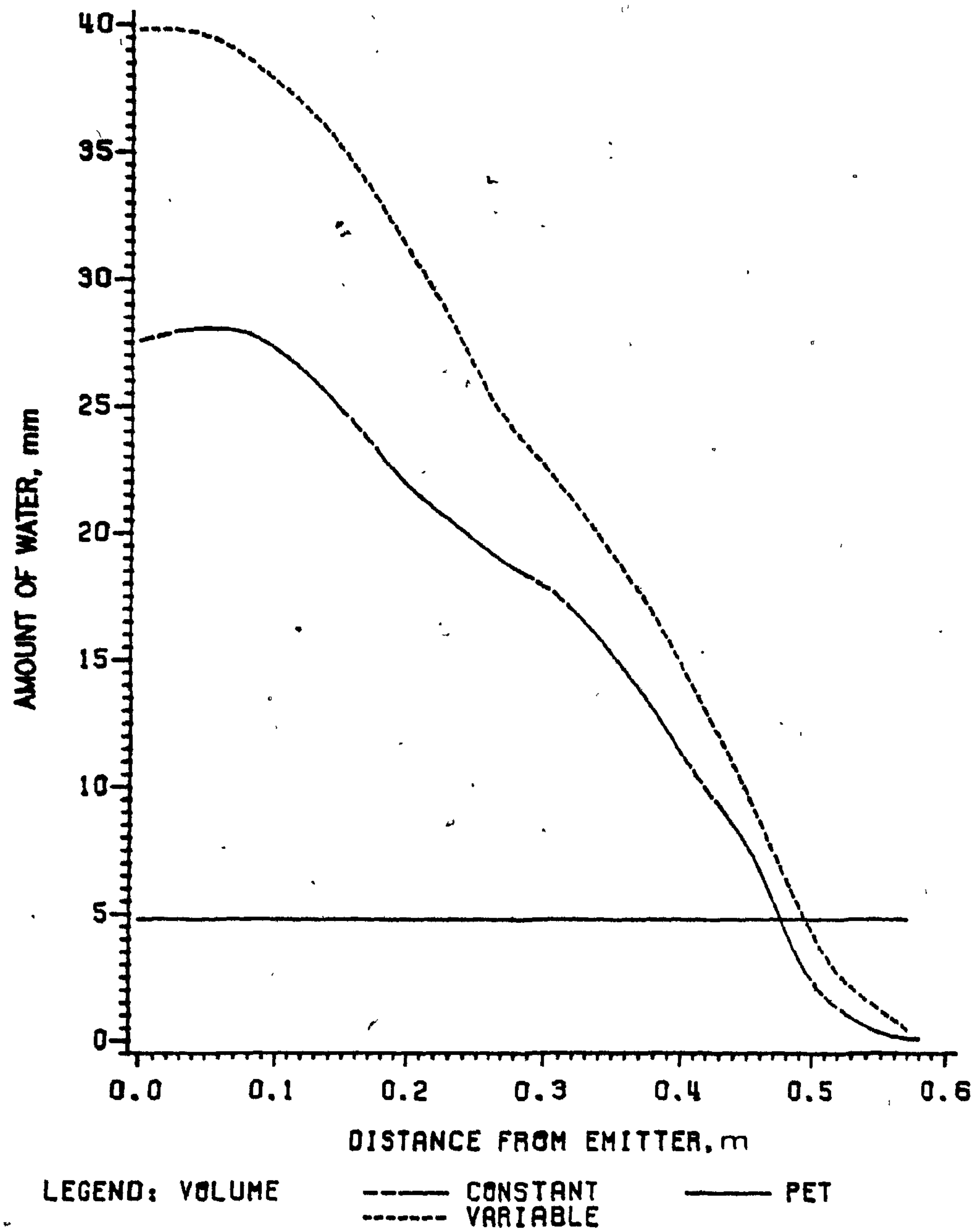

Figure 6.23. Water input predicted along horizontal distance with an irrigation application of 12 L using constant and variable volume soil rings.

Table 6.9. Summary of simulation results obtained for sesititivity of various parameters.

	Hydraulic Conductivity		
K_s ($m^1.day^{-1}$)	3.56	4.35	5.14
Replenished R (m)	0.46	0.47	0.48
Replenished Z (m)	0.79	0.79	0.84
Area (m^2)	0.67	0.70	0.72
RWE (%)	26.5	27.5	28.5
Storage (%)	49.3	47.4	45.6
Loss (%)	19.4	20.3	21.1
Input WRA (%)	95.3	95.3	95.1
Input BRA (%)	4.2	4.2	4.3
Simulated (%)	99.5	99.5	99.5
Error (%)	0.5	0.5	0.5
Total (%)	100.0	100.0	100.0

	Amount of Water		
TQ (L)	16.0	12.0	24.0
Replenished R (m)	0.51	0.47	0.57
Depth (m)	0.85	0.79	> 0.90
Area (m^2)	0.81	0.70	1.0
RWE (%)	23.9	27.5	19.8
Storage (%)	45.4	47.4	41.3
Loss (%)	26.4	20.3	35.9
Input WRA (%)	95.7	95.3	96.9
Input BRA (%)	3.8	4.2	2.7
Simulated (%)	99.5	99.5	99.6
Error (%)	0.5	0.5	0.4
Total (%)	100.0	100.0	100.0

continued...

Table 6.9 continued......

	Root Zone Depth		
Depth (m)	0.48	0.36	0.60
Replenished R (m)	0.47	0.47	0.47
Replenished Z (m)	0.79	0.79	0.79
Area (m^2)	0.70	0.70	0.71
RWE (%)	27.8	27.5	27.9
Storage (%)	59.9	47.4	65.9
Loss (%)	7.4	20.3	1.1
Input WRA (%)	95.1	95.3	94.9
Input BRA (%)	4.4	4.2	4.5
Simulated (%)	99.5	99.5	99.5
Error (%)	0.5	0.5	0.5
Total (%)	100.0	100.0	100.0

	Initial Soil Moisture Content		
IMC $m^3.m^{-3}$	0.07	0.085	0.10
Replenished R (m)	0.47	0.47	0.50
Replenished Z (m)	0.73	0.79	> 0.90
Area (m^2)	0.68	0.70	0.78
RWE (%)	24.6	27.5	31.2
Storage (%)	57.3	47.4	34.8
Loss (%)	15.0	20.3	26.5
Input WRA (%)	96.9	95.3	92.5
Input BRA (%)	3.4	4.2	7.0
Simulated (%)	100.3	99.5	99.5
Error (%)	-0.3	0.5	0.5
Total (%)	100.0	100.0	100.0

continued...

Table 6.9 continued....

	Daily Potential Evapotranspiration			
PET (mm)	0.0	2.5	5.0	7.5
Replenished R (m)	0.64	0.51	0.47	0.43
Replenished Z (m)	0.82	0.80	0.79	0.79
Area (m^2)	1.29	0.83	0.70	0.59
RWE (%)	0.0	16.5	27.5	35.1
Storage (%)	72.9	67.7	47.4	38.8
Loss (%)	26.5	23.2	20.3	17.8
Input WRA (%)	99.5	97.2	95.3	91.7
Input BRA (%)	0.0	2.3	4.2	7.8
Simulated (%)	99.5	99.5	99.5	99.5
Error (%)	0.5	0.5	0.5	0.5
Total (%)	100.0	100.0	100.0	100.0

	Volume of Soil Ring	
Volume of each ring (m^3)	0.0061	Variable
Simulated Area (m^2)	1.12	1.37
Replenished R (m)	0.48	0.47
Replenished Z (m)	0.73	0.79
Area (m^2)	0.72	0.70
RWE (%)	28.3	27.5
Storage (%)	51.6	47.4
Loss (%)	15.9	20.3
Input WRA (%)	95.8	95.3
Input BRA (%)	4.0	4.2
Simulated (%)	99.8	99.5
Error (%)	0.2	0.5
Total (%)	100.0	100.0

CHAPTER VII

SUMMARY

A computer model based on the principle of mass conservation and Darcy's law was formulated using the Continuous System Modeling Program (CSMP) to study the soil moisture migration from a drip source under supplementary irrigation conditions considering root water extraction (RWE). The RWE was assumed to be equal to evapotranspiration (ET) and was considered as a function of soil moisture content, depth of root zone and the time of the day.

The soil properties needed for the model are unsaturated hydraulic conductivity as a function of moisture content and the moisture retention characteristics. To estimate the ET, the temperatures, the latitude and the time of the day of the location are needed. The RWE patterns with respect to the depth from the soil surface are also required.

The field experiments were conducted with predetermined rates and amounts of water applied continuously from a point source on five different soils in newly-developed dwarf-apple orchards located in southwestern Quebec. The soils were sandy and sandy loam. Undisturbed soil samples were taken to determine the bulk density, hydraulic conductivity, and soil moisture retention characteristics. The soil samples were taken from the soil profile before and immediately after irrigation application to determine moisture content by the gravimetric

method.

The model was solved using axisymmetric soil volumes. The soil was assumed to be homogeneous, isotropic and non-swelling. Hysteresis was not considered. No flow conditions across the boundaries of the finite soil cylinder were fixed. The root zone depth was specified at the interface between the soil rings along the horizontal direction. The initial soil moisture contents in the soil profile were considered to form horizontal moisture planes and were specified at the center of the rings. The simulations were continued after the cessation of irrigation until the time equivalent to an arbitrary 12-hour AMT (actual migration time for the total irrigation water).

The soil moisture contents in the soil profile predicted with this model were compared with the observed data and good agreement was found. The sensitivity of the model to the rate of emitter discharge, amount of water, initial moisture content, hydraulic conductivity, root zone depth, amount of RWE was examined. It was found that the distribution of soil moisture is dependent on the amount of water, the soil moisture retention characteristics, the initial moisture content and the amount of RWE. It is independent of emitter discharge rate and root zone depth.

CHAPTER VIII

CONCLUSIONS

Based on the results of this investigation the following conclusions were drawn:

1. The model can be used to predict soil moisture migration in the soil in the presence of, or without an apple tree.
2. The soil moisture retention characteristic curve is the basic requirement for generating data for designing a drip system. Parameters such as potential evapotranspiration, root zone depth and others can be estimated. The functions of unsaturated hydraulic conductivity versus moisture content, root zone depth versus root water extraction fraction and moisture content vs AET/PET can be derived or estimated.
3. The moisture content profiles simulated and observed were in close agreement with each other. This indicates that this model is reliable for predicting moisture migration from a drip source.
4. The loss of water increased with the increase in the amount of water applied. Higher amounts of water gave wider and deeper migration of water in the soil.
5. The loss of water tends to increase with a decrease in the discharge rate but this minor difference did not affect the general pattern of moisture distribution.

6. The soil moisture distributions obtained with mesh sizes ranging from 0.05 to 0.08 m and variable mesh size were in close agreement with each other. The larger mesh size simulations tend to show less water input under the emitter. When the volume of the rings was held constant the large mesh size close to the emitter gave lower water input when compared to the simulations with constant mesh sizes. Therefore, the large mesh size especially close to the emitter should be avoided.

7. The water input is not evenly distributed along the horizontal distance from the emitter when the discharge from a point source is considered. There is loss of water below root zone and temporary saturation under the emitter.

8. The circular loop emitter when compared to the point emitter gave better water input distribution and no loss of water below root zone.

9. The wetting front moves as a step function of horizontal distance from the vertical axis passing through the emitter and the vertical distance from the soil surface. The step size is equivalent to the mesh size.

10. At an arbitrary actual migration time (AMT) of 12-hours for total irrigation water, there was no difference in width or depth and iso-soil moisture content curves obtained at different discharge rates for the same amount of water.

11. The distribution of water is dependent on the amount of water applied, but it is independent of the rate of its application.

12. The migration of soil water depends on the initial soil moisture content.

13. The moisture migration is not dependent on the root zone depth.

14. The percentage of irrigation water stored within the root zone is higher with lower amounts of water application.

15. The net amount of water available for wetting and redistribution in the soil is the result of the amount of water input by irrigation, the initial moisture content, and depletion due to root water extraction. Consequently, the distribution of moisture would be according to the net amount of water available in the soil.

16. The moisture content in the soil tends to approach field capacity

17. The simulation accounts for more than 97 percent of the total irrigation water.

18. The relationship between wetted area and total amount of irrigation water applied can be represented by:

$$A_2 = A_1 \sqrt{TQ_2 / TQ_1}$$

where TQ is the total amount of water, L ; A is the replenished area, m^2. Subscripts 1 and 2 refer to the amount of water and the corresponding replenished area.

19. The pulse irrigation results are similar to continuous irrigation application when compared to its average (half) discharge rate. Thus, the pulse irrigation is a method of application to reduce the discharge rate with high discharging emitters.

To summarize, the soil moisture distribution from a point source is dependent on the amount of water remaining in the soil and soil moisture retention characteristics. It is independent of the root zone depth, and of the rate or method of water application.

CHAPTER IX

CONTRIBUTION TO KNOWLEDGE

The application of drip irrigation to irrigated agriculture is a recent development in Quebec. It is being used in dwarf-apple orchards and for vegetable and other small fruit production. Although investigations have been carried out previously on drip irrigation under laboratory and arid field conditions, the results cannot be applied to the climatic conditions exsisting in the province of Quebec.

In this work a simulation model has been developed to predict soil moisture migration from drip sources in the orchards. The root water extraction term and emitter discharge combined with the flow equation has been solved using the concept of mass conservation and Darcy's law. A macroscopic approach has been used to estimate the root water extraction term. The model is formulated using the Continuous System Modeling Program (CSMP).

The combination of Darcy's law, the concept of mass conservation and the RWE term as a function of θ, Z and t has not been used before, especially under the conditions prevailing in humid areas. Also, no work has been reported on the prediction of soil moisture distribution from a pulse method of drip irrigation.

In previous studies, the initial soil moisture has been assumed to be uniform throughout the finite soil volume. In this study, the initial soil moisture was considered to be uniform with respect to the radial distance from the emitter, but to be variable vertically in the soil profile due to rainfall, evaporanspiration and drainage.

This thesis contributes to the knowledge of drip irrigation as follows:

1. A simulation model was developed to predict soil moisture distribution from a point source for irrigation of dwarf-apple trees.
2. The root water extraction term as a function of θ, Z and t is defined.
3. After rainfall the moisture content is considered to be the same with respect to the horizontal direction from an emitter, but it varies vertically in the soil profile. Thus, the moisture content observed in the soil profile before the start of experiments has been used for simulations.
4. The model is formulated to accept variable and constant mesh sizes.
5. The concept of a replenished wetting front is proposed and is used and investigated.
6. The concept of actual migration time for the total irrigation water (AMT) has been defined and used to study the soil moisture migration for different discharge rates, and methods of irrigation application.
7. The simulations were continued after the termination of irrigation until a time equivalent to the 12-hours AMT which allows sufficient time for redistribution of soil moisture.
8. The simulations have been done for the continuous and pulse methods of drip irrigation application and the results have been compared.

9. The empirical relation between initial replenished area obtained with a certain amount of water and a subsequent replenished area obtained with a different amount of water was found.

10. The moisture migration within a finite soil volume depends on the final amount of water (SWA_{fi}) which can be determined from the following relationship:

$$SWA_{fi} = SWA_{in} + TQ - RWE ,$$

where SWA_{in} is the initial amount of water in soil; TQ is the total amount of water applied; RWE is the root water extraction.

11. The storage of water within the root zone, the loss of water beyond the root zone, and the root water extraction are estimated.

12. The soil moisture migration from a circular loop emitter is predicted and compared with that obtained from a point source.

CHAPTER X

SUGGESTIONS FOR FUTURE RESEARCH

The simulation model developed in this study can be used to predict soil moisture distribution from a point source under homogeneous conditions. In the field the soil is seldom homogeneous. The soil properties vary within the soil profile. The root water extraction (RWE) patterns, as a function of depth, are required for this model. The RWE patterns may differ in the layered soils. Also, the properties of soil containing roots differ from the soil with no roots. This model does not differentiate between the two soil conditions. It is recommended that research be done on layered soils to study the root water extraction patterns so that the model can be modified to be applicable to layered soils.

This model considers the moving boundary as a step function of the distance from an emitter, the step being equal to the mesh size. Additional research should be done to account for the moving boundary conditions as a function of soil moisture content at least for saturation under the emitter. This can be done by developing a model which permits the use of varying mesh sizes during simulation.

The model should be modified to account for soil heterogeneity and anisotropy to increase the accuracy of the simulated results. Also, the effects of cloud cover during the day-time and hysteresis on the soil moisture migration need to be considered in further research.

Simulation studies should be carried out to study the distribution of irrigation water considering overlapping of wetting fronts from adjacent emitters. The distance between emitters should be determined when the distribution of soil moisture from a point source is the same as that from a line source irrigation water application.

Research is needed to study the moisture migration from a circular loop source and its placement with respect to a tree. Further studies are needed for the developement of circular loop emitters which can meet the irrigation needs of a tree. Also, research should be conducted to study the potential of circular loop emitters in the development of new orchards.

Drip irrigation from a point source is applied to vegetable crops cultivated in rows under controlled conditions in greenhouses in Quebec. Under these conditions the information on the estimation of evapotranspiration and RWE patterns is not available in the literature. Research in this field is required for the development of a model applicable to the greenhouse situation.

Under supplementary irrigation conditions the irrigation water requirement and the area to be irrigated are less than those required under dry conditions. The undulating topography of the orchards needs special care in designing an irrigation system for emitter discharge uniformity. Work is needed in order to determine the water requirements and the minimum area to be irrigated.

Clogging of emitters is observed by the farmers in the orchards and greenhouses. No study has been done in Quebec on the subject. It is suggested that the cause of the problem be determined and that research and development be carried out to alleviate the problem.

Fertilizers are applied through drip irrigation systems. From a point source water input to the soil under the emitter is high causing a temporary saturation and loss of water. Research is needed to study the distribution of fertilizers in soil with the irrigation system and its effect on root development and crop response.

REFERENCES

Armsrong C.F. and T.V. Wilson. 1983. Computer model for moisture distribution in stratified soils under a trickle source. Trans. Amer. Soc. Agr. Eng., 26:1704-1709.

ASAE Engineering Practice: ASAE EP405. 1983. Design, installation, and performance of trickle irrigation systems. Agricultural Engineers Handbook of Standards 1983. Amer. Soc. Agr. Eng., St. Joseph, MI.

Ashcroft, G., D.D. Marsh, D.D. Evans and L. Boersma. 1962. Numerical method for solving the diffusion equation, 1: Horizontal flow in semi-infinite media. Soil Sci. Soc. Amer. Proc., 26:522-525.

Ayers, H.D. 1965. Water deficit and irrigation needs in Ontario. Can. Agr. Eng., 7:37-39.

Baier, W. and G.W. Robertson. 1965. Estimation of latent evaporation from simple weather observation. Can. J. Plant Sci., 45:276-284.

Baier, W. and G.W. Robertson. 1966. A new versatile soil moisture budget. Can. J. Plant Sci., 46:299-315.

Baier, W. and G.W. Robertson. 1967. Estimating supplemental irrigation water requirements for climatological data. Can. Agr. Eng., 8:46-50.

Beek, J. and M.J. Frissel. 1973. Simulation of Nitrogen Behaviour in Soils. Center for Agricultural Publishing and Documentation, Wageningen, the Netherlands, 67p.

Beese, F, R.R. van der Ploeg and W. Richter. 1977. Test of a soil water model under field conditions. Soil Sci. Soc. Amer. J., 41:979-984.

Belmans, J, J. Feyen and D. Hillel. 1979. An attempt at experimental validation of macroscopic-scale models of soil moisture extraction by roots. Soil Sci., 127:174-186

Ben-Asher, J. 1979. Trickle irrigation timing and its effect on plant and soil water status. Agr. Water Manage., 2:225-232.

Ben-Asher, J., D.O. Lomen, and A.W. Warrick. 1978. Linear and nonlinear models of infiltration from a point source. Soil Sci. Soc. Amer. J., 42:3-6.

Bhattacharya, A.K. 1977. Hydrologic and Economic Models for Subsurface Drainage. Ph.D. thesis, McGill University, Montreal, Canada.

Bhuiyan, S.I., E.A. Hiler, C.H.M. van Bavel, and A.R. Aston. 1971. Dynamic simulation of vertical infiltration into unsaturated soils. Water Resour. Res., 7:1597-1606.

Brandt, A., E. Bresler, N. Diner, I. Ben-Asher, J. Heller, and D. Goldberg. 1971. Infiltration from a trickle source: I. Mathematical models. Soil Sci. Soc. Amer. Proc., 35:675-682.

Brennan, R.D. and M.Y. Silberberg. 1968. The System/360 continuous system modeling program. Simulation, 11:301-308.

Bresler, E. 1975. Two-dimensional transport of solutes during nonsteady infiltration from a trickle source. Soil Sci. Soc. Amer. Proc., 39:604-613.

Bresler, E., J. Heller, N. Diner, I. Ben-Asher, A. Brandt, and D. Goldberg. 1971. Infiltration from a trickle source: II. Experimental data and theoretical predictions. Soil Sci. Soc. Amer. Proc., 35:683-689.

Bresler, E., W.D. Kemper and R.J. Hanks. 1969. Infiltration, redistribution and subsequent evaporation of water from soil as affected by wetting rate and hysteresis. Soil Sci. Soc. Amer. Proc., 33:832-839.

Carter, N., A.F.G. Dixen and R. Rabbinge. 1982. Cereal Aphid Population Biology, Simulation and Prediction. Centre for Agricultural Publishing and Documentation, Wageningen, the Netherlands, 91p.

Curry, R.B. 1969. Dynamic modeling of plant growth. ASAE Paper No. 69-939.

Day, P.R. and J.N. Luthin. 1956. A numerical solution of the differential equation of flow for a vertical drainage problem. Soil Sci. Soc. Amer. Proc., 20:443-447.

de Wit, C.T., J. Goudriaan, H.H. van Laar, F.W.T. Penning de Vries, R. Rabbinge, H. van Keulen, W. Louwerse, L.Sibma and de Jonge. 1978. Simulation of Assimilation, Respiration and Transpiration of Crops. Center for Agricultural Publshing and Documentation, Wageningen, the Netherlands, 140p.

de Wit, C.T. and H. van Keulen. 1972. Simulation of transport processes in soils. Center for Agricultural Publishing and Documentation, Wageningen, 100p.

Edwards, W.M., R.R. van der Ploeg and W. Ehlers. 1979. A numerical study of the effects of noncapillary-sized pores upon infiltration. Soil Sci. Soc. Amer. J., 43:851-856.

Feddes, R.A. 1981. Water use models for assesing root zone modification. In G.F. Arkin and H.M. Taylor (eds.) Modifying the Root Environment to Reduce Crop Stress. Amer. Soc. Agr. Eng., 4:345-390.

Feddes, R.A., E. Bresler and S.P. Neuman. 1974 Field test of modified numerical model for water uptake by root systems. Water Resour. Res., 10:1199-1206.

Feddes, R.A, P. Kowalik, K. Kolinska-Malinka and H. Zaradny. 1976. Simulation of field water uptake by plant using a soil water dependent root extraction function. J. Hydrol., 31:13-26.

Feddes, R.A., S.P. Neuman, and E. Bresler. 1975. Finite element analysis of two-dimensional flow in soils considering water uptake by roots. II. Field application. Soil Sci. Soc. Amer. Proc., 39:231-237.

Freeze, R.A. 1971. Three-dimensional transient saturated - unsaturated flow in a groundwater basin. Water Resour. Res., 7:347-366.

Gardner, W.R. 1960. Dynamic aspect of water availability to plants. Soil Sci., 89:63-73.

Gardner, W.R. 1964. Relation of root distribution to water uptake and availability. Agron. J., 56:41-45.

Gardner, W.R. and C.F. Ehlig. 1962. Some observations on the movement of water to plant roots. Agron. J., 54:453-456.

Goldberg, D., and M. Shmueli. 1970. Drip irrigation - a method used under arid and desert conditions of high water and soil salinity. Trans. Amer. Soc. Agr. Eng., 13:38-41.

Hanks, R.J., and S.A. Bowers. 1962. Numerical solution of the moisture flow equation for infiltration into layered soils. Soil Sci. Soc. Amer. Proc., 26:530-534.

Hanks, R.J., A. Klute, and E. Bresler. 1969. Numerical method for estimating infiltration, redistribution, drainage, and evaporation of water from soil. Water Resour. Res., 5:1064-1069.

Hansen, V.E., O.W. Israelsen and G.E. Stringham. 1980. Irrigation Principles and Practices. 4th ed. John Wiley & Sons, Toronto, 417p.

Hillel, D. 1977. Computer Simulation of Soil-Water Dynamics: A Compendium of Recent Work. IDRC, Ottawa, Canada, 214p.

Hillel, D., H. Talpaz and H. van Keulen. 1975c. A macroscopic scale model of water uptake by non-uniform root system and of water and salt movement in the soil profile. Soil Sci., 121:242-255.

Hillel, D., C.H.M. van Bavel and H. Talpaz. 1975a. Dynamic simulation of water storage in fallow soil as affected by soil mulch of hydrophobic aggregates. Soil Sci. Soc. Amer. Proc., 39:826-833.

Hillel, D., C. van Beek and H. Talpaz. 1975b. A microscopic-scale model of soil water uptake and salt movement to plant roots. Soil Sci., 120:385-399.

Holmes, R.M. and G.W. Robertson, 1957. Conversion of latent evaporation to potential evapotranspiration. Can. J. Plant Sci., 38:164-172.

Holmes, R.M. and G.W. Robertson, 1963. Application of the relatioship between actual and potential evapotranspiration in dry land agriculture. Trans. Amer. Soc. Agr. Eng., 6:65-67.

Hunter, A.S. and O.J. Kelly. 1946. A new technique for studying the absorption of moisture and nutrient from soil by roots. Soil Sci., 62:441-450.

IBM Corporation. 1972. System/360 Continuous Systems Modeling Program. User's Manual, 5th edition, GH20-0367-4. Data Processing Division, IBM, White Plains, New York 10604.

Jackson, R.D. 1972. On the calculation of hydraulic conductivity. Soil Sci. Soc. Amer. Proc., 36:380-382.

Jensen, M.E. and R.J. Hanks. 1967. Nonsteady-state drainage from porous media. J Irri. & Drainage Div., ASCE, Proc. Paper, 93:209-231.

Jutras, P.J., K.C. Khatri and R.S. Broughton. 1983. Drip irrigation potential in Quebec. ASAE Paper No. 83-2029.

Karmeli, D. and G. Peri. 1974. Basic principles of pulse irrigation. J Irri. & Drainage Div., ASCE, Proc. Paper, 100:309-319.

Klute, A. 1952. A numerical method for solving the flow equation for water in unsaturated materials. Soil Sci., 73:105-116.

Klute, A. 1965. Laboratory measurement of hydraulic conductivity of saturated soil. In Method of Soil Analysis, Amer. Soc. Agron., Monograph, 9:210-221.

Kramer, P.J. 1969. Plant and Soil Water Relationships - A Modern Synthesis. McGraw-Hill Book Co., New York, 482p.

Lake, E.B., and R.S. Broughton. 1969. Irrigation requirements in southwestern Quebec. Can. Agr. Eng., 11:28-32.

Lambe, T.W. 1951. Soil Testing for Engineers. John Wiley & Sons, Inc., New York, 165p.

Levin, I., R. Assaf, and B. Bravdo. 1972. Effect of irrigation treatments for apple trees on water uptake from differnt soil layers. J. Amer. Soc. Hort. Sc., 97:521-526.

Levin, I., R. Assaf and B. Bravdo. 1979a. Soil moisture and root distribution in an apple orchard irrigated by tricklers. Plant and Soil, 52:31-40.

Levin, I., P.C. van Rooyen, and F.C. van Rooyen. 1979b. The effect of discharge rate and intermittent water application by point-source irrigation on the soil moisture distribution pattern. Soil Sci. Soc. Amer. J., 43:8-16.

Mailloux, A. and G. Godbout. 1954. Etude pédologique des sols des comtés de Huntingdon et Beauharnois. Province de Québec, Ministère de l'Agriculture, Québec.

Marshall, T.J. and J.W. Holmes. 1979. Soil Physics. Cambridge University Press, Cambridge, 1st ed., 345p.

Merrill, S.D., P.A.C. Ratts, and C. Dirksen. 1978. Laterally confined flow from a point source at the surface of an inhomogeneous soil column. Soil Sci. Soc. Amer. J., 42:851-857.

Miller, E.E., and A. Klute. 1967. The dynamics of soil water. In R.M. Hagan et al. (ed.). Irrigation of Agricultural Lands. Amer. Soc. Agron., Monograph, 11:222-237.

Molz, F.J. 1981. Models for water transport in the soil-plant system: A review. Water Resour. Res., 17:1245-1260.

Molz, F.J., and I. Remson. 1970. Extraction term models of soil moisture use by transpiring plants. Water Resour. Res., 6:1347-1356.

Molz, F.J., and I. Remson. 1971. Application of an extraction term model to the study of moisture flow to plant roots. Agron. J., 63:72-77.

Morris, G.H. and D. Hillel. 1983. A model for root growth and water uptake accounting for photosynthesis, respiration, transpiration, and soil hydraulics. In D. Hillel (ed.) Advances in Irrigation, Academic Press New York, 2:273-333.

Mostaghimi, S., J.K. Mitchell, and W.D. Lembke. 1981a. Effect of discharge rate on distribution of moisture in heavy soils irrigated from a trickle source. ASAE Paper No. 81-2081.

Mostaghimi, S., J.K. Michell, and W.D. Lembke. 1981b. Effect of pulsed trickling on moisture distribution patterns in heavy soils. ASAE Paper No. 81-2553.

Neuman, S.P., R.A. Feddes and E. Bresler. 1975. Finite element analysis of two-dimensional flow in soils considering water uptake by roots: I. Theory. Soil Sci. Soc. Amer. Proc., 39:224-230.

Nimah, M.N., and R.J. Hanks. 1973a. Model for estimating soil water, plant and atmospheric interrelations, I: Description and sensitivity. Soil Sci. Soc. Amer. Proc., 37:522-527.

Nimah, M.N., and R.J. Hanks. 1973b. Model for estimating soil water, plant and atmospheric interrelations, II: Field test of model. Soil Sci. Soc. Amer. Proc., 37:528-532.

Padmakumari, O. and R.K. Sivanappan. 1979. Wetting patterns for varying rates of dripper discharge. Madras Agr. J., 66:271-272.

Pair C.H., W.W. Hinz, C. Reid and K.R. Frost (eds.) 1975. Sprinkler Association, Silver Spring, Maryland, 615p.

Pall, R., R. Jarret and C.T. Morrow. 1978. A simple finite element method of infiltration. ASAE Paper No. 78-2068.

Pall, R., R. Jarret and C.T. Morrow. 1979. Explicit numerical method of infiltration for layerd soils. ASAE Paper No. 79-2033.

Pall, R. 1980. Simulation of soil moisture flow from a trickle source considering root water uptake by an apple tree. Ph.D. Thesis, The Pennsylvania State University, University Park, PA.

Pall, R., C.T. Morrow, D.D. Fritton, and A.R. Jarret. 1981. Modeling moisture flow from a trickle source in the presence of an apple tree. ASAE Paper No. 81-2079.

Peters, R.B. 1965. Water availability. In C.A. Black et al. (eds.) Method of Soil Analysis, Part 1. Amer. Soc. Agron., 9:279-285.

Philip, J.R. 1955. Numerical solution of equation of the diffusion type with diffusivity concentration dependent. Trans. Faraday Soc., 51:885-892.

Philip, J.R., and R.I. Forrester. 1975. Steady infiltration from buried, surface, and perched point and line sources in heterogeneous soils: II. Flow details and discussions. Soil Sci. Soc. Amer. Proc., 39:408-414.

Raats, P.A.C. 1971. Steady infiltration from point sources, cavities, and basins. Soil Sci. Soc. Amer. Proc., 35:689-694.

Rose, C.W., and W.R. Stern. 1967. Determination of withdrawal of water from soil by crop roots as a function of depth and time. Aust. J. Soil Res., 5:11-19.

Rubin, J. 1968. Theoretical analysis of two-dimentional, transient flow of water in unsaturated and partly unsaturated soils. Soil Sci. Soc. Amer. Proc., 32:607-615.

Russelo, D., S. Edey and J. Godfrey. 1974. Selected Tables and Conversions Use in Agrometeorology and Related Fields. Publication 1522, Canada Dept. of Agr., Ottawa. 275p.

Scott, E.J., R.J. Hanks, D.B. Peters and A. Klute. 1962. Power series solution of the one-dimensional flow equation for exponential and linear diffusivity functions. U.S. Dept. of Agr., Agr. Res. Ser., 41-64:1-39.

Soomro, G.M., P.J. Jutras, K.C. Khatri. 1983. Response of semi-dwarf apple trees to supplementary drip irrigation. ASAE Paper No. 83-2028.

van Bavel, C.H.M., G.B. Stirk, and K.J. Brust. 1968a. Hydraulic properties of a clay loam and field measurement of water uptake by roots: I. Interpretation of water content and pressure profiles. Soil Sci. Soc. Amer. Proc., 32:310-317.

van Bavel, C.H.M., K.J. Brust, and G.B. Stirk. 1968b. Hydraulic properties of a clay loam soil and field measurement of water uptake by roots: II. The water balance of the root zone. Soil Sci. Soc. Amer. Proc., 32:317-321.

van der Ploeg, R.R. 1974. Simulation of moisture transfer in soils: One dimensional infiltration. Soil Sci. 118:349-357.

van der Ploeg, R.R., and P. Benecke. 1974. Unsteady unsaturated n-dimensional moisture flow in soil: A computer simulation program. Soil Sci. Soc. Amer. Proc., 38:881-885.

Warrick, A.W., and D.O. Lomen. 1974. Linearized moisture flow solution for point, line, and strip sources. Proc. Second Inter'l Drip Irrig. Cong., San Diego, CA, pp 228-233.

Verma, S.C. and H.R. Whiteley. 1981. Simulating irrigation need from climatological records. ASAE Paper No. 81-419.

Westwood, M.N. 1978. Temperate-zone Pomology. W.H. Freeman and Co., San Francisco, 428p.

Whisler, F.D., A. Klute and R.J. Millington. 1968. Analysis of steady state evapotranspiration from a soil column. Soil Sci. Soc. Amer. Proc., 32:167-174.

Wierenga, P.J. and de Wit, C.T. 1970. Simulation of heat transfer in soils. Soil Sci. Soc. Amer. Proc., 34:845-847.

Willoughby, P., and B. Cockroft. 1974. Changes in root patterns of peach trees under trickle irrigation. Proc. Second Inter'l Drip Irrig. Cong., San Diego, CA, pp 439-442.

Withers, B. and S. Vipond. 1974. Irrigation: Design and Practice. B.T. Batsford Ltd., London, 306p.

Zur, B. 1976. The pulsed irrigation principle for controlled soil wetting. Soil sci., 22:282-291.

APPENDICES

APPENDIX A

LISTING OF THE COMPUTER PROGRAM

```
*                CONTINUOUS SYSTEM MODELING PROGRAM                    *
*                            VERSION 1.3                               *

************************************************************************

*          THIS PROGRAM SIMULATES SOIL MOISTURE DISTRIBUTION           *
*           FROM A POINT SOURCE IRRIGATION OF AN APPLE TREE            *
*                                                                      *
*          SITE = ROUGEMONT ORCHARD SITE 1                             *
*          RATE OF EMITTER DISCHARGE  = 2.0 L/H                        *
*          AMOUNT OF IRRIGATION WATER = 12 LITERS                      *
*          DATE = 24-8-1980                                            *
*          METHOD OF DRIP IRRIGATION APPLICATION = CONTINUOUS          *
*                                                                      *
************************************************************************

*                DESCRIPTION OF VARIABLES                              *

*  A        A DUMMY VARIABLE
*  AEPE     AET/PET RATIO OF EACH SOIL RING W.R.T TOTAL PET
*  AEPEAR   AET/PET RATIO OVER AN AREA OF RING FROM BOTTOM TO SURFACE
*  AEPEL    AET/PET RATIO LOCAL TO A RING, W.R.T LOCAL PET
*  AET      ROOT WATER EXTRACTION OR ACTUAL EVAPOTRANSPIRATION, MM

*  AETALL   AET OVER ALL THE AREA OF THE SOIL CYLINDER, MM
*  AETAR    AET OVER AN AREA OF RING, MM
*  AETPET   AET/PET, RATIO OVER ALL THE AREA OF THE SOIL CYLINDER
*  ARNGIJ   AREA OF A SOIL RING FROM INSIDE OR OUTSIDE
*  ARNGJ    AREA OF A SOIL RING FROM TOP OR BOTTOM

*  AVDELR   RADIAL DISTANCE BETWEEN TWO ADJACENT RINGS, CM
*  AVDELZ   DEPTH DISTANCE BETWEEN TWO OVERLYING RINGS, CM
*  AVKR     AVERAGE K OF SOIL RINGS (I,J) AND (I,J-1), CM/MIN
*  AVKZ     AVERAGE K OF SOIL RINGS (I,J) AND (I-1,J), CM/MIN
*  CUMIRR   CUMULATIVE IRRIGATION IN COLUMN, PERCENT

*  CUMPC1   CUMULATIVE DELTA STORAGE IN EACH ROW, PERCENT
*  CUMPC2   CUMULATIVE DELTA STORAGE IN EACH COLUMN, PERCENT
*  CUMPC3   CUMULATIVE DELTA STORAGE IN EACH COLUMN BEYOND ROOT ZONE, %
*  CUMPC4   CUMULATIVE RWE FROM EACH ROW, PERCENT
*  CUMPC5   CUMULATIVE RWE FROM EACH COLUMN, PERCENT
```

```
*  CUMPC6  CUMULATIVE IRRIGATION WATER INPUT IN EACH ROW, PERCENT
*  DELST   CHANGE IN STORAGE, CM3/CM3/MIN
*  DELT    A SYSTEM VARIABLE FOR TIME INCREMENT, MIN
*  DELTAR  WIDTH OF A SOIL RING, CM
*  DELTAZ  THICKNESS OF A SOIL RING, CM

*  DSLSPC  CHANGE OF STORAGE (LOSS) BELOW ROOT ZONE, PERCENT
*  DSRZPC  CHANGE OF STORAGE WITHIN ROOT ZONE, PERCENT
*  DSSCPC  CHANGE OF STORAGE WITHIN THE SOIL CYLINDER, PERCENT
*  DSTBMM  DELTA STORAGE IN EACH COLUMN BEYOND RZ, MM
*  DSTBRZ  CHANGE OF STORAGE BELOW ROOT ZONE, L

*  DSTCBR  DELTA STORAGE IN EACH COLUMN, BEYOND RZ, PERCENT
*  DSTCMM  DELTA STORAGE IN EACH COLUMN, MM
*  DSTCOL  CHANGE OF STORAGE WITHIN A COLUMN, PERCENT
*  DSTROW  CHANGE OF STORAGE WITHIN A ROW, PERCENT
*  DSTWRZ  CHANGE OF STORAGE WITHIN ROOT ZONE, L

*  DSTWSC  CHANGE OF STORAGE WITHIN SOIL CYLINDER, L
*  EQHR    EMITTER DISCHARGE RATE, L/HR
*  EQMIN   EMITTER DISCHARGE RATE, ML/MIN
*  EQMIN1  A DUMMY VARIABLE
*  ERRPC   ERROR BETWEEN SIMULATED AND APPLIED IRRIGATION, PERCENT

*  FINTIM  A SYSTEM VARIABLE FOR FINISHING THE SIMULATION, MIN
*  GPOT    GRAVITY POTENTIAL, CM
*  HBOUND  MATRIC POTENTIAL AT SATURATION, CM
*  HPOT    HYDRAULIC POTENTIAL AT THE CENTER OF RING (I,J), CM
*  I       SUBSCRIPT I REPRESENTS RING NUMBER FROM THE SOIL SURFACE
*          OR DEPTH AT THE TOP OF A SOIL RING

*  IMAX    NUMBER OF SOIL RINGS IN Z DIRECTION
*  IMAX1   NUMBER OF BOUNDARIES OF I SOIL RINGS, ONE MORE THAN IMAX
*  IMC     INITIAL VOLUMETRIC SOIL MOISTURE CONTENT IN A RING CM3/CM3
*  IRRCOL  IRRIGATION APPLICATION IN EACH COLUMN, PERCENT
*  IRRIMM  IRRIGATION APPLICATION IN EACH COLUMN, MM

*  IRRLIT  IRRIGATION APPLICATION, L
*  IRRROW  IRRIGATION APPLICATION IN EACH ROW, PERCENT
*  ITHETA  INITIAL VOLUMETRIC SOIL MOISTURE CONTENT IN A RING CM3/CM3
*  J       SUBSCRIPT REPRESENTING RING NUMBER FROM CENTER OF FINITE SOIL
*          OR INNER RADIUS OF A RING

*  JMAX    NUMBER OF SOIL RINGS IN RADIAL DIRECTION
*  JMAX1   NUMBER OF RADII OR BOUNDARIES OF J RINGS
*  K       HYDRAULIC CONDUCTIVITY, FUNCTION OF THETA, CM/MIN
*  KSAT    SATURATED HYDRAULIC CONDUCTIVITY, CM/MIN
*  LDMIN   LENGTH OF THE DAY, MIN
```

```
*    M        INTEGER VARIABLE
*    MC       MOISTURE CONTENT AT EACH TIME STEP, CM3/CM3
*    MCWIL    LOWER LIMIT OF SOIL MOISTURE CONTENT NEAR TO WILTING, CM3/CM3
*    MC50AV   MC AT 50 PERCENT AVAILABLE MOISTURE, CM3/CM3
*    MPDEN    A DENOMINATOR USED IN CALCULATING RWE

*    MPOT     MATRIC POTENTIAL IN EACH SOIL RING (I,J), CM
*    MP50AV   MATRIC POTENTIAL AT 50 PERCENT AVAILABLE MOISTURE, CM
*    N        NUMBER OF ROWS WITHIN ROOT ZONE FROM SOIL SURFACE
*    OLREST   A DUMMY VARIABLE EQUIVALENT TO REST
*    PET      POTENTIAL EVAPOTRANSPIRATION, CM/DAY

*    PETCU    CUMULATIVE PET DURING SIMULATION TIME, MM
*    PETCUM   CUMULATIVE PET DURING SIMULATION, CM
*    PI       CONSTANT=3.14159
*    PRDEL    A SYSTEM VARIABLE FOR OUTPUT PRINTING INTERVAL, MM
*    P1       TIME INTERVAL FOR PULSE IRRIGATION, MIN

*    P2       TIME INTERVAL FOR GENERATION OF IMPULSES, MIN
*    RADDIS   RADIAL DISTANCE FROM AXIS TO THE CENTER OF EACH J RING, CM
*    RADRNG   INNER RADIUS OF RING (J), CM
*    REST     AMOUNT OF EXCESS WATER THAT MOVES TO NEXT RING, CM3
*    RWE      ROOT WATER EXTRACTION FROM A SOIL RING, CM3/CM3

*    RWECMM   RWE FROM EACH COLUMN, MM
*    RWECOL   RWE FROM EACH COLUMN, PERCENT
*    RWECUM   CUMULATIVE ROOT WATER EXTRACTION, CM3
*    RWEDM    A DUMMY VARIABLE EQUAL TO RWEZP
*    RWELIT   RWE, L

*    RWEMDR   ROOT WATER EXTRACTION- MAXIMUM MIDDAY RATE, CM/MIN
*    RWEMP    ROOT WATER EXTRACTION AS A FUNCTION OF MATRIC POTENTIAL
*    RWEPC    RWE, PERCENTAGE OF TOTAL IRRIGATION WATER
*    RWER     RWE RATE AS A FUNCTION OF TIME, DEPTH, AND MPOT, CM/MIN
*    RWEROW   RWE FROM EACH ROW, PERCENT

*    RWET     RWE RATE A FUNCTION OF TIME IN MINUTES FROM SUNRISE, CM/MIN
*    RWEZ     RWE FROM A SOIL RING AS A FUNCTION OF Z, FRACTION
*    RWEZF    ROOT WATER EXTRACTION AT DEPTH Z, FRACTION
*    RWEZP    RWE - FUNCTION OF Z, MC, AND TIME, CM3/CM3/MIN
*    RZD      ROOT ZONE DEPTH, CM

*    RZDF     ROOT ZONE DEPTH FRACTION OF TOTAL
*    RZDRWE   ROOT ZONE DEPTH FRACTION OF TOTAL VS RWE FRACTION
*    T        TIME AT SIMULATION AFTER SUNRISE
*    THETAS   VOLUMETRIC MOISTURE CONTENT AT SATURATION, CM3/CM3
*    THK      SOIL MOISTURE CONTENT VS K, TABLE

*    THMPOT   SOIL MOISTURE CONTENT VS MATRIC POTENTIAL, TABLE
*    TIME     A SYSTEM VARIABLE REPRESENTS TIME OF SIMULATION, MIN
```

```
*  TIMHR    TIME OF SIMULATION, HOUR
*  TRUN     TIME OF IRRIGATION APPLICATION, MIN
*  TSTART   TIME AT THE START OF DISCHARGE AFTER SUNRISE, MIN

*  TSTOP    TIME AT THE STOP OF DISCHARGE AFTER SUNRISE, MIN
*  TWOPI    CONSTANT EQUAL TO PI*2.0
*  VOLRNG   VOLUME OF A SOIL RING, CM3
*  VWACCT   VOLUME OF WATER ACCOUNTED FOR, BY SIMUATION, PERCENT
*  VWAPPL   VOLUME OF WATER APPLIED, CM3

*  VWBRZI   INITIAL VOLUME OF WATER BELOW ROOT ZONE, L
*  VWBRZT   VOLUME OF WATER BEYOND ROOT ZONE AT TIME, L
*  VWCBRI   INITIAL VOLUME OF WATER IN COLUMN BELOW ROOT ZONE, L
*  VWCBRT   VOL OF WATER IN A COLUMN BELOW ROOT ZONE AT SPECIFIED TIME, L
*  VWCOLI   INITIAL VOLUME OF WATER IN COLUMN, L

*  VWCOLT   VOLUME OF WATER IN A COLUMN I AT TIME SPECIFIED, L
*  VWERR    DIFFERENCE BETWEEN SIMULATED AND APPLIED AMOUNT OF WATER, L
*  VWROWI   INITIAL VOLUME OF WATER IN A ROW J, CM3
*  VWROWT   VOLUME OF WATER IN A ROW J AT SPECIFIED TIME, CM3
*  VWSIMU   VOLUME OF WATER SIMULATED AT TIME SPECIFIED, L

*  VWWRNG   VOLUME OF WATER IN A SOIL RING, CM3
*  VWWRZI   INITIAL VOLUME OF WATER WITHIN ROOT ZONE, L
*  VWWRZT   VOLUME OF WATER WITHIN ROOT ZONE AT TIME SPECIFIED, L
*  VWWSCI   INITIAL VOLUME OF WATER WITHIN SOIL CYLINDER, L
*  VWWSCT   VOLUME OF WATER WITHIN SOIL CYLINDER AT TIME SPECIFIED, L

*  WRTDEL   OUTPUT INTERVAL USED IN THIS PROGRAM, MIN
*  Y        A DUMMY VARIABLE
*  Z        DEPTH FROM THE SOIL SURFACE, CM

****************************************************************************

*                             COMPUTER PROGRAM

****************************************************************************

/     REAL DELST(15,11),MC(15,11),IMC(15,11),VOLRNG(15,11),ARNGIJ(15,11)
/     REAL HPOT(15,11),MPOT(15,11) ,AVKR(15,11),AVKZ(15,11),K(15,11)
/     REAL RWEZP(15,11),RWE(6,11),AET(15,11),AEPE(15,11),AEPEL(15,11)
/     REAL RWEDM(6,11),IRRIMM(11),RWECMM(11),RWECOL(11),DSTBMM(11)
/     REAL DSTCMM(11),CUMPC1(11),CUMPC2(11),CUMPC3(11),CUMPC5(11)
/     REAL CUMIRR(11),IRRCOL(11),RWEROW(15),CUMPC4(15),IRRROW(15)
/     REAL CUMPC6(15)

STORAGE ITHETA(165),RADRNG(12),DELTAR(11),AVDELR(11),ARNGJ(11),Z(16)
STORAGE DELTAZ(15),AVDELZ(15),RWEZF(16),RZDF(15),RWEZ(15),DSTROW(15)
STORAGE AETAR(11),AEPEAR(11),RADDIS(11),GPOT(15),VWROWI(15),VWROWT(15)
STORAGE VWCOLI(11),VWCOLT(11),DSTCOL(11),VWCBRI(11),VWCBRT(11)
```

```
STORAGE DSTCBR(11)

/     EQUIVALENCE (DELST1,DELST(1,1)),(MC1,MC(1,1)),(RWE1,RWE(1,1))
/     EQUIVALENCE (IMC1,IMC(1,1)),(RWEDM1,RWEDM(1,1))

FIXED I,J,IMAX,JMAX,M,JMAX1,IMAX1,N

*********************************************************************
INITIAL
*********************************************************************

* INPUT INITIAL SOIL MOISTURE CONTENT OF ALL THE SOIL RINGS
TABLE ITHETA(1-165)=22*0.078,44*.0.080,99*0.085

* INPUT INNER RADII OF SOIL AND OUTER BOUNDARY, CM
TABLE RADRNG(1-12)=0.0,6.,12.0,18.,24.,30.,36.,42.,48.,54.,60.,66.0

* INPUT DEPTH AT THE TOP OF SOIL RINGS AND BOTTOM BOUNDARY, CM
TABLE Z(1-16)=0.0,6.,12.,18.,24.,30.,36.,42.,48.,54.,60.,66.,72.0,...
  78.0,84.0,90.0

* SOIL MOISTURE CONTENT, (CM3/CM3) VS MATRIC POTENTIAL, (CM)
 FUNCTION THMPOT=...
 (0.060,0.9000E+04),(0.070,0.2000E+04),(0.080,0.8000E+03),...
 (0.090,0.5000E+03),(0.100,0.3000E+03),(0.110,0.1850E+03),...
 (0.120,0.9500E+02),(0.130,0.8000E+02),(0.140,0.7300E+02),...
 (0.150,0.6700E+02),(0.160,0.6100E+02),(0.170,0.5700E+02),...
 (0.180,0.5300E+02),(0.190,0.5000E+02),(0.200,0.4700E+02),...
 (0.210,0.4500E+02),(0.220,0.4300E+02),(0.230,0.4050E+02),...
 (0.240,0.3900E+02),(0.250,0.3750E+02),(0.260,0.3600E+02),...
 (0.270,0.3470E+02),(0.280,0.3350E+02),(0.290,0.3200E+02),...
 (0.300,0.3050E+02),(0.310,0.2850E+02),(0.320,0.2650E+02),...
 (0.330,0.2450E+02),(0.340,0.2250E+02),(0.350,0.1950E+02),...
 (0.360,0.1700E+02),(0.370,0.1000E+02)

* SOIL MOISTURE CONTENT, (CM3/CM3) VS HYDRAULIC CONDUCTIVITY, (CM/MIN)
 FUNCTION THK=...
 (0.060,0.1641E-08),(0.070,0.4451E-07),(0.080,0.4207E-06),...
 (0.090,0.1998E-05),(0.100,0.7262E-05),(0.110,0.2336E-04),...
 (0.120,0.7947E-04),(0.130,0.2215E-03),(0.140,0.4910E-03),...
 (0.150,0.9329E-03),(0.160,0.1603E-02),(0.170,0.2567E-02),...
 (0.180,0.3896E-02),(0.190,0.5675E-02),(0.200,0.7996E-02),...
 (0.210,0.1096E-01),(0.220,0.1467E-01),(0.230,0.1926E-01),...
 (0.240,0.2486E-01),(0.250,0.3162E-01),(0.260,0.3969E-01),...
 (0.270,0.4924E-01),(0.280,0.6045E-01),(0.290,0.7354E-01),...
 (0.300,0.8874E-01),(0.310,0.1064E+00),(0.320,0.1268E+00),...
 (0.330,0.1506E+00),(0.340,0.1783E+00),(0.350,0.2110E+00),...
 (0.360,0.2501E+00),(0.370,0.3020E+00)

* DEPTH FROM SOIL SURFACE (FRACTION OF TOTAL) VS RWE (FRACTION OF TOTAL)
```

```
FUNCTION RZDRWE=(0.0,0.0),(0.1,0.16),(0.2,0.32),(0.3,0.46),...
(0.4,0.59),(0.5,0.72),(0.6,0.80),(0.7,0.86),(0.8,0.91),...
(0.9,0.96),(1.0,1.0)

* INPUT PARAMETERS
PARAMETER IMAX=15,JMAX=11,RZD=36.0,THETAS=0.37,MCWIL=0.06,TRUN=360.0
PARAMETER HBOUND=0.0,KSAT=0.302,PI=3.14159,MC50AV=0.083,P1=30.0
PARAMETER PET=0.49,TSTART=264.0,EQHR=2.0,LDMIN=823.0,WRTDEL=60.0

NOSORT
      JMAX1=JMAX+1
      IMAX1=IMAX+1
      TWOPI=2.0*PI
      EQMIN=EQHR*1000./60.0
      EQMIN1=EQMIN
      RWEMDR=PET*PI/2.0/LDMIN
      P2=P1*2.0

* ASSIGN THE INITIAL SOIL MOISTURE CONTENT TO SOIL RINGS (I,J), CM3/CM3
      DO 10 I=1,IMAX
      DO 10 J=1,JMAX
      M=(I-1)*JMAX+J
10    IMC(I,J)=ITHETA(M)

* CALCULATE THE WIDTH OF EACH OF THE SOIL RINGS, CM
      DO 20 J=1,JMAX
20    DELTAR(J)=RADRNG(J+1)-RADRNG(J)

* CALCULATE THE DISTANCE FROM AN EMITTER TO THE CENTER OF EACH RING, CM
      DO 30 J=1,JMAX
30    RADDIS(J)=RADRNG(J)+0.5*DELTAR(J)

* CALCULATE THE TOP OR BOTTOM AREA OF EACH SOIL RING, CM2
      DO 40 J=1,JMAX
40    ARNGJ(J)=(RADRNG(J+1)**2-RADRNG(J)**2)*PI

* CALCULATE RADIAL DISTANCE BETWEEN TWO CONTACTING RINGS, CM
      AVDELR(1)=DELTAR(1)/2.0
      DO 50 J=2,JMAX
50    AVDELR(J)=(DELTAR(J-1)+DELTAR(J))/2.0

* CALCULATE THE THICKNESS OF EACH OF THE SOIL RINGS, CM
      DO 60 I=1,IMAX
60    DELTAZ(I)=Z(I+1)-Z(I)

* CALCULATE THE GRAVITY POTENTIAL AT THE CENTER OF EACH SOIL RING, CM
      DO 70 I=1,IMAX
70    GPOT(I)=Z(I)+0.5*DELTAZ(I)

* CALCULATE DEPTH DISTANCE BETWEEN TWO CONTACTING RINGS, CM
```

```
      AVDELZ(1)=DELTAZ(1)/2.0
      DO 80 I=2,IMAX
80    AVDELZ(I)=(DELTAZ(I-1)+DELTAZ(I))/2.0

* CALCULATE THE INNER AREA OF CONTACT OF EACH SOIL RING, CM2
      DO 90 I=1,IMAX
      DO 90 J=1,JMAX
90    ARNGIJ(I,J)=DELTAZ(I)*TWOPI*RADRNG(J)

* CALCULATE THE VOLUME OF EACH OF THE SOIL RINGS, CM3
      DO 100 I=1,IMAX
      DO 100 J=1,JMAX
100   VOLRNG(I,J)=DELTAZ(I)*ARNGJ(J)

* CALCULATE RWE TERM FOR A SOIL RING WITH RESPECT TO ITS POSITION
* FROM SOIL SURFACE, FRACTION OF TOTAL

      RWEZF(1)=0.0
      DO 120 M=2,IMAX1
      I=M-1
      RZDF(I)=Z(M)/RZD
      IF(RZDF(I).EQ.1.0) N=I
      IF(RZDF(I).GT.1.0) GO TO 110
      RWEZF(M)=AFGEN(RZDRWE,RZDF(I))
      RWEZ(I)=RWEZF(M)-RWEZF(M-1)
      GO TO 120
110   RWEZ(I)=0.0
120   CONTINUE

* CALCULATE MPOT AT 50 PERCENT AVAILABLE SOIL MOISTURE AND DENOMINATOR
      MP50AV=-AFGEN(THMPOT,MC50AV)
      MPDEN=-15000.-(MP50AV)

* CALCULATE INITIAL VOLUME OF WATER WITHIN EACH ROW, EACH COLUMN WITHIN
* ROOT ZONE AND  EACH COLUMN BELOW ROOT ZONE, CM3

      DO 140 I=1,IMAX
      DO 140 J=1,JMAX
      VWWRNG=IMC(I,J)*VOLRNG(I,J)
      VWROWI(I)=VWROWI(I)+VWWRNG
      IF(I.GT.N)GO TO 130
      VWCOLI(J)=VWCOLI(J)+VWWRNG
      GO TO 140
130   VWCBRI(J)=VWCBRI(J)+VWWRNG
140   CONTINUE

* CALCULATE VOLUME OF WATER WITHIN & BELOW RZ AND SOIL CYLINDER, L
      DO 145 J=1,JMAX
      VWWRZI=VWWRZI+VWCOLI(J)
145   VWBRZI=VWBRZI+VWCBRI(J)
```

```
      VWWRZI=VWWRZI/1000.
      VWBRZI=VWBRZI/1000.
      VWWSCI=VWWRZI+VWBRZI

***********************************************************************
DYNAMIC
***********************************************************************

      MC1=INTGRL(IMC1,DELST1,165)
      RWE1=INTGRL(0.,RWEDM1,66)
      PETCUM=INTGRL(0.,RWET)
      VWAPPL=INTGRL(0.,EQMIN)

**********************************
NOSORT
**********************************

* KEEP SOIL MOISTURE CONTENT WITHIN UPPER AND LOWER LIMITS
      DO 150 J=1,JMAX
      DO 150 I=1,IMAX
      IF(MC(I,J).GT.THETAS) MC(I,J)=THETAS
      IF(MC(I,J).LT.MCWIL) MC(I,J)=MCWIL
150   CONTINUE

* CALCULATE MATRIC AND HYDRAULIC POTENTIALS IN EACH SOIL RING, CM
      DO 160 I=1,IMAX
      DO 160 J=1,JMAX
      K(I,J)=AFGEN(THK,MC(I,J))
      MPOT(I,J)=-AFGEN(THMPOT,MC(I,J))
160   HPOT(I,J)=MPOT(I,J)-GPOT(I)

* CALCULATE WEIGHTED AVERAGE OF K BETWEEN TWO SOIL RINGS, R-DIRECTION
      DO 170 I=1,IMAX
      DO 170 J=2,JMAX
170   AVKR(I,J)=(K(I,J-1))

* CALCULATE WEIGHTED AVERAGE OF K BETWEEN TWO SOIL RINGS, Z-DIRECTION
      DO 180 J=1,JMAX
      AVKZ(1,J)=(KSAT+K(I,J))/2.0
      DO 180 I=2,IMAX
180   AVKZ(I,J)=(K(I-1,J))


* CALCULATE RWE TERM AS A FUNCTION OF TIME AFTER SUNRISE, CM/MIN
190   T=TSTART+TIME
      IF(T-LDMIN) 200,210,210
200   RWET=RWEMDR*SIN(PI*T/LDMIN)
      GO TO 220
210   RWET=0.0
```

```
220   DO 9999 I=1,IMAX
      DO 9999 J=1,JMAX

* CALCULATE RWE TERM W.R.T MATRIC POTENTIAL IN A RING, FRACTION OF TOTAL
230   IF(MPOT(I,J).LE.(-15000.)) GO TO 240
      IF(MPOT(I,J).GE.(MP50AV)) GO TO 250
      RWEMP=(-15000.-MPOT(I,J))/MPDEN
      GO TO 260
240   RWEMP=0.0
      GO TO 260
250   RWEMP=1.0

* CALCULATE RWE FROM A RING AS A FUNCTION OF Z, MPOT AND TIME, CM3/MIN
260   RWER=RWET*RWEMP*RWEZ(I)
      RWEZP(I,J)=RWER*ARNGJ(J)
      IF(I.GT.N)GO TO 270
      RWEDM(I,J)=RWEZP(I,J)

* TRANSFER THE CONTROL TO A SOIL RING ACCORDING TO ITS POSITION
270   IF(I.EQ.1.AND.J.EQ.1) GO TO 2000
      IF(I.LT.IMAX.AND.J.EQ.1) GO TO 3000
      IF(I.EQ.IMAX.AND.J.EQ.1) GO TO 4000
      IF(I.EQ.1.AND.J.LT.JMAX) GO TO 6000
      IF(I.EQ.IMAX.AND.J.LT.JMAX) GO TO 5000
      IF(I.EQ.1.AND.J.EQ.JMAX) GO TO 7000
      IF(I.LT.IMAX.AND.J.EQ.JMAX) GO TO 8000
      IF(I.EQ.IMAX.AND.J.EQ.JMAX) GO TO 9000


*  CALCULATE DELTA STORAGE IN SOIL RING (I,J) 1<I<IMAX; 1<J<JMAX

1000  DELST(I,J)=(-RWEZP(I,J)...
        +AVKR(I,J)*ARNGIJ(I,J)*(HPOT(I,J-1)-HPOT(I,J))/AVDELR(J)...
        -AVKR(I,J+1)*ARNGIJ(I,J+1)*(HPOT(I,J)-HPOT(I,J+1))/AVDELR(J+1)...
        +AVKZ(I,J)*ARNGJ(J)*(HPOT(I-1,J)-HPOT(I,J))/AVDELZ(I)...
        -AVKZ(I+1,J)*ARNGJ(J)*(HPOT(I,J)-HPOT(I+1,J))/AVDELZ(I+1))...
        /VOLRNG(I,J)
        GO TO 9999

*  CALCULATE DELTA STORAGE IN SOIL RING (1,1)
*  IRRIGATION WATER FROM A POINT SOURCE IS APPLIED ON THIS RING

2000  CONTINUE

*************************************************************************

**               DO YOU WANT IRRIGATION BY PULSE METHOD ?
**   IF YES REMOVE THE STARS (*) FROM COLUMN ONE OF THE FOLLOWING TWO
**   CSMP STATEMENTS AND CHECK THE PARAMETER TRUN WHICH MUST BE TWICE
**   (IF PULSES ARE A SQUARE WAVE FUNCTION OF TIME) THE TRUN REQUIRED
```

```
**  REQUIRED FOR CONTINUOUS IRRIGATION, REPLACE STARS BACK OTHERWISE.

*     Y=PULSE(P1,IMPULS(0.,P2))
*     EQMIN=EQMIN1*Y

*******************************************************************************

      IF(TIME.GT.TRUN) EQMIN=0.0
      REST=EQMIN-...
      (+AVKZ(I,J)*ARNGJ(J)*(HBOUND-HPOT(I,J)))/AVDELZ(I)
      IF(REST) 2100,2200,2200
2100  DELST(I,J)=(EQMIN-RWEZP(I,J)...
       -AVKR(I,J+1)*ARNGIJ(I,J+1)*(HPOT(I,J)-HPOT(I,J+1))/AVDELR(J+1)...
       -AVKZ(I+1,J)*ARNGJ(J)*(HPOT(I,J)-HPOT(I+1,J))/AVDELZ(I+1))...
       /VOLRNG(I,J)
      GO TO 9999

2200  DELST(I,J)=(-RWEZP(I,J)...
       +AVKZ(I,J)*ARNGJ(J)*(HBOUND-HPOT(I,J))/AVDELZ(I)...
       -AVKR(I,J+1)*ARNGIJ(I,J+1)*(HPOT(I,J)-HPOT(I,J+1))/AVDELR(J+1)...
       -AVKZ(I+1,J)*ARNGJ(J)*(HPOT(I,J)-HPOT(I+1,J))/AVDELZ(I+1))...
       /VOLRNG(I,J)
      GO TO 9999

*  CALCULATE DELTA STORAGE IN SOIL RING (I,J)  1<I<IMAX; J=1

3000  DELST(I,J)=(-RWEZP(I,J)...
       -AVKR(I,J+1)*ARNGIJ(I,J+1)*(HPOT(I,J)-HPOT(I,J+1))/AVDELR(J+1)...
       +AVKZ(I,J)*ARNGJ(J)*(HPOT(I-1,J)-HPOT(I,J))/AVDELZ(I)...
       -AVKZ(I+1,J)*ARNGJ(J)*(HPOT(I,J)-HPOT(I+1,J))/AVDELZ(I+1))...
       /VOLRNG(I,J)
      GO TO 9999

*  CALCULATE DELTA STORAGE IN SOIL RING (I,J)  I=IMAX; J=JMAX

4000  DELST(I,J)=(-RWEZP(I,J)...
       -AVKR(I,J+1)*ARNGIJ(I,J+1)*(HPOT(I,J)-HPOT(I,J+1))/AVDELR(J+1)...
       +AVKZ(I,J)*ARNGJ(J)*(HPOT(I-1,J)-HPOT(I,J))/AVDELZ(I))...
       /VOLRNG(I,J)
      GO TO 9999

*  CALCULATE DELTA STORAGE IN SOIL RING (I,J) I=IMAX;  1<J<JMAX

5000  DELST(I,J)=(-RWEZP(I,J)...
       +AVKR(I,J)*ARNGIJ(I,J)*(HPOT(I,J-1)-HPOT(I,J))/AVDELR(J)...
       -AVKR(I,J+1)*ARNGIJ(I,J+1)*(HPOT(I,J)-HPOT(I,J+1))/AVDELR(J+1)...
       +AVKZ(I,J)*ARNGJ(J)*(HPOT(I-1,J)-HPOT(I,J))/AVDELZ(I))...
       /VOLRNG(I,J)
      GO TO 9999
```

```
*  CALCULATE DELTA STORAGE IN SOIL RING (I,J) I=1, 1<J<JMAX

6000 IF (REST) 6400,6400,6100
6100 OLREST=REST
     REST=OLREST-...
      (+AVKZ(I,J)*ARNGJ(J)*(HBOUND-HPOT(I,J))/AVDELZ(I))
     IF (REST) 6200,6300,6300
6200 DELST(I,J)=(OLREST-RWEZP(I,J)...
      +AVKR(I,J)*ARNGIJ(I,J)*(HPOT(I,J-1)-HPOT(I,J))/AVDELR(J)...
      -AVKR(I,J+1)*ARNGIJ(I,J+1)*(HPOT(I,J)-HPOT(I,J+1))/AVDELR(J+1)...
      -AVKZ(I+1,J)*ARNGJ(J)*(HPOT(I,J)-HPOT(I+1,J))/AVDELZ(I+1))...
      /VOLRNG(I,J)
     GO TO 9999

6300 DELST(I,J)=(-RWEZP(I,J)...
      +AVKZ(I,J)*ARNGJ(J)*(HBOUND-HPOT(I,J))/AVDELZ(I)...
      +AVKR(I,J)*ARNGIJ(I,J)*(HPOT(I,J-1)-HPOT(I,J))/AVDELR(J)...
      -AVKR(I,J+1)*ARNGIJ(I,J+1)*(HPOT(I,J)-HPOT(I,J+1))/AVDELR(J+1)...
      -AVKZ(I+1,J)*ARNGJ(J)*(HPOT(I,J)-HPOT(I+1,J))/AVDELZ(I+1))...
      /VOLRNG(I,J)
     GO TO 9999

6400 DELST(I,J)=(-RWEZP(I,J)...
      +AVKR(I,J)*ARNGIJ(I,J)*(HPOT(I,J-1)-HPOT(I,J))/AVDELR(J)...
      -AVKR(I,J+1)*ARNGIJ(I,J+1)*(HPOT(I,J)-HPOT(I,J+1))/AVDELR(J+1)...
      -AVKZ(I+1,J)*(HPOT(I,J)-HPOT(I+1,J))*ARNGJ(J)/AVDELZ(I+1))...
      /VOLRNG(I,J)
     GO TO 9999

*  CALCULATE DELTA STORAGE IN SOIL RING (I,J) I=1, J=JMAX

7000 DELST(I,J)=(-RWEZP(I,J)...
      +AVKR(I,J)*ARNGIJ(I,J)*(HPOT(I,J-1)-HPOT(I,J))/AVDELR(J)...
      -AVKZ(I+1,J)*ARNGJ(J)*(HPOT(I,J)-HPOT(I+1,J))/AVDELZ(I+1))...
      /VOLRNG(I,J)
     GO TO 9999

*  CALCULATE DELTA STORAGE IN SOIL RING (I,J) 1<I<IMAX; J=JMAX

8000 DELST(I,J)=(-RWEZP(I,J)...
      +AVKR(I,J)*ARNGIJ(I,J)*(HPOT(I,J-1)-HPOT(I,J))/AVDELR(J)...
      +AVKZ(I,J)*ARNGJ(J)*(HPOT(I-1,J)-HPOT(I,J))/AVDELZ(I)...
      -AVKZ(I+1,J)*ARNGJ(J)*(HPOT(I,J)-HPOT(I+1,J))/AVDELZ(I+1))...
      /VOLRNG(I,J)
     GO TO 9999

*  CALCULATE DELTA STORAGE IN SOIL RING (I,J) I=IMAX; J=JMAX

9000 DELST(I,J)=(-RWEZP(I,J)...
      +AVKR(I,J)*ARNGIJ(I,J)*(HPOT(I,J-1)-HPOT(I,J))/AVDELR(J)...
```

```
     +AVKZ(I,J)*ARNGJ(J)*(HPOT(I-1,J)-HPOT(I,J))/AVDELZ(I))...
     /VOLRNG(I,J)

9999  CONTINUE

**********************************************************************
* OUTPUT AND SOME CALCULATIONS AT WRTDEL INTERVAL
**********************************************************************

      IF(TIME.EQ.FINTIM) GO TO 403
      IF(TIME.EQ.840.) GO TO 403
400   A=IMPULS(0.,WRTDEL)
      IF(A*KEEP.LT.1.0)GO TO 999
      GO TO 405

* WRITING OF THE VOLUMETRIC MC IN EACH SOIL RING,
403   IF(KEEP.LT.1.0)GO TO 999
405   TIMHR=TIME/60.
      WRITE(6,600)
      WRITE(6,610)TIMHR
      WRITE(6,620)
      WRITE(6,630)(RADDIS(J),J=1,JMAX)
      DO 410 I=1,IMAX
410   WRITE(6,640)GPOT(I),(MC(I,J), J=1,JMAX)

      IF(TIME.EQ.0.0)GO TO 999

* CONVERT VOULME OF WATER APPLIED IN LITERS
      IRRLIT=VWAPPL/1000.

* CALCULATE VOLUME OF WATER IN EACH COLUMN WITHIN ROOT ZONE, IN EACH
* COLUMN BELOW ROOT ZONE, IN EACH ROW, CM3

      DO 420 J=1,JMAX
      VWCOLT(J)=0.0
420   VWCBRT(J)=0.0
      DO 440 I=1,IMAX
      VWROWT(I)=0.0
      DO 440 J=1,JMAX
      VWWRNG=MC(I,J)*VOLRNG(I,J)
      VWROWT(I)=VWROWT(I)+VWWRNG
      IF(I.GT.N)GO TO 430
      VWCOLT(J)=VWCOLT(J)+VWWRNG
      GO TO 440
430   VWCBRT(J)=VWCBRT(J)+VWWRNG
440   CONTINUE

* CALCULATE VOLUME OF WATER CONTENT WITHIN AND BELOW ROOT ZONE, L
      VWWRZT=0.0
      VWBRZT=0.0
```

```
      DO 445 J=1,JMAX
      VWWRZT=VWWRZT+VWCOLT(J)
445   VWBRZT=VWBRZT+VWCBRT(J)
      VWWRZT=VWWRZT/1000.
      VWBRZT=VWBRZT/1000.

* CALCULATE DELTA STORAGE IN EACH ROW, PERCENT
      DO 450 I=1,IMAX
450   DSTROW(I)=(VWROWT(I)-VWROWI(I))/VWAPPL*100.

* CALCULATE CUMULATIVE DELTA STORAGE IN EACH ROW, PERCENT
      CUMPC1(1)=DSTROW(1)
      DO 451 I=2,IMAX
451   CUMPC1(I)=CUMPC1(I-1)+DSTROW(I)

* CALCULATE ROOT WATER EXTRACTION FROM EACH ROW, CM3
      DO 452 I=1,N
      RWEROW(I)=0.0
      DO 452 J=1,JMAX
452   RWEROW(I)=RWEROW(I)+RWE(I,J)

* CALCULATE ROOT WATER EXTRACTION FROM EACH ROW, PERCENT
      DO 453 I=1,N
453   RWEROW(I)=RWEROW(I)/VWAPPL*100.

* CALCULATE CUMULATIVE ROOT WATER EXTRACTION FROM EACH ROW, PERCENT
      CUMPC4(1)=RWEROW(1)
      DO 454 I=2,IMAX
454   CUMPC4(I)=CUMPC4(I-1)+RWEROW(I)

* CALCULATE IRRIGATION APPLICATION IN EACH ROW, PERCENT
      DO 455 I=1,IMAX
455   IRRROW(I)=RWEROW(I)+DSTROW(I)

* CALCULATE CUMULATIVE IRRIGATION APPLICATION IN EACH ROW, PERCENT
      CUMPC6(1)=IRRROW(1)
      DO 456 I=2,IMAX
456   CUMPC6(I)=CUMPC6(I-1)+IRRROW(I)

* WRITE DEL STORAGE AND CUM DEL STORAGE IN EACH ROW, PERCENT
      WRITE(6,825)TIMHR
      WRITE(6,830)
      WRITE(6,855)(Z(I),I=2,IMAX1)
      WRITE(6,850)(DSTROW(I),I=1,IMAX)
      WRITE(6,855)(CUMPC1(I),I=1,IMAX)

* WRITE RWE AND CUMULATIVE RWE FROM EACH ROW, PERCENT
      WRITE(6,835)
      WRITE(6,850)(RWEROW(I),I=1,IMAX)
      WRITE(6,855)(CUMPC4(I),I=1,IMAX)
```

```
* WRITE IRRIGATION AND CUM IRRIGATION APPLICATION IN EACH ROW, PERCENT
      WRITE(6,840)
      WRITE(6,850)(IRRROW(I),I=1,IMAX)
      WRITE(6,855)(CUMPC6(I),I=1,IMAX)

* CALCULATE DELTA STORAGE IN EACH COLUMN, CM3
      DO 458 J=1,JMAX
      DSTCOL(J)=VWCOLT(J)-VWCOLI(J)
458   DSTCBR(J)=VWCBRT(J)-VWCBRI(J)

* CALCULATE ROOT WATER EXTRACTION FROM EACH COLUMN OF THE SOIL, CM3
      DO 460 J=1,JMAX
      RWECOL(J)=0.0
      DO 460 I=1,N
460   RWECOL(J)=RWECOL(J)+RWE(I,J)

* CALCULATE CUMULATIVE RWE FROM THE SOIL CYLINDER, PERCENT
      RWECUM=0.0
      DO 465 J=1,JMAX
465   RWECUM=RWECUM+RWECOL(J)
      RWELIT=RWECUM/1000.

* CALCULATE DELTA STORAGE IN EACH COLUMN, MM
      DO 467 J=1,JMAX
      DSTCMM(J)=DSTCOL(J)/ARNGJ(J)*10.
467   DSTBMM(J)=DSTCBR(J)/ARNGJ(J)*10.

* CALCULATE RWE & IRRIGATION FROM EACH COLUMN, MM
      DO 470 J=1,JMAX
      RWECMM(J)=RWECOL(J)/ARNGJ(J)*10.
470   IRRIMM(J)=RWECMM(J)+DSTCMM(J)+DSTBMM(J)

* CALCULATIONS TO ACCOUNT FOR WATER DISTRIBUTION
      VWWSCT=VWWRZT+VWBRZT
      DSTWRZ=VWWRZT-VWWRZI
      DSTBRZ=VWBRZT-VWBRZI
      DSTWSC=VWWSCT-VWWSCI
      VWSIMU=DSTWSC+RWELIT
      VWERR=IRRLIT-VWSIMU
      VWACCT=VWSIMU/IRRLIT*100.0

* CALCULATE DELTA STORAGE IN EACH COLUMN, PERCENT
      DO 475 J=1,JMAX
      DSTCOL(J)=DSTCOL(J)/VWAPPL*100.
475   DSTCBR(J)=DSTCBR(J)/VWAPPL*100.

* CALCULATE CUMULATIVE DELTA STORAGE IN EACH COLUMN, PERCENT
      CUMPC2(1)=DSTCOL(1)
      CUMPC3(1)=DSTCBR(1)
```

```
      DO 480 J=2,JMAX
      CUMPC2(J)=CUMPC2(J-1)+DSTCOL(J)
480   CUMPC3(J)=CUMPC3(J-1)+DSTCBR(J)

* CALCULATE ROOT WATER EXTRACTION FROM EACH COLUMN, PERCENT
      DO 482 J=1,JMAX
482   RWECOL(J)=RWECOL(J)/VWAPPL*100.

* CALCULATE CUMULATIVE ROOT WATER EXTRACTION FROM EACH COLUMN, PERCENT
      CUMPC5(1)=RWECOL(1)
      DO 483 J=2,JMAX
483   CUMPC5(J)=CUMPC5(J-1)+RWECOL(J)

* CALCULATE IRRIGATION APPLICATION IN EACH COLUMN, PERCENT
      DO 485 J=1,JMAX
485   IRRCOL(J)=DSTCOL(J)+DSTCBR(J)+RWECOL(J)

* CALCULATE CUMULATIVE IRRIGATION APPLICATION IN EACH COLUMN, PERCENT
      CUMIRR(1)=IRRCOL(1)
      DO 490 J=2,JMAX
490   CUMIRR(J)=CUMIRR(J-1)+IRRCOL(J)

* WRITE DISTANCE FROM EMITTER, DEL STORAGE WITHIN AND BELOW RZ, PERCENT
      WRITE(6,930)
      WRITE(6,940)(RADRNG(J),J=2,JMAX1)
      WRITE(6,945)(DSTCOL(J),J=1,JMAX)
      WRITE(6,950)(CUMPC2(J),J=1,JMAX)
      WRITE(6,952)(DSTCBR(J),J=1,JMAX)
      WRITE(6,953)(CUMPC3(J),J=1,JMAX)
      WRITE(6,954)(RWECOL(J),J=1,JMAX)
      WRITE(6,955)(CUMPC5(J),J=1,JMAX)
      WRITE(6,956)(IRRCOL(J),J=1,JMAX)
      WRITE(6,957)(CUMIRR(J),J=1,JMAX)

* WRITE DELTA STORAGE, RWE AND IRRIGATION IN EACH COLUMN, MM
      WRITE(6,958)
      WRITE(6,959)(RADDIS(J),J=1,JMAX)
      WRITE(6,960)(DSTCMM(J),J=1,JMAX)
      WRITE(6,962)(DSTBMM(J),J=1,JMAX)

      WRITE(6,965)(RWECMM(J),J=1,JMAX)
      WRITE(6,970)(IRRIMM(J),J=1,JMAX)

* WRITING OF THE WATER DISTRIBUTION WITHIN SOIL CYLINDER, L
      WRITE(6,710)
      WRITE(6,720)
      WRITE(6,730)VWWRZI,VWWRZT,DSTWRZ,RWELIT
      WRITE(6,740)VWBRZI,VWBRZT,DSTBRZ
      WRITE(6,750)VWWSCI,VWWSCT,DSTWSC,RWELIT
```

```
* WRITE IRRI APPLIED AND SIMULATED, ERROR & SIMULATED IRRI, PERCENT
      WRITE(6,760)
      WRITE(6,770)IRRLIT,VWSIMU,VWERR,VWACCT

999   CONTINUE

***********************************************************************
TERMINAL
***********************************************************************

* RWE OUTPUT AND SOME CALCULATIONS AT TERMINATION OF SIMULATION RUN

500   PETCU=PETCUM*10.0
      DO 510 J=1,JMAX
      AETAR(J)=0.0
      AEPEAR(J)=0.0
      DO 510 I=1,N
      AET(I,J)=RWE(I,J)*10.0/ARNGJ(J)
      AEPE(I,J)=AET(I,J)/PETCU
      AEPEL(I,J)=AEPE(I,J)/RWEZ(I)
      AETAR(J)=AETAR(J)+AET(I,J)
510   AEPEAR(J)=AEPEAR(J)+AEPE(I,J)

* WRITE ROOT WATER EXTRACTION, FROM EACH SOIL RING, MM
520   WRITE(6,780)
      WRITE(6,610)TIMHR
      WRITE(6,650)
      WRITE(6,630)(RADRNG(J+1),J=1,JMAX)
      DO 530 I=1,N
530   WRITE(6,640)Z(I+1),(AET(I,J), J=1,JMAX)

* WRITE RWE/PETCUM, FROM EACH SOIL RING, RATIO
      WRITE(6,660)
      DO 540 I=1,N
540   WRITE(6,640)Z(I+1),(AEPE(I,J), J=1,JMAX)

* WRITE RWE/(PETCUM*RWEZ(I)) FOR EACH SOIL RING, RATIO
      WRITE(6,670)
      DO 550 I=1,N
550   WRITE(6,640)Z(I+1),(AEPEL(I,J), J=1,JMAX)

* WRITE RWE FROM THE SOIL SURFACE FROM EACH WIDTH OF SOIL RING, MM
      WRITE(6,680)
      WRITE(6,640)RZD,(AETAR(J), J=1,JMAX)

* WRITE RWE/PETCUM FROM THE SOIL SURFACE FROM EACH WIDTH OF RING, RATIO
      WRITE(6,690)
      WRITE(6,640)RZD,(AEPEAR(J), J=1,JMAX)

      WRITE(6,700)PETCU,EQHR
```

```
* CALCULATIONS FOR SIMULATED WATER DISTRIBUTION W.R.T WATER APPLIED.
      AETALL=RWECUM/(PI*RADRNG(JMAX1)**2.)*10.
      AETPET=AETALL/PETCU
      ERRPC=VWERR/IRRLIT*100.
      DSRZPC=DSTWRZ/IRRLIT*100.
      DSLSPC=DSTBRZ/IRRLIT*100.
      DSSCPC=DSTWSC/IRRLIT*100.
      RWEPC=RWECUM/VWAPPL*100.

* WRITING OF THE WATER DISTRIBUTION ACCOUNTED FOR BY SIMULATION RUN
      WRITE(6,600)
      WRITE(6,610)TIMHR
      WRITE(6,790)
      WRITE(6,800)
      WRITE(6,810)AETALL,PETCU,AETPET
      WRITE(6,920)N
      WRITE(6,820)MP50AV
      WRITE(6,860)VWACCT
      WRITE(6,870)ERRPC
      WRITE(6,880)DSRZPC
      WRITE(6,890)DSLSPC
      WRITE(6,900)DSSCPC
      WRITE(6,910)RWEPC

************************************************************************
*              FORMAT STATEMENTS FOR WRITING SIMULATION RESULTS
************************************************************************

600   FORMAT('1','SIMULATION OF DRIP IRRIGATION (CONTINUOUS   ) AT THE RA
     $TE OF 2.00 L/H'/' FOR 6 HOURS FILED=RM1, TOTAL APPLICATION=12.00 L
     $, DATE= 24-08-1980')
610   FORMAT(/1X,'TIME=',F6.2,' HOURS')
620   FORMAT('0','VOLUMETRIC MOISTURE CONTENT IN THE SOIL RINGS, M3/M3 ,
     $ Z AND R IN CM')
630   FORMAT(/1X,' Z/R   ',F6.1,10F8.1/)
640   FORMAT(1X,F5.1,11F8.4)

650   FORMAT(//1X,'ROOT WATER EXTRACTION FROM EACH SOIL RING, MM, Z AND
     $R IN CM'/)
660   FORMAT(//1X,'RWE/PETCUM FROM EACH SOIL RING WITHIN ROOT ZONE, RATI
     $O'/)
670   FORMAT(//1X,'RWE/PET FROM EACH DEPTH AND WIDTH WITHIN ROOT ZONE,
     $RATIO'/)
680   FORMAT(//1X,'RWE FROM TOTAL ROOT ZONE DEPTH AND EACH WIDTH OF SOIL
     $ CYLINDER, MM'/)
690   FORMAT(//1X,'RWE/PETCUM FROM TOTAL ROOT ZONE DEPTH AND EACH WIDTH
     $OF RING,  RATIO'/)
700   FORMAT(/1X,'PETCUM=',F12.4,' MM',4X,'Q EMITTER =',F6.2,' L/H')
```

```
710   FORMAT(/1X,' ACCOUNTING OF THE VOLUME OF WATER FOR THE FINITE SOIL
     $ CYLINDER, L')
720   FORMAT('0',24X,'INITIAL     FINAL     DEL STORAGE      RWECUM')
730   FORMAT('0','WITHIN ROOT ZONE =',3F12.3,F15.3)
740   FORMAT(' ','BELOW  ROOT ZONE =',3F12.3)
750   FORMAT(' ','TOTAL            =',3F12.3,F15.3)

760   FORMAT(/1X,T24,'APPLIED (L)',T36,'SIMULATED (L)',
     $T51,'ERROR (L)',T61,'ACCOUNTED (PC)')
770   FORMAT('0','VOLUME OF WATER  = ',4F12.3)
780   FORMAT('1',' ACCOUNTING OF ROOT WATER EXTRACTION AND POTENTIAL EVA
     $POTRANSPIRATION'//)
790   FORMAT('0',' VALUES OVER THE AREA OF THE SOIL CYLINDER AT THE END
     $OF SIMULATION RUN'///)
800   FORMAT(8X,'AET(MM)     PET(MM)     AET/PET')
810   FORMAT(/'   ',3F12.4///)
820   FORMAT(/8X,'MPOT AT 50 PER CENT AVILABLE MOISTURE  =',F10.3,' CM')

825   FORMAT('1','TIME=',F6.2,' HOURS')
830   FORMAT(/1X,'DELTA STORAGE IN EACH ROW OF SOIL RINGS, PC, 1ST LINE
     $= DEPTH (CM), 2ND LINE= DEL STORAGE, PC, 3RD LINE=CUMULTIVE, PC'/)
835   FORMAT(/1X,'RWE AND CUM RWE IN EACH ROW, PERCENT'/)
840   FORMAT(/1X,'IRRIGATION AND CUM IRRIGATION APPLICATION TO EACH ROW,
     $PERCENT'/)
850   FORMAT('0',15F8.3)
855   FORMAT(1X,15F8.3)

860   FORMAT(//8X,'VOLUME OF WATER ACCOUNTED, PERCENT      =',F10.3)
870   FORMAT(/8X,'VOLUME OF WATER ERROR, PERCENT          =',F10.3)
880   FORMAT(/8X,'DELTA STORAGE ROOT ZONE, PERCENT        =',F10.3)
890   FORMAT(/8X,'DELTA STORAGE BELOW ROOT ZONE, PERCENT  =',F10.3)
900   FORMAT(/8X,'DELTA STORAGE SOIL CYLINDER, PERCENT    =',F10.3)
910   FORMAT(/8X,'ROOT WATER EXTRACTION, PERCENT          =',F10.3)
920   FORMAT(/8X,'NUMBER OF RING ROWS WITHIN ROOT ZONE    =',I7)

930   FORMAT(////1X,'DEL STORAGE & CUM DEL STORAGE WITHIN AND BELOW RZ,
     $ RWE & CUM RWE, AND IRRI & CUM IRRIGATION IN EACH COLUMN, PC'/)
940   FORMAT(1X,'DISTANCE       (CM) =',11F8.3/)
945   FORMAT(1X,'DEL STO RZ,      PC =',11F8.3)
950   FORMAT(1X,'CUM DEL STO RZ,  PC =',11F8.3/)
952   FORMAT(1X,'DEL STO BRZ,     PC =',11F8.3)
953   FORMAT(1X,'CUM DEL STO BRZ, PC =',11F8.3/)
954   FORMAT(1X,'RWE,             PC =',11F8.3)
955   FORMAT(1X,'CUM RWE,         PC =',11F8.3/)
956   FORMAT(1X,'IRRIGATION,      PC =',11F8.3)
957   FORMAT(1X,'CUM IRRIGATION,  PC =',11F8.3/)

958   FORMAT(/1X,'DEL STORAGE, WITHIN AND BELOW ROOT ZONE, RWE AND IRRIG
     $ATION APPLICATION IN EACH COLUMN, MM'/)
959   FORMAT(1X,'DISTANCE       (CM) =',11F8.3)
```

```
960   FORMAT(/1X,'STORAGE WRZ     (MM) =',11F8.3)
962   FORMAT(1X,'STORAGE BRZ      (MM) =',11F8.3)
965   FORMAT(1X,'RWE              (MM) =',11F8.3)
970   FORMAT(1X,'IRRIGATION       (MM) =',11F8.3)

*********************************************
* SIMULATION RUN CONTROL STATEMENTS
*********************************************

TIMER FINTIM=900.,DELT=15.0,PRDEL=15.
METHOD MILNE
END
STOP
ENDJOB
```

APPEDIX B

FIGURES OF VARIOUS EXPERIMENTS AND SIMULATIONS

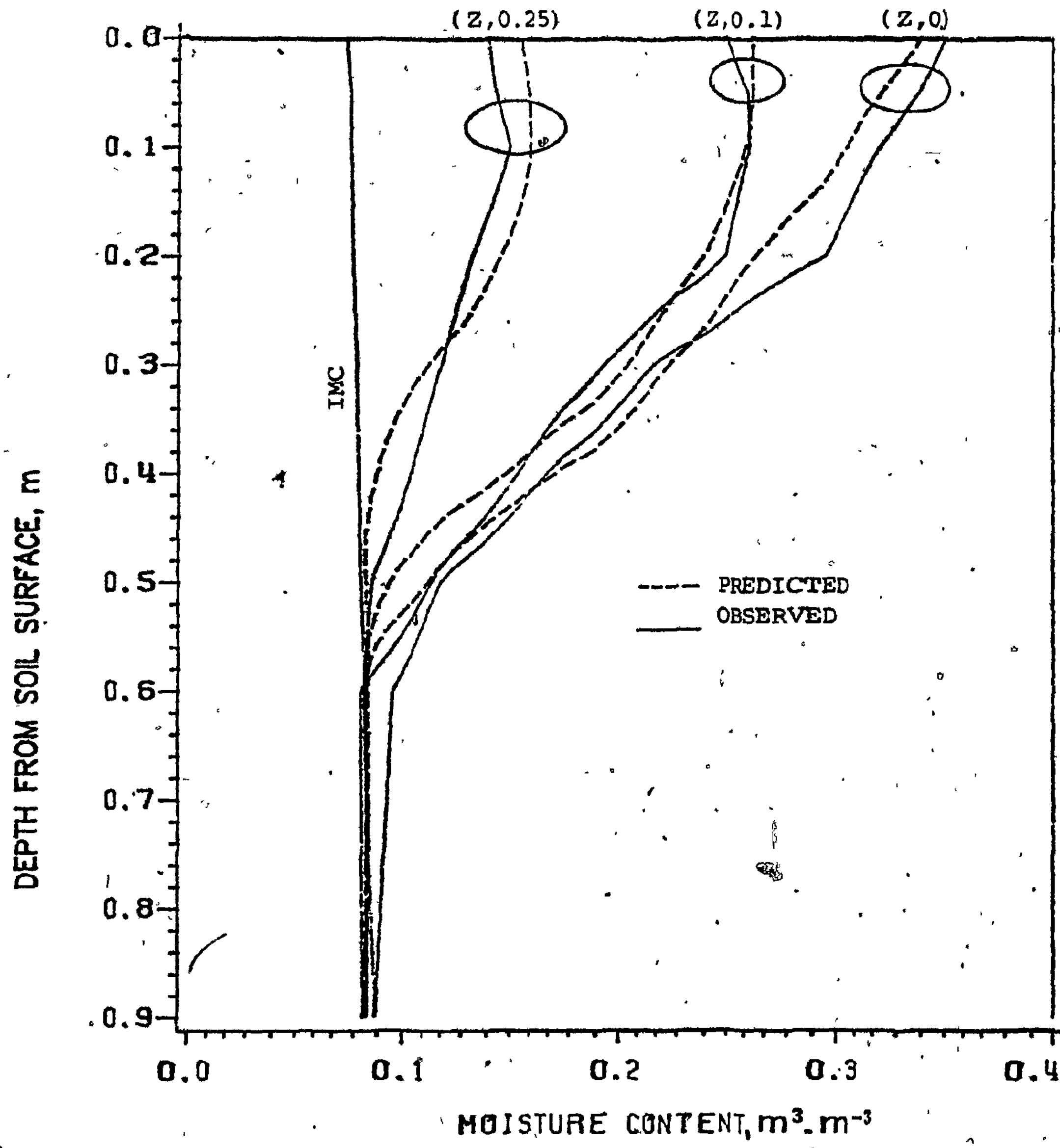

Figure B.1. Soil moisture content profiles before and after 12 L of water applied at 4 $L.h^{-1}$ at Rougemont orchard site 1.

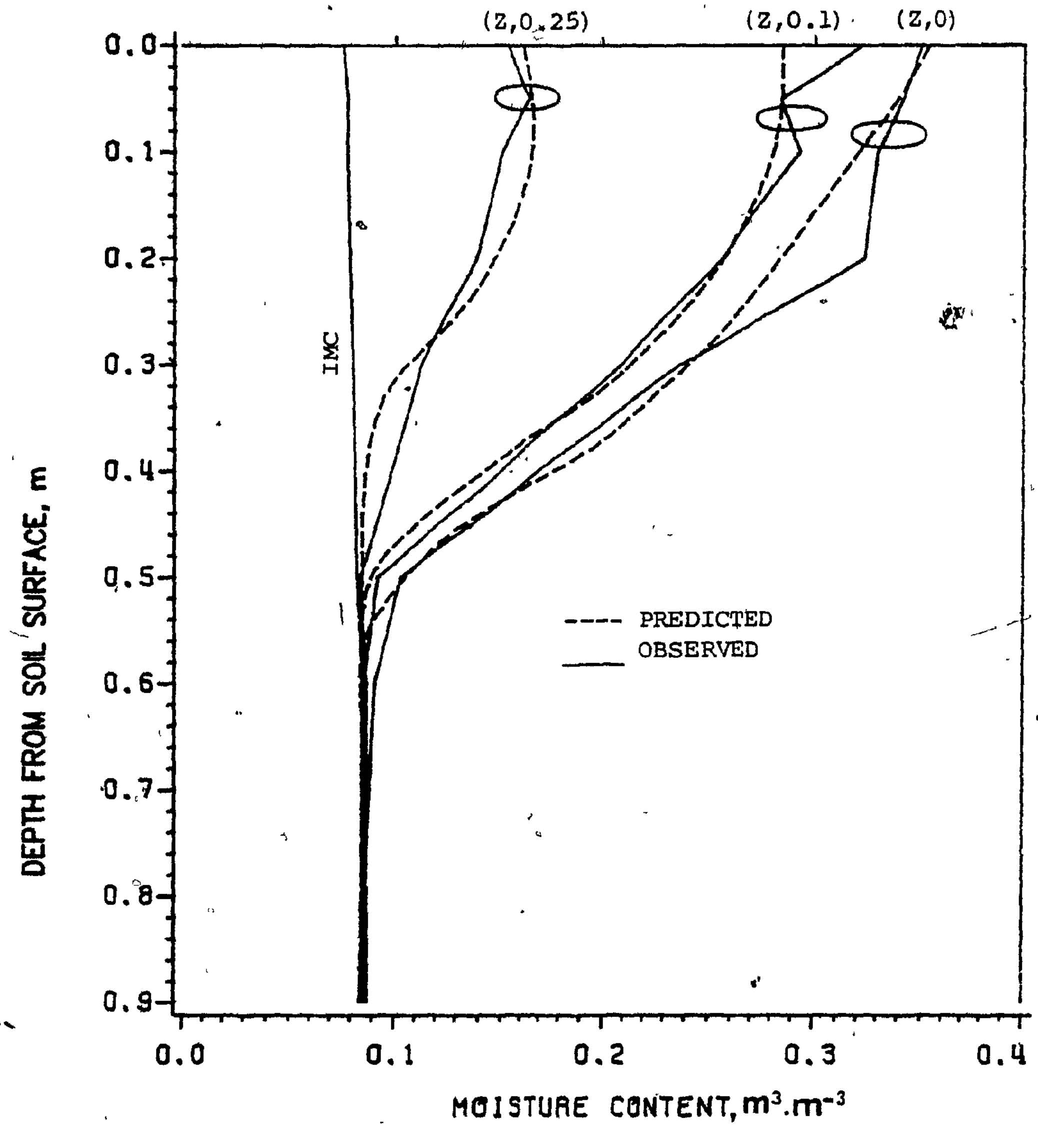

Figure B.2. Soil moisture content profiles before and after 12 L of water applied at 6 $L.h^{-1}$ at Rougemont orchard site 1.

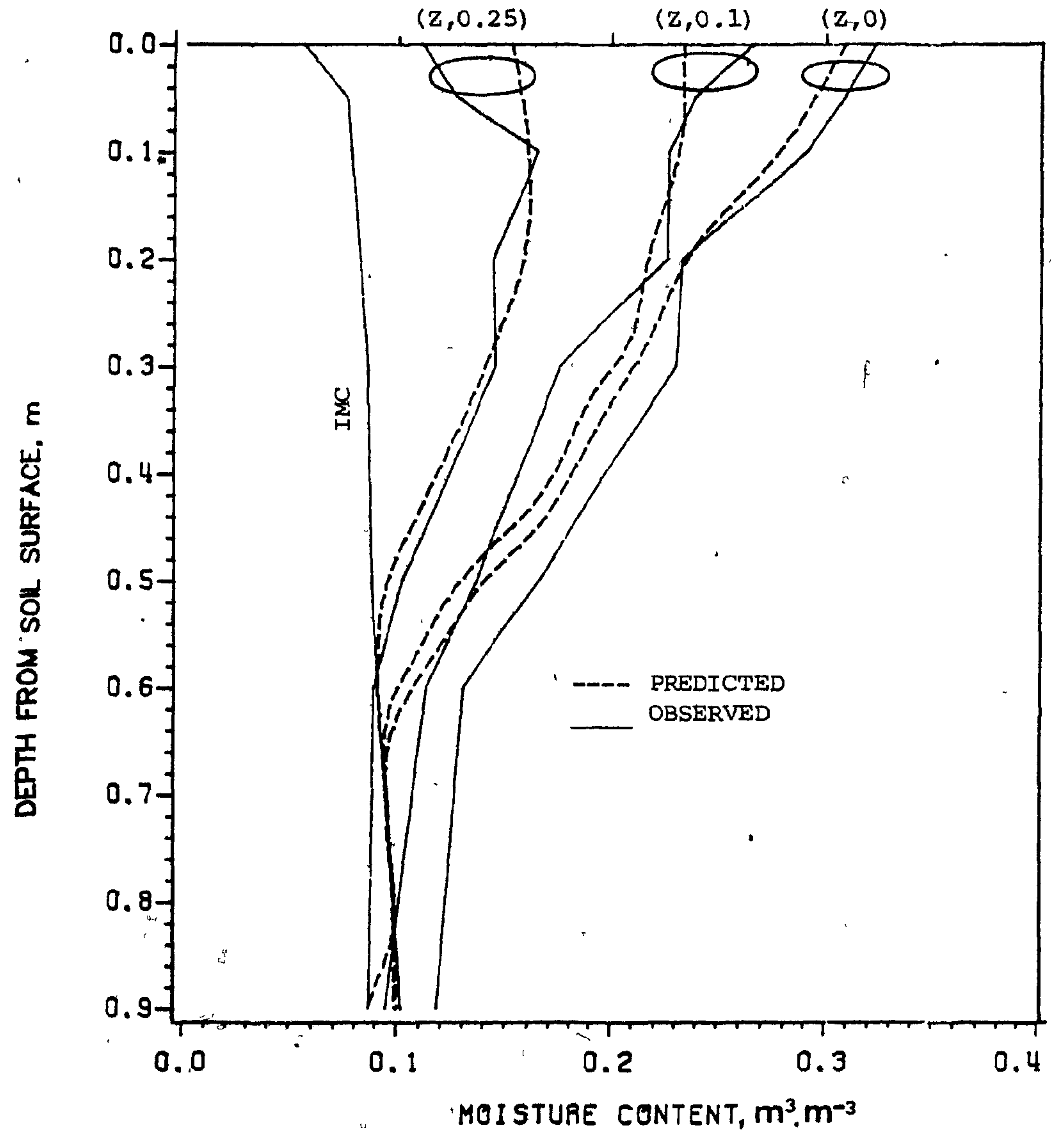

Figure B.3. Soil moisture content profiles before and after 16 L of water applied at 2 $L.h^{-1}$ at Rougemont orchard site 1.

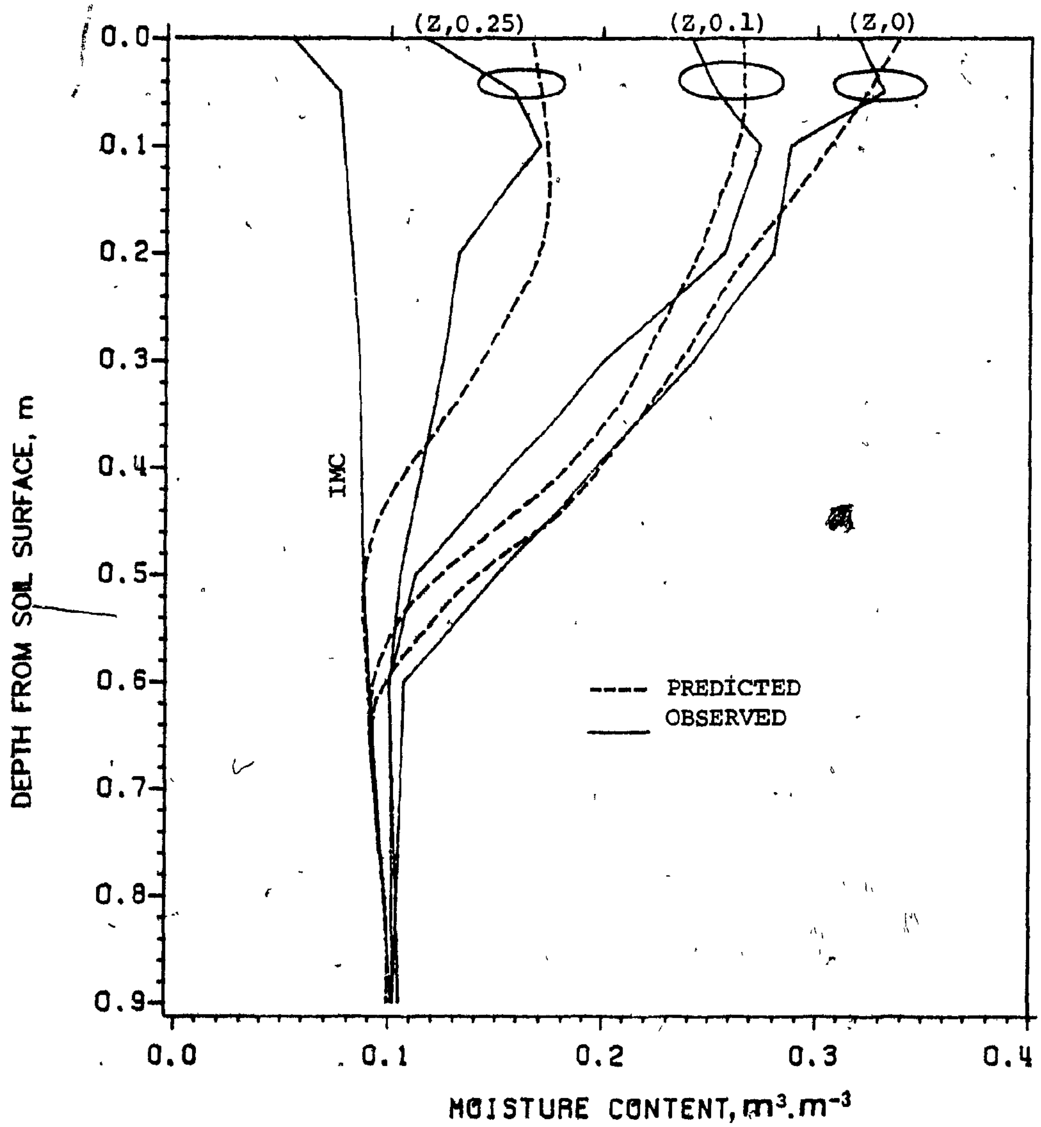

Figure B.4. Soil moisture content profiles before and after 16 L of water applied at 4 $L.h^{-1}$ at Rougemont orchard site 1.

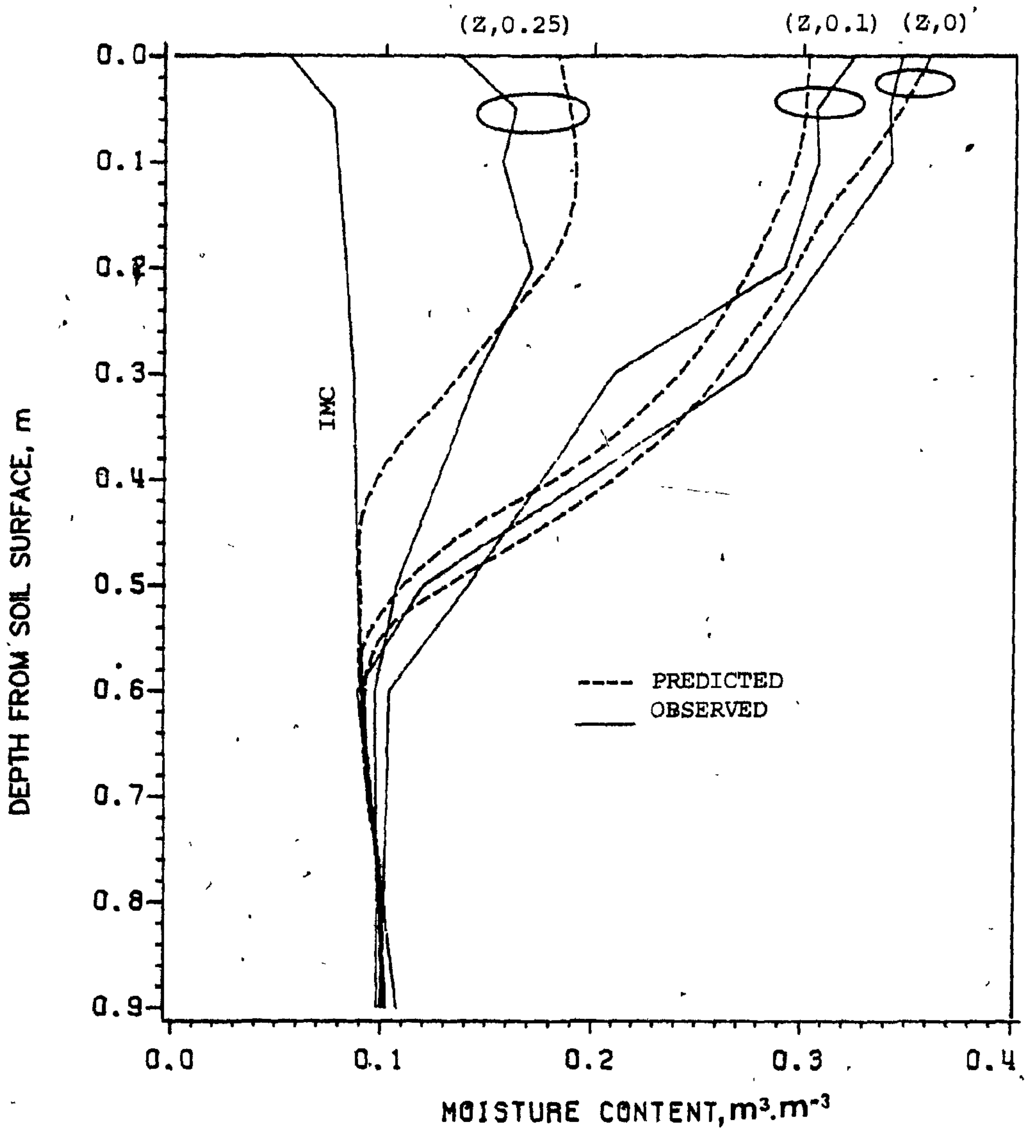

Figure B.5. Soil moisture content profiles before and after 16 L of water applied at 8 $L.h^{-1}$ at Rougemont orchard site 1.

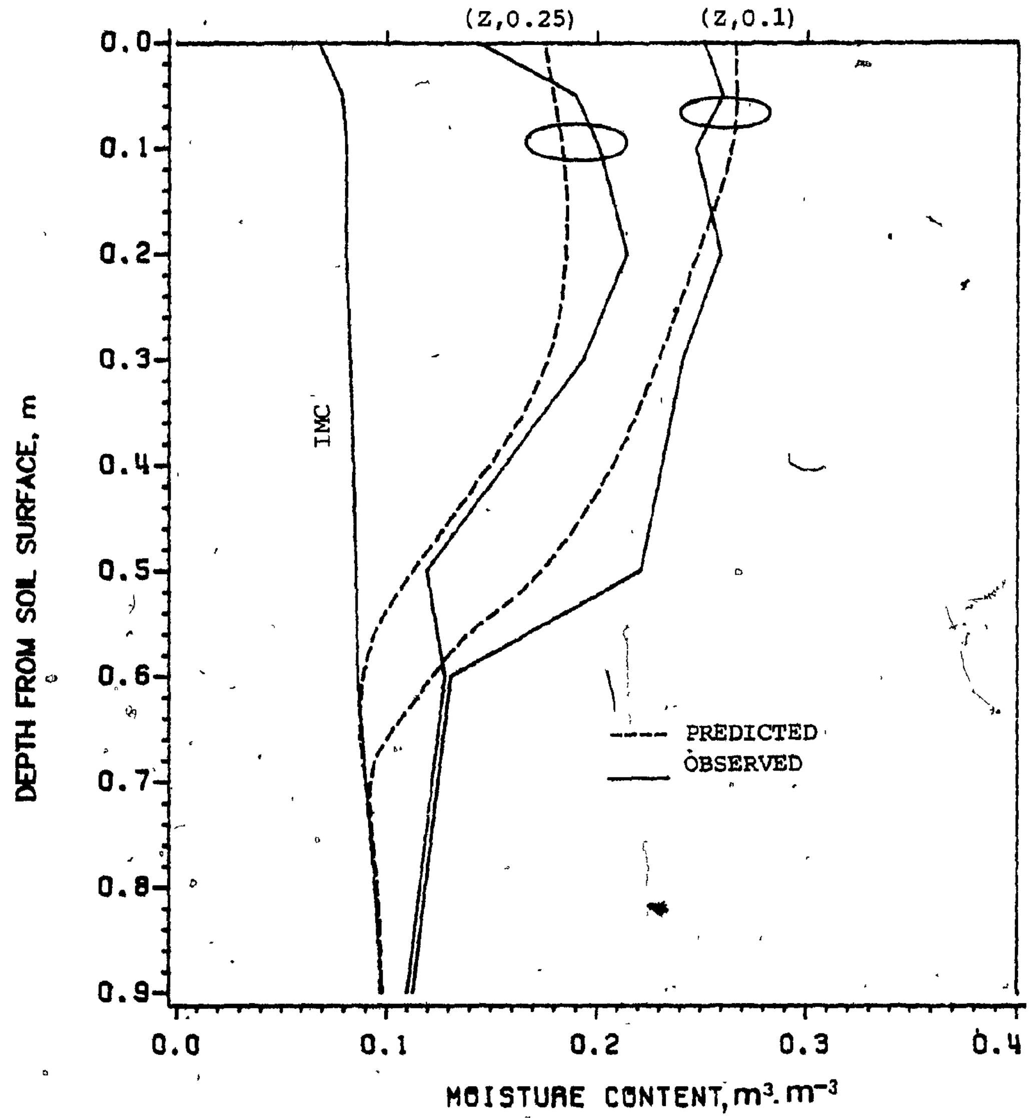

Figure B.6. Soil moisture content profiles before and after 24 L of water applied at 4 $L.h^{-1}$ at Rougemont orchard site 1.

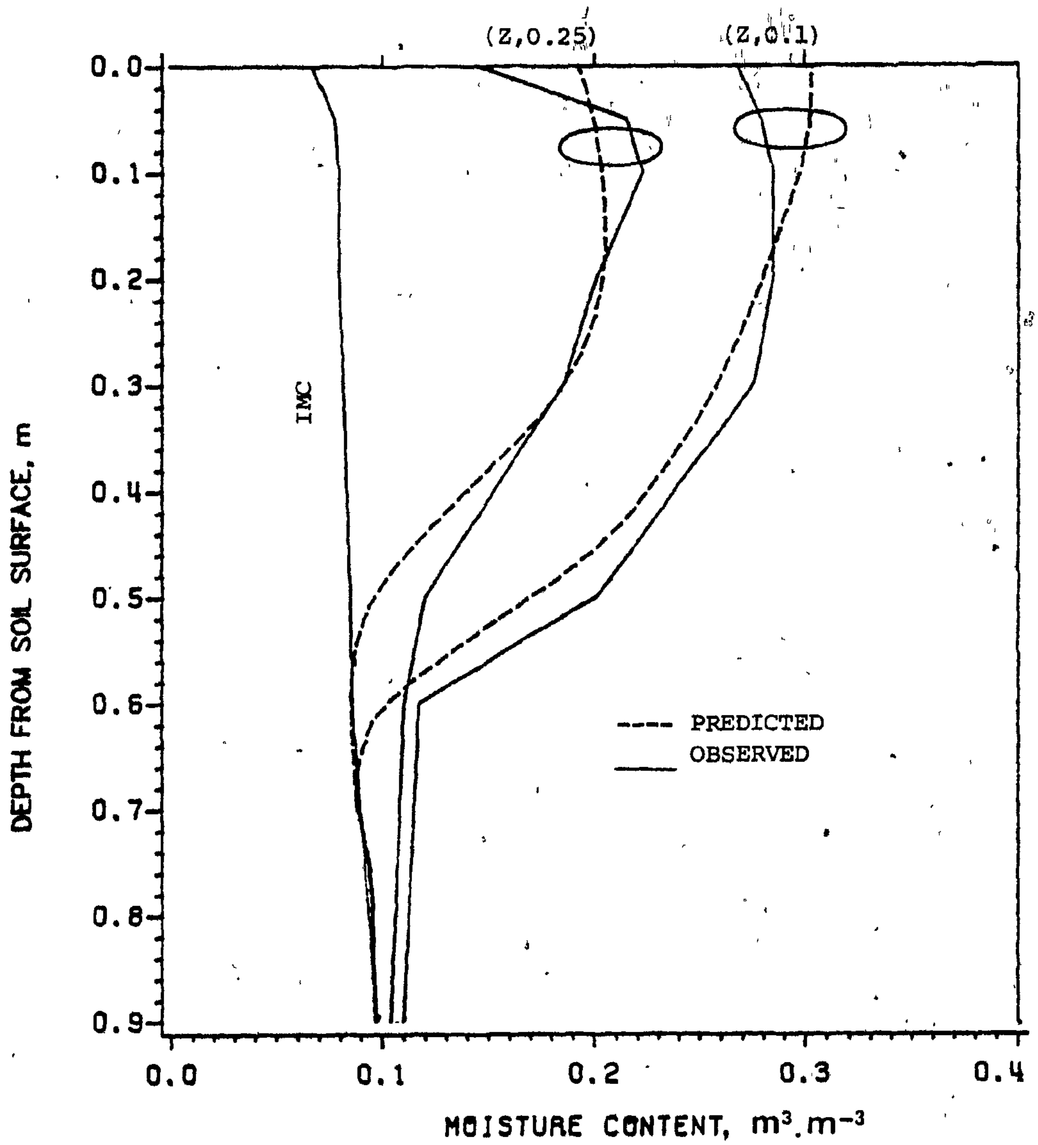

Figure B.7. Soil moisture content profiles before and after 24 L of water applied at 8 $L.h^{-1}$ at Rougemont orchard site 1.

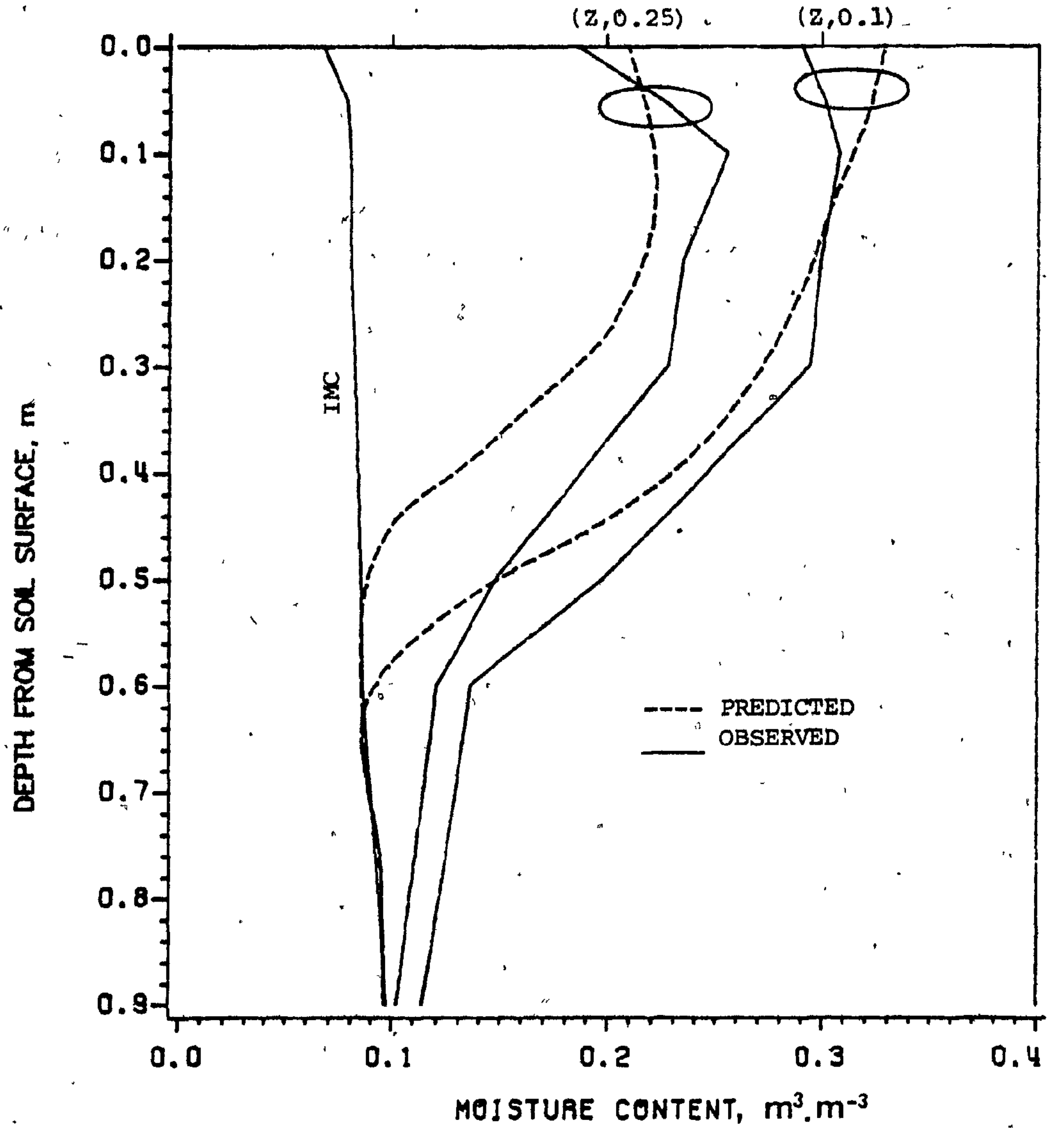

Figure B.8. Soil moisture content profiles before and after 24 L of water applied at 12 $L.h^{-1}$ at Rougemont orchard site 1.

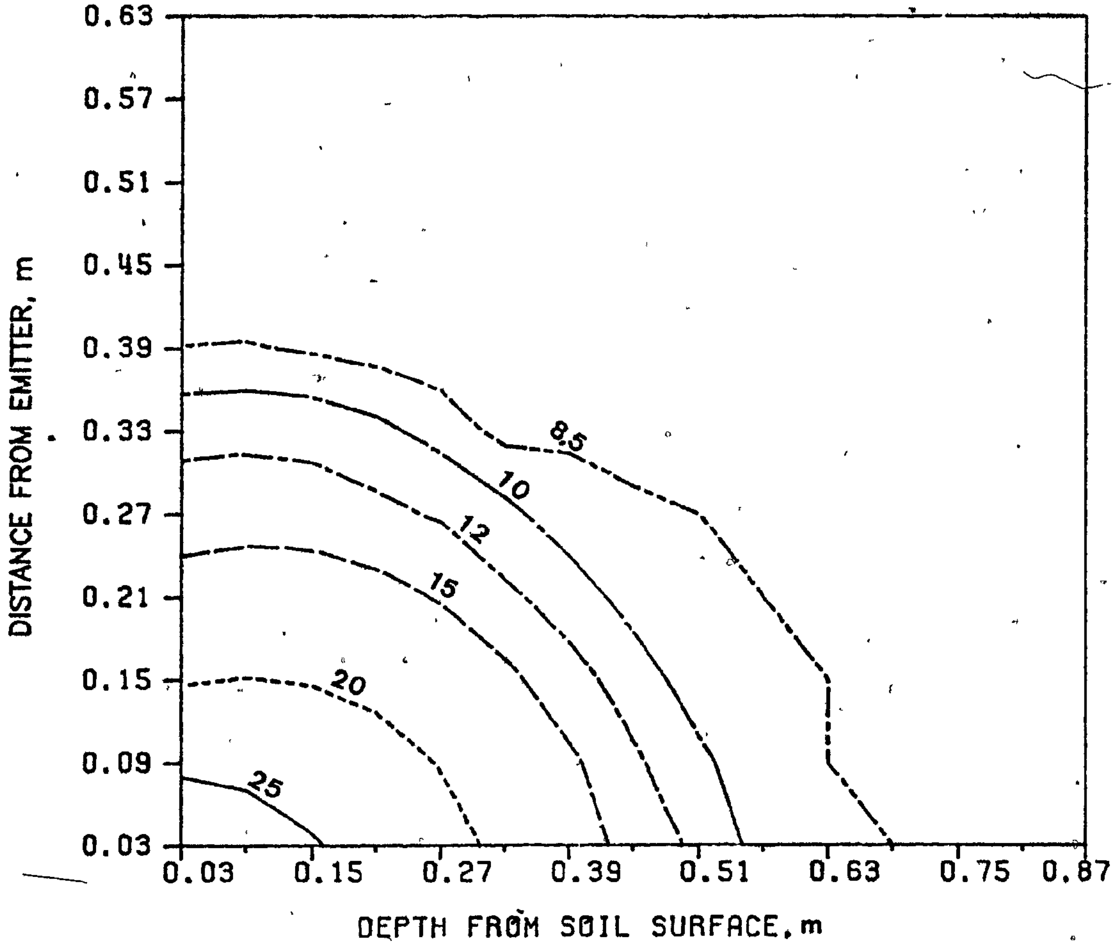

Figure B.9. Equimoisture curves at the cessation of irrigation water application of 12 L with discharge rate of 2 $L.h^{-1}$ for Rougemont orchard site 1. (Numbers labeling curves indicate soil moisture content, percent)

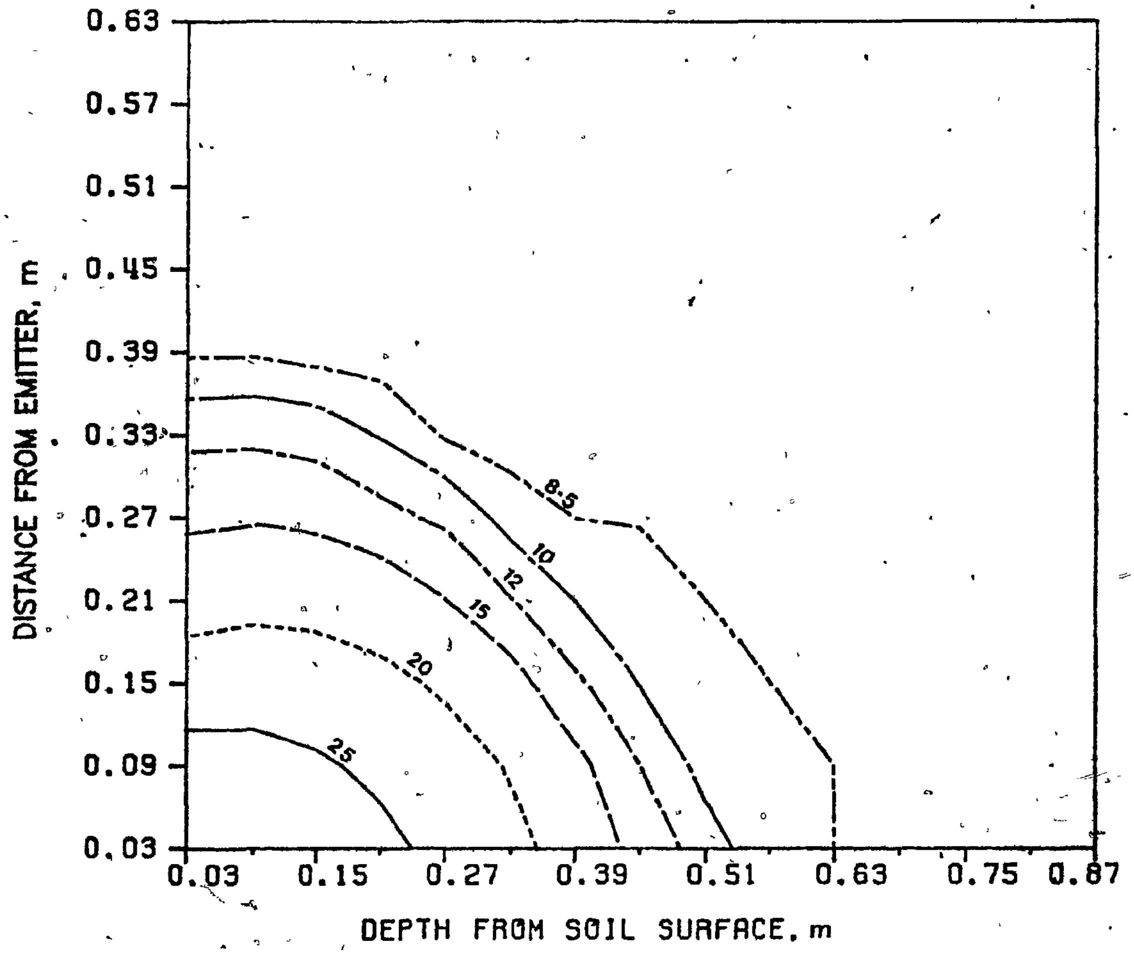

Figure B.10. Equimoisture curves at the cessation of irrigation water application of 12 L with discharge rate of 4 $L.h^{-1}$ for Rougemont orchard site 1. (Numbers labeling curves indicate soil moisture content, percent)

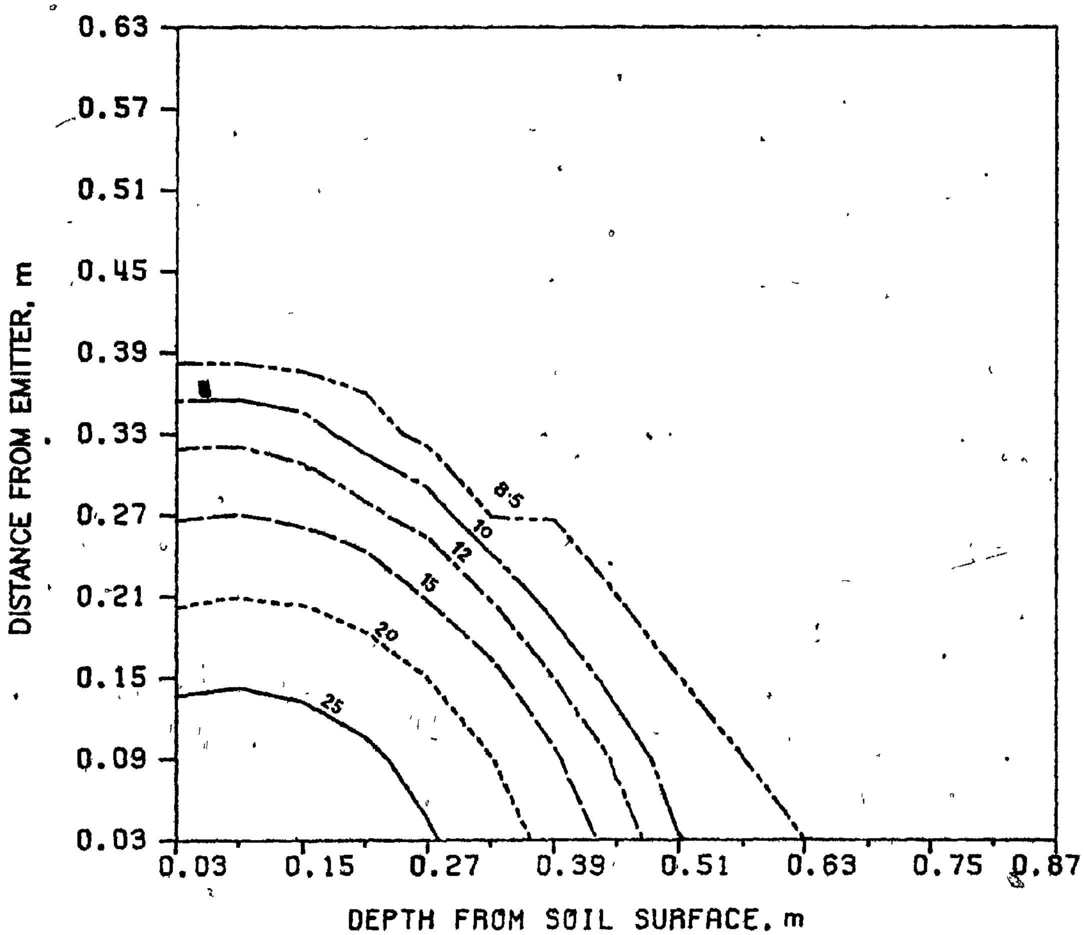

Figure B.11. Equimoisture curves at the cessation of irrigation water application of 12 L with discharge rate of 6 $L.h^{-1}$ for Rougemont orchard site 1. (Numbers labeling curves indicate soil moisture content, percent)

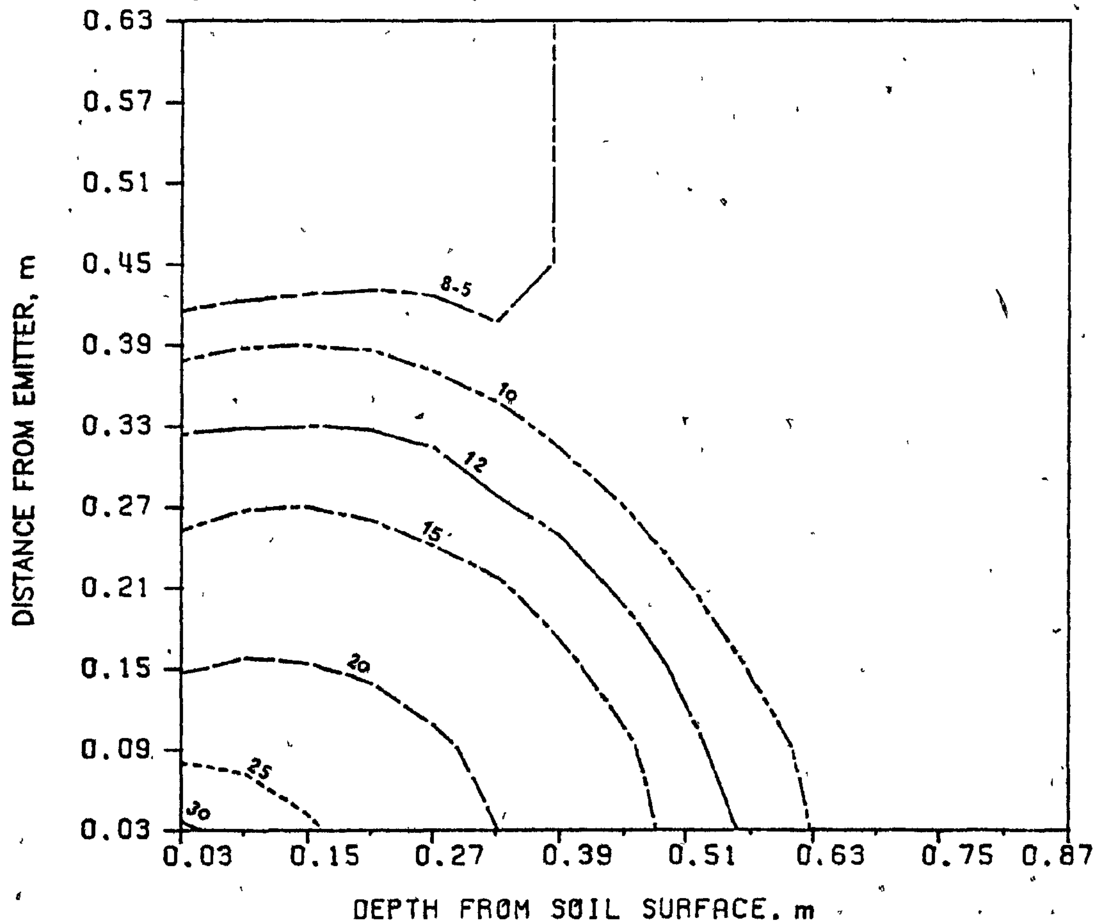

Figure B.12. Equimoisture curves at the cessation of irrigation water application of 16 L with discharge rate of 2 $L.h^{-1}$ for Rougemont orchard site 1.

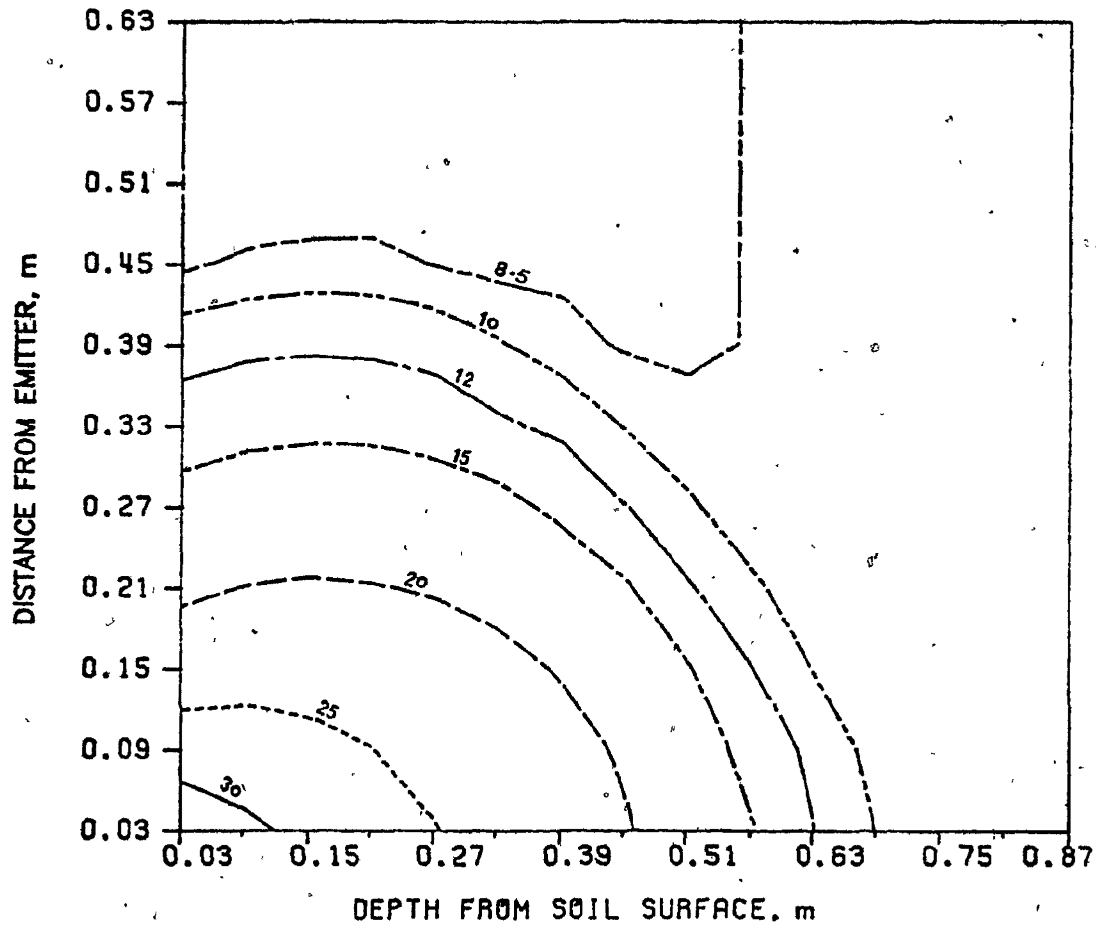

Figure B.13. Equimoisture curves at the cessation of irrigation water application of 24 L with discharge rate of 4 $L.h^{-1}$ for Rougemont orchard site 1. (Numbers labeling curves indicate soil moisture content, percent)

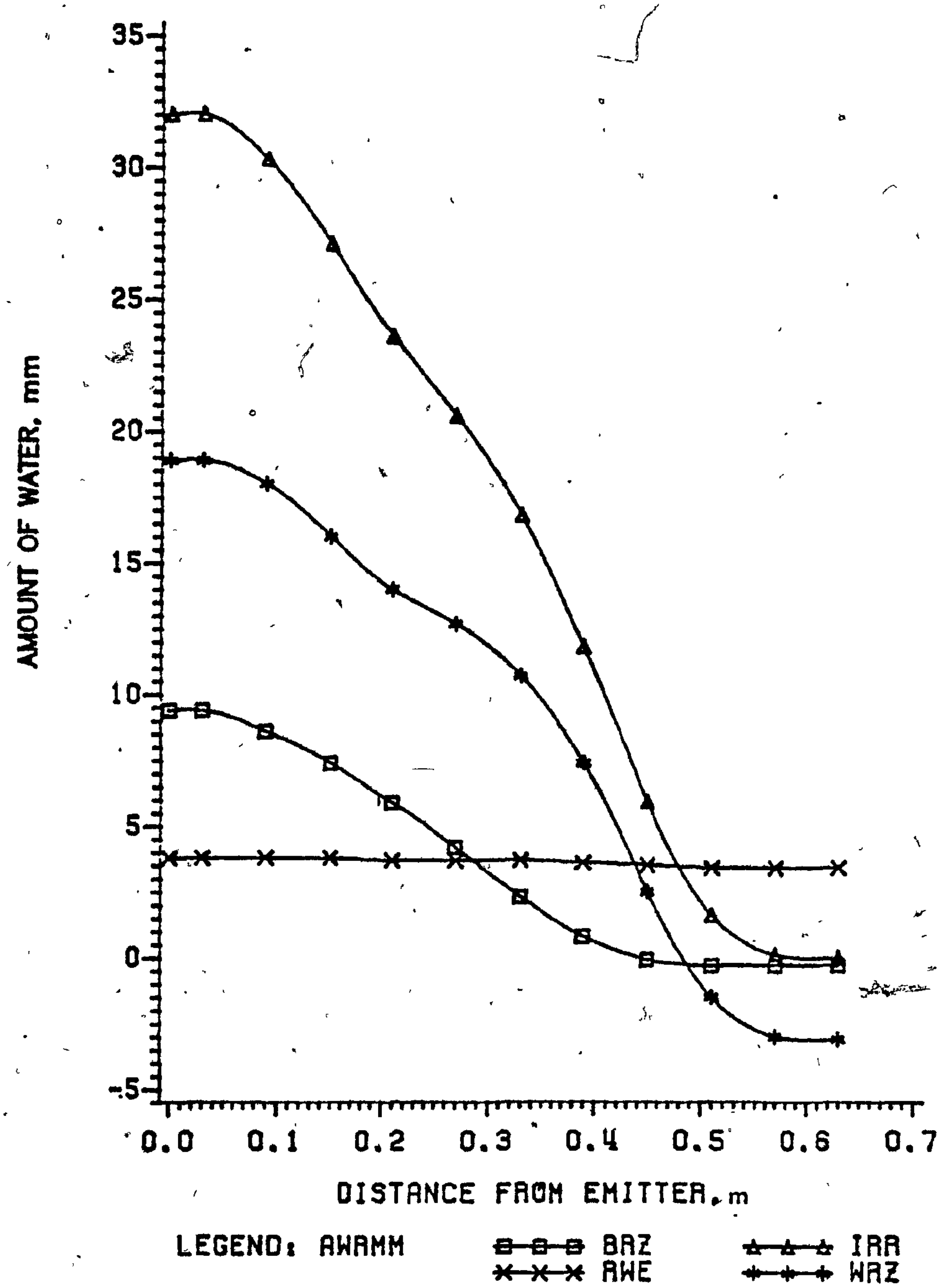

Figure B.14. Distribution of 12 L of water along horizontal distance with discharge rate of 2 $L.h^{-1}$ (expressed in mm) for Rougemont orchard site 1.

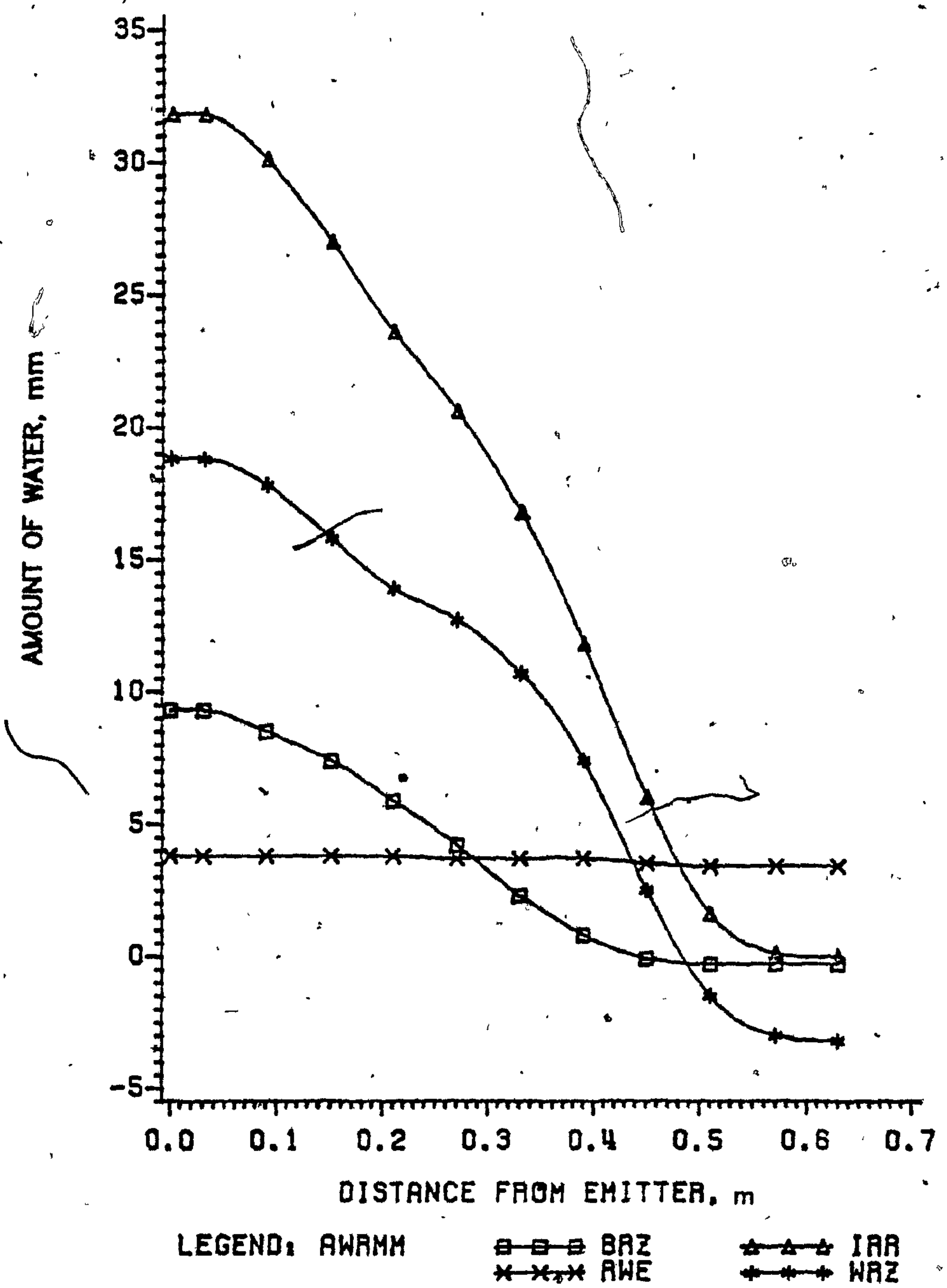

Figure B.15. Distribution of 12 L of water along horizontal distance with pulse discharge rate of 4 $L.h^{-1}$ (expressed in mm) for Rougemont orchard site 1.

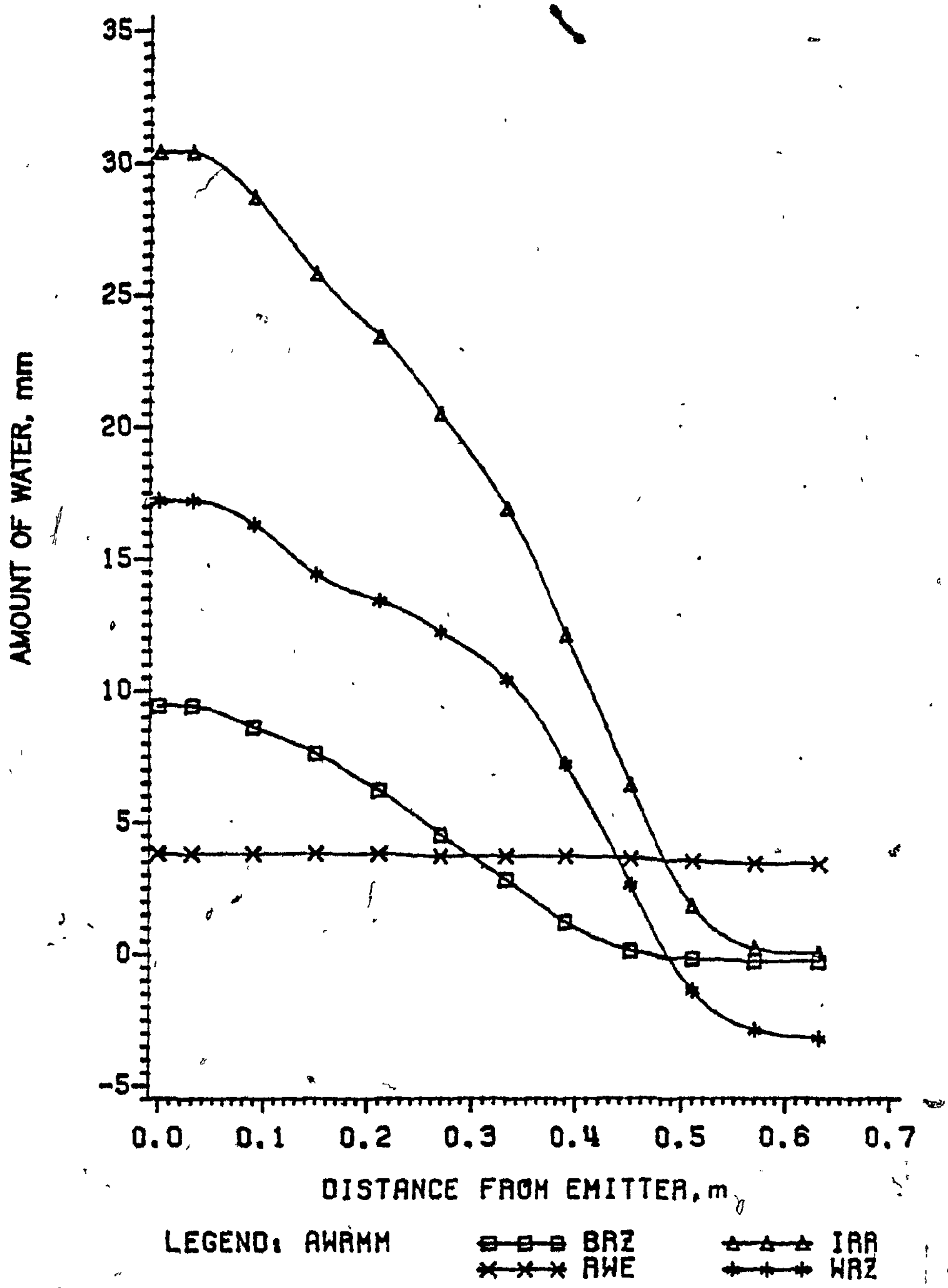

Figure B.16. Distribution of 12 L of water along horizontal distance with discharge rate of 4 $L.h^{-1}$ (expressed in mm) for Rougemont orchard site 1.

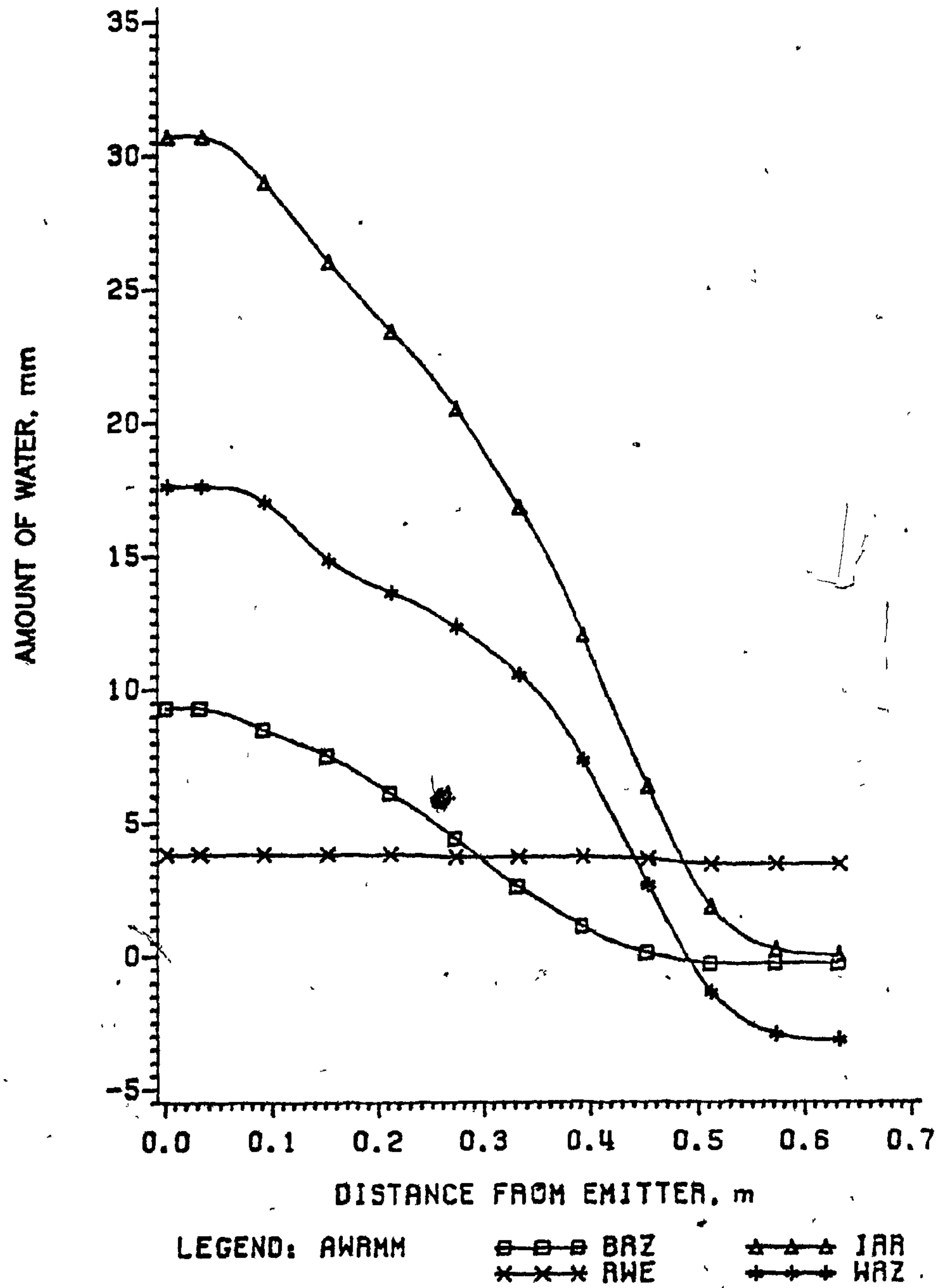

Figure B.17. Distribution of 12 L of water along horizontal distance with pulse discharge rate of 6 L.h^{-1} (expressed in mm) for Rougemont orchard site 1.

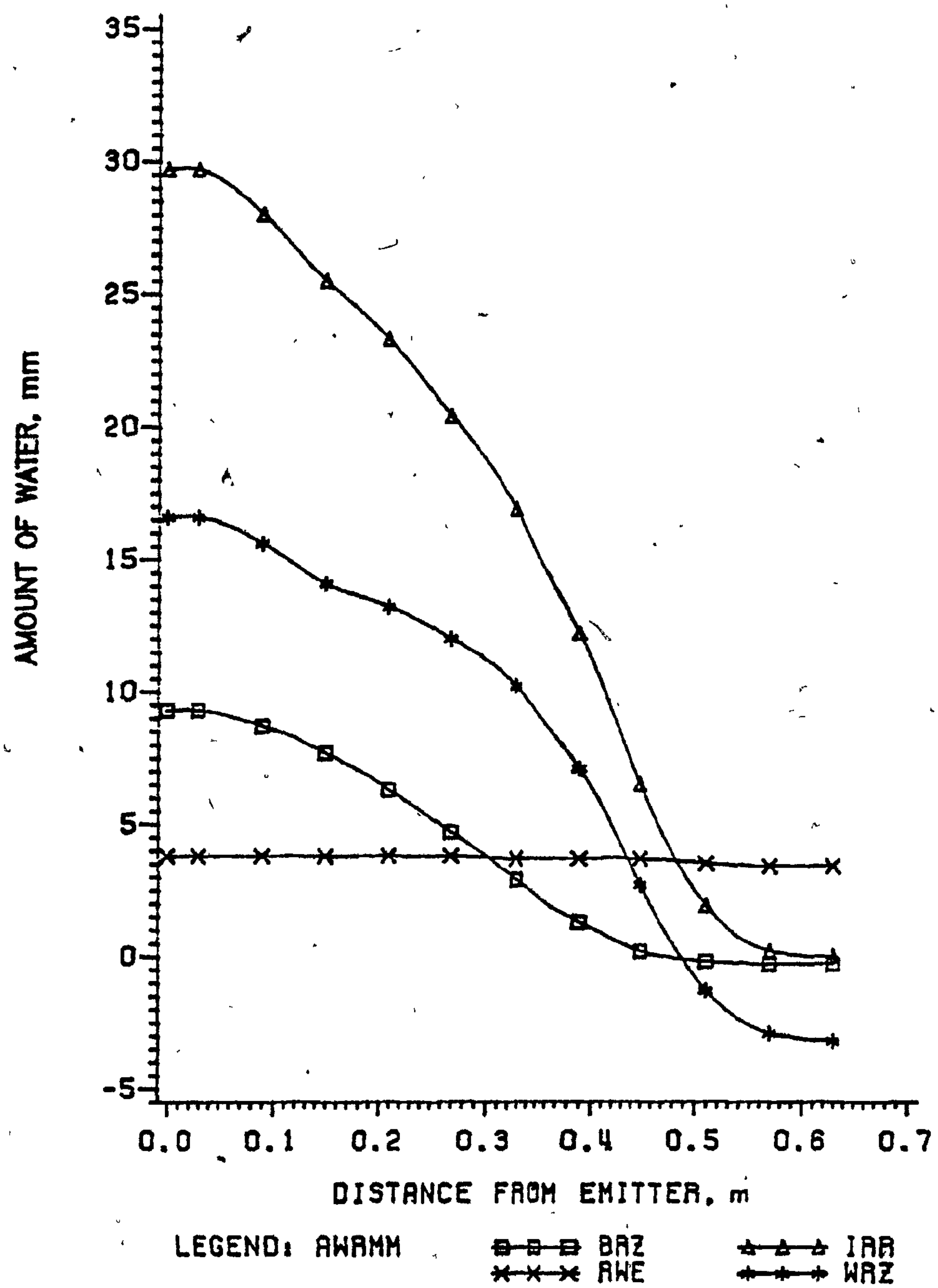

Figure B.18. Distribution of 12 L of water along horizontal distance with discharge rate of 6 $L.h^{-1}$ (expressed in mm) for Rougemont orchard site 1.

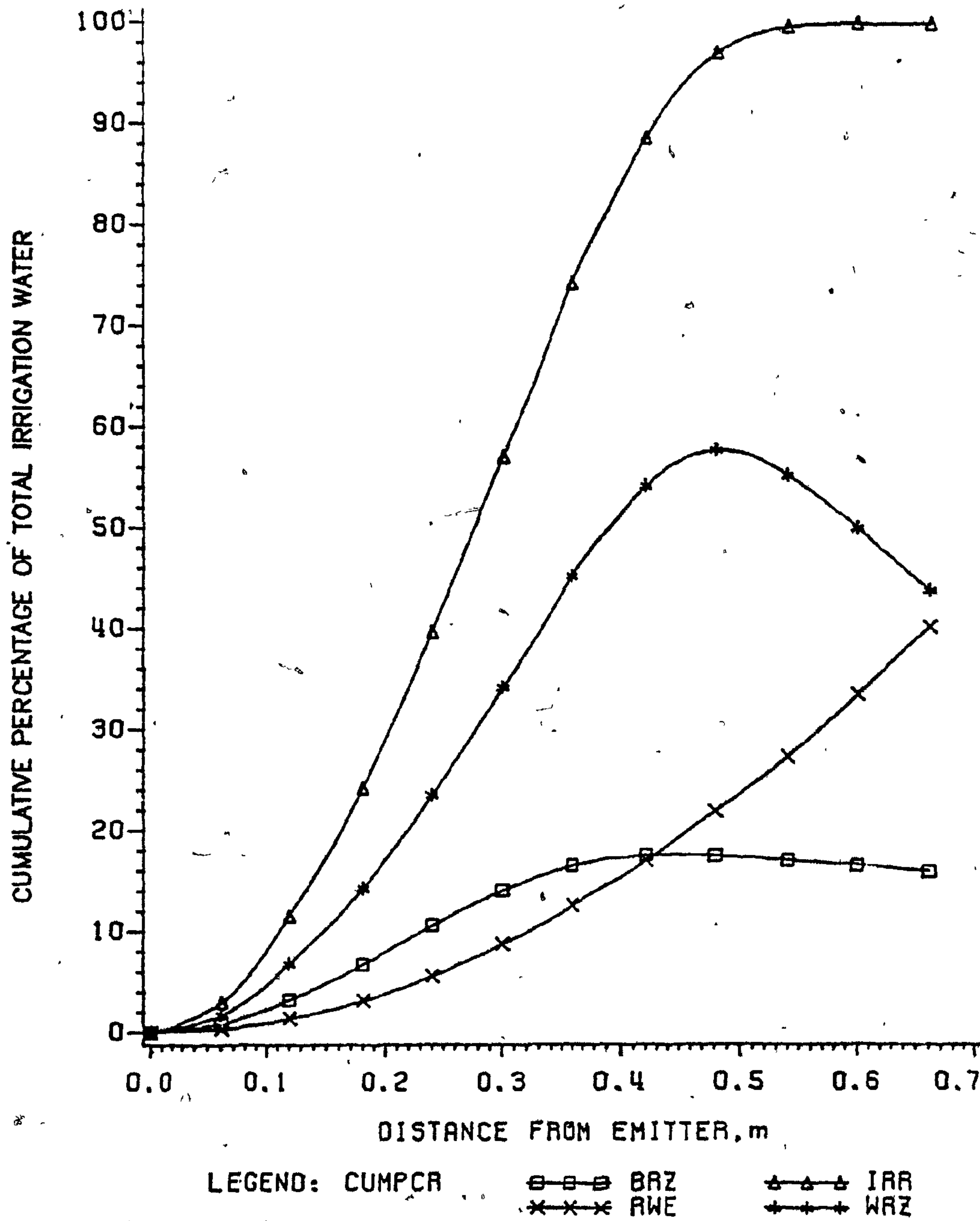

Figure B.19. Distribution of 12 L of water along horizontal distance with discharge rate of 2 $L.h^{-1}$ (expressed as percentage) for Rougemont orchard site 1.

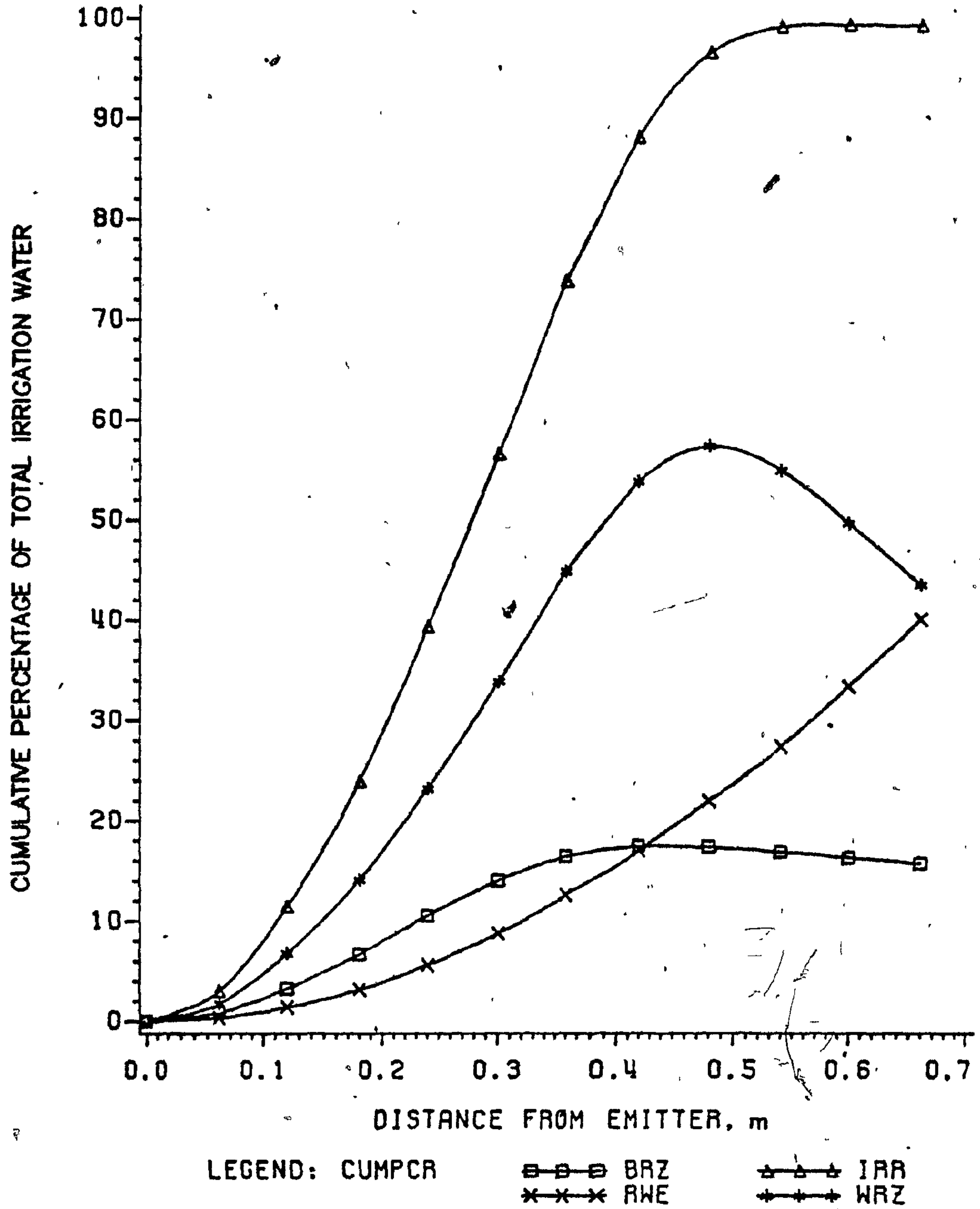

Figure B.20. Distribution of 12 L of water along horizontal distance with pulse discharge rate of 4 $L.h^{-1}$ (expressed as percentage) for Rougemont orchard site 1.

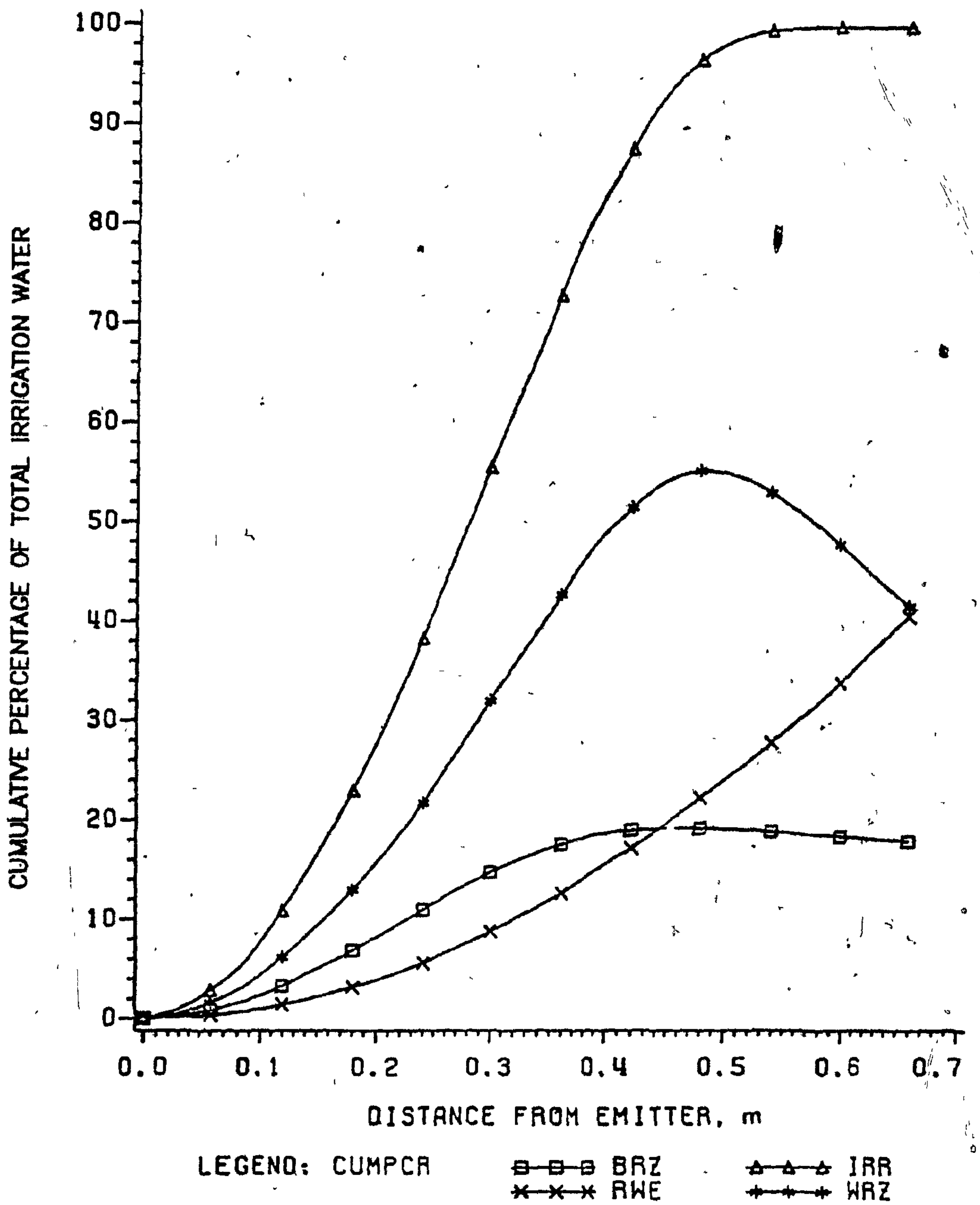

Figure B.21. Distribution of 12 L of water along horizontal distance with discharge rate of 4 $L.h^{-1}$ (expressed as percentage) for Rougemont orchard site 1.

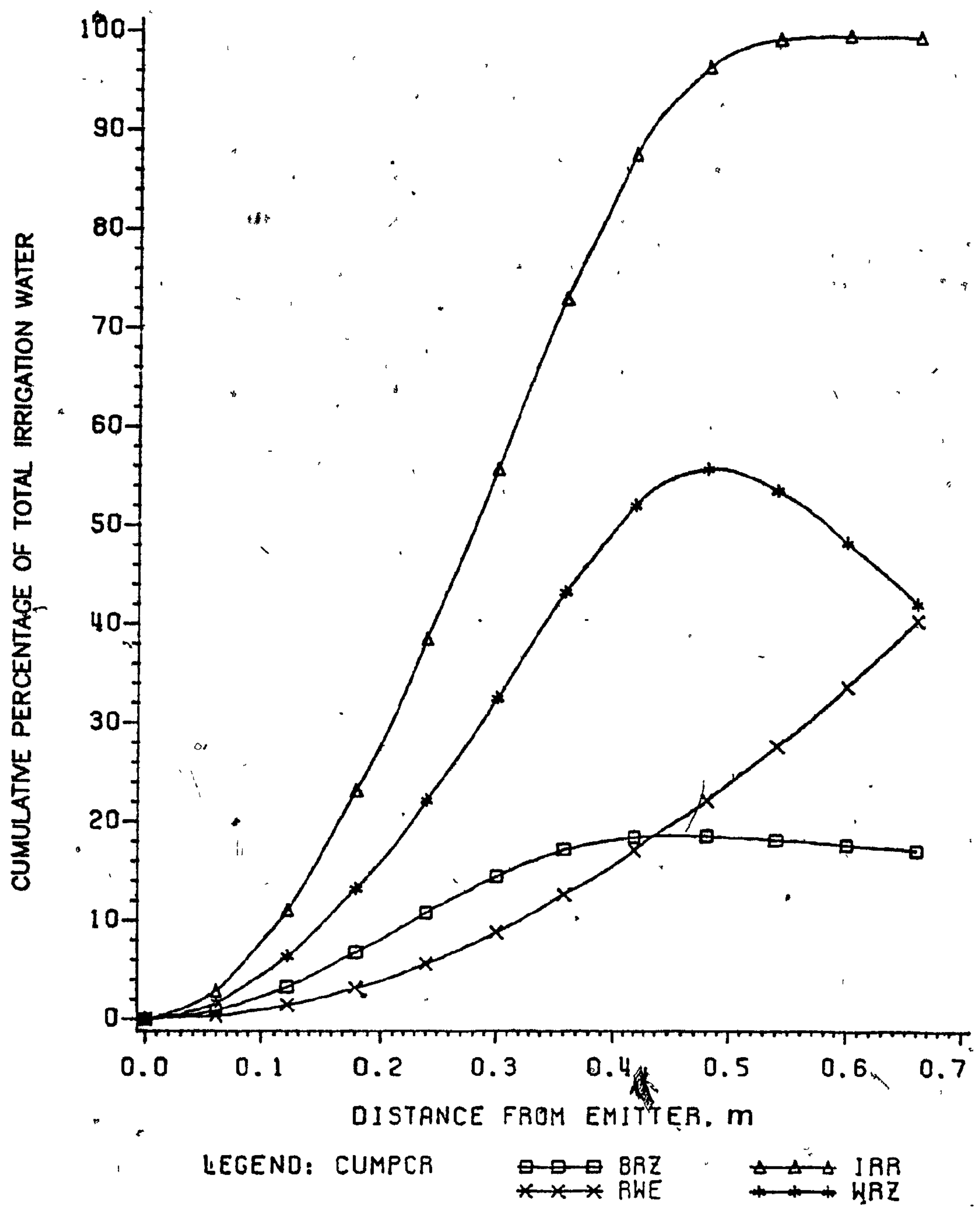

Figure B.22. Distribution of 12 L of water along horizontal distance with pulse discharge rate of 6 L.h^{-1} (expressed as percentage) for Rougemont orchard site 1.

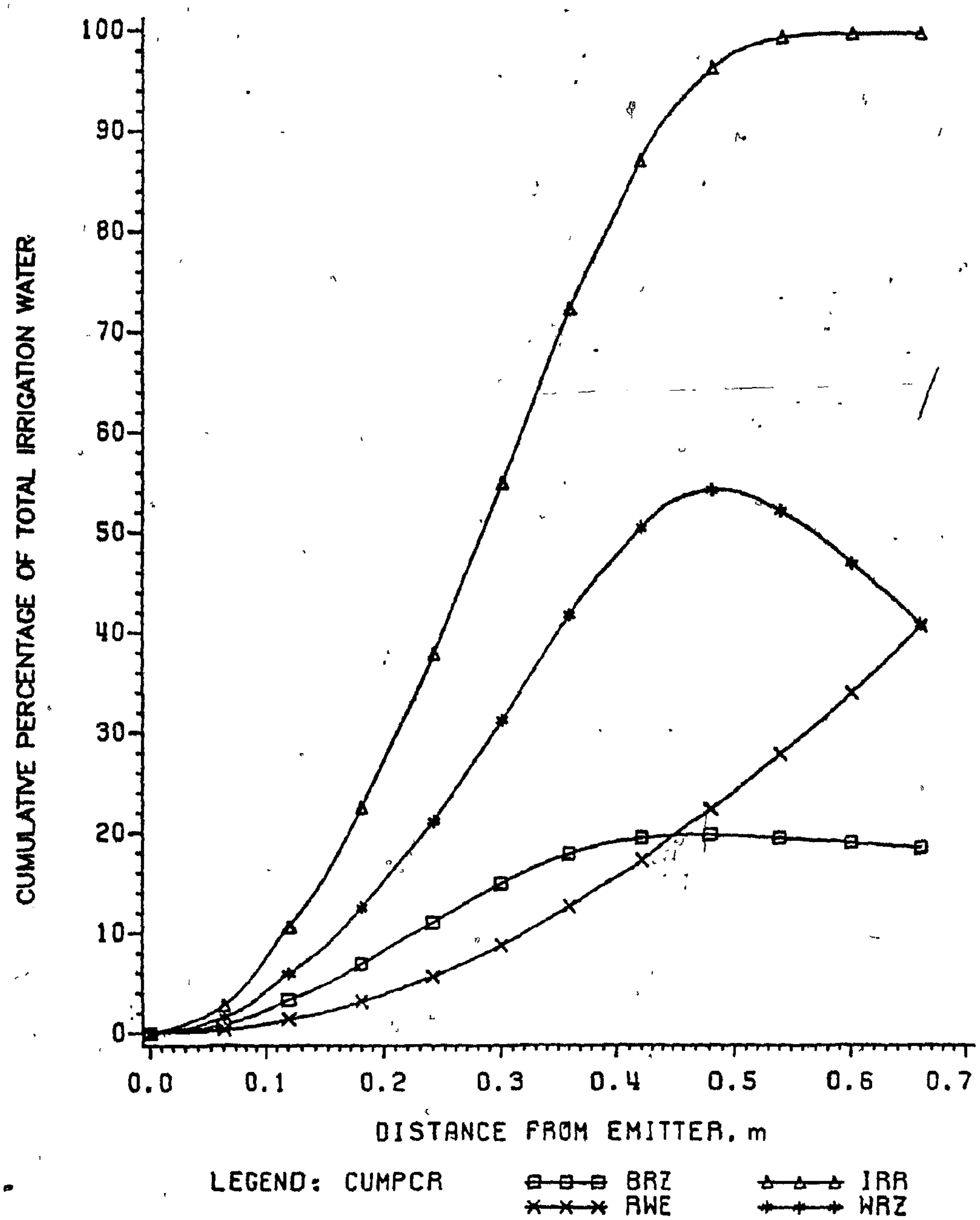

Figure B.23. Distribution of 12 L of water along horizontal distance with discharge rate of 6 $L.h^{-1}$ (expressed as percentage) for Rougemont orchard site 1.

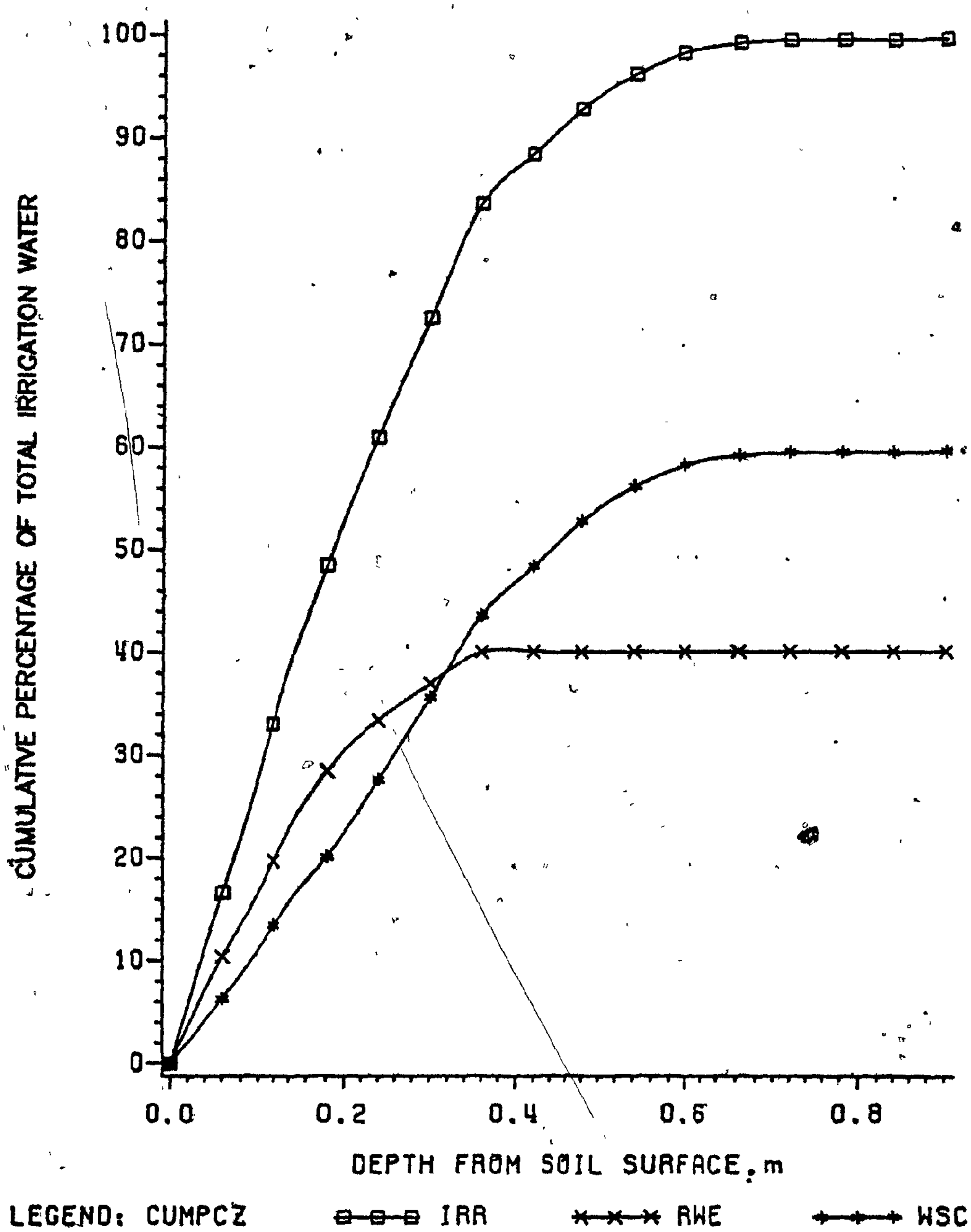

Figure B.24. Distribution of 12 L of water in soil profile with discharge rate of 2 $L.h^{-1}$ for Rougemont orchard site 1.

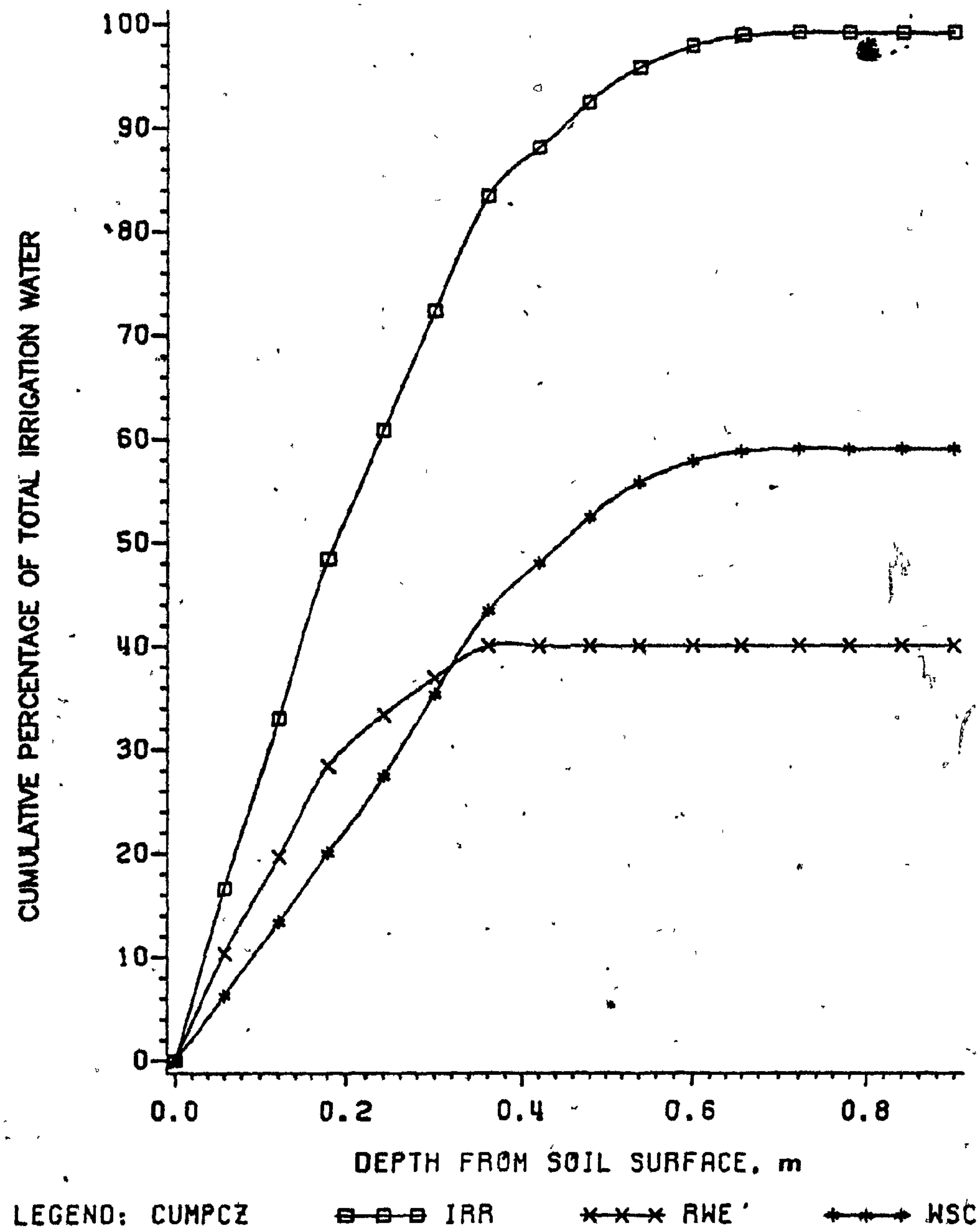

Figure B.25. Distribution of 12 L of water in soil profile with pulse discharge rate of 4 L.h^{-1} for Rougemont orchard site 1.

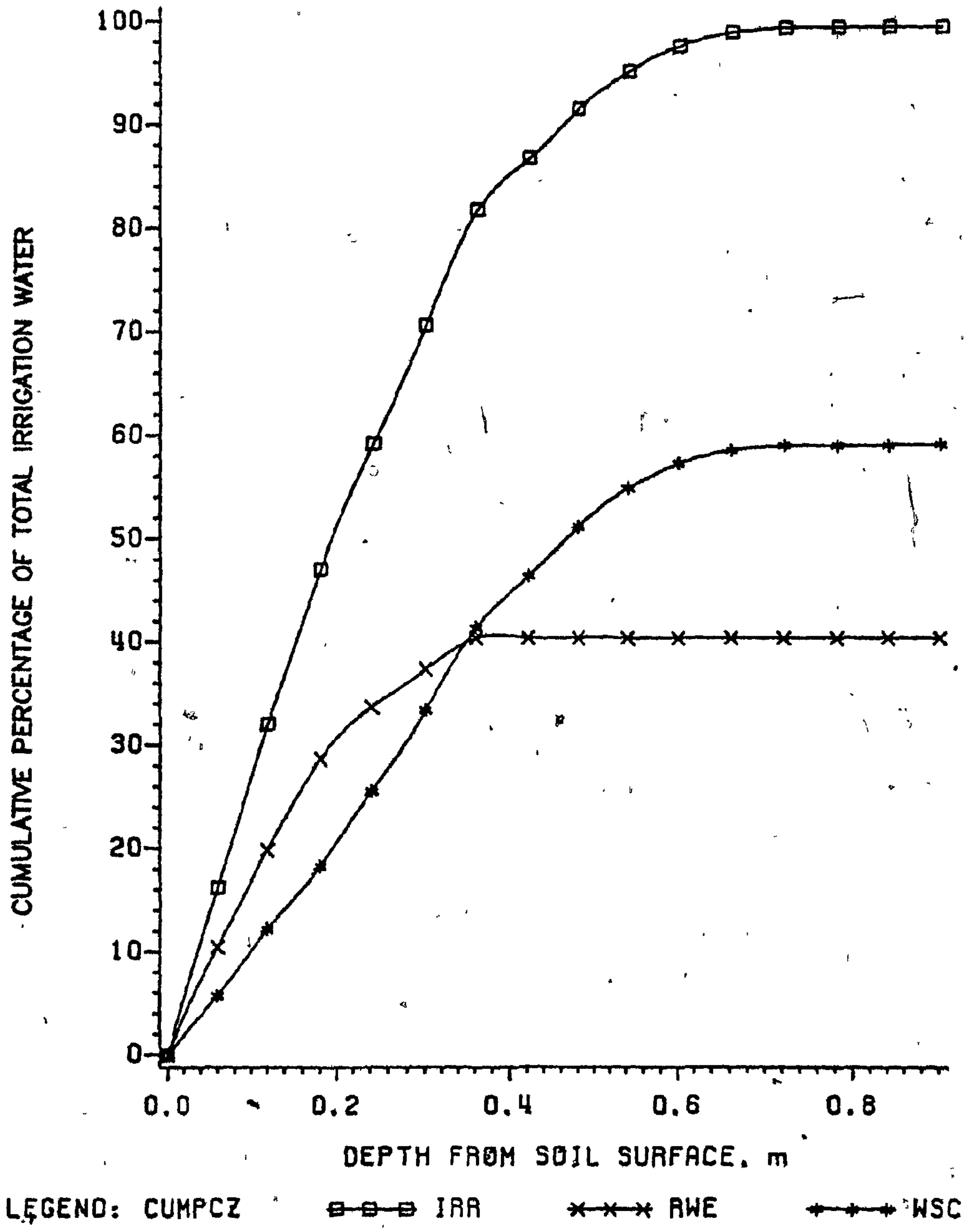

Figure B.26. Distribution of 12 L of water in soil profile with discharge rate of 4 $L.h^{-1}$ for Rougemont orchard site 1.

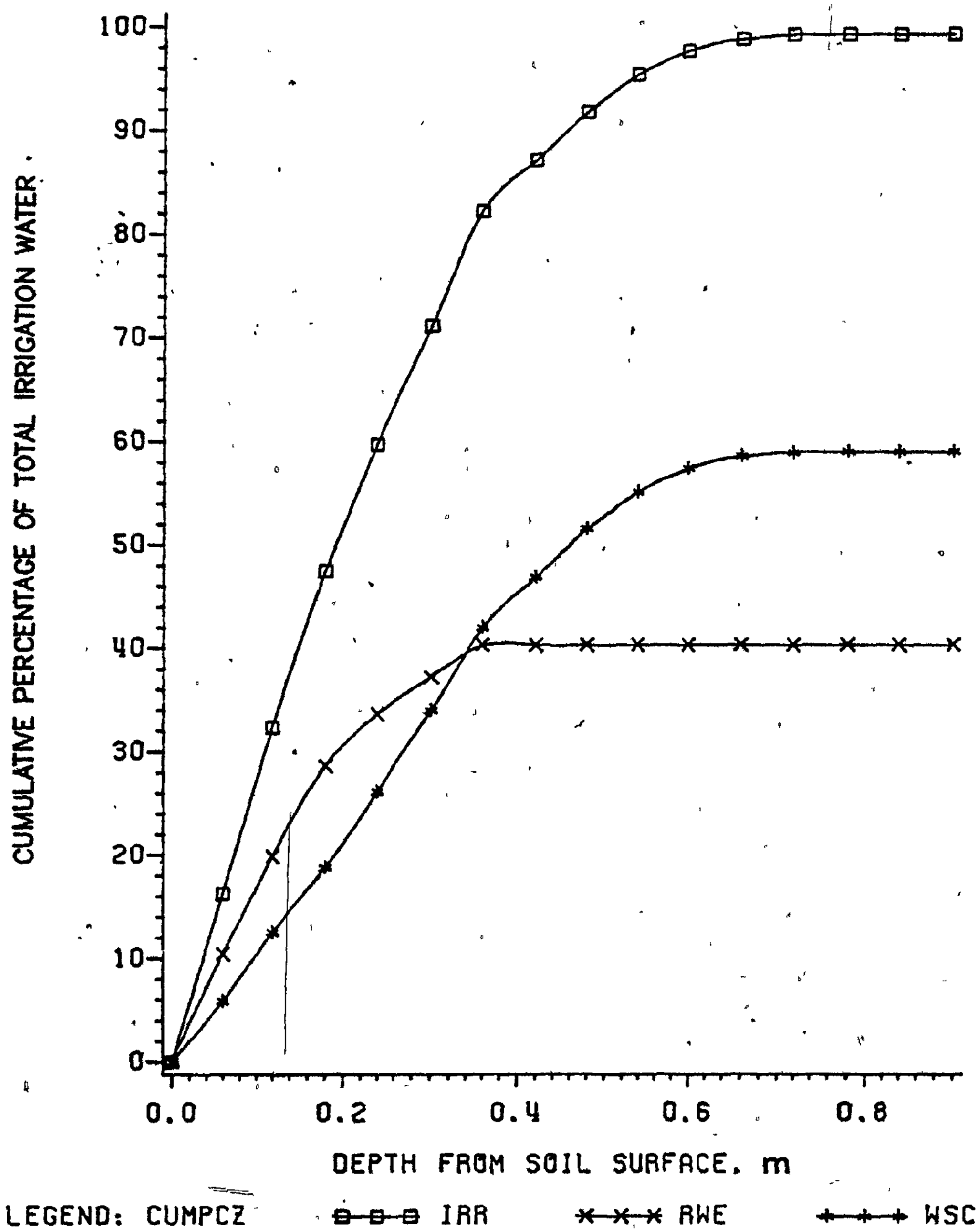

Figure B.27. Distribution of 12 L of water in soil profile with pulse discharge rate of 6 $L.h^{-1}$ for Rougemont orchard site 1.

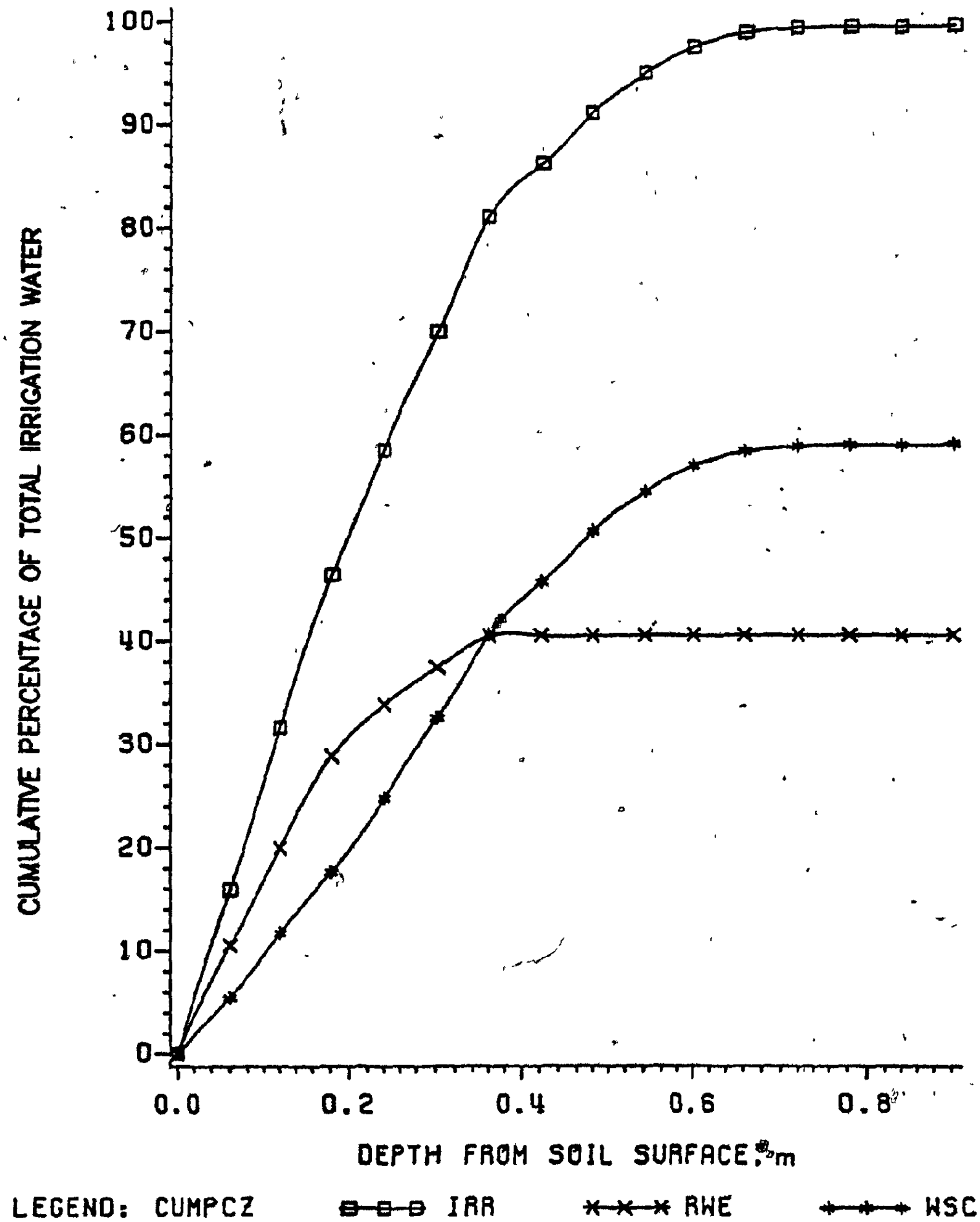

Figure B.28. Distribution of 12 L of water in soil profile with discharge rate of 6 $L.h^{-1}$ for Rougemont orchard site 1.

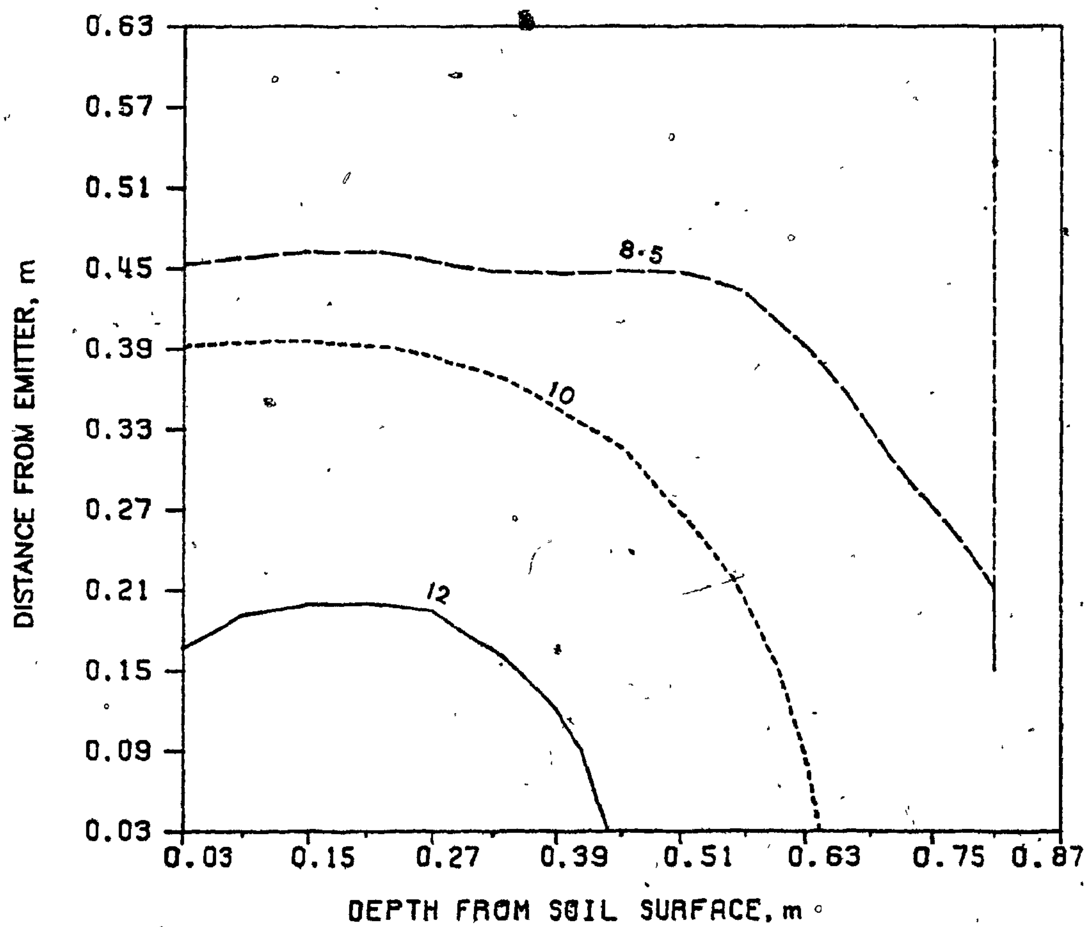

Figure B.29. Equimoisture curves after redistribution of irrigation water application of 12 L with discharge rate of 2 $L.h^{-1}$ for Rougemont orchard site 1. (Numbers labeling curves indicate soil moisture content, percent)

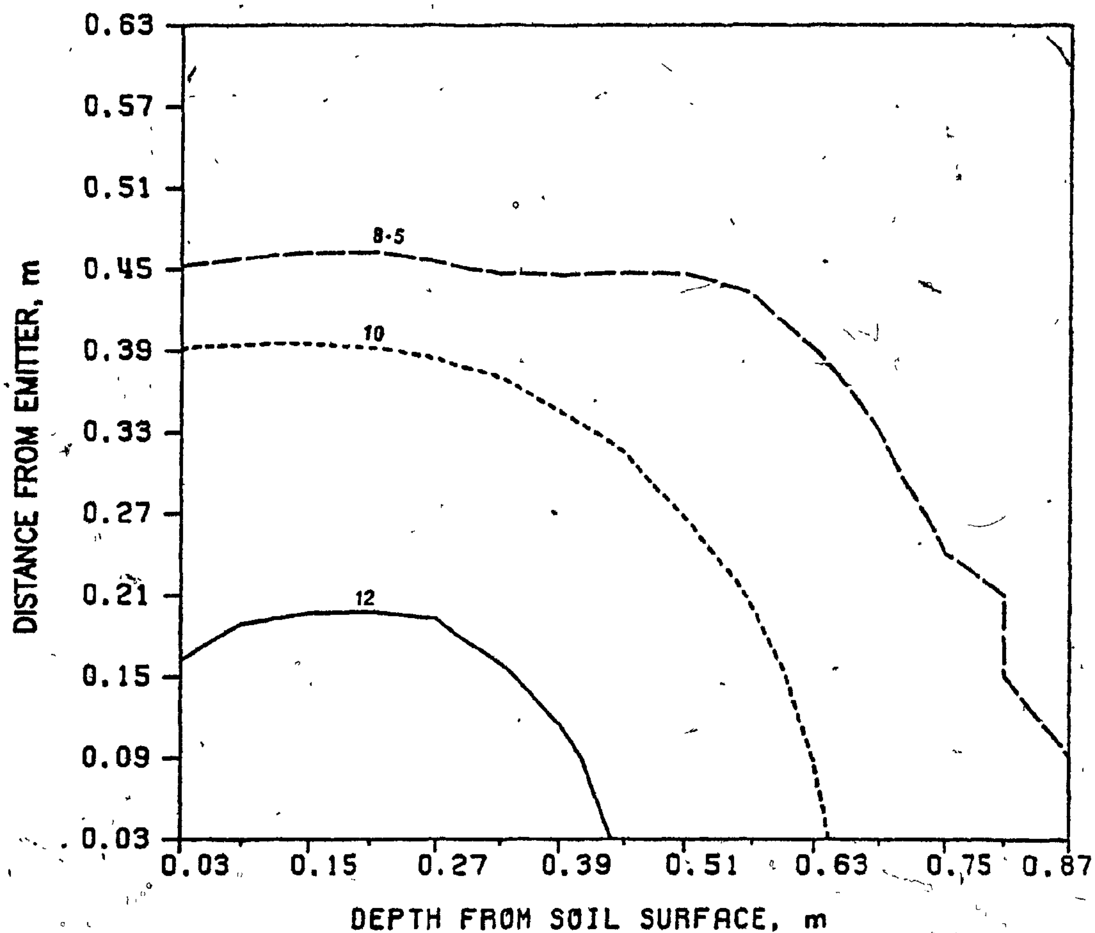

Figure B.30. Equimoisture curves after redistribution of irrigation water pulse application of 12 L with discharge rate of 4 $L.h^{-1}$ for Rougemont orchard site 1. (Numbers labeling curves indicate soil moisture content, percent)

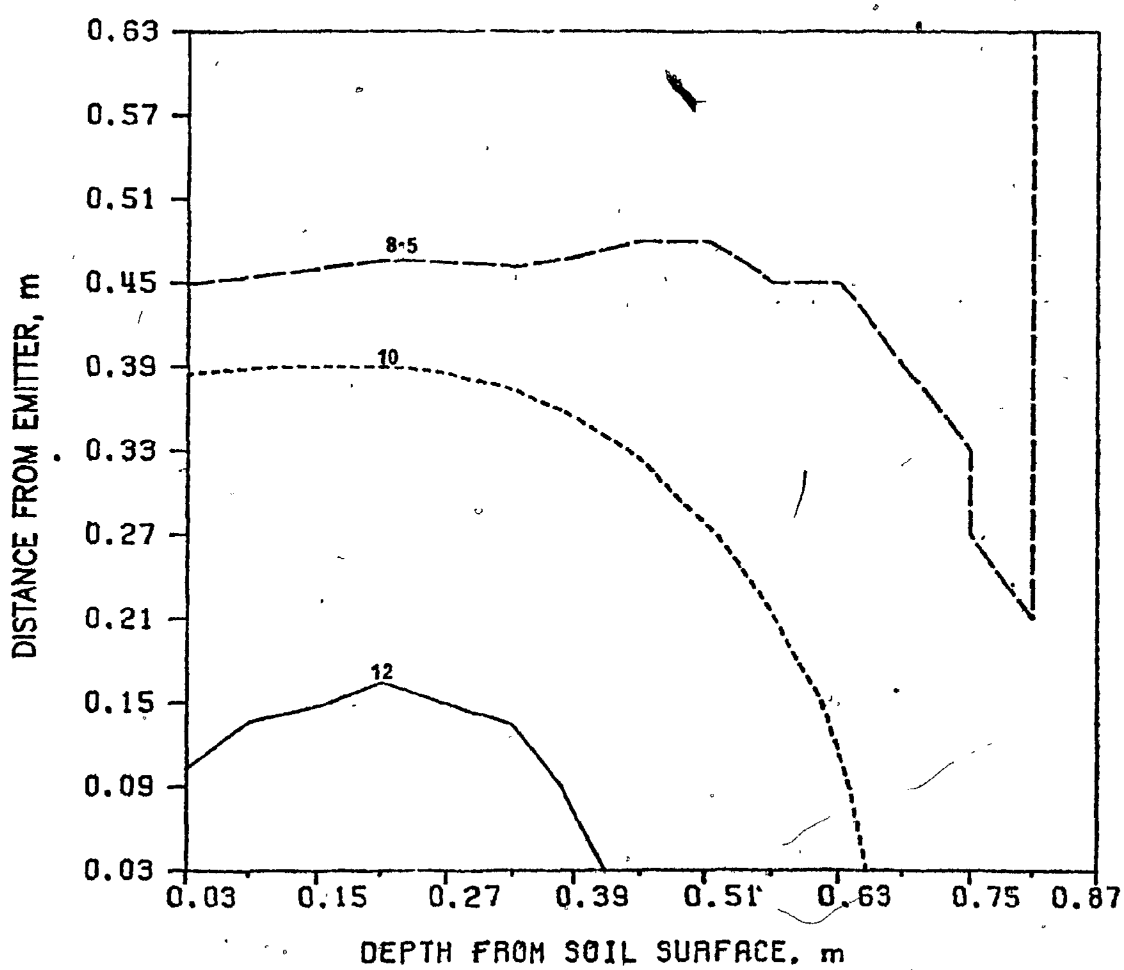

Figure B.31. Equimoisture curves after redistribution of irrigation water application of 12 L with discharge rate of 4 L.h^{-1} for Rougemont orchard site 1. (Numbers labeling curves indicate soil moisture content, percent)

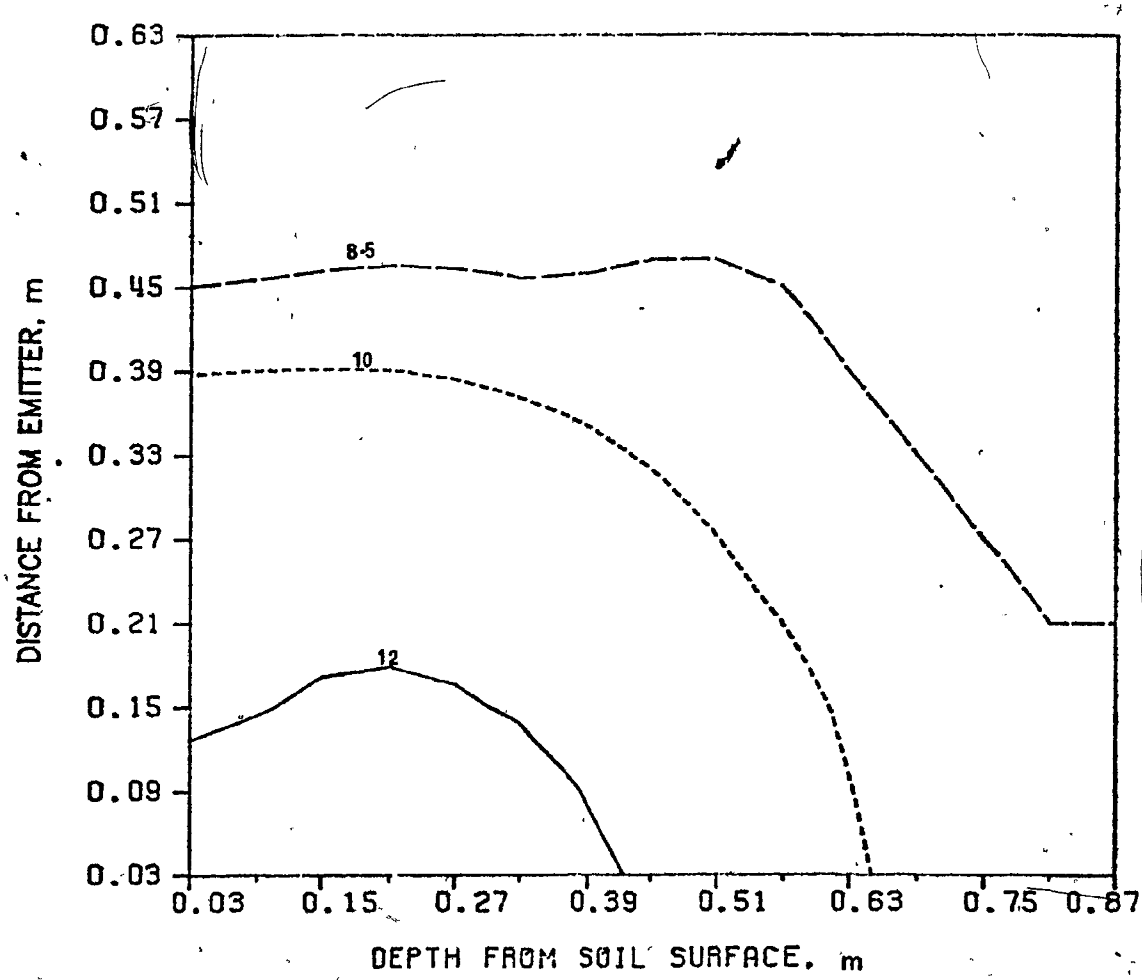

Figure B.32. Equimoisture curves after redistribution of irrigation water pulse application of 12 L with discharge rate of 6 $L.h^{-1}$ for Rougemont orchard site 1. (Numbers labeling curves indicate soil moisture content, percent)

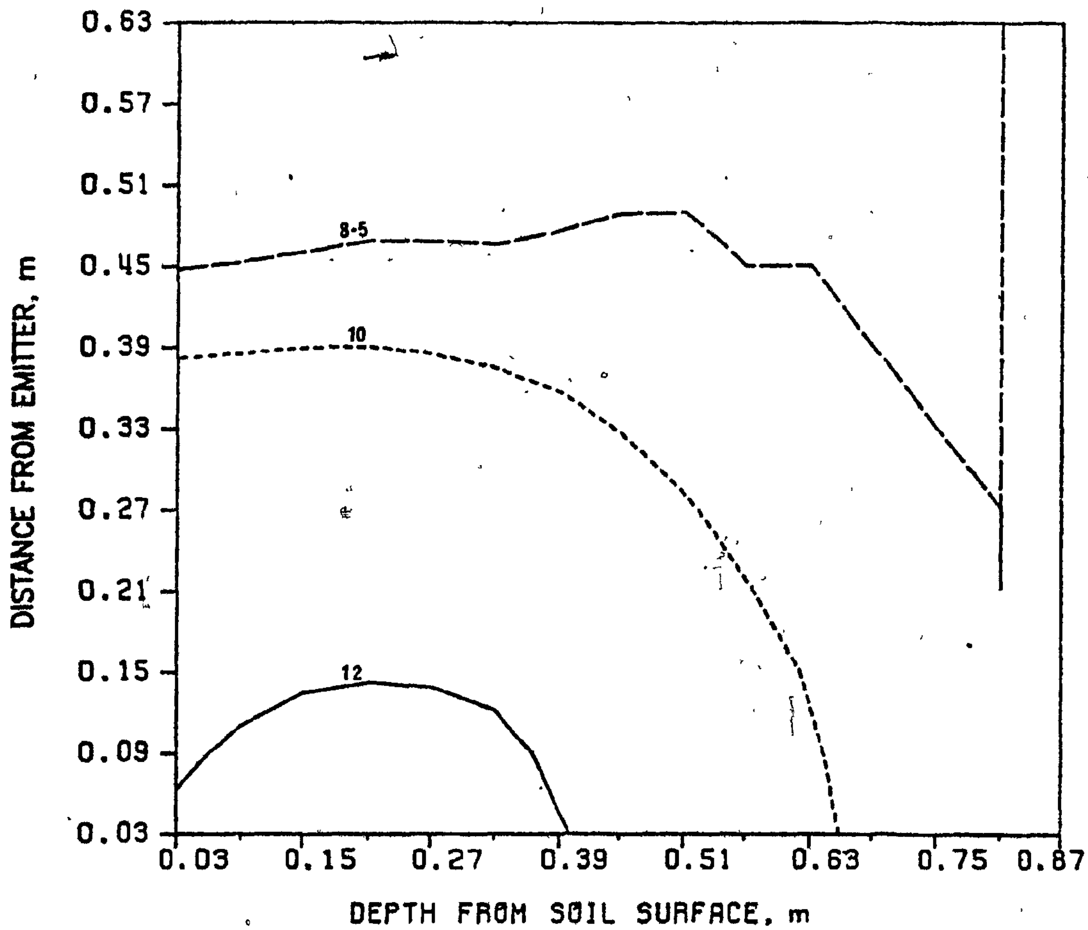

Figure B.33. Equimoisture curves after redistribution of irrigation water application of 12 L with discharge rate of 6 $L.h^{-1}$ for Rougemont orchard site 1. (Numbers labeling curves indicate soil moisture content, percent)

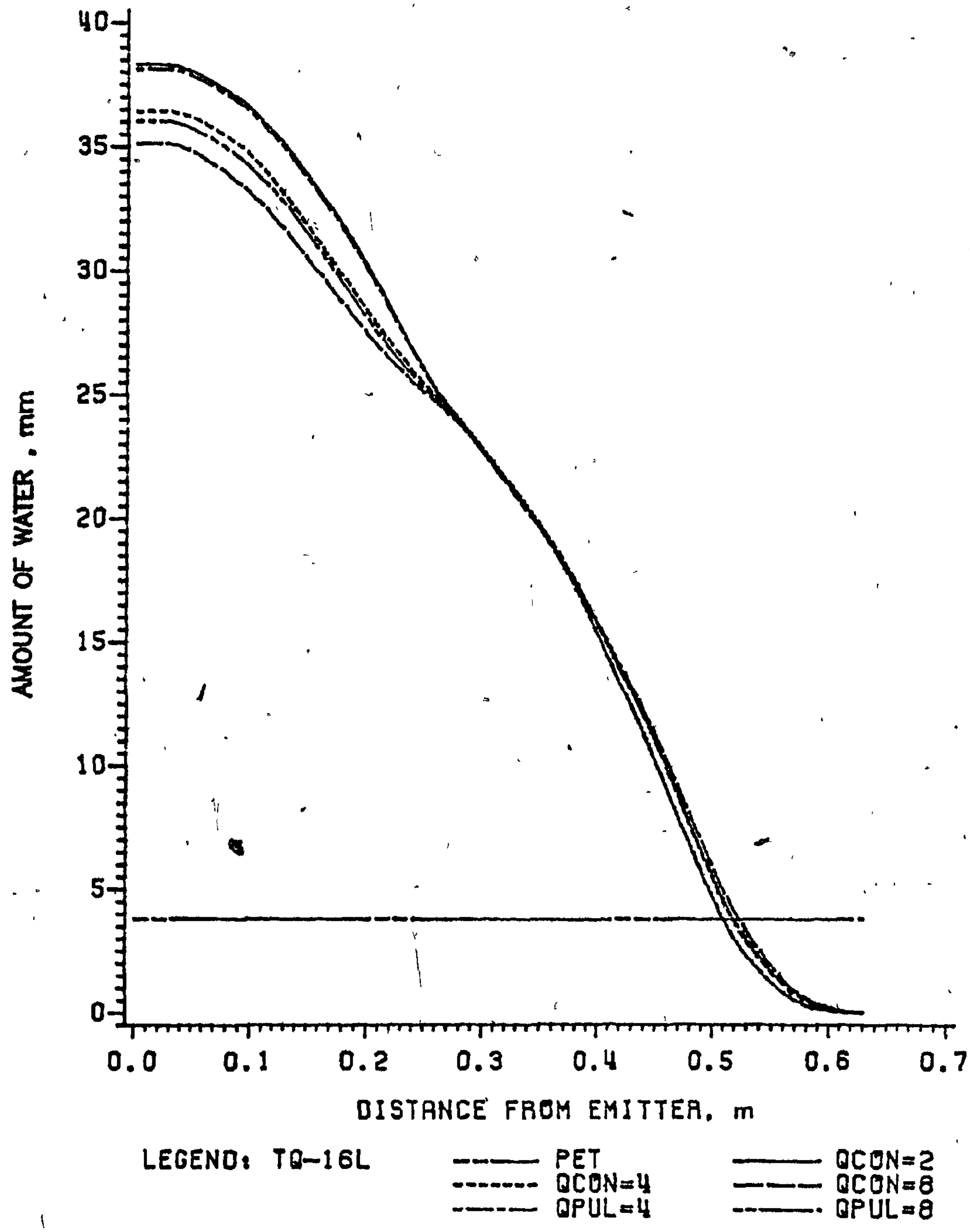

Figure B.34. Water input predicted along horizontal distance with an irrigation application of 16 L at different discharge rates for Rougemont orchard site 1.

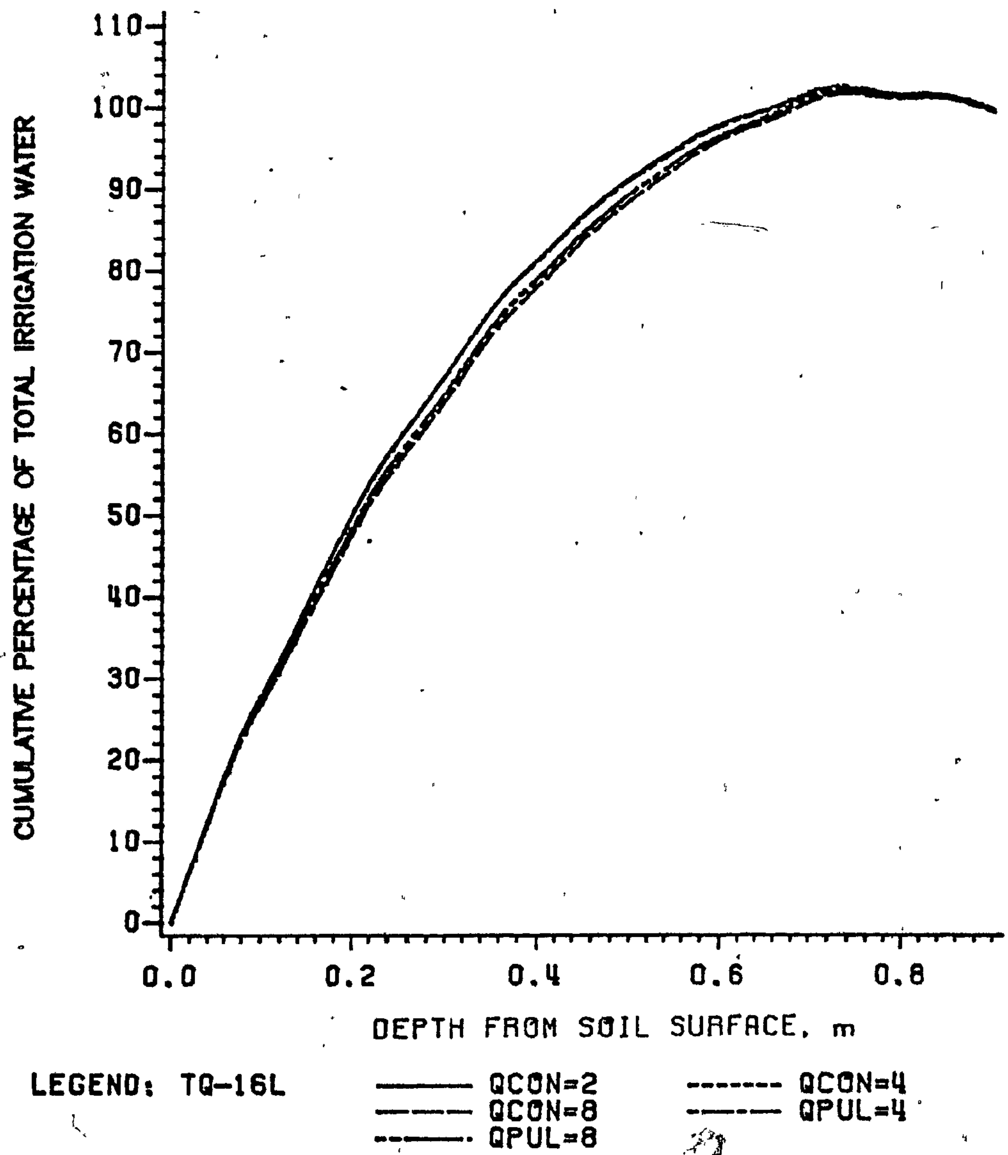

Figure B.35. Water input predicted in soil profile with an irrigation application of 16 L at different discharge rates for Rougemont orchard site 1.

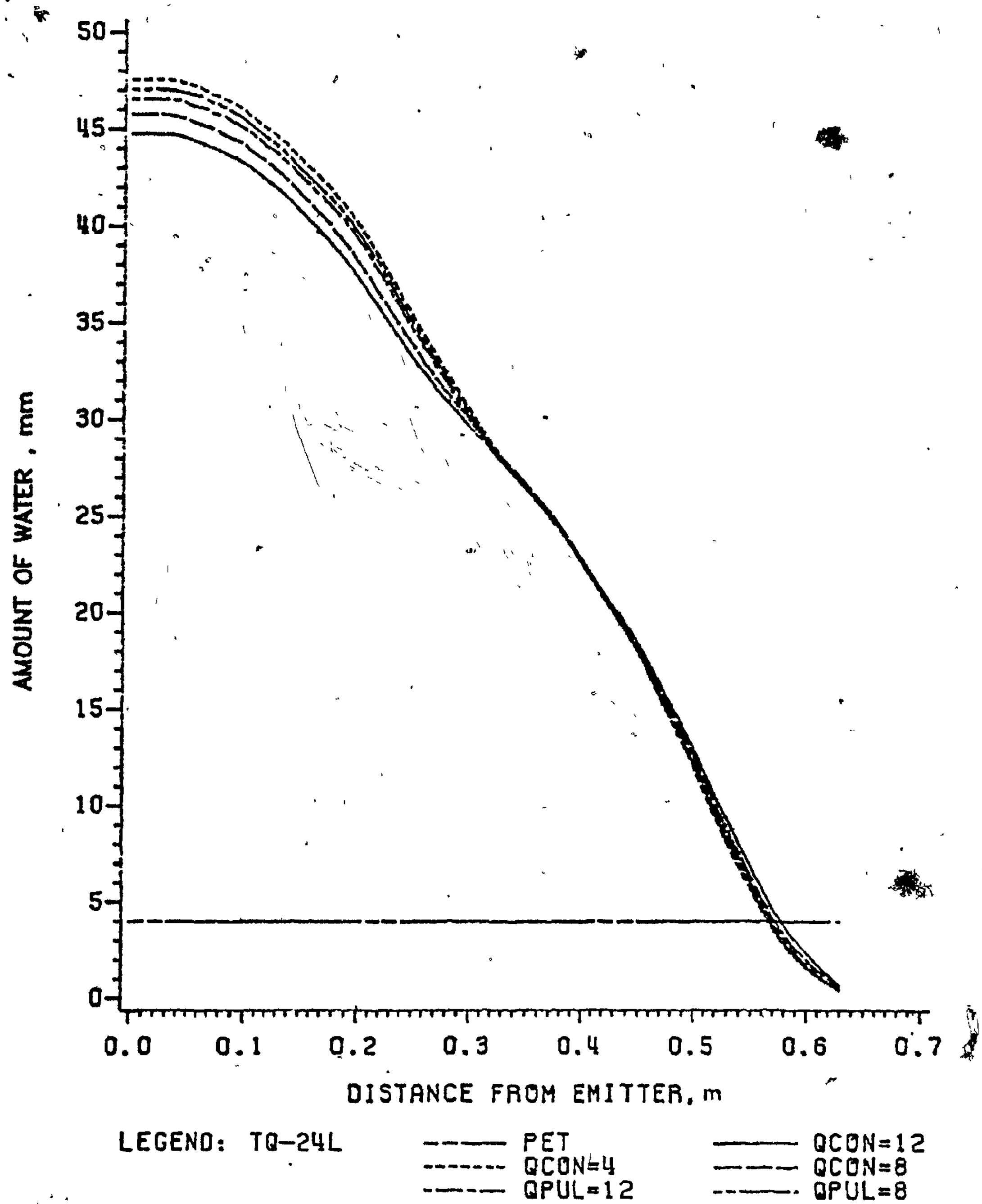

Figure B.36. Water input predicted along horizontal distance with an irigation application of 24 L at different discharge rates for Rougemont orchard site 1.

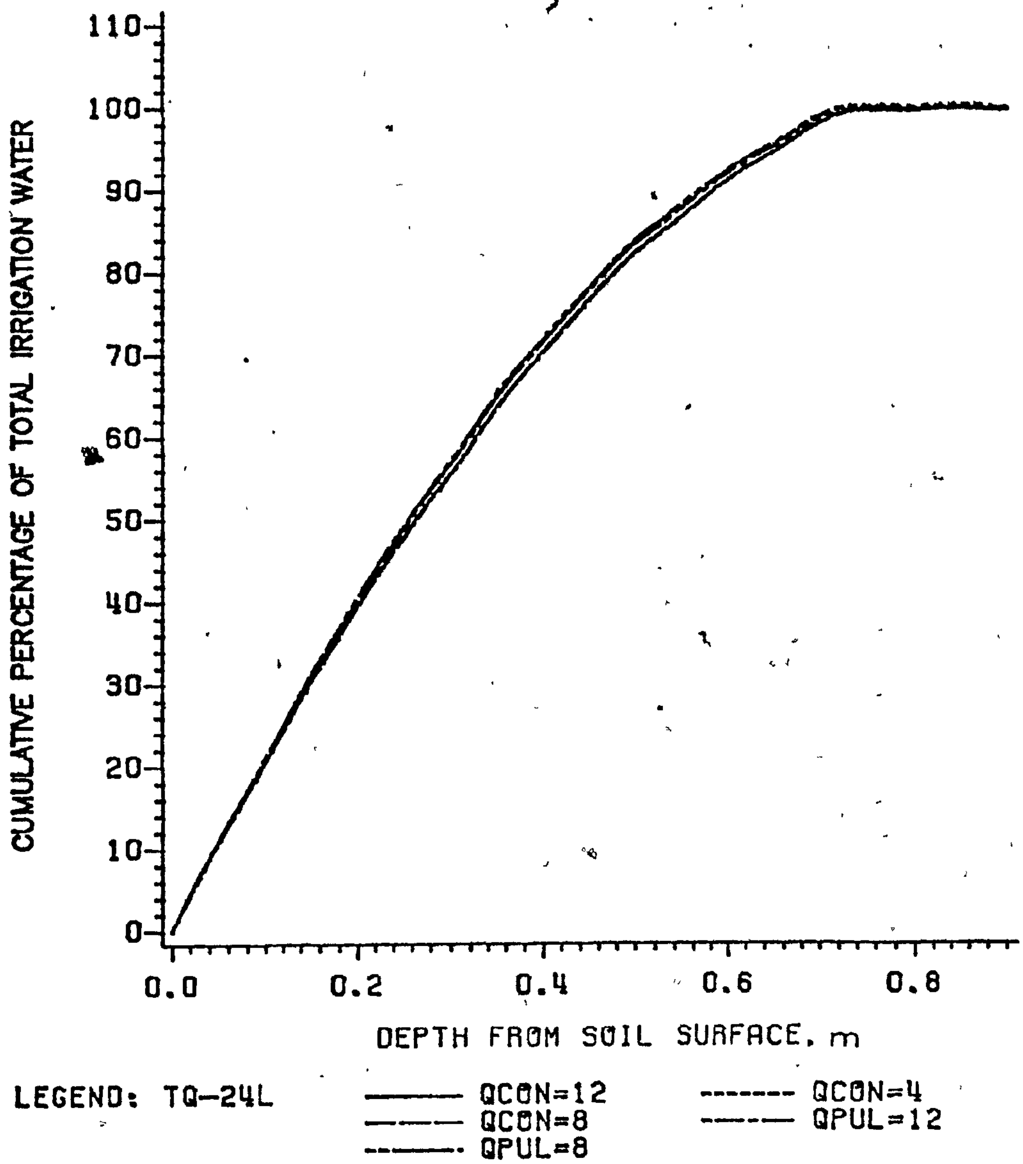

Figure B.37. Water input predicted in soil profile with an irrigation application of 24 L at different discharge rates for Rougemont orchard site 1.

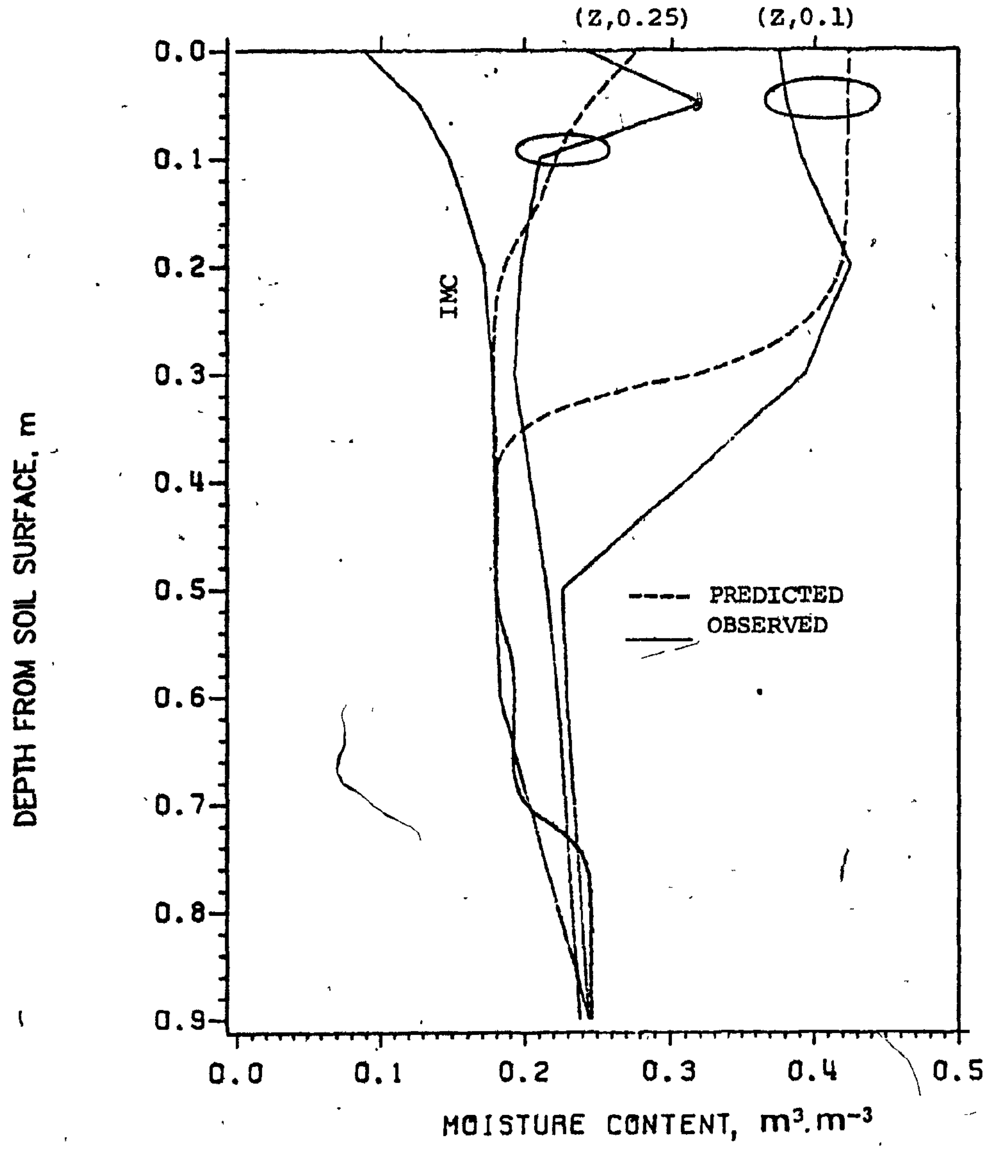

Figure B.38. Soil moisture content profiles before and after 12 L of water applied at 4 $L.h^{-1}$ at Rougemont orchard site 2.

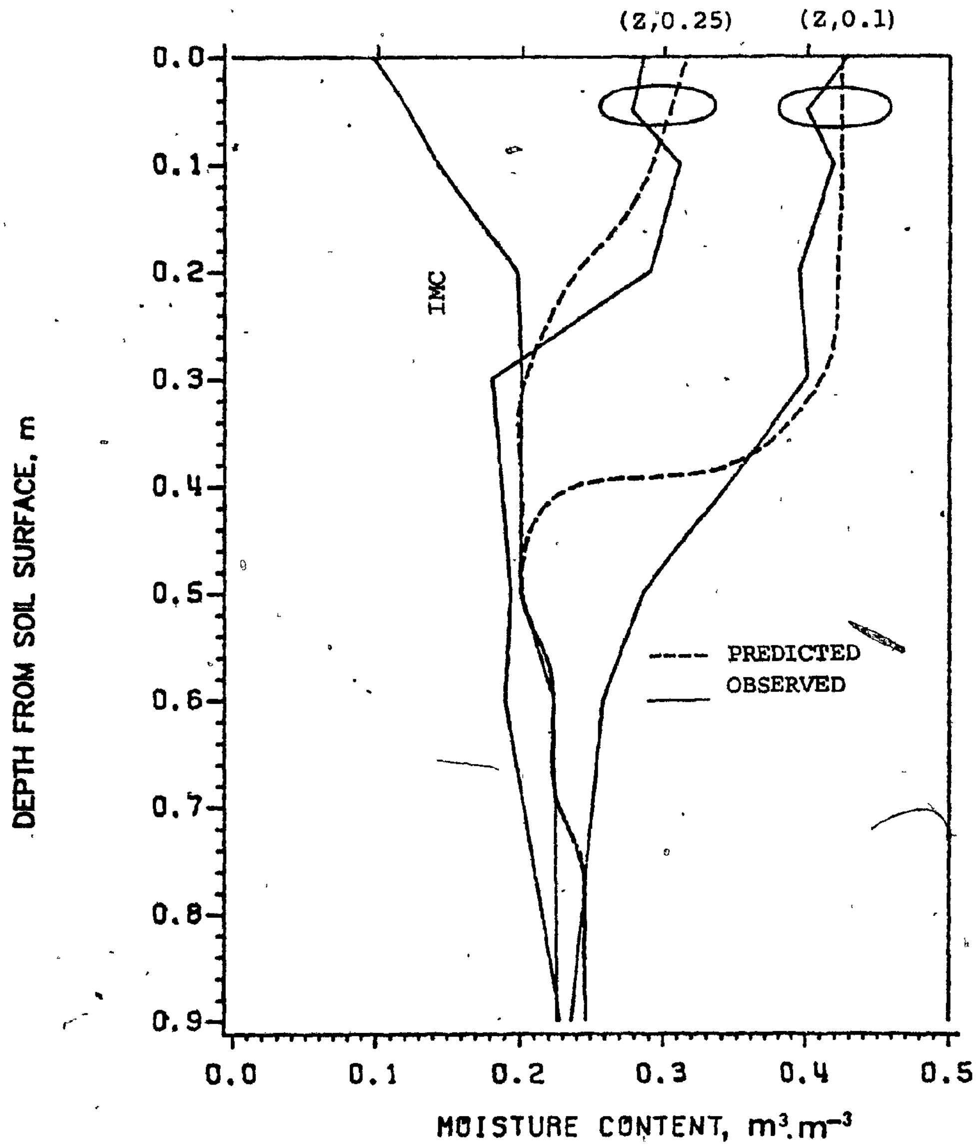

Figure B.39. Soil moisture content profiles before and after 16 L of water applied at 4 $L.h^{-1}$ at Rougemont orchard site 2.

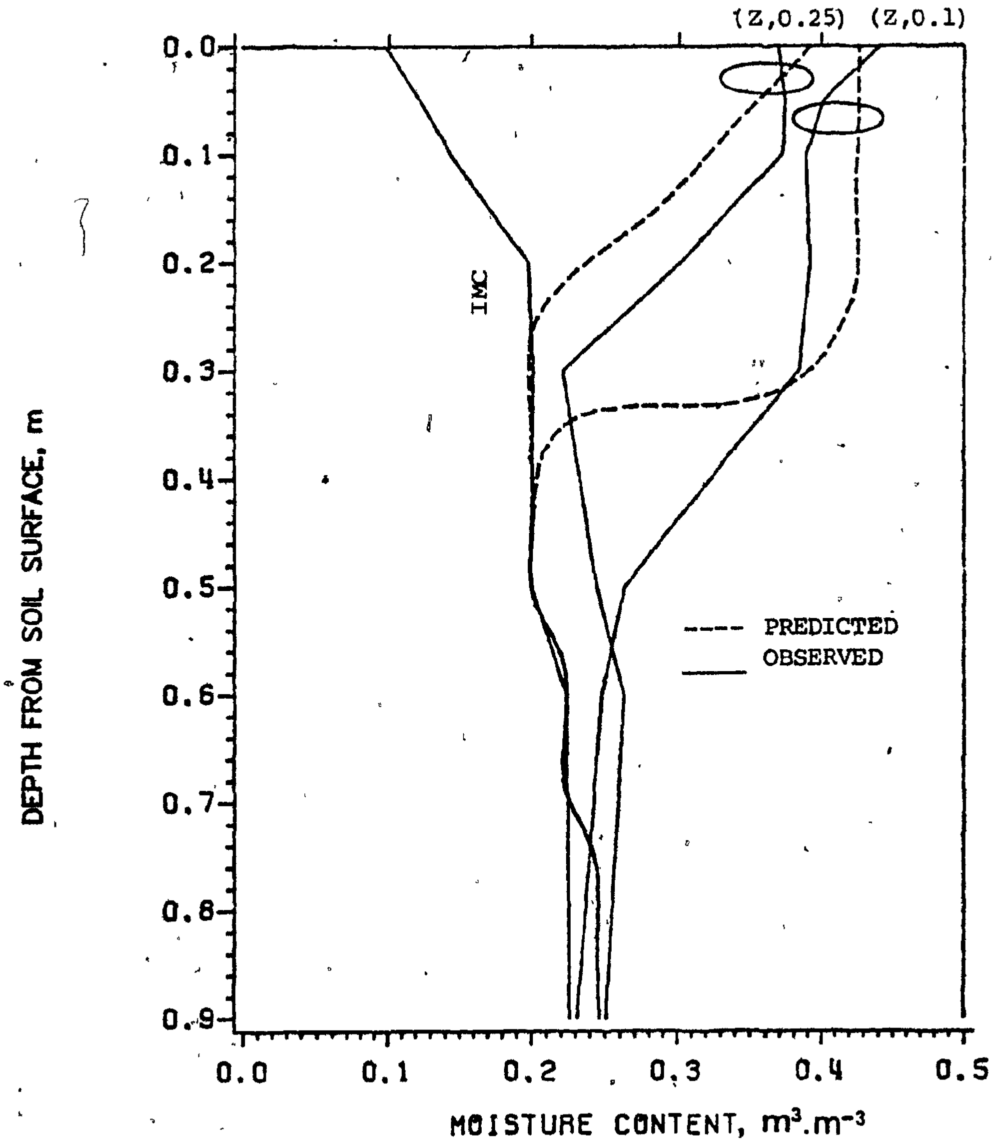

Figure B.40. Soil moisture content profiles before and after 16 L of water applied at 8 $L.h^{-1}$ at Rougemont orchard site 2.

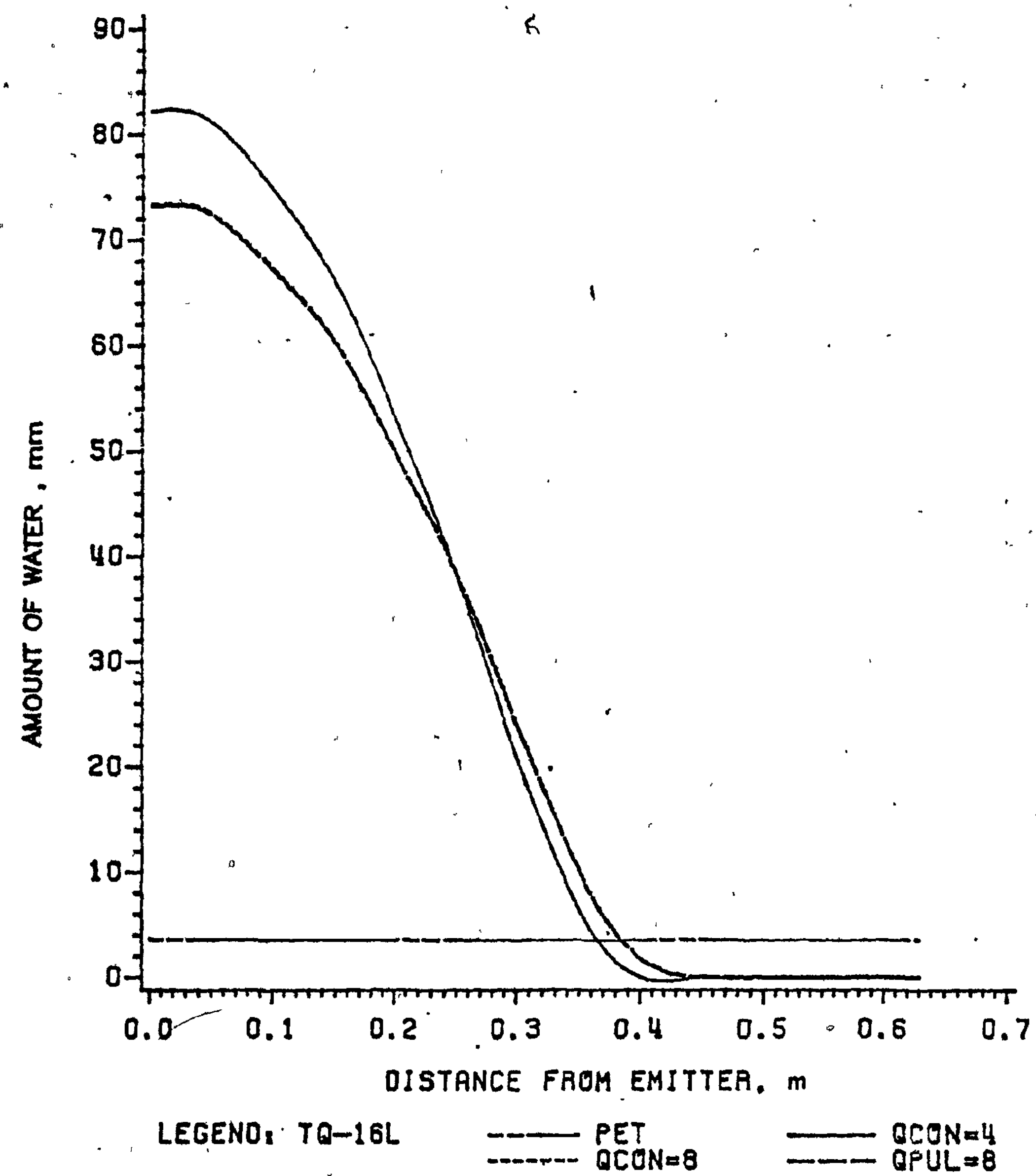

Figure B.41. Water input predicted along horizontal distance with an irrigation application of 16 L at different discharge rates for Rougemont orchard site 2.

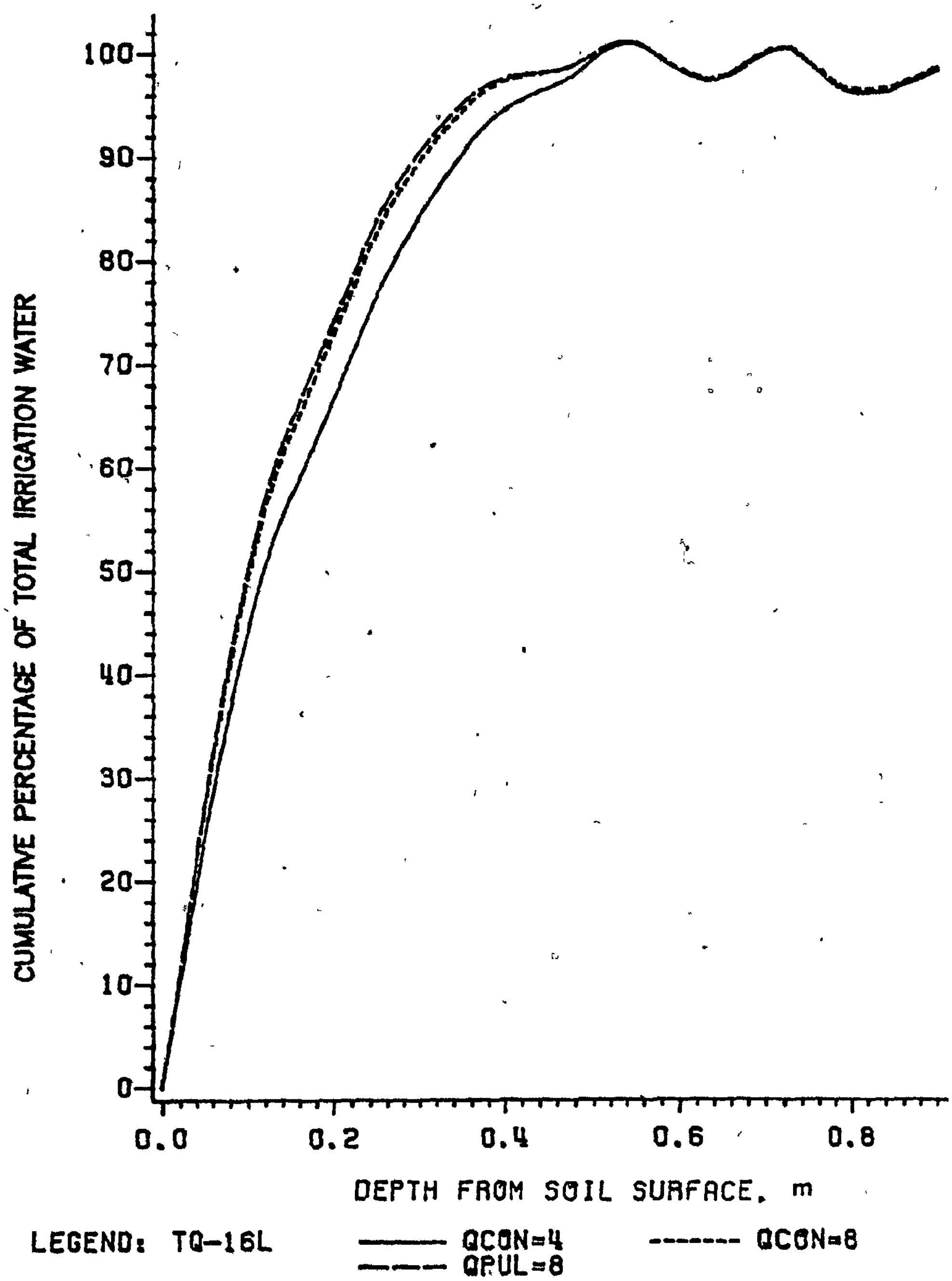

Figure B.42. Water input predicted in soil profile with an irrigation application of 16 L at different discharge rates for Rougemont orchard site 2.

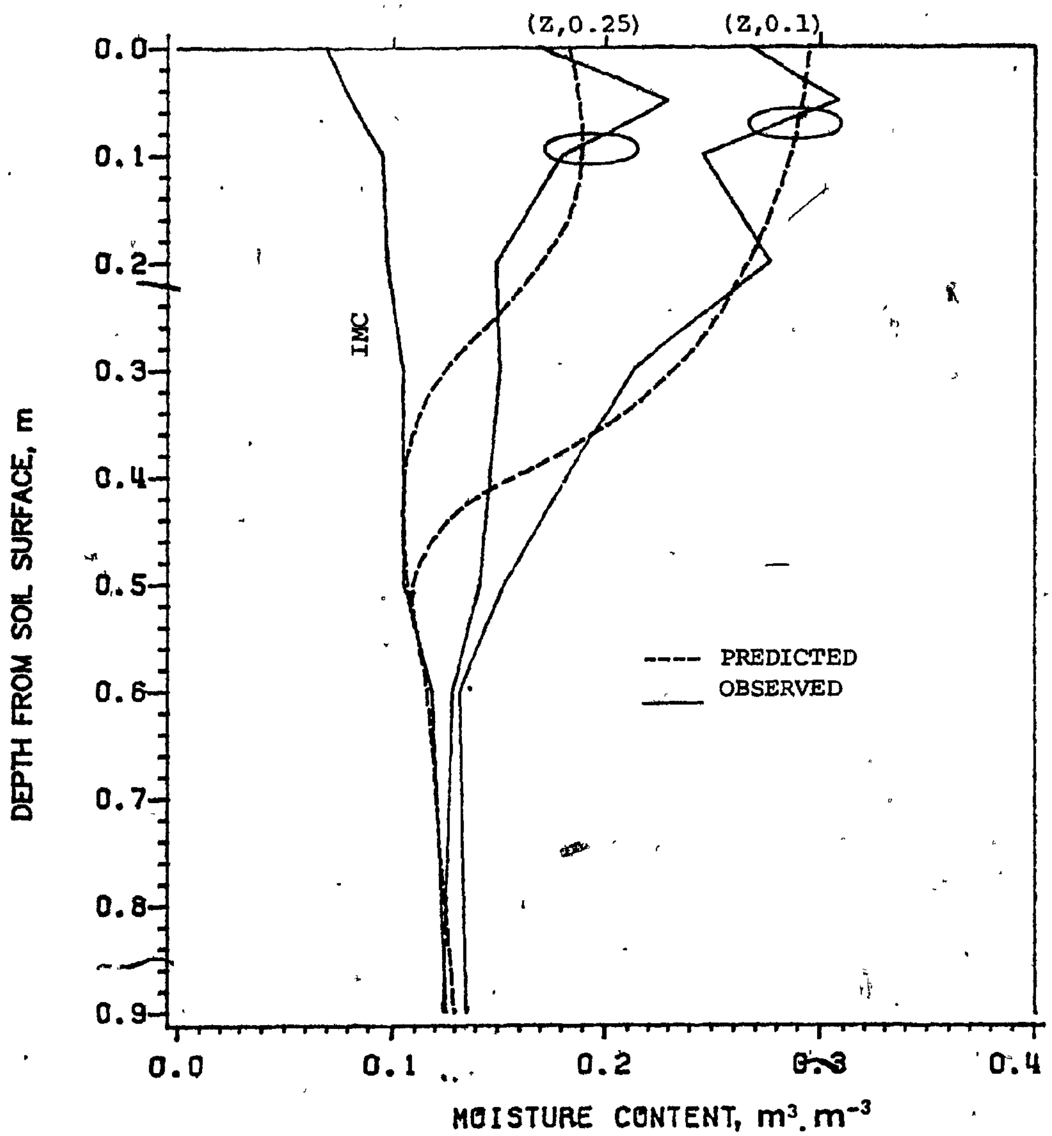

Figure B.43. Soil moisture content profiles before and after 12 L of water applied at 4 $L.h^{-1}$ at Rougemont orchard site 3.

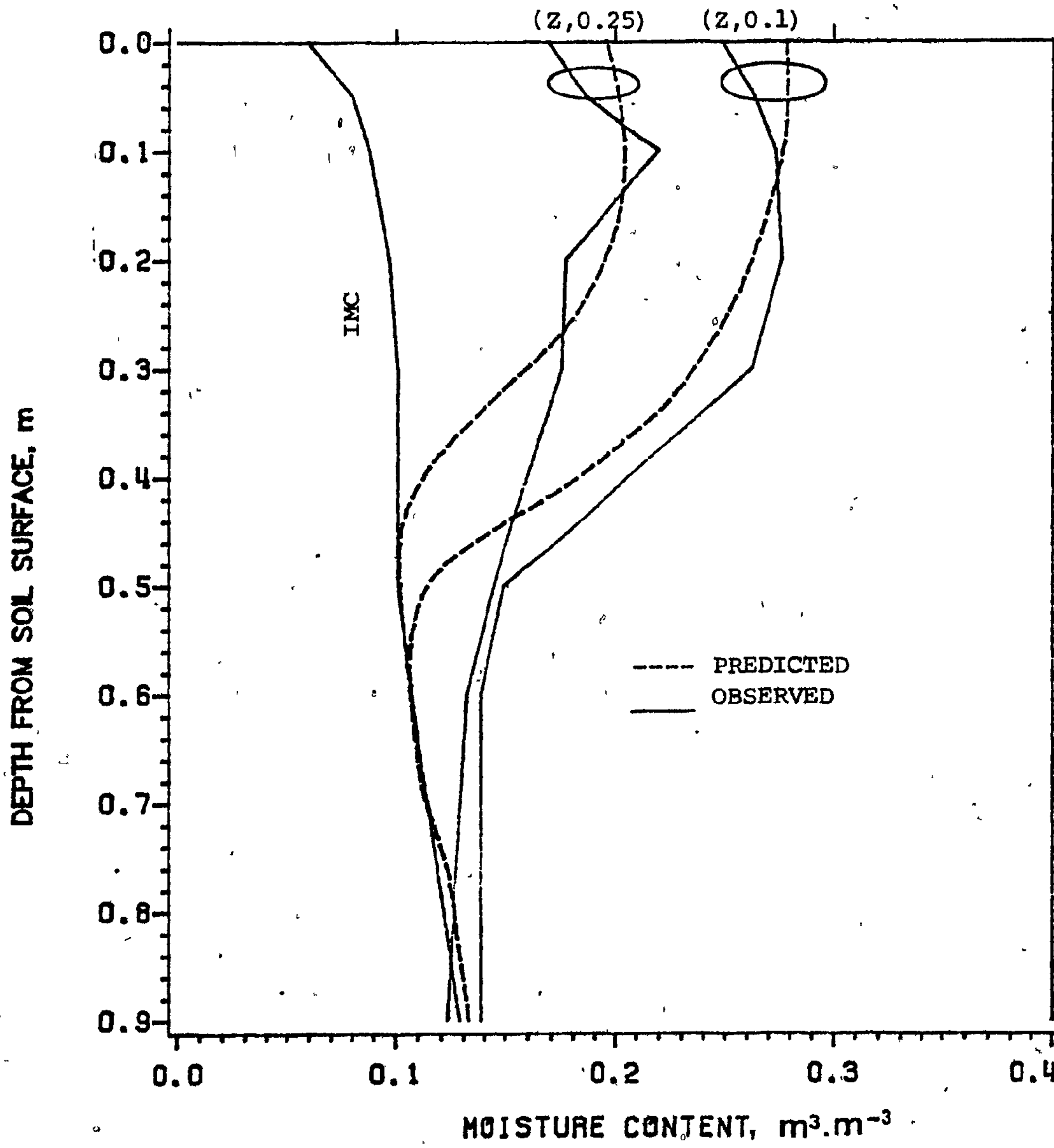

Figure B.44. Soil moisture content profiles before and after 16 L of water applied at 4 $L.h^{-1}$ at Rougemont orchard site 3.

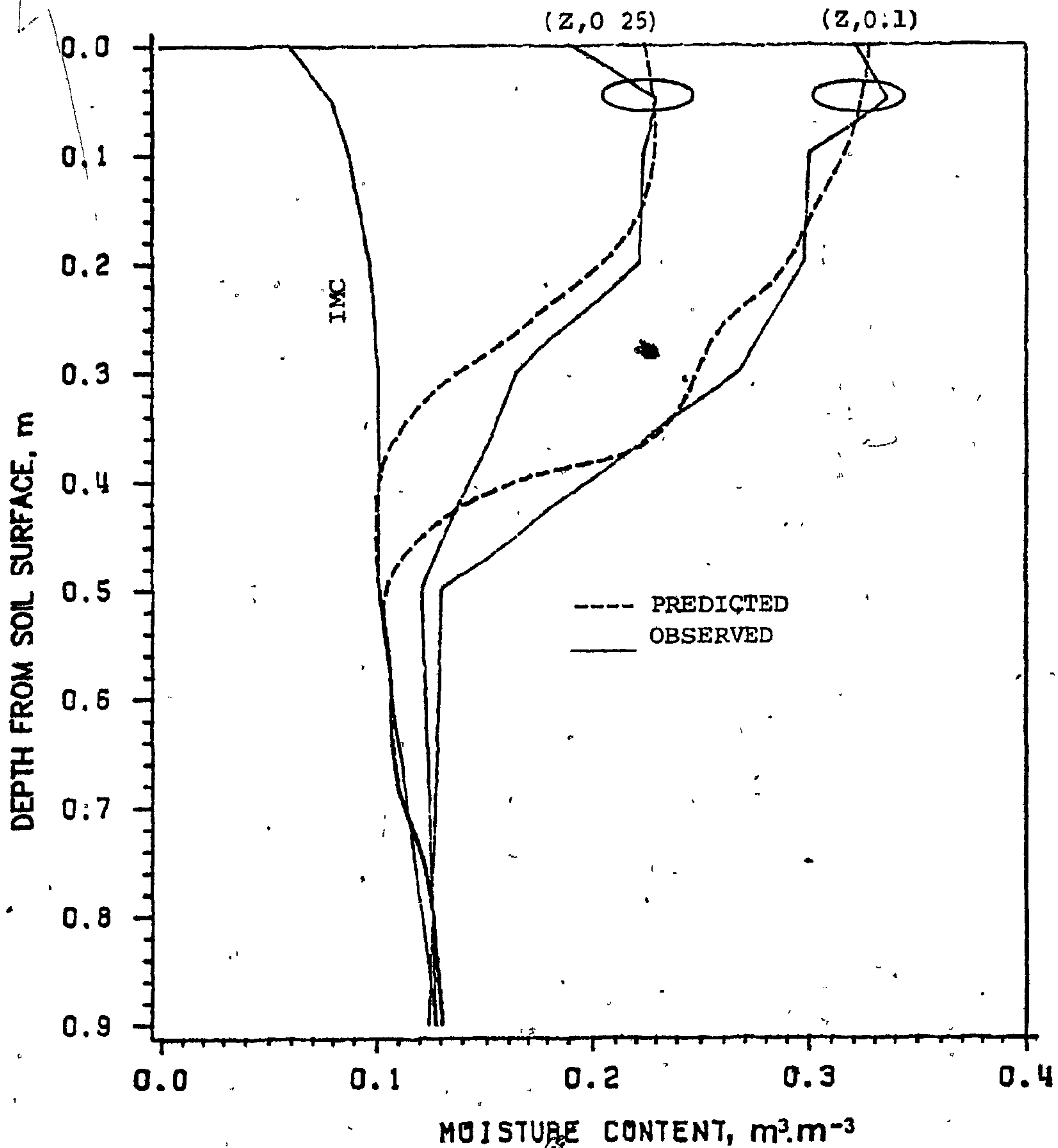

Figure B.45. Soil moisture content profiles before and after 16 L of water applied at 8 $L.h^{-1}$ at Rougemont orchard site 3.

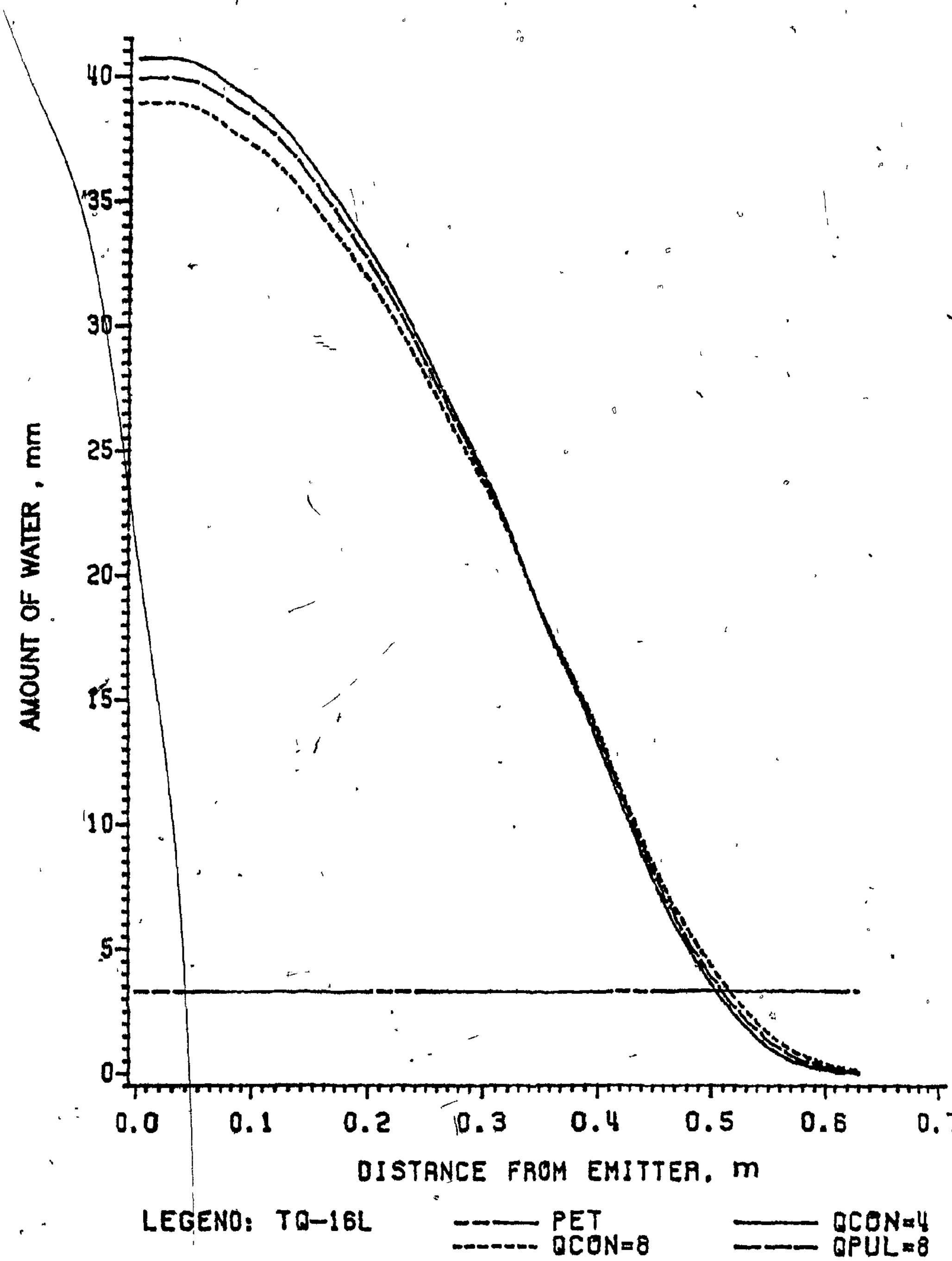

Figure B.46. Water input predicted along horizontal distance with an irrigation application of 16 L at different discharge rates for Rougemont orchard site 3.

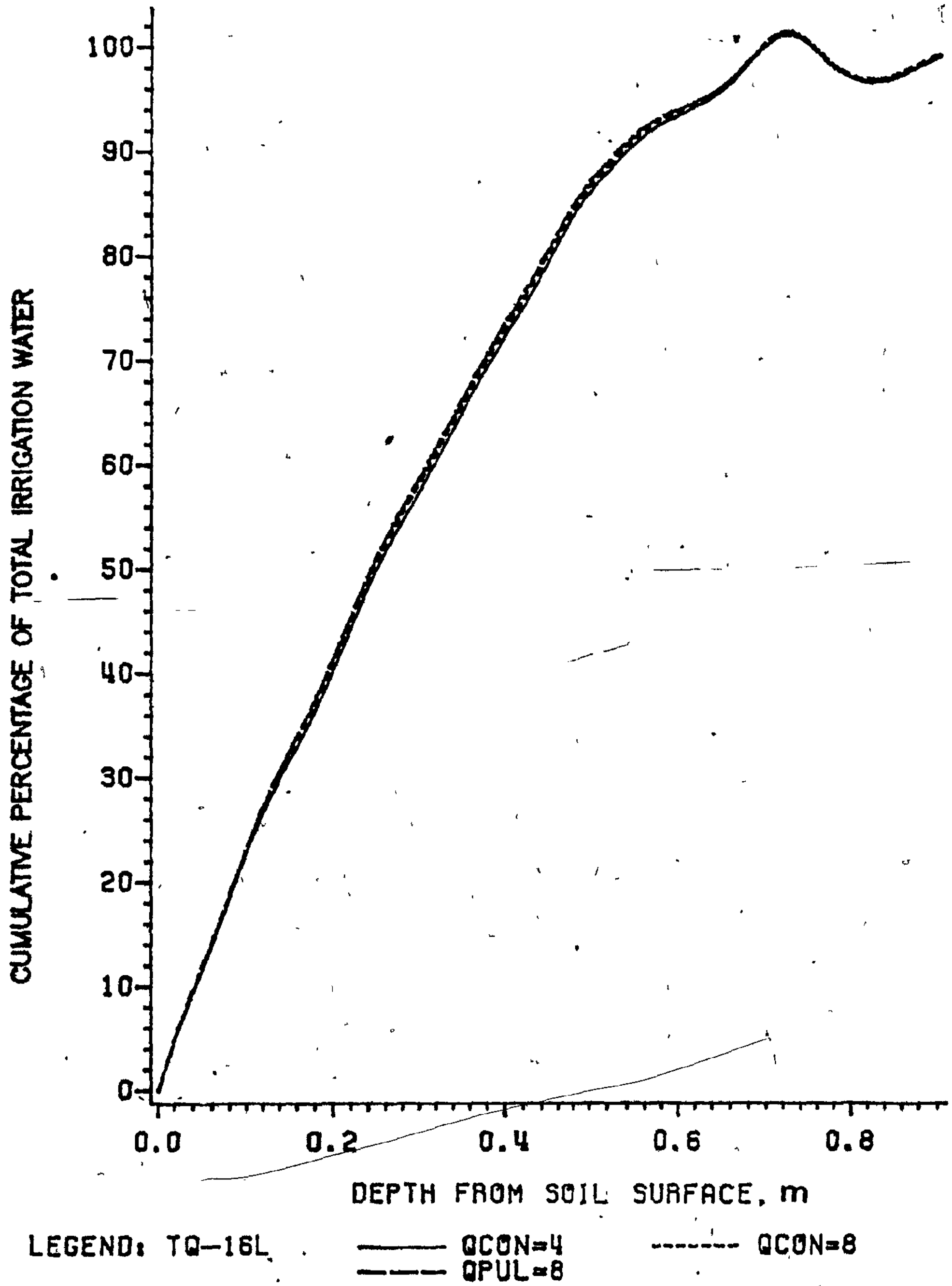

Figure B.47. Water input predicted in soil profile with an irrigation application of 16 L at different discharge rates for Rougemont orchard site 3.

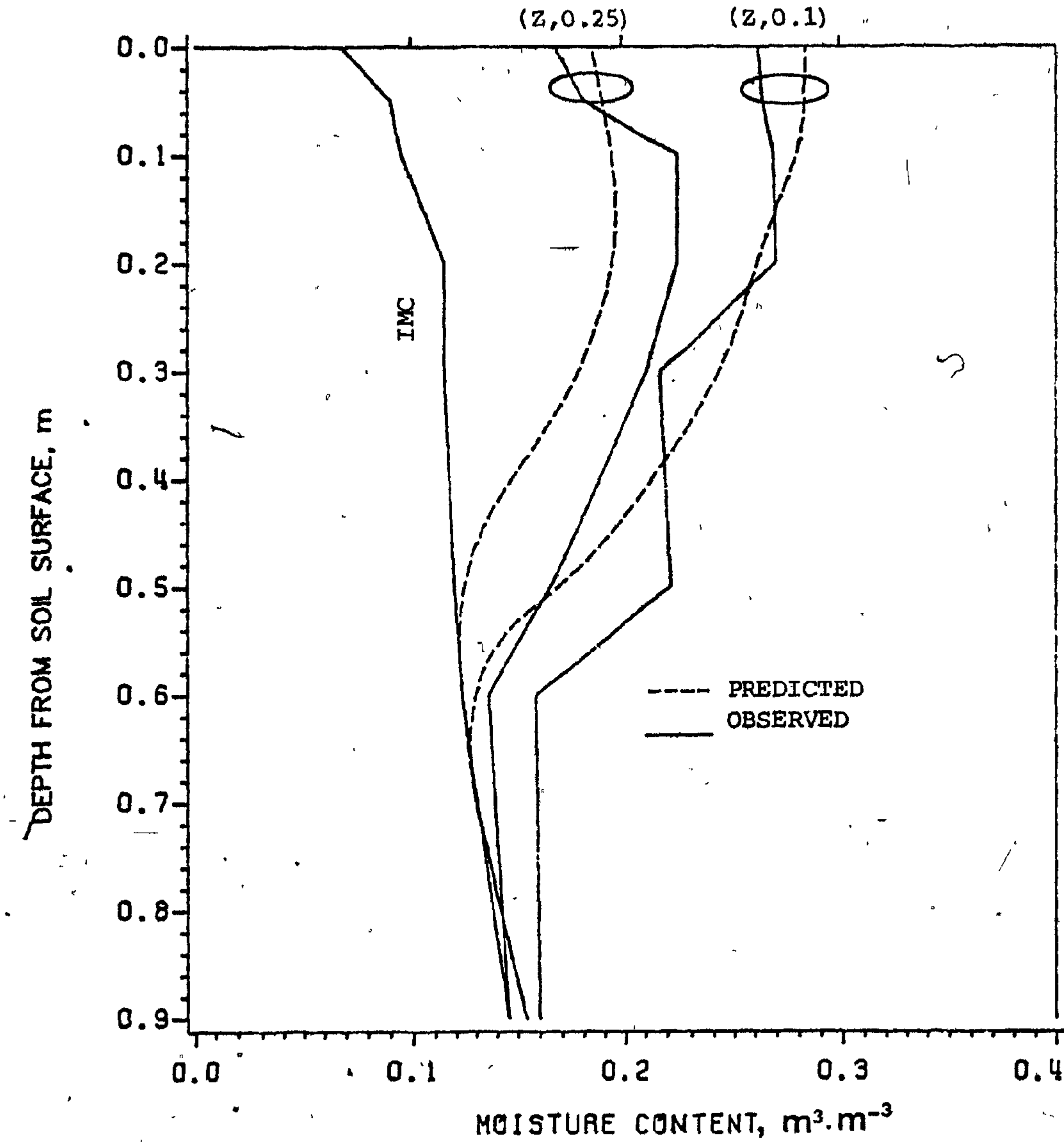

Figure B.48. Soil moisture content profiles before and after 16 L of water applied at 8 $L.h^{-1}$ at Rockburn orchard site 1.

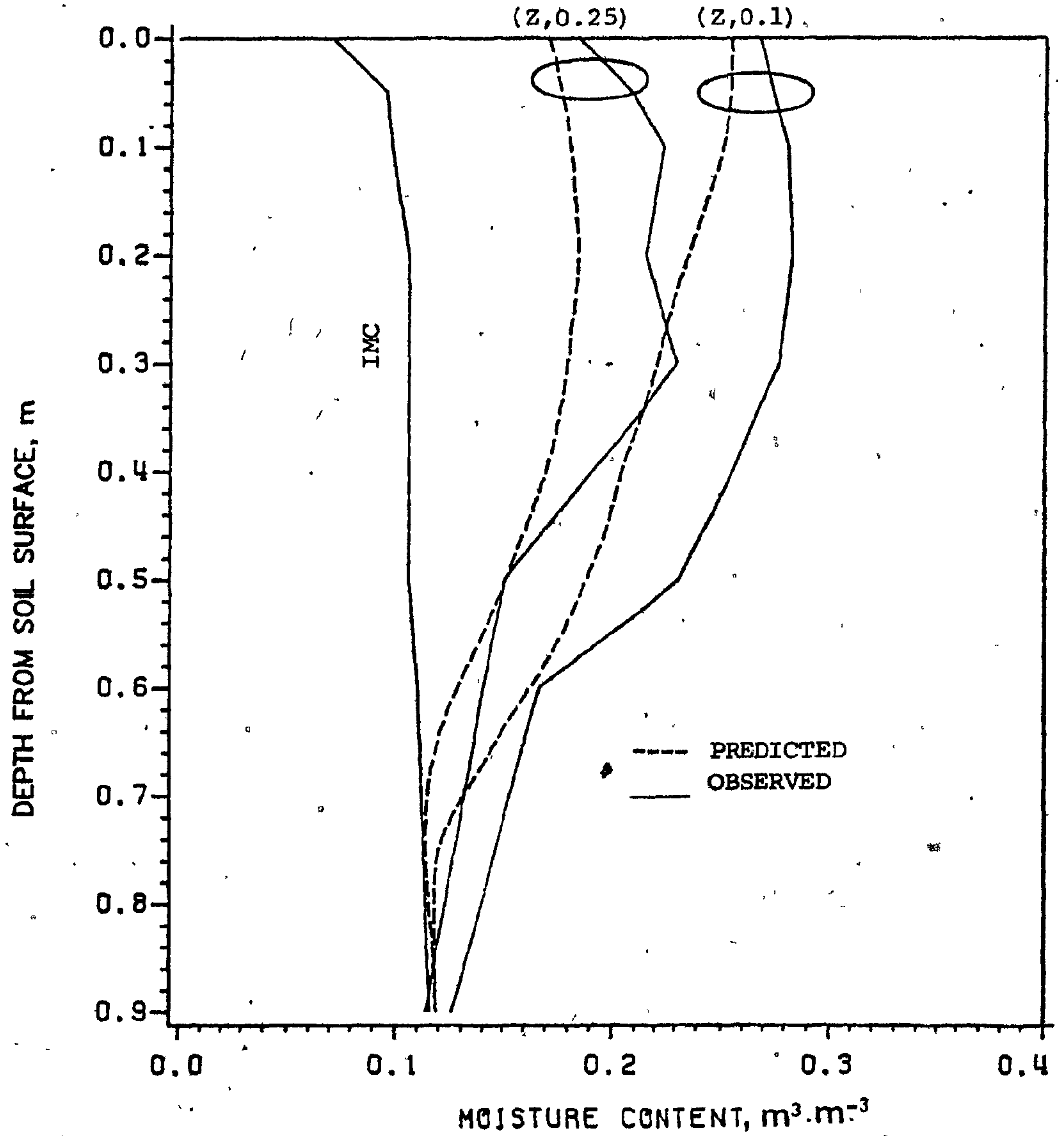

Figure B.49 Soil moisture content profiles before and after 24 L of water applied at 4 $L.h^{-1}$ at Rockburn orchard site 1.

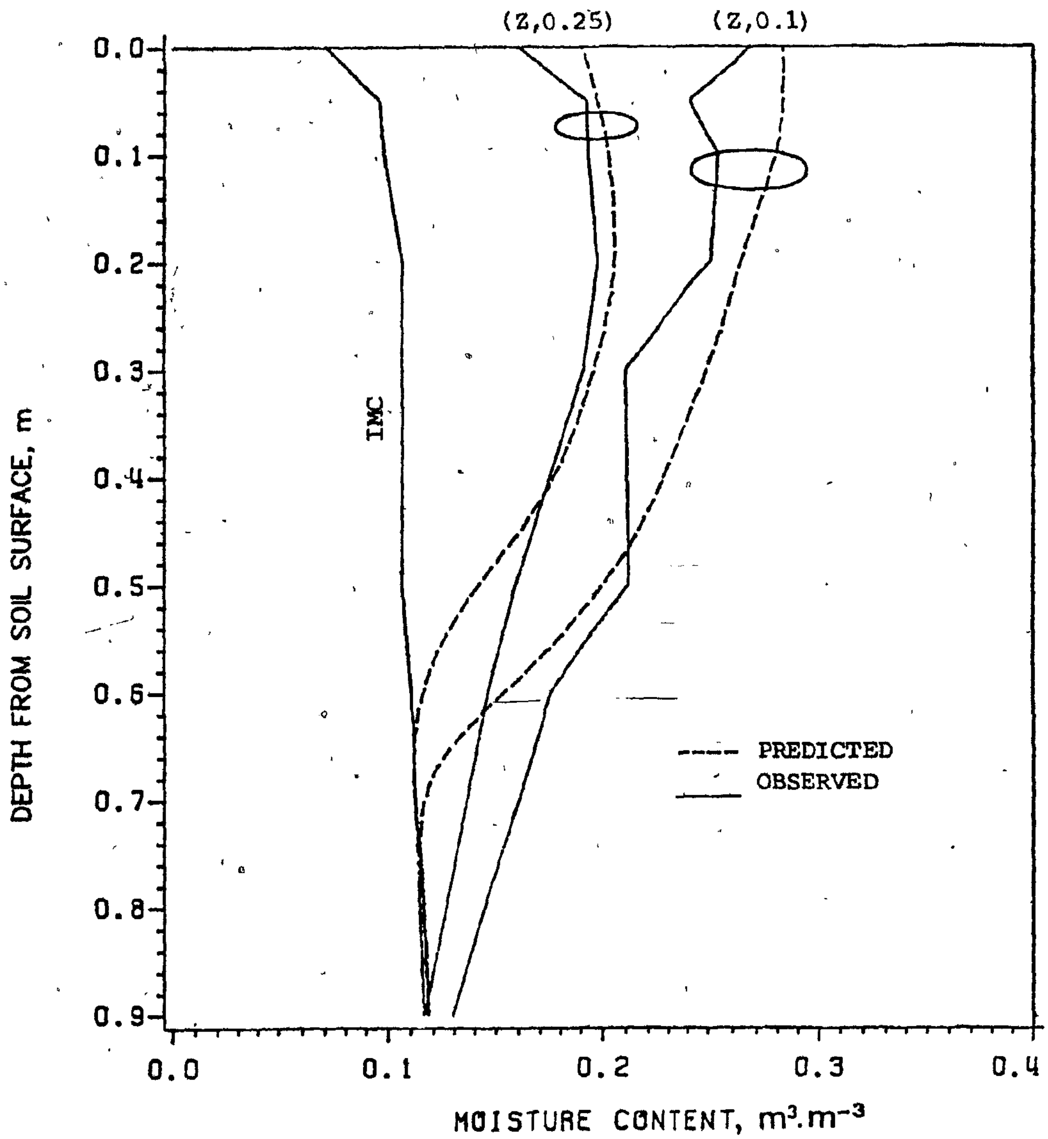

Figure B.50 Soil moisture content profiles before and after 24 L of water applied at 8 $L.h^{-1}$ at Rockburn orchard site 1.

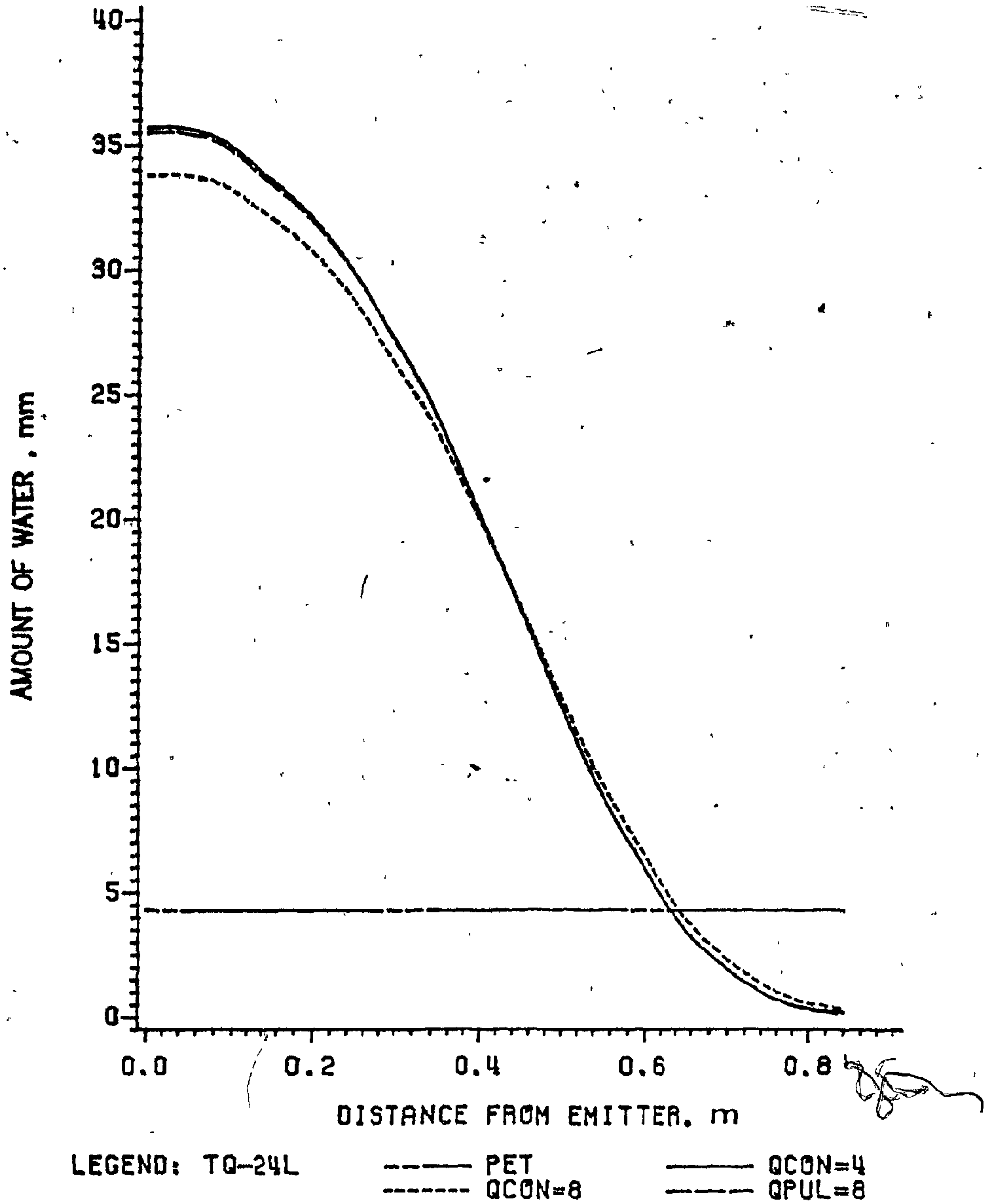

Figure B.51. Water input predicted along horizontal distance with an irrigation application of 24 L at different discharge rates for Rockburn orchard site 1.

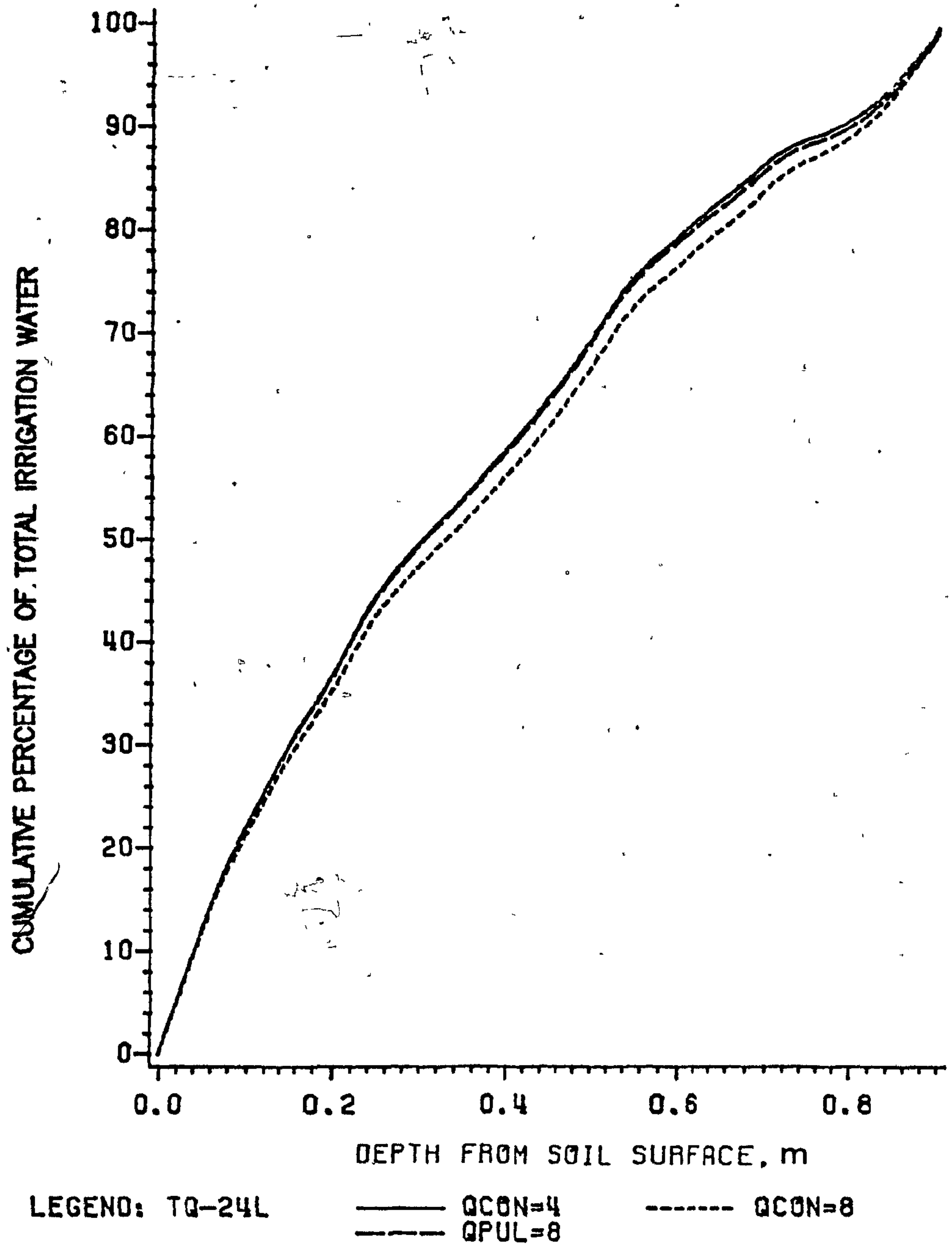

Figure B.52. Water input predicted in soil profile with an irrigation application of 24 L at different discharge rates for Rockburn orchard site 1.

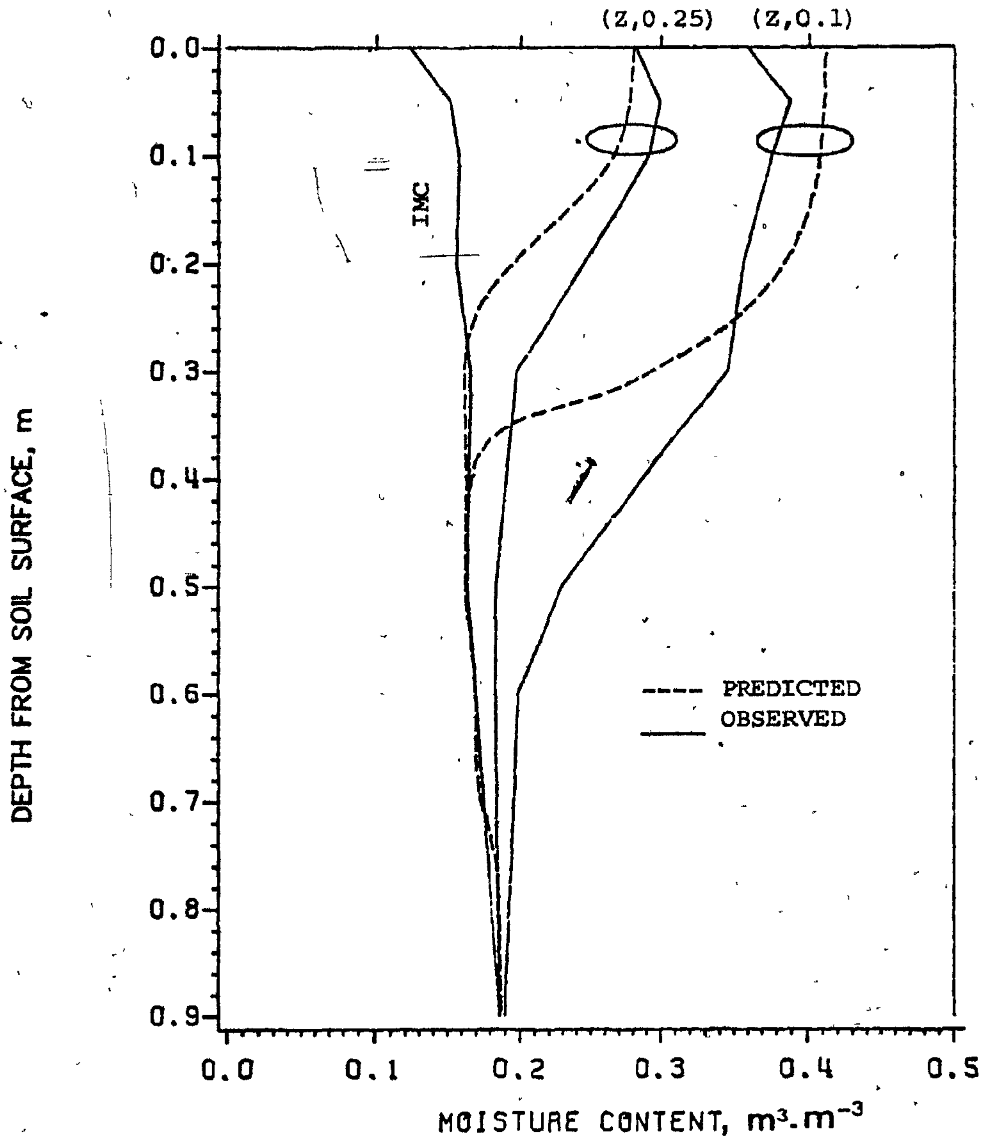

Figure B.53. Soil moisture content profiles before and after 12 L of water applied at 4 $L.h^{-1}$ at Rockburn orchard site 2.

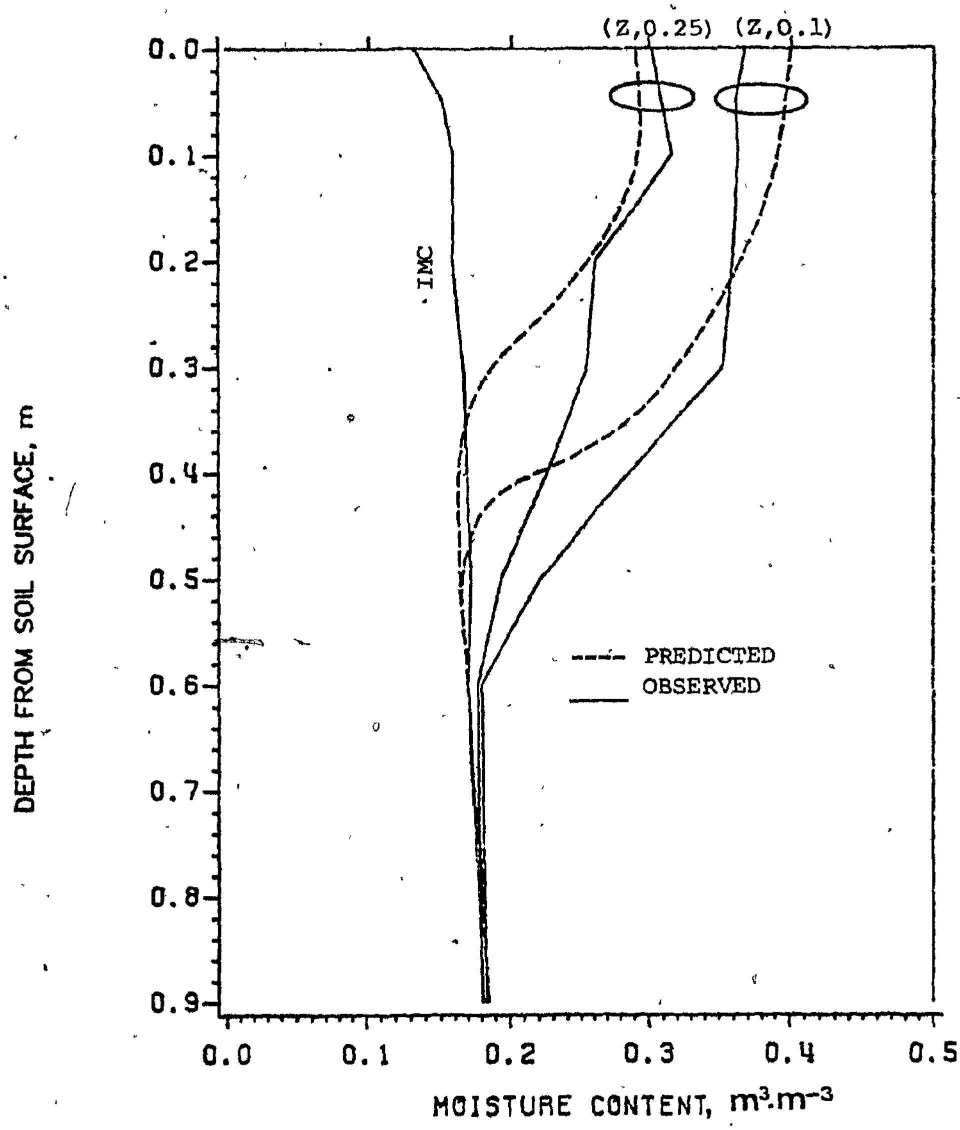

Figure B.54. Soil moisture content profiles before and after 16 L of water applied at 2 $L.h^{-1}$ at Rockburn orchard site 2.

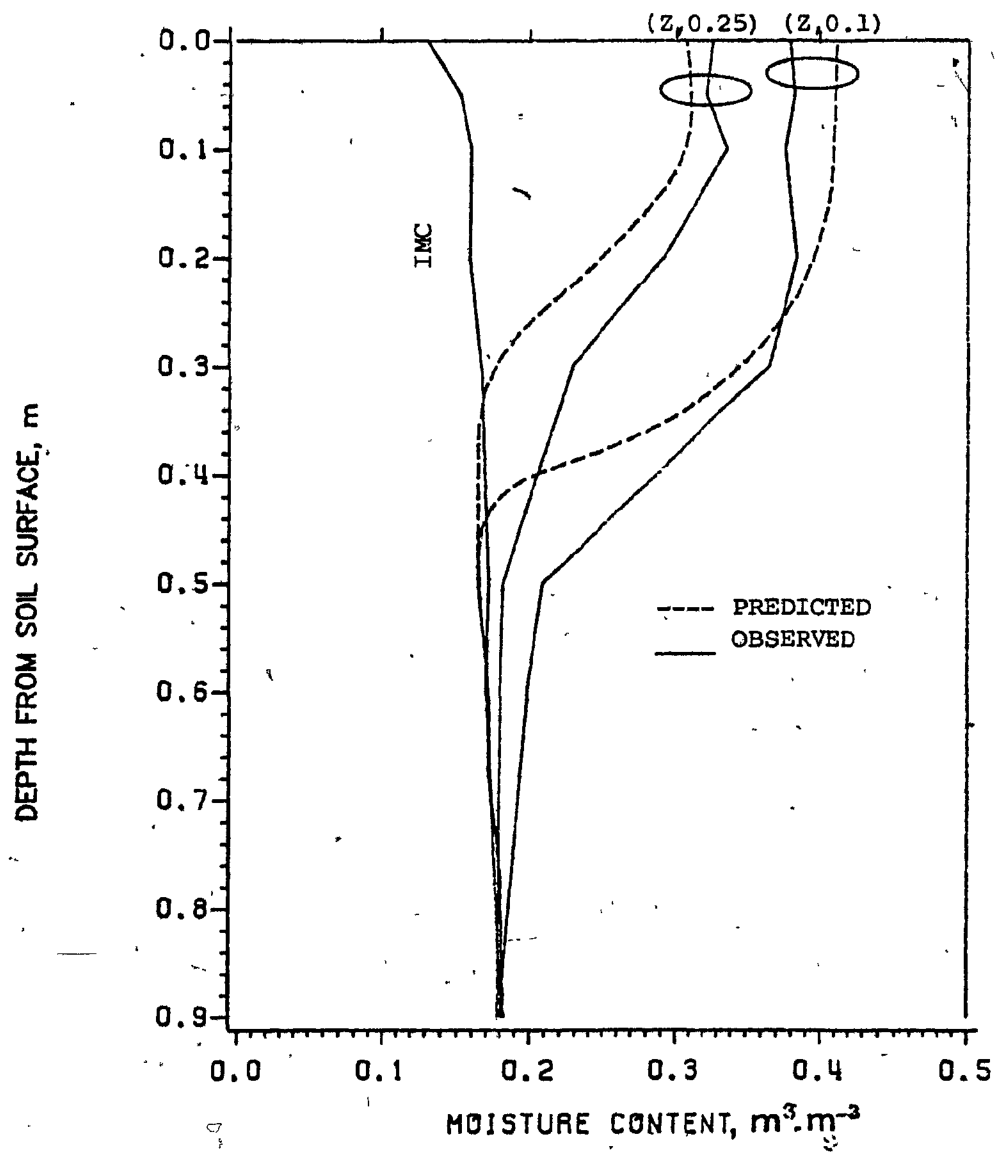

Figure B.55. Soil moisture content profiles before and after 16 L of water applied at 4 $L.h^{-1}$ at Rockburn orchard site 2.

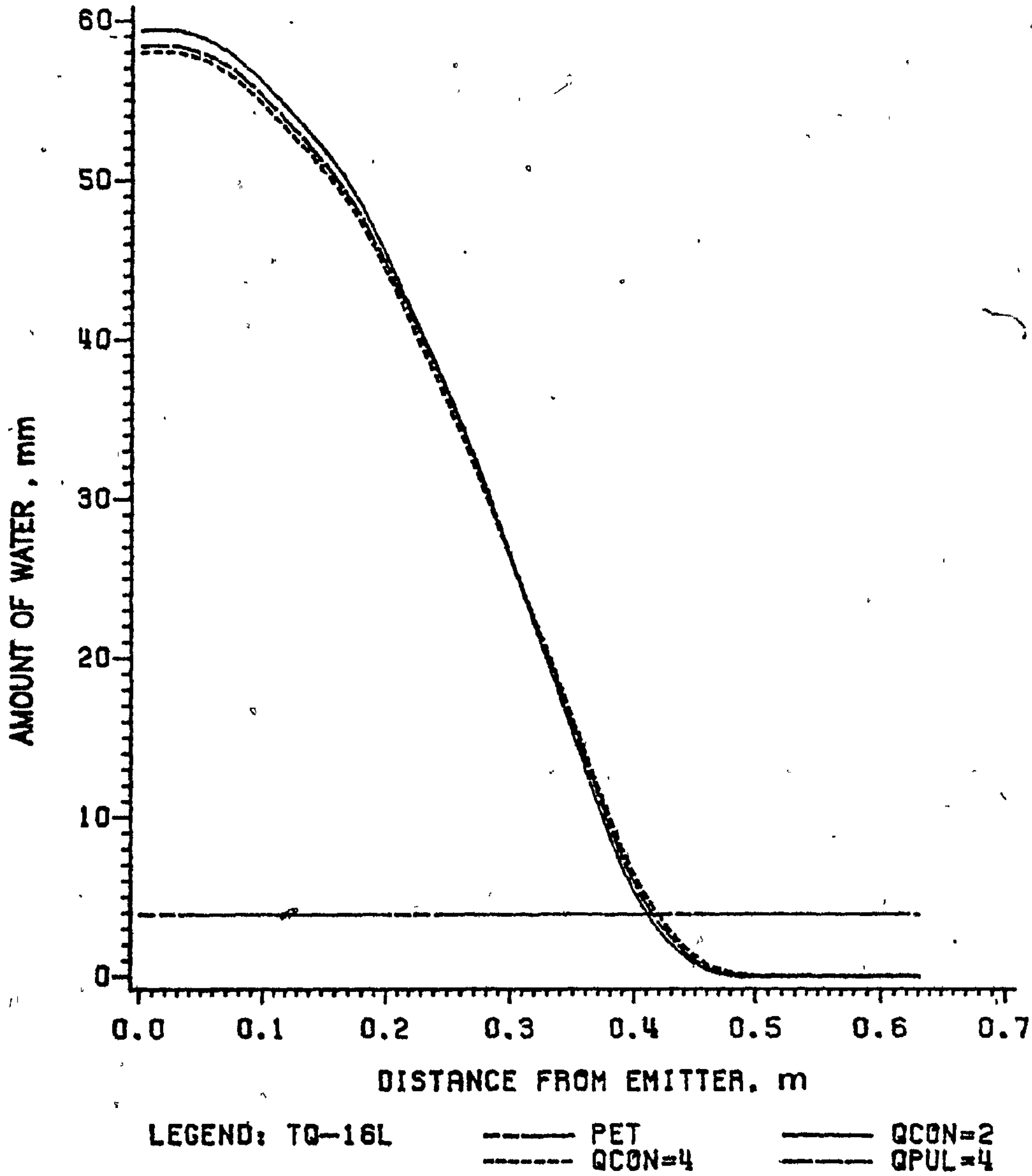

Figure B.56. Water input predicted along horizontal distance with an irrigation application of 16 L at different discharge rates for Rockburn orchard site 2.

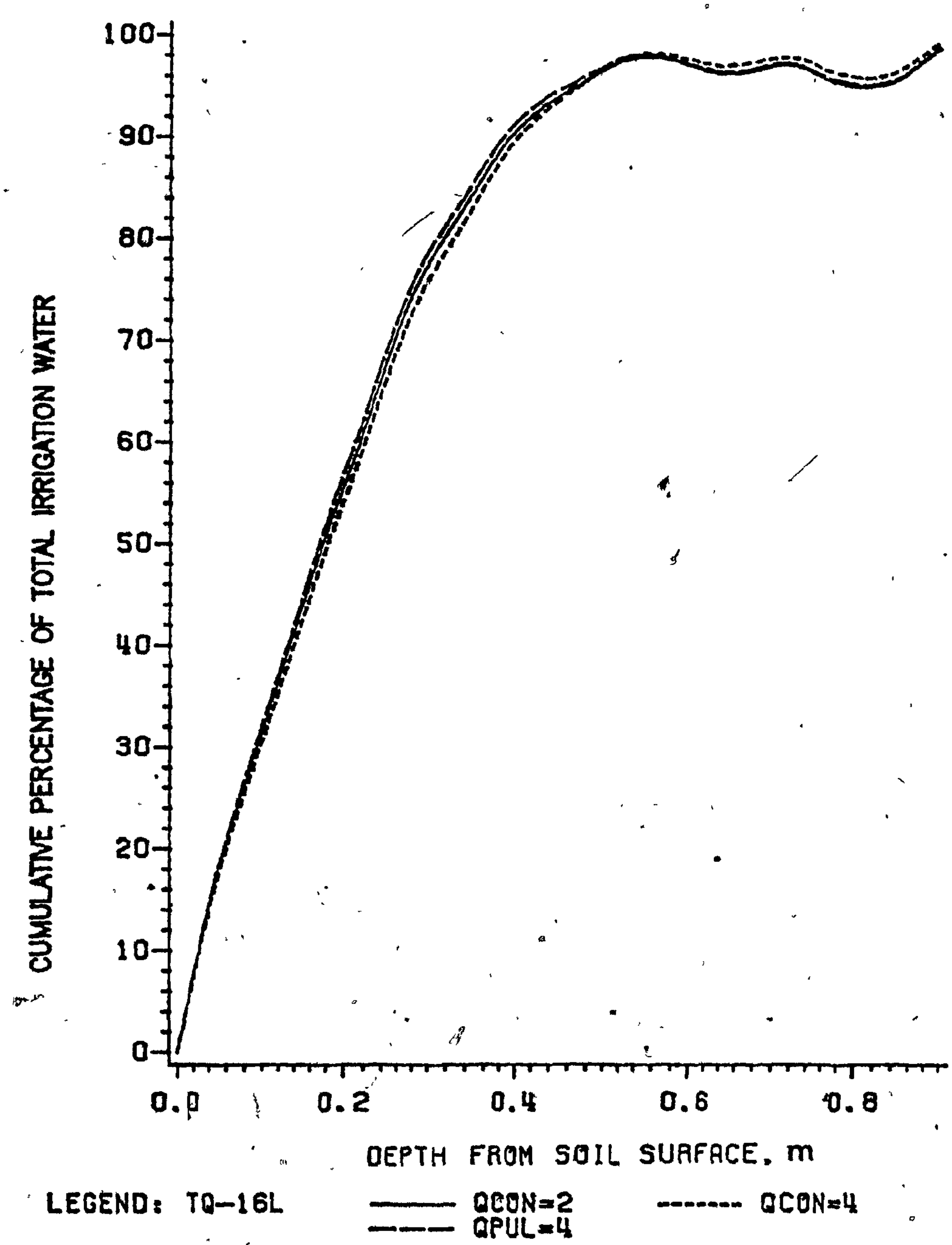

Figure B.57. Water input predicted in soil profile with an irrigation application of 16 L at different discharge rates for Rockburn orchard site 2.

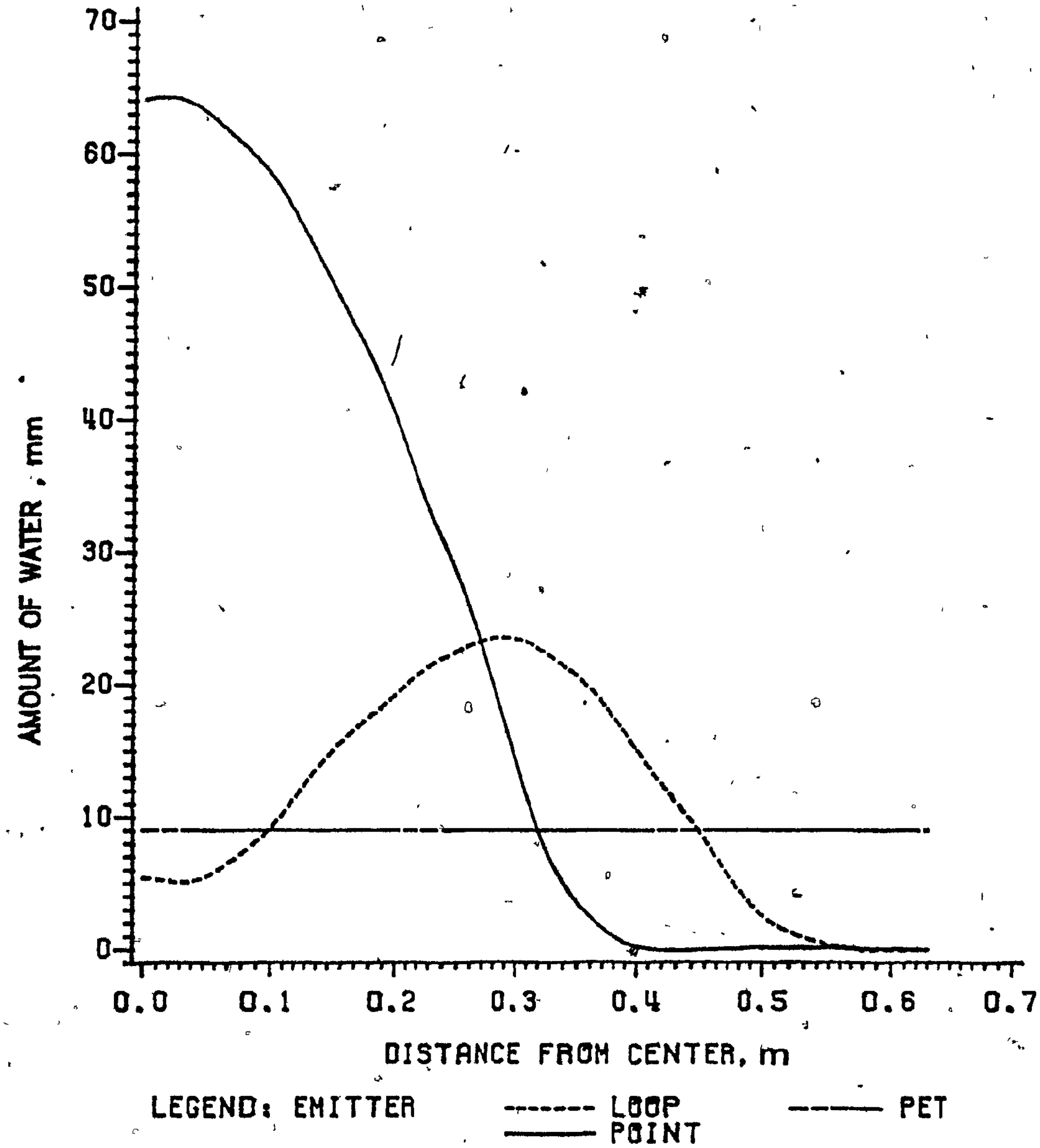

Figure B.58. Water input predicted along horizontal distance with an irrigation application of 12 L from a point and a circular loop source for Rougemont orchard site 2.

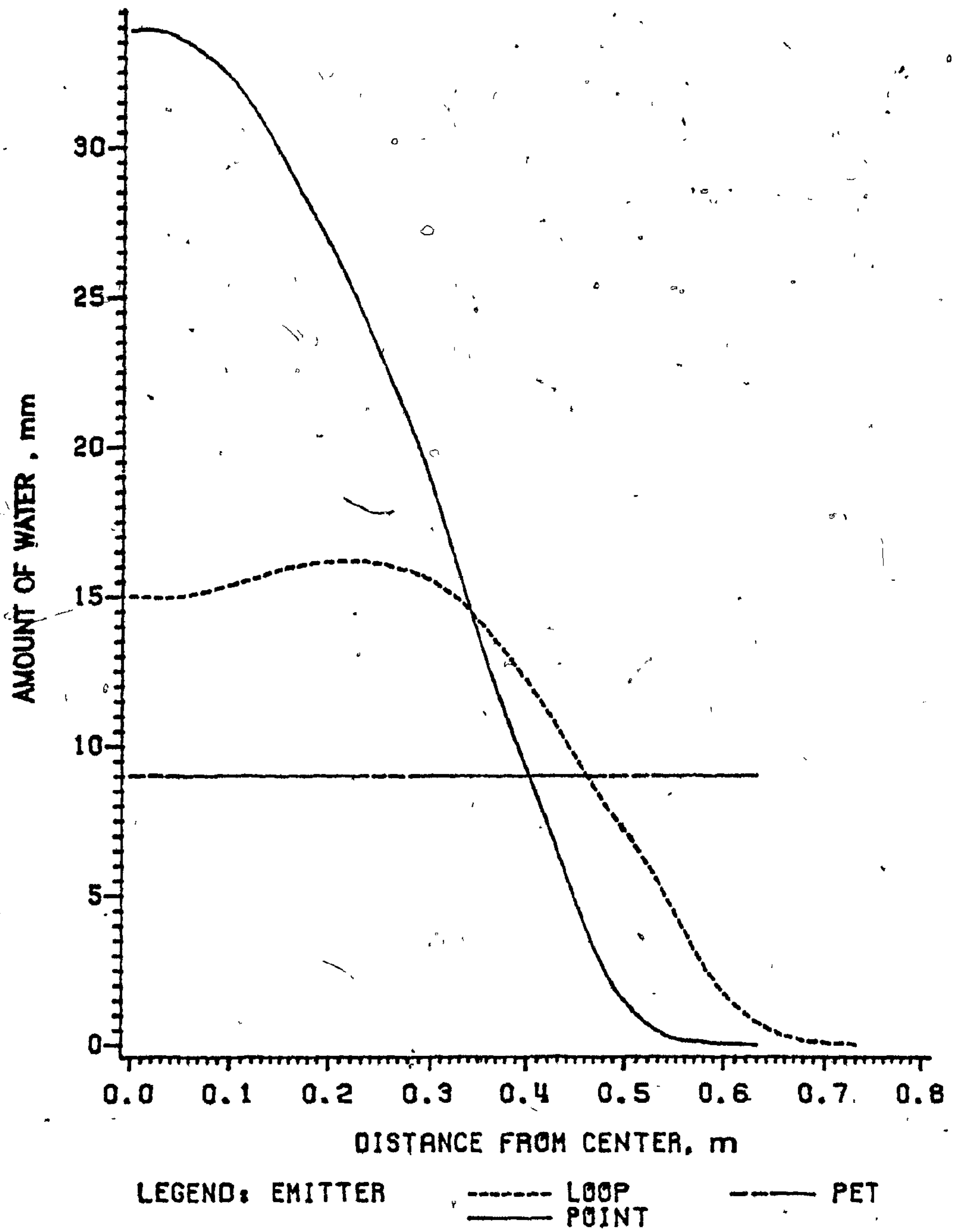

Figure B.59. Water input predicted along horizontal distance with an irrigation application of 12 L from a point and a circular loop source for Rougemont orchard site 3.

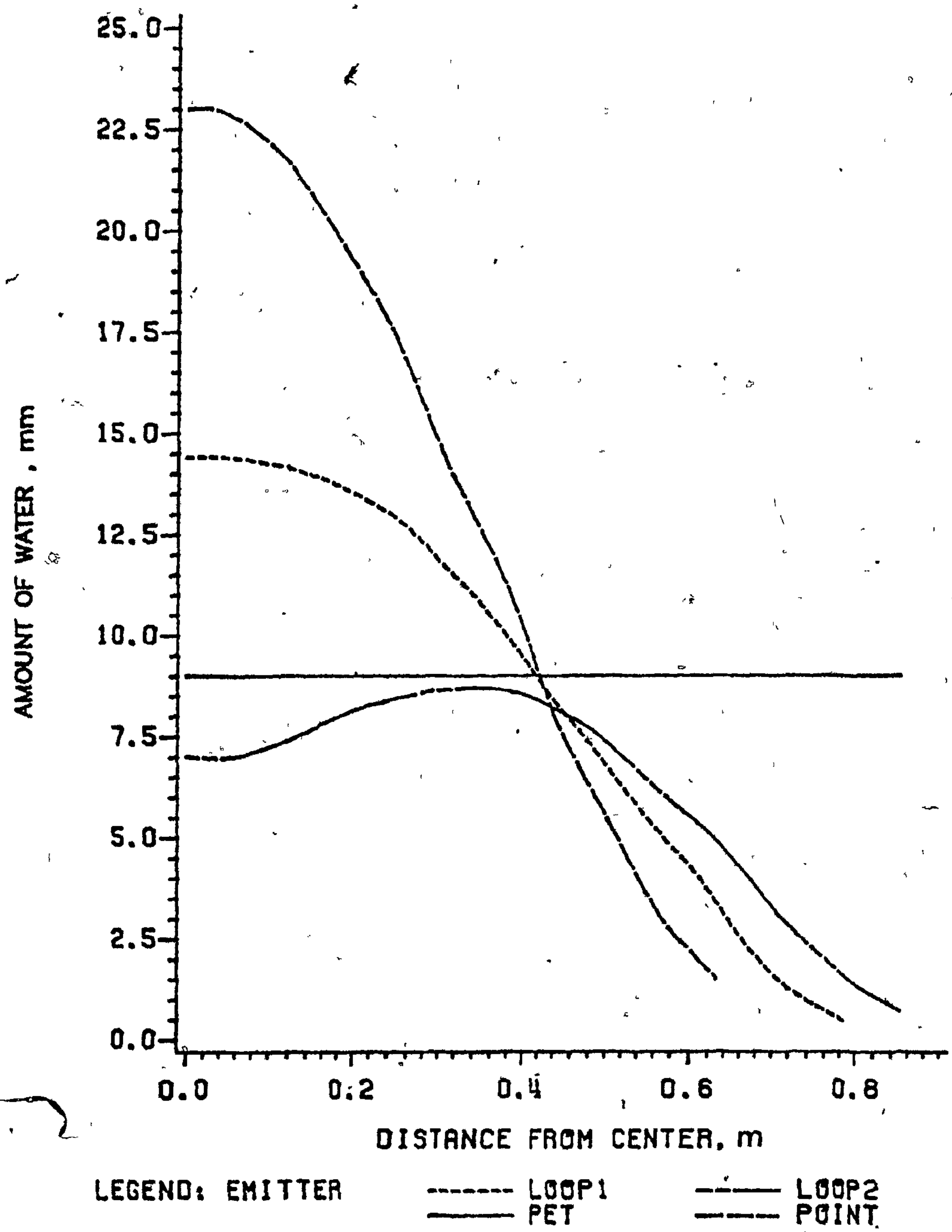

Figure B.60. Water input predicted along horizontal distance with an irrigation application of 12 L from a point and a circular loop source for Rockburn Orchard Site 1. (LOOP1: R=0.3 m, LOOP2: R=0.42 m)

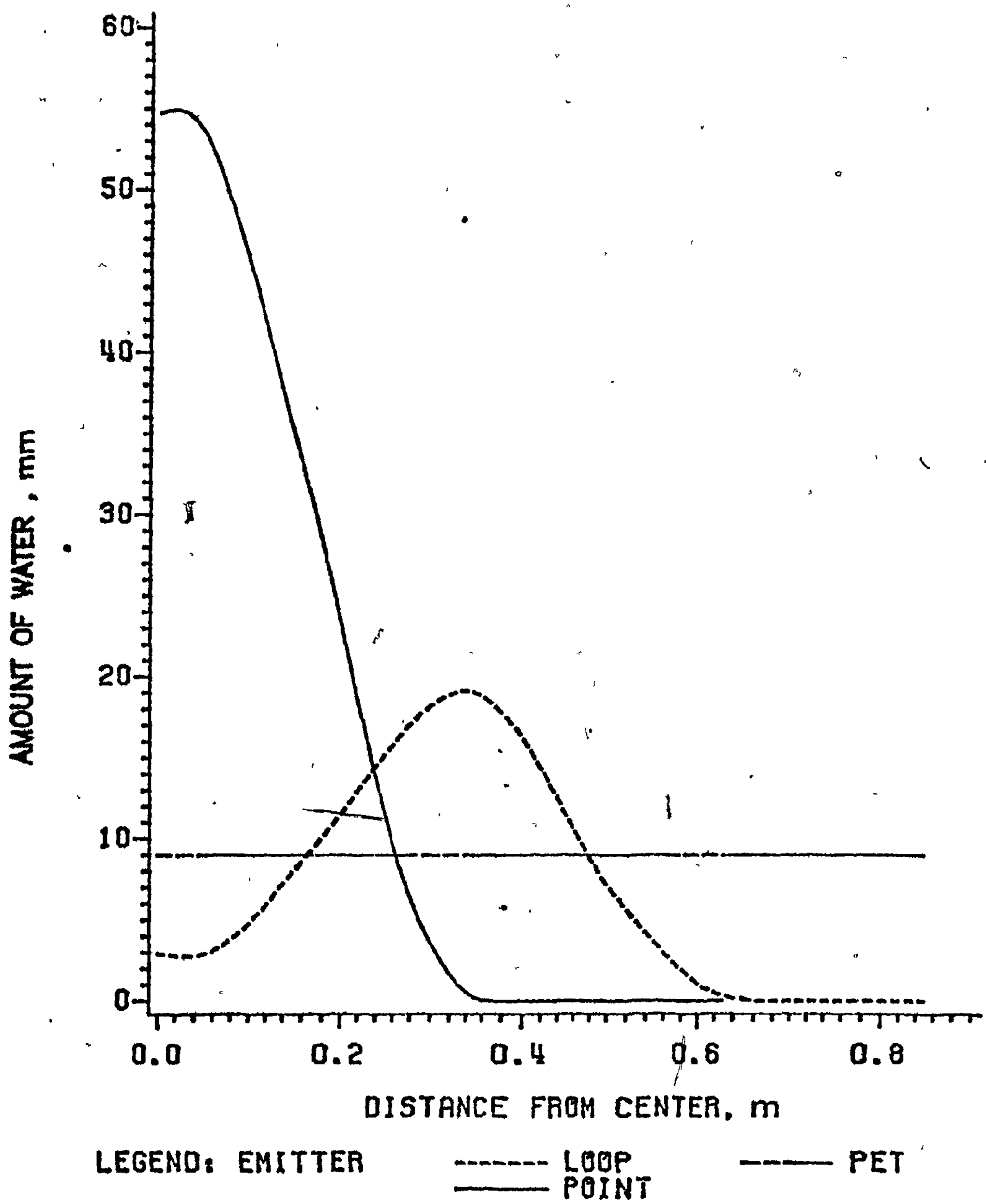

Figure B.61. Water input predicted along horizontal distance with an irrigation application of 12 L from a point and a circular loop source for Rockburn orchard site 2.

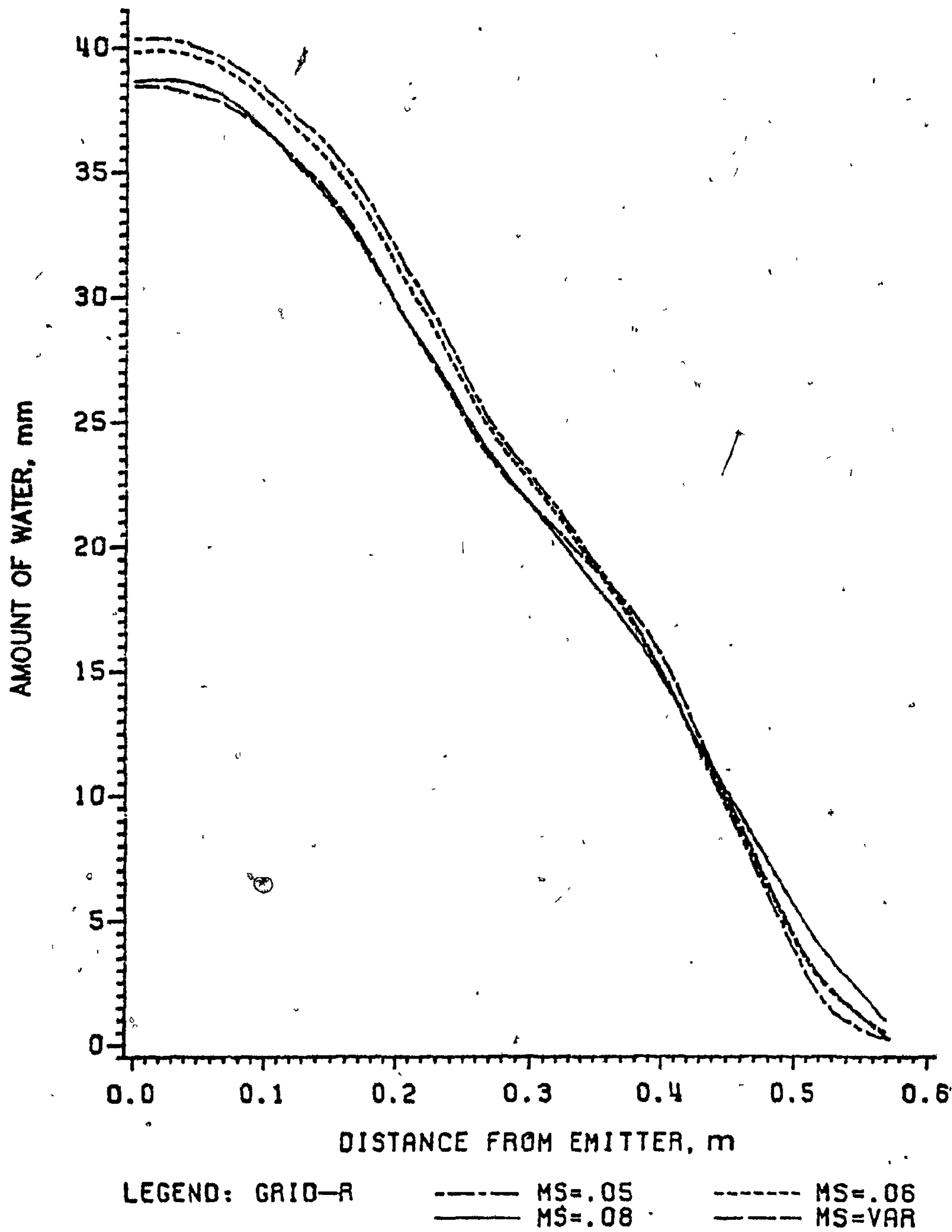

Figure B.62. Water input predicted along horizontal distance with an irrigation application of 12 L and different mesh sizes in radial direction.

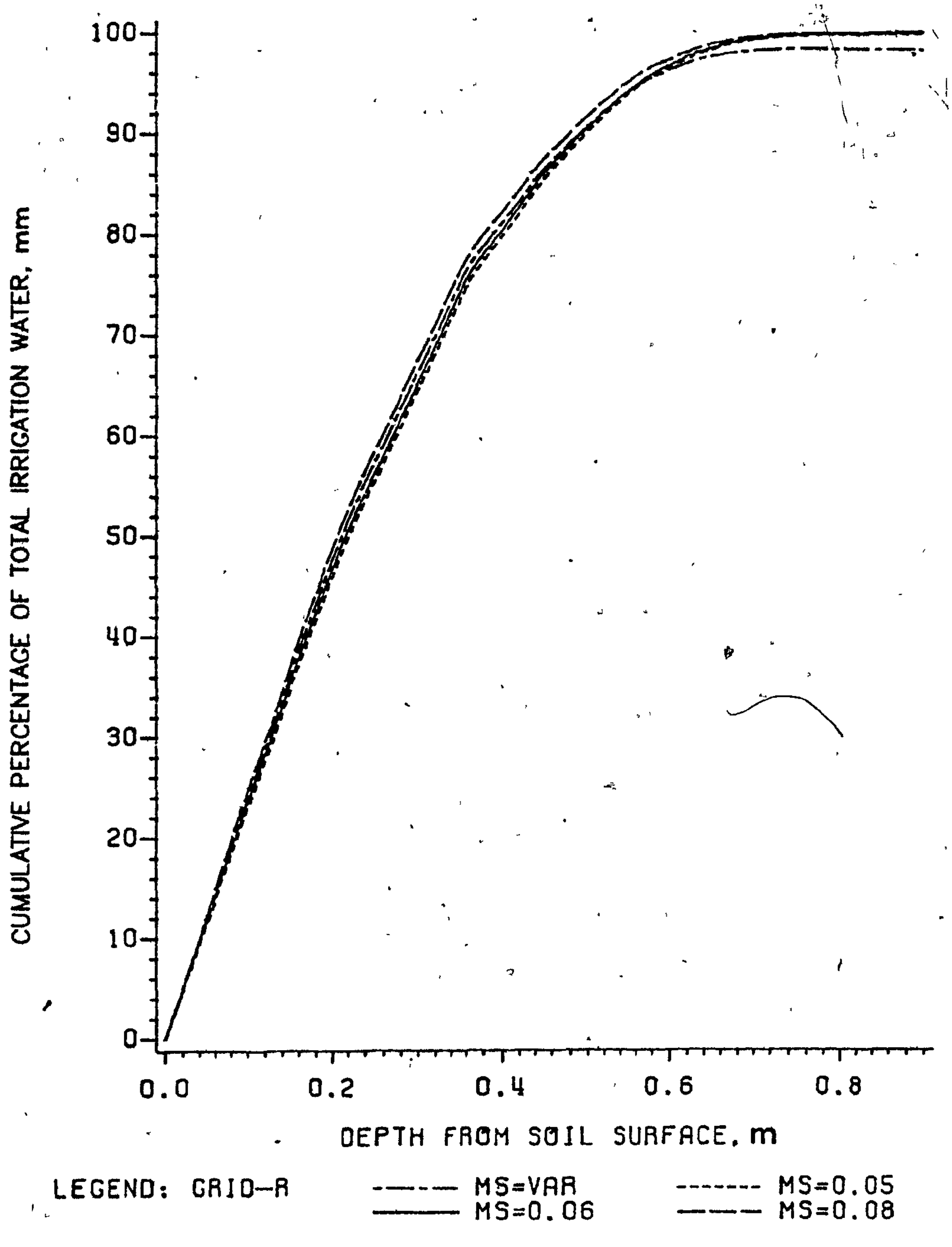

Figure B.63. Water input predicted in soil profile with an irrigation application of 12 L and different mesh sizes in radial direction.

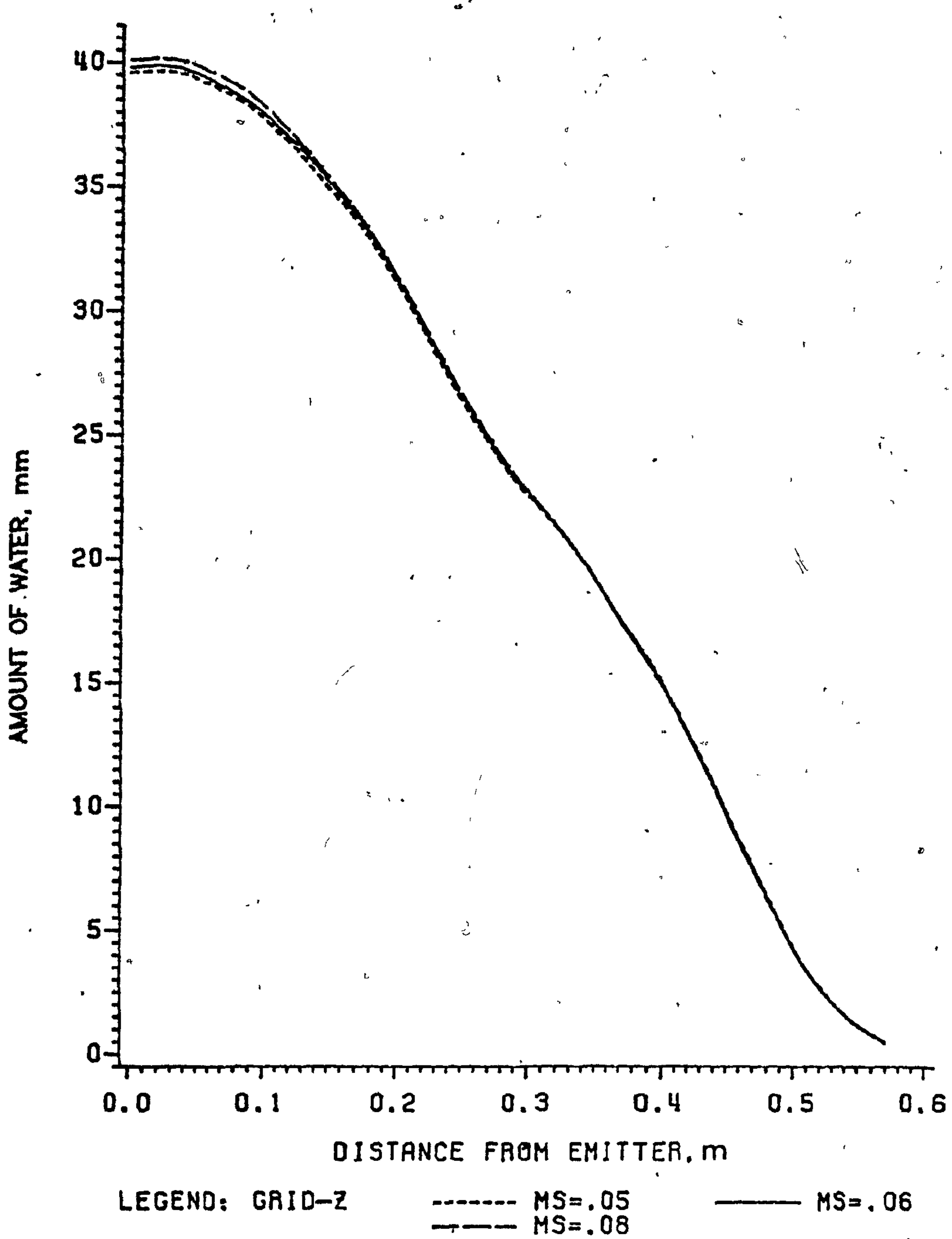

Figure B.64. Water input predicted along horizontal distance with an irrigation application of 12 L and different mesh sizes in vertical direction.

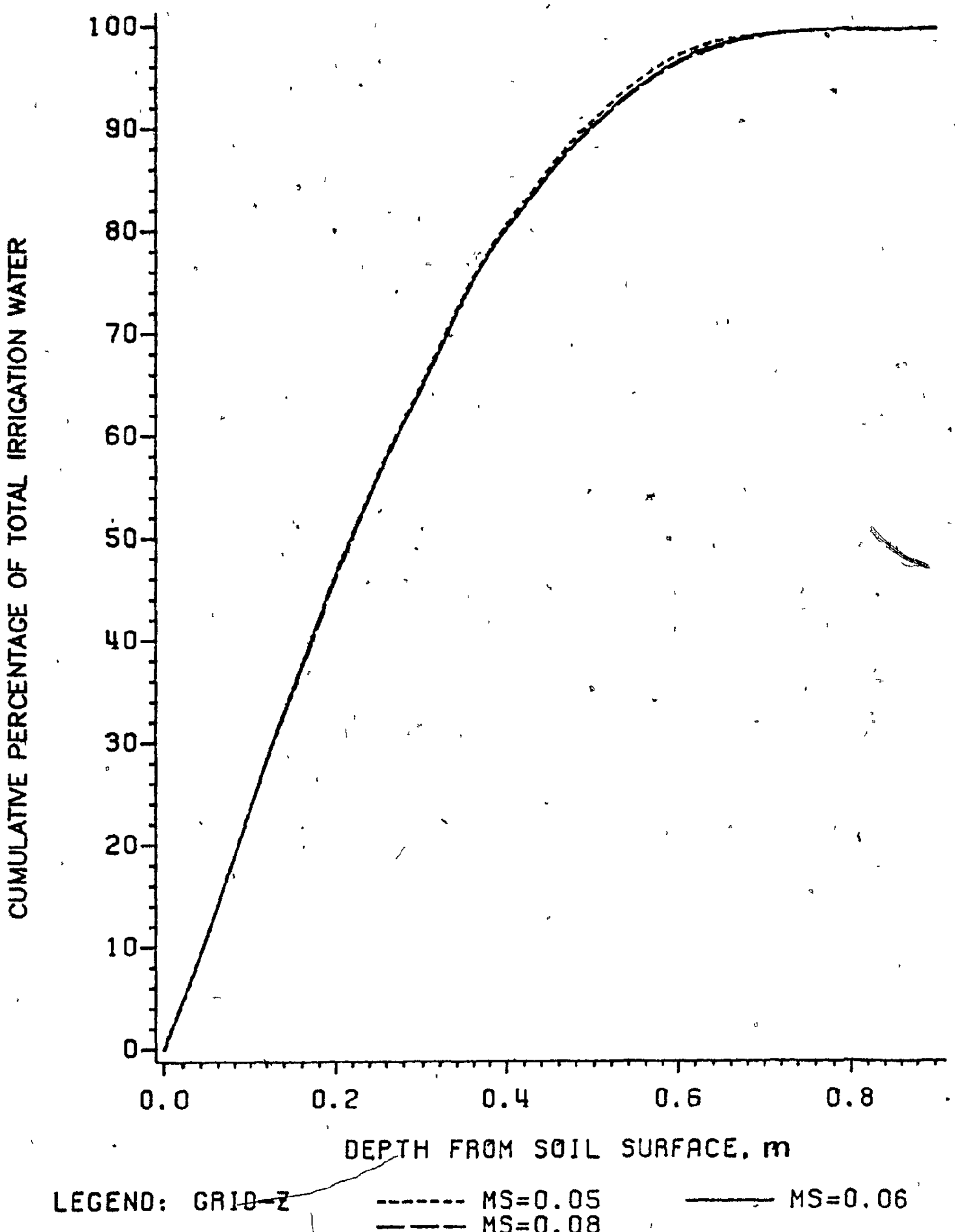

Figure B.65. Water input predicted in soil profile with an irrigation application of 12 L and different mesh sizes in vertical direction.

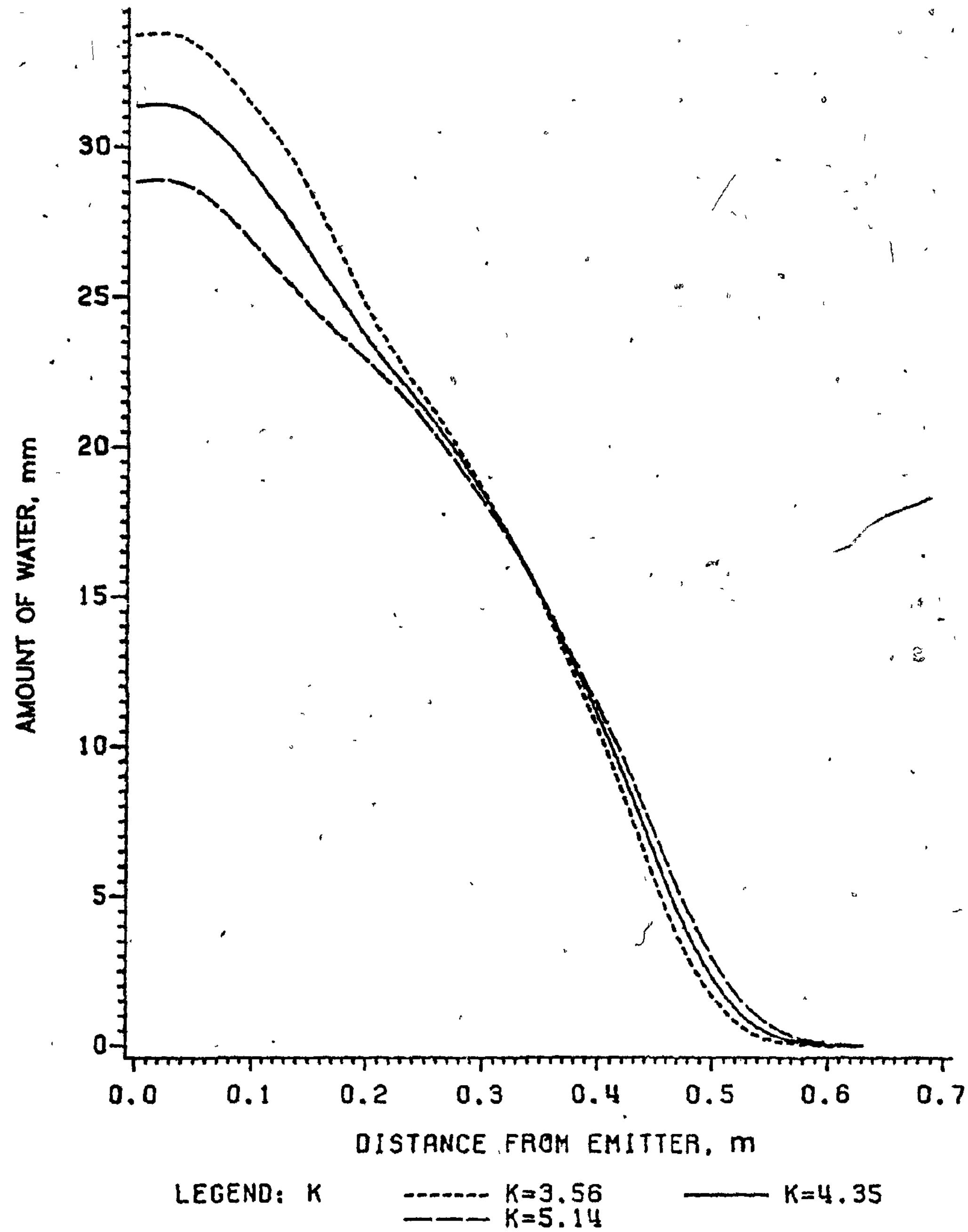

Figure B.66. Water input predicted along horizontal distance with an irrigation application of 12 L and different hydraulic conductivity values.

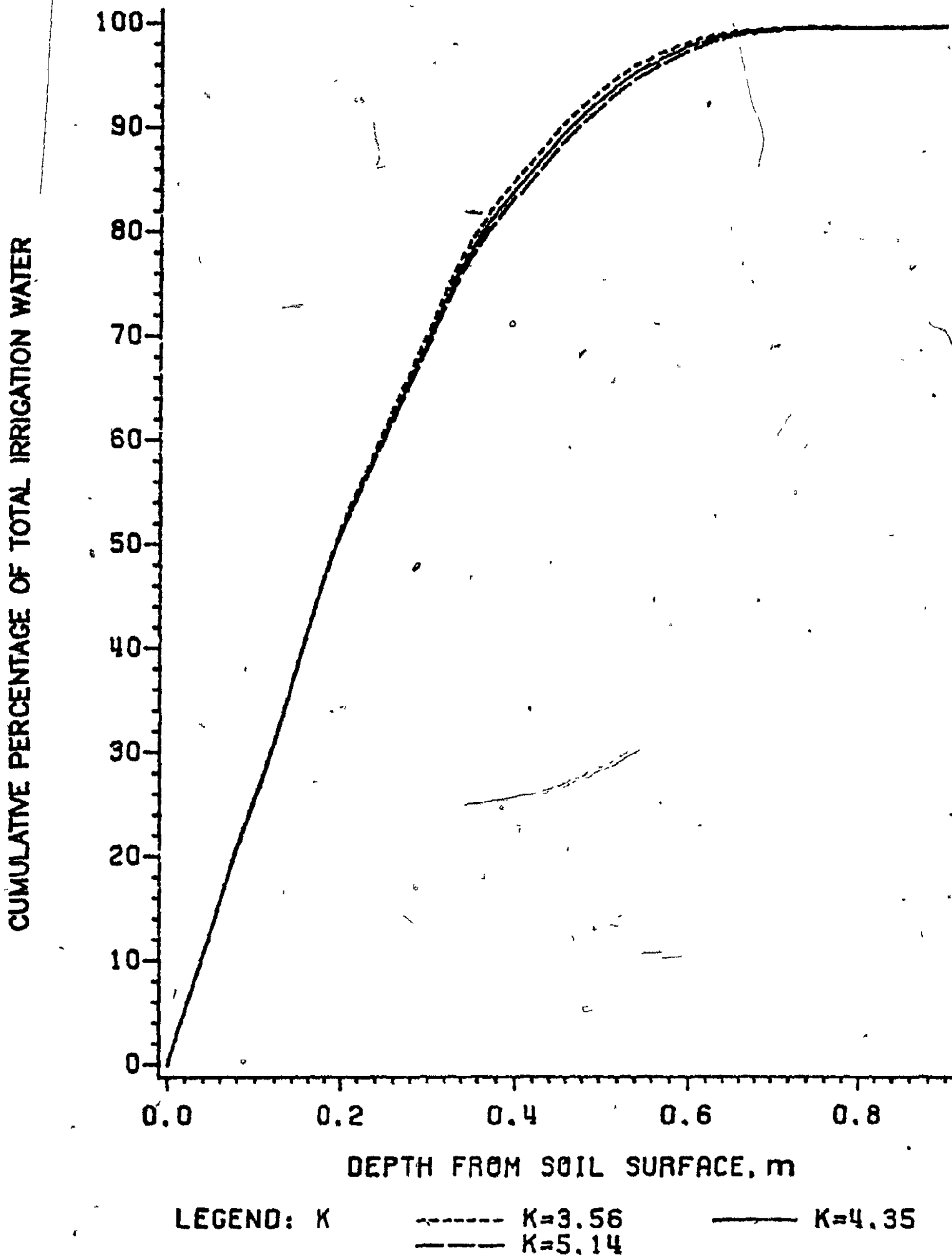

Figure B.67. Water input predicted in soil profile with an irrigation application of 12 L and different hydraulic conductivity values.

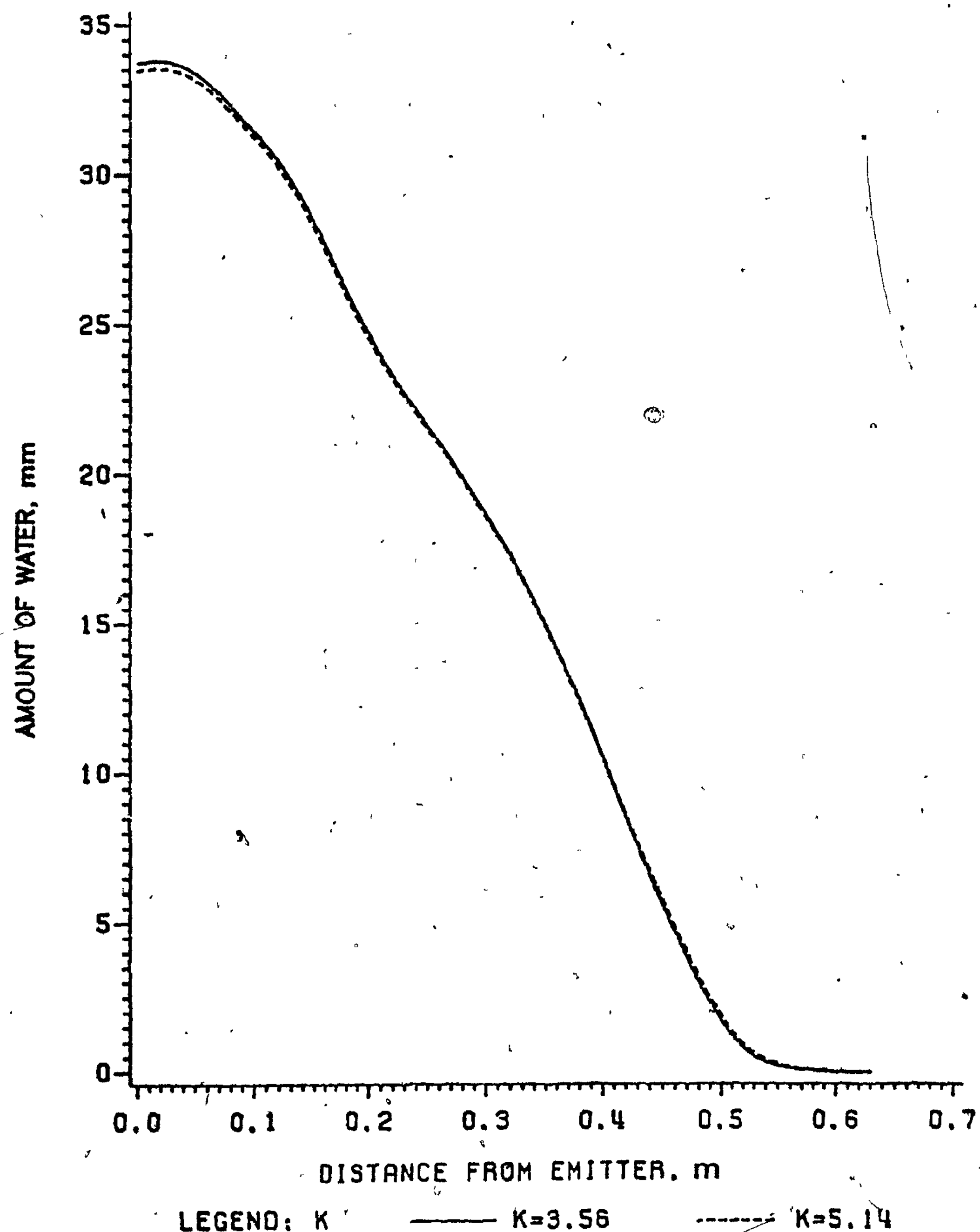

Figure B.68. Water input predicted along horizontal distance with an irrigation application of 12 L for K=3.56 $m.day^{-1}$ at t=15 h and K=5.14 $m.day^{-1}$ at t=13 h.

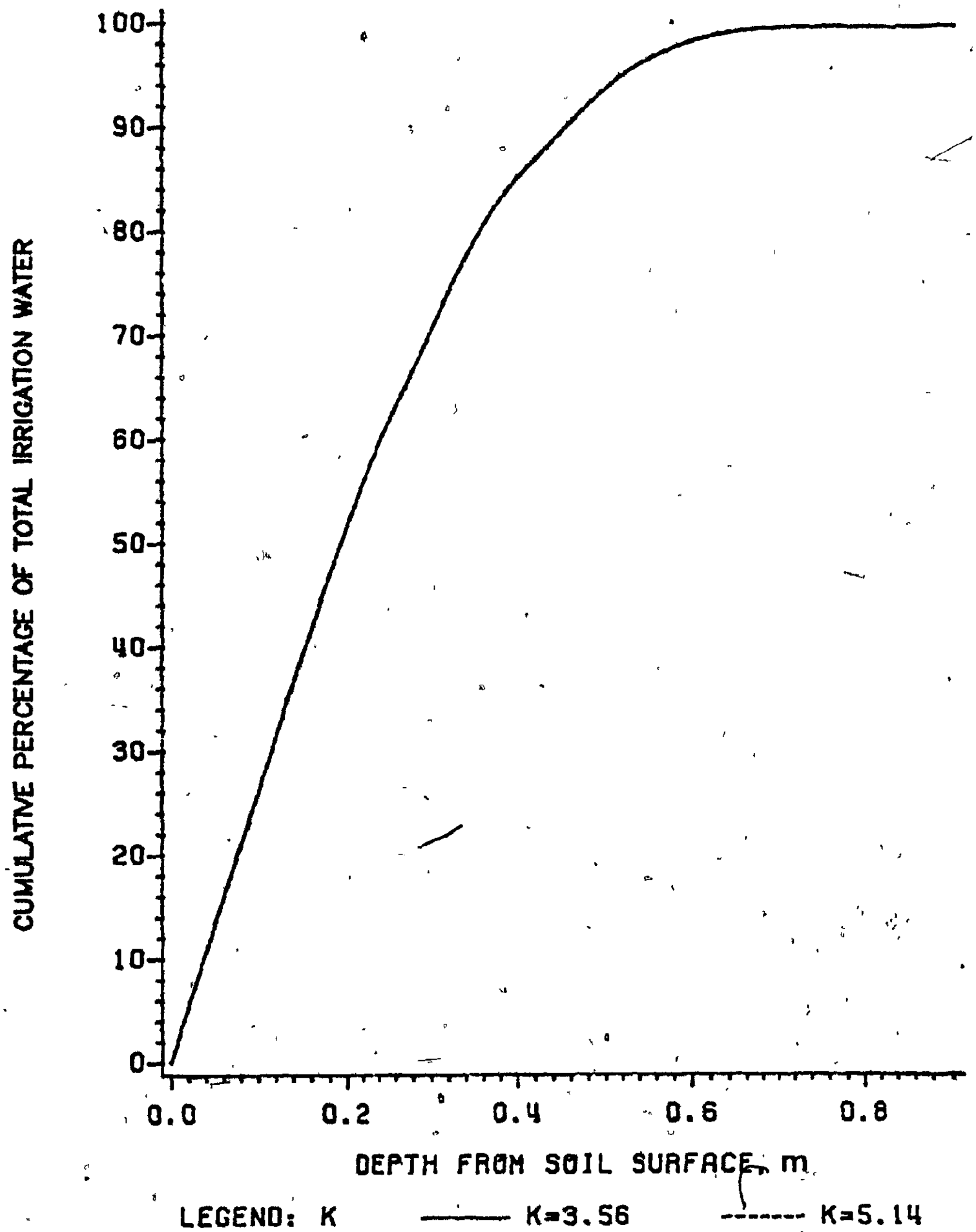

Figure B.69. Water input predicted in soil profile with an irrigation application of 12 L for K = 3.56 $m.day^{-1}$ at t=15 h and K = 5.14 $m.day^{-1}$ at t=13 h.

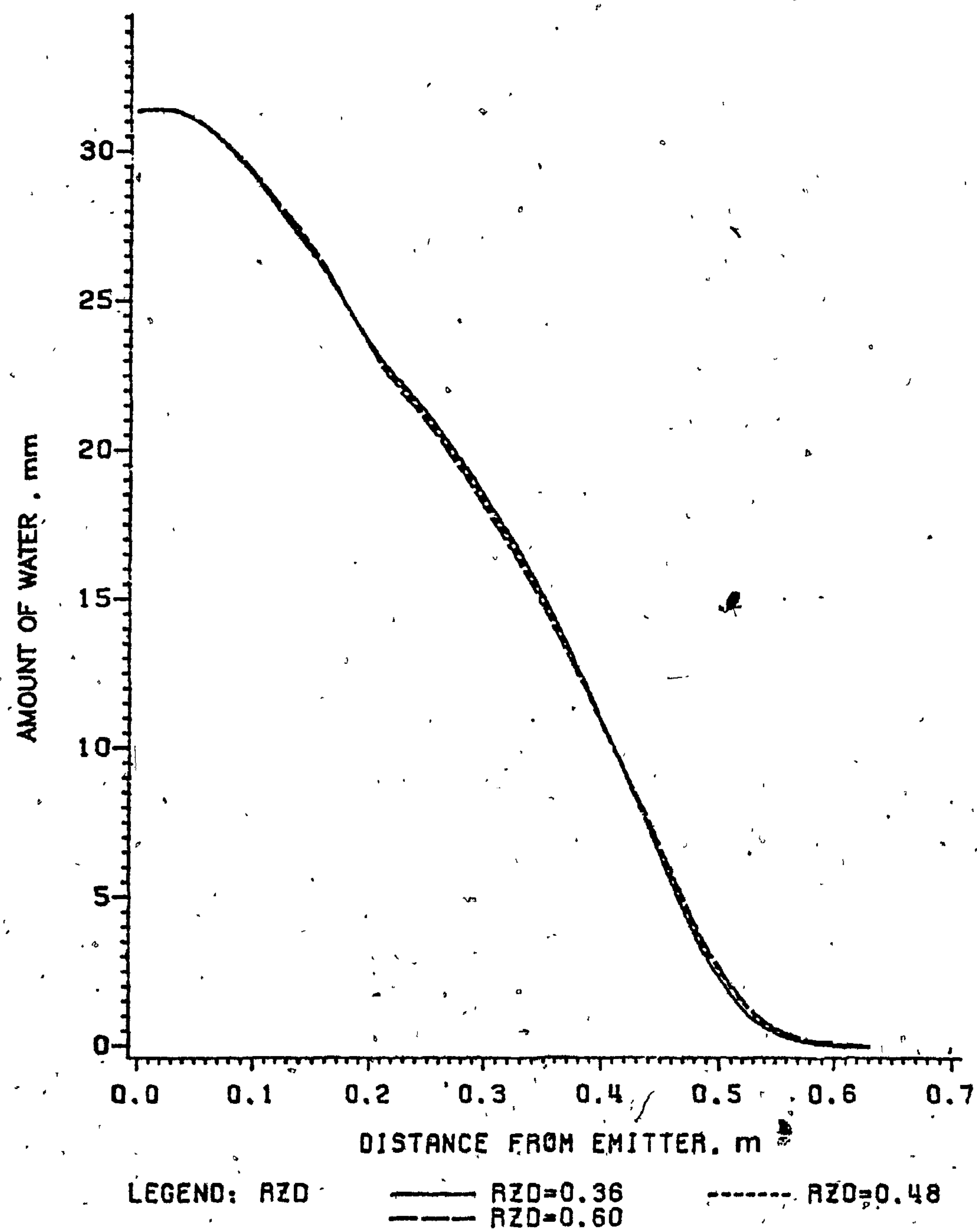

Figure B.70. Water input predicted along horizontal distance with an irrigation application of 12 L and different root zone depths.

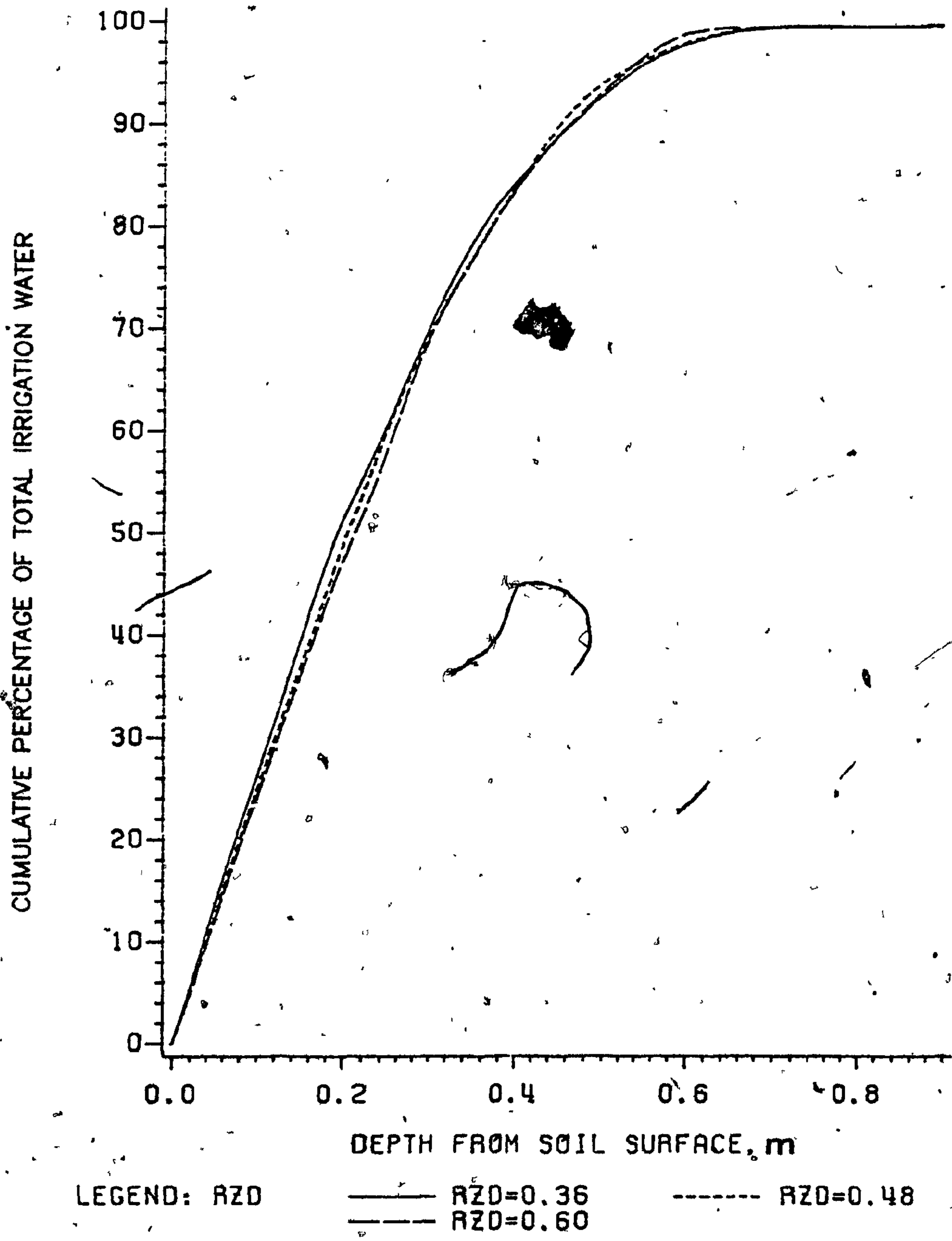

Figure B.71. Water input predicted in soil profile with an irrigation application of 12 L and different root zone depths.

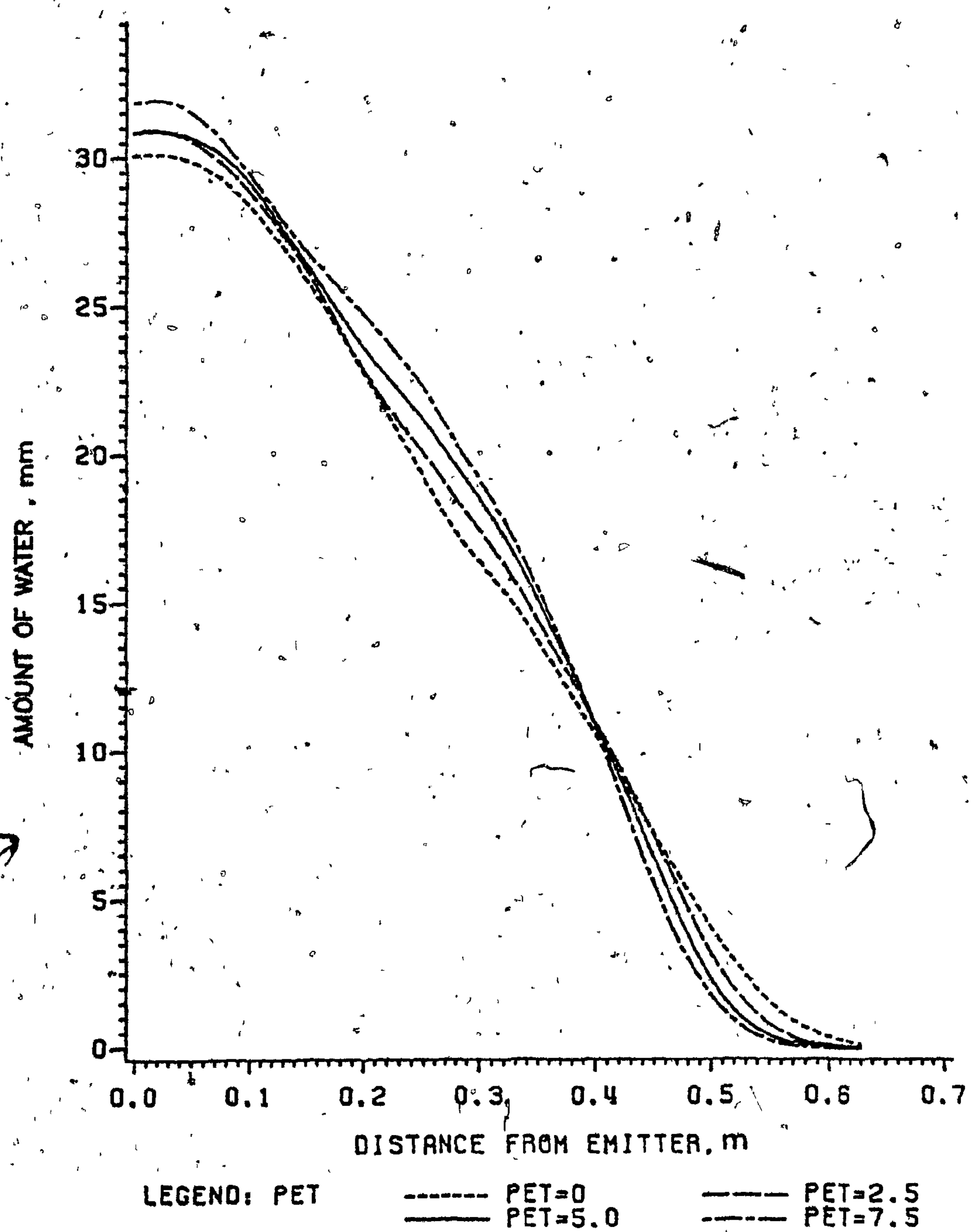

Figure B.72. Water input predicted along horizontal distance with an irrigation application of 12 L and different PET values.

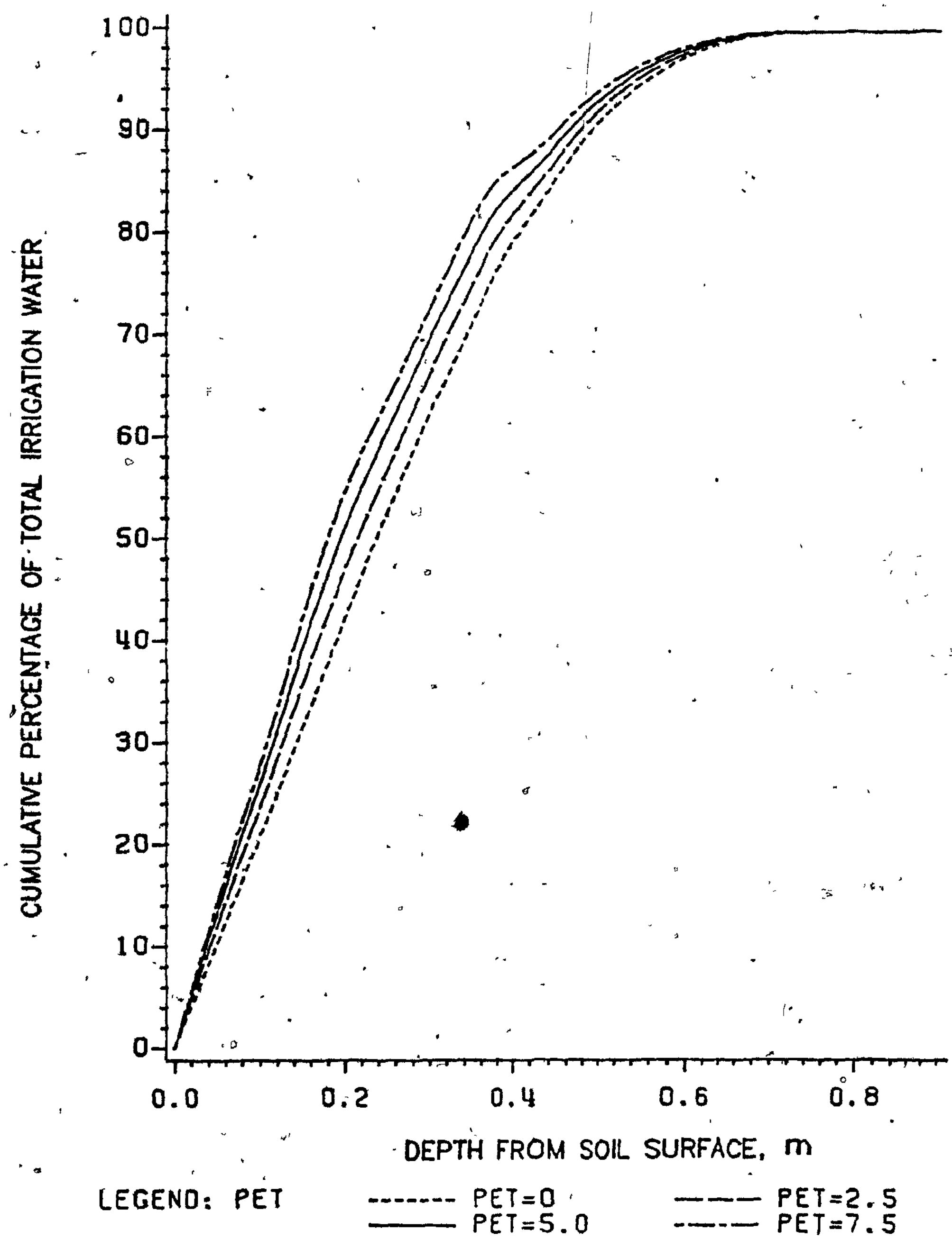

Figure B.73. Water input predicted in soil profile with an irrigation application of 12 L and different PET values.